# A role for Syndecan-4 and PCP signalling in controlling directional migration of neural crest cells in vivo

**Helen Katherine Matthews**

A Thesis submitted for the Degree of Doctor of Philosophy
University College London
2008

Department of Anatomy & Developmental Biology
University College London
London





ProQuest LLC
789 East Eisenhower Parkway
P.O. Box 1346
Ann Arbor, MI 48106-1346

## ABSTRACT

The neural crest (NC) is an embryonic population of cells, which delaminate from the neural tube epithelium to become vigorous migratory cells that colonise the entire embryo and give rise to many different derivatives. Neural crest migration requires activation of the non-canonical Wnt/planar cell polarity (PCP) signalling pathway, but it is not known exactly how this pathway controls cell migration. Here I show that the PCP ligand, Wnt11R, and the downsteam PCP element, Dishevelled, are essential for neural crest migration in *Xenopus laevis* embryos. Additionally, the proteoglycan, Syndecan-4, interacts with Dishevelled to control NC migration. A detailed examination of neural crest cell behaviour in *Xenopus* and zebrafish embryos shows that, in the absence of Dishevelled or Syndecan-4, cells are motile but lack the persistent migration that allows them to reach their target tissue. Furthermore, Dishevelled and Syndecan-4 control directional migration by regulating the polarised formation of cell protrusions. They also regulate the formation of paxillin-containing focal contacts *in vitro* and *in vivo*. Rho GTPase activity was measured using FRET analysis in neural crest cells migrating *in vitro* and *in vivo* after interfering with Syndecan-4/PCP signalling. I demonstrate that Syndecan-4 acts as a potent inhibitor of Rac, while Dishevelled activates RhoA. In addition, I show that RhoA inhibits Rac in neural crest cells. So, modulation of Rac by Syndecan-4 and PCP signalling allows the polarised formation of cell protrusions required for persistent NC migration. Finally I show that cell-cell contact inhibition of locomotion, dependent on PCP signalling, contributes to the initial polarity of the cell by inhibiting cell protrusions. Thus I present a model whereby neural crest cells are able to establish and maintain a directed migration by the integration of signals from cell-cell interactions mediated by PCP signalling and from the extracellular matrix via Syndecan-4.

I, Helen Katherine Matthews, confirm that the work presented in this thesis is my own. Where information has been derived from other sources, I confirm that this has been indicated in the thesis.

Signed..... Date.....

# TABLE OF CONTENTS


LIST OF FIGURES ..... 6
ABBREVIATIONS ..... 8
ACKNOWLEDGEMENTS ..... 9

**1. GENERAL INTRODUCTION ..... 10**

1.1. THE MIGRATING CELL ..... 10
1.2. THE NEURAL CREST ..... 12
*1.2.1. Neural crest specification ..... 12*
*1.2.2. Epithelial to mesenchymal transition ..... 14*
*1.2.3. Migration and differentiation ..... 15*
*1.2.4. Neural crest migration in Xenopus and zebrafish ..... 16*
1.3. A MOLECULAR BASIS FOR NEURAL CREST MIGRATION ..... 17
*1.3.1. Extracellular matrix components ..... 18*
*1.3.2. Inhibitory signals ..... 19*
*1.3.3. The case for chemoattraction ..... 19*
1.4. THE ROLE OF NON-CANONICAL WNT/PLANAR CELL POLARITY SIGNALLING ..... 21
*1.4.1. PCP signalling in Drosophila ..... 22*
*1.4.2. PCP signalling in vertebrates ..... 22*
*1.4.3. PCP signalling in the neural crest ..... 26*
1.5. SYNDECAN-4: A NEW ELEMENT OF THE PCP PATHWAY ..... 26
1.6. SUMMARY AND AIMS ..... 28

**2. MATERIALS & METHODS ..... 29**

2.1. SOLUTIONS AND MEDIA ..... 29
2.2. OBTAINING *XENOPUS* EMBRYOS ..... 30
2.3. OBTAINING ZEBRAFISH EMBRYOS ..... 31
2.4. SYNTHESIS OF ANTISENSE RNA PROBES FOR *IN SITU* HYBRIDISATION ..... 31
2.5. WHOLE MOUNT *IN SITU* HYBRIDISATION ..... 31
2.6. DOUBLE *IN SITU* HYBRIDISATION ..... 32
2.7. SYNTHESIS OF MRNA/MORPHOLINOS FOR MICROINJECTION ..... 33
2.8. MICROINJECTION IN *XENOPUS* AND ZEBRAFISH ..... 33
2.9. *XENOPUS* MICROMANIPULATION: ANIMAL CAP AND DLMZ DISSECTION ..... 34
2.10. *XENOPUS* MICROMANIPULATION: NEURAL CREST GRAFT EXPERIMENT ..... 34
2.11. PHOTOGRAPHY OF *XENOPUS* & ZEBRAFISH EMBRYOS ..... 34
2.12. *IN VITRO* CULTURE OF *XENOPUS* NC CELLS ..... 34
2.13. TIME-LAPSE ANALYSIS OF NC CELLS *IN VITRO* ..... 35
2.14. IMMUNOSTAINING OF FOCAL CONTACTS *IN VITRO* ..... 36
2.15. TIME-LAPSE ANALYSIS OF ZEBRAFISH NC *IN VIVO* ..... 36
2.16. WHOLE MOUNT IMMUNOSTAINING IN ZEBRAFISH ..... 37
2.17. CRYOSTAT SECTIONS ..... 38
2.18. FRET ANALYSIS ..... 38
2.19. STATISTICAL ANALYSIS ..... 39

**3. RESULTS: THE ROLE OF PCP SIGNALLING IN NEURAL CREST MIGRATION ..... 40**

3.1. INTRODUCTION ..... 40
*3.1.1. Non-canonical wnt ligands ..... 41*
*3.1.2. Dishevelled is an important modulator of wnt signalling ..... 41*
3.2. PCP PATHWAY GENES ARE EXPRESSED IN AND AROUND THE CRANIAL NEURAL CREST ..... 44
3.3. PCP SIGNALLING IS ESSENTIAL FOR CRANIAL NEURAL CREST MIGRATION ..... 46
3.4. WNT/PCP LIGANDS ARE EXPRESSED AROUND THE PRE-MIGRATORY NEURAL CREST ..... 49
3.5. WNT11R IS REQUIRED FOR NEURAL CREST MIGRATION ..... 53
3.6. DSH LOCALISES AT THE CELL MEMBRANE IN MIGRATING NEURAL CREST CELLS ..... 58
3.7. DISCUSSION ..... 60

**4. RESULTS: THE ROLE OF SYNDECAN-4 IN NEURAL CREST MIGRATION ..... 63**

4.1. INTRODUCTION ..... 63
*4.1.1. The domain structure of Syndecan-4 ..... 63*
*4.1.2. Interaction with the PCP pathway ..... 66*

4.2. *SYN4* IS EXPRESSED IN THE MIGRATING NEURAL CREST ..... 66
4.3. SYN4 IS REQUIRED FOR NEURAL CREST MIGRATION ..... 68
4.4. SYN4 IS NOT INVOLVED IN NC SPECIFICATION ..... 71
4.5. SYN4 INTERACTS WITH THE PCP PATHWAY IN THE NEURAL CREST ..... 72
4.6. THE PDZ AND PKCα BINDING DOMAINS OF SYN4 ARE REQUIRED FOR ITS ACTION IN THE NC 75
4.7. DISCUSSION ..... 78

**5. RESULTS: A CELLULAR BASIS FOR THE EFFECT OF SYN4 AND PCP SIGNALLING IN NEURAL CREST MIGRATION ..... 82**

5.1. INTRODUCTION ..... 82
*5.1.1. Cell protrusions and the actin cytoskeleton ..... 82*
*5.1.2. Attachment to the substrate ..... 83*
5.2. SYN4/PCP SIGNALLING AFFECTS THE PERSISTENCE BUT NOT THE SPEED OF NEURAL CREST CELL MIGRATION ..... 85
5.3. SYN4 AND PCP SIGNALLING CONTROL THE DIRECTIONALITY OF CELL PROTRUSIONS. ..... 93
5.4. SYN4 AND DSH SIGNALLING CONTROL THE FORMATION OF PAXILLIN-CONTAINING FOCAL CONTACTS *IN VITRO* ..... 99
5.5. SYN4 AND DSH SIGNALLING AFFECT P-PAXILLIN DISTRIBUTION *IN VIVO* ..... 100
5.6. FOCAL ADHESION KINASE (FAK) IS REQUIRED FOR NC MIGRATION *IN VIVO* BUT NOT *IN VITRO* 109
5.7. FRNK TREATMENT RESULTS IN THE STABILISATION OF FOCAL CONTACTS *IN VITRO* AND *IN VIVO* 115
5.8. DISCUSSION ..... 119

**6. RESULTS: SYNDECAN-4 AND PCP SIGNALLING CONTROL SMALL GTPASE ACTIVITY ..... 124**

6.1. INTRODUCTION ..... 124
*6.1.1. Rac, RhoA and Cdc42 in cell migration ..... 124*
*6.1.2. Using FRET to measure small GTPase activity ..... 126*
6.2. SYN4 CONTROLS RAC ACTIVITY BUT NOT RHOA OR CDC42 ..... 127
6.3. DISHEVELLED CONTROLS RHOA ACTIVITY BUT NOT RAC OR CDC42 ..... 128
6.4. ROK REPRESSES RAC IN THE NEURAL CREST ..... 133
6.5. RAC AND ROK ARE REQUIRED FOR DIRECTED MIGRATION OF NEURAL CREST CELLS ..... 135
6.6. RAC AND ROK CONTROL THE FORMATION OF CELL PROTRUSIONS AND FOCAL CONTACTS IN NEURAL CREST CELLS ..... 136
6.7. INHIBITION OF RAC IS ABLE TO RESCUE THE EFFECT OF *SYN4* MO ON FOCAL CONTACT FORMATION. ..... 142
6.8. DISCUSSION ..... 144

**7. RESULTS: PCP SIGNALLING CONTROLS 'CONTACT INHIBITION OF LOCOMOTION' IN NEURAL CREST CELLS ..... 149**

7.1. INTRODUCTION ..... 149
7.2. LEADING NEURAL CREST CELLS BEHAVE DIFFERENTLY TO NON-LEADING CELLS *IN VITRO* .. 150
7.3. CONTACT INHIBITION OF LOCOMOTION OCCURS BETWEEN NEURAL CREST CELLS *IN VITRO* AND *IN VIVO* ..... 151
7.4. DSH SPONTANEOUSLY LOCALISES TO CELL CONTACTS UPON A COLLISION ..... 155
7.5. SYN4 DOES NOT SHOW SPECIFIC LOCALISATION AT CELL CONTACTS ..... 155
7.6. INHIBITION OF DSH/PCP LIMITS CONTACT INHIBITION IN THE NEURAL CREST. ..... 159
7.7. DISCUSSION ..... 165

**8. GENERAL DISCUSSION ..... 169**

8.1. A MOLECULAR MODEL OF NEURAL CREST MIGRATION ..... 169
*8.1.1. The interaction between Syn4 and PCP signalling ..... 170*
*8.1.2. Alternative intracellular signalling pathways ..... 173*
*8.1.3. The role of the extracellular matrix ..... 175*
*8.1.4. The role of external signalling molecules ..... 177*
*8.1.5. Collective versus individual cell migration ..... 179*
8.2. THE NEURAL CREST AS AN EXAMPLE OF CELL MIGRATION *IN VIVO* ..... 181

**9. REFERENCES ..... 185**

## LIST OF FIGURES


**1. GENERAL INTRODUCTION ..... 10**

FIGURE 1.1. DEVELOPMENT OF THE NEURAL CREST ..... 13
FIGURE 1.2 PCP SIGNALLING CONTROLS DIVERSE DEVELOPMENTAL PROCESSES ..... 23
FIGURE 1.3 THE WNT SIGNALLING PATHWAY IN VERTEBRATES ..... 25

**2. MATERIALS & METHODS ..... 29**

**3. RESULTS: THE ROLE OF PCP SIGNALLING IN NEURAL CREST MIGRATION ..... 40**

FIGURE 3.1. THE CENTRAL ROLE OF DISHEVELLED IN WNT SIGNALLING ..... 43
FIGURE 3.2. PCP COMPONENTS ARE EXPRESSED IN AND AROUND THE NEURAL CREST ..... 45
FIGURE 3.3. PCP SIGNALLING IS REQUIRED FOR CRANIAL NEURAL CREST MIGRATION IN *XENOPUS* . 48
FIGURE 3.4. *WNT11* AND *WNT5A* ARE EXPRESSED IN AND AROUND THE NEURAL CREST ..... 51
FIGURE 3.5. *WNT11* AND *WNT11R* SURROUND THE NEURAL CREST BEFORE MIGRATION ..... 52
FIGURE 3.6. WNT11R IS REQUIRED FOR NEURAL CREST MIGRATION IN *XENOPUS* ..... 56
FIGURE 3.7. WNT11R IS NON CELL-AUTONOMOUS IN ITS CONTROL OF NEURAL CREST MIGRATION . 57
FIGURE 3.8. DISHEVELLED LOCALISES TO THE CELL MEMBRANE IN MIGRATING NC CELLS ..... 59

**4. RESULTS: THE ROLE OF SYNDECAN-4 IN NEURAL CREST MIGRATION ..... 63**

FIGURE 4.1. DOMAIN STRUCTURE AND SEQUENCE OF SYNDECAN-4 ..... 65
FIGURE 4.2. SYNDECAN-4 IS EXPRESSED IN THE MIGRATING NEURAL CREST ..... 67
FIGURE 4.3. INHIBITION OR OVEREXPRESSION OF SYN4 INHIBITS CRANIAL NC MIGRATION ..... 69
FIGURE 4.4. THE EFFECT OF SYN4 IS CELL AUTONOMOUS ..... 70
FIGURE 4.5. SYNDECAN-4 DOES NOT AFFECT NEURAL CREST INDUCTION ..... 73
FIGURE 4.6. THE EFFECT OF SYN4 MO CAN BE RESCUED BY ACTIVATION OF DSH ..... 74
FIGURE 4.7. SYN4 IS REQUIRED FOR TRANSLOCATION OF DSH TO THE MEMBRANE IN MIGRATING NC CELLS ..... 76
FIGURE 4.8. THE $PIP_2$ AND PDZ BINDING DOMAINS OF SYN4 ARE REQUIRED FOR ITS ACTION IN THE NEURAL CREST ..... 77

**5. RESULTS: A CELLULAR BASIS FOR THE EFFECT OF SYN4 AND PCP SIGNALLING IN NEURAL CREST MIGRATION ..... 82**

FIGURE 5.1. SYN4 IS REQUIRED FOR PERSISTENT MIGRATION OF NEURAL CREST CELLS *IN VITRO* ..... 88
FIGURE 5.2. SYN4 MRNA AFFECTS THE PERSISTENCE AND VELOCITY OF NEURAL CREST MIGRATION *IN VITRO*. ..... 89
FIGURE 5.3. DISHEVELLED AFFECTS THE PERSISTENCE OF NEURAL CREST MIGRATION *IN VITRO* ..... 91
FIGURE 5.4. SYN4 IS REQUIRED FOR PERSISTENT MIGRATION *IN VIVO*. ..... 94
FIGURE 5.5. SYN4 AND DSH CONTROL THE FORMATION OF CELL PROTRUSIONS *IN VITRO* ..... 97
FIGURE 5.6. SYN4 AND DSH CONTROL THE FORMATION OF CELL PROTRUSIONS *IN VIVO* ..... 98
FIGURE 5.7. SYN4 AFFECTS THE FORMATION OF FOCAL CONTACTS *IN VITRO* ..... 102
FIGURE 5.8. DSH AFFECTS THE FORMATION OF FOCAL CONTACTS *IN VITRO* ..... 102
FIGURE 5.9. SYN4 AND DSH CONTROL FOCAL CONTACT FORMATION *IN VIVO* IN ZEBRAFISH ..... 107
FIGURE 5.10. SYN4 AND DSH CONTROL FOCAL CONTACT FORMATION *IN VIVO* IN *XENOPUS* ..... 107
FIGURE 5.11. FAK IS REQUIRED FOR NEURAL CREST MIGRATION IN *XENOPUS* EMBRYOS ..... 111
FIGURE 5.12. FRNK AFFECTS THE SPEED OF NEURAL CREST CELL MIGRATION IN ZEBRAFISH EMBRYOS ..... 112
FIGURE 5.13. FRNK AFFECTS THE VELOCITY BUT NOT PERSISTENCE OF NEURAL CREST CELL MIGRATION *IN VITRO* ..... 114
FIGURE 5.14. FRNK STABILISES FOCAL CONTACTS IN NEURAL CREST CELLS *IN VITRO* ..... 116
FIGURE 5.15. FRNK STABILISES FOCAL CONTACTS IN NEURAL CREST CELLS *IN VIVO* ..... 118

**6. RESULTS: SYNDECAN-4 AND PCP SIGNALLING CONTROL SMALL GTPASE ACTIVITY ..... 124**

FIGURE 6.1. *SYN4* MO AFFECTS RAC ACTIVITY BUT NOT RHOA OR CDC42 ..... 129
FIGURE 6.2. DISHEVELLED AFFECTS RHOA ACTIVITY BUT NOT RAC OR CDC42 ..... 130
FIGURE 6.3. SYN4 AFFECTS RAC WHILE DSH AFFECTS RHOA *IN VIVO* ..... 132

FIGURE 6.4. ROK REPRESSES RAC IN NEURAL CREST CELLS MIGRATING *IN VITRO* ..... 134
FIGURE 6.5. RAC AND ROK ARE REQUIRED FOR PERSISTENT MIGRATION *IN VITRO* ..... 138
FIGURE 6.6. RAC AND ROK CONTROL THE FORMATION OF CELL PROTRUSIONS *IN VITRO* ..... 139
FIGURE 6.7. RAC AND ROK CONTROL FOCAL CONTACTS *IN VITRO* ..... 141
FIGURE 6.8. THE EFFECT OF *SYN4* MO ON FOCAL CONTACTS CAN BE RESCUED BY INHIBITION OF RAC. ..... 143

**7. RESULTS: PCP SIGNALLING CONTROLS 'CONTACT INHIBITION OF LOCOMOTION' IN NEURAL CREST CELLS ..... 149**

FIGURE 7.1. LEADING NEURAL CREST CELLS BEHAVE DIFFERENTLY TO NON-LEADING CELLS *IN VITRO* ..... 153
FIGURE 7.2. CONTACT INHIBITION OF LOCOMOTION OCCURS IN THE NEURAL CREST ..... 154
FIGURE 7.3. DISHEVELLED LOCALISES TO POINTS OF CONTACT BETWEEN NEURAL CREST CELLS ... 157
FIGURE 7.4 LOCALISATION OF SYNDECAN-4 IN NEURAL CREST CELLS ..... 158
FIGURE 7.5. DISHEVELLED IS REQUIRED FOR THE PERSISTENT MIGRATION OF 'LEADING' NEURAL CREST CELLS ..... 162
FIGURE 7.6. PCP SIGNALLING IS REQUIRED FOR CONTACT INHIBITION OF LOCOMOTION ..... 163
FIGURE 7.7. DISHEVELLED IS REQUIRED CELL-AUTONOMOUSLY FOR CONTACT INHIBITION ..... 164

**8. GENERAL DISCUSSION ..... 169**

FIGURE 8.1. MODEL OF NEURAL CREST MIGRATION ..... 171

**9. REFERENCES ..... 185**

## ABBREVIATIONS

| | | | |
|---|---|---|---|
| **BMP** | Bone morphogenetic protein | **GFP** | Green fluorescent protein |
| **CBD** | Central binding domain | **HSPG** | Heperan sulphate proteoglycan |
| **CE** | Convergent extension | **JNK** | Jun kinase |
| **CFP** | Cyan fluorescent protein | **MMP** | Matrix metalloprotease |
| **DCC** | Deleted in colorectal cancer | **Mo** | Morpholino |
| **DLMZ** | Dorsal lateral marginal zone | **NC** | Neural crest |
| **DRG** | Dorsal root ganglia | **PCP** | Planar cell polarity |
| **Dsh** | Dishevelled | **PKC** | Protein kinase C |
| **ECM** | Extra-cellular matrix | **$PIP_2$** | Phosphatidylinositol (3,4)-bisphosphate |
| **EMT** | Epithelial mesenchymal transition | **PNS** | Peripheral nervous system |
| **FA** | Focal adhesion | **ppax** | Phospho-paxillin |
| **FAK** | Focal adhesion kinase | **RA** | Retinoic acid |
| **FDX** | Fluorescein dextran | **RDX** | Rhodamine dextran |
| **FGF** | Fibroblast growth factor | **RFP** | Red fluorescent protein |
| **FRET** | Fluorescent resonance energy transfer | **ROK** | RhoA Kinase |
| **FRNK** | FAK-related non kinase | **SDF** | Stromal cell derived factor |
| **Fzd** | Frizzled | **SEM** | Scanning electron microscopy |
| **GAG** | Glycosaminoglycan | **Syn4** | Syndecan-4 |
| **GAP** | GTPase activating protein | **WASP** | Wiskott–Aldrich syndrome protein |
| **GDNF** | Glial cell derived neurotrophic factor | **WAVE** | WASP family Verprolin-homologous protein |
| **GEF** | Guanine nucleotide exchange factor | **YFP** | Yellow fluorescent protein |

**ACKNOWLEDGEMENTS**

Firstly, I am indebted to my supervisor, Roberto Mayor, for his continued advice, support and kind encouragement. I would also like to express gratitude to all my friends in the Mayor lab, past and present, with a special mention to Jaime de Calisto, Lorena Marchant and Sei Kuriyama for their guidance in the lab. Many thanks must also be expressed to Les Dale, Claudio Stern, Masa Tada, Tim Geach, Carlos Carmona-Fontaine and Ben Steventon for their lively discussion and constructive comments on my work.

I would also like to acknowledge my collaborators: Maddy Parsons, who carried out the analysis of the FRET data, Carlos Carmona-Fontaine for his help with the statistical analysis, Sei Kuriyama for construction of the Syn4 mutants and Chaudhary Riaz for providing SEM images of the neural crest. Thanks also to Maria Christodoulou, with whose kind help I was able to visulise focal contacts in neural crest cells. I also thank Juan Larrain, Florence Broders-Bondon, Anne Ridley, Sean Megason, Robert Kelsh, M. Matsuda, Klaus Hahn and Masa Tada for supplying reagents.

Finally I would like to express my immense gratitude to my partner, Matthew, and to my parents, June and Tony, for their unending love and support.

# 1. GENERAL INTRODUCTION

## 1.1. The migrating cell

The ability of a cell to move in a directed manner from one location to another is a fundamental requirement for almost all biological systems. In multi-cellular organisms, this requirement begins in the embryo, where a multitude of different processes are dependent on the correct movement of large numbers of cells. These range from the intricate movements of gastrulation, to the precision guidance of neurons in the developing nervous system (Keller, 2005; Locascio and Nieto, 2001). In the adult too, cell migration plays a vital role in many systems including the immune system, epithelial tissue renewal and wound healing. Cell migration defects can contribute to the pathology of many diseases including vascular diseases such as atherosclerosis, and chronic inflammatory diseases like asthma and multiple sclerosis (Luster et al., 2005; Ridley et al., 2003). Likewise, metastasis in cancer is caused by mis-regulation of the normal cell migration machinery and results in cells that are normally static becoming aggressively motile and invasive (Yamaguchi et al., 2005). With such a vital role for cell migration in development and disease, it is of little wonder that scientists devote much time studying this process, and in recent years there have been major advances in our understanding of cell motility.

The co-ordinated movement of a cell is a hugely complex process that requires the co-operation and integration of many different sub-cellular machinery. For a cell to travel in a purposeful manner, it must first 'know' which direction to go. This can be achieved by sensing environmental cues such as chemokines, migration-promoting agents that attract motile cells (Van Haastert and Devreotes, 2004). Upon receiving a chemotactic signal, the cell must become polarised in the direction of migration. This requires complete structural re-organisation including restructuring of the actin cytoskeleton, microtubule network and Golgi apparatus. The cell must then produce a protrusion either in the form of a broad sheet-like lamellipodium or spiky filopodium, which are driven by polymerisation of actin at the leading edge. Cell protrusions attach to the underlying substrate at points known as focal contacts, clusters of proteins that physically link the actin cytoskeleton to the extracellular matrix and allow the cell to exert traction against its surroundings. Finally, at the rear

of the cell, attachments to the substrate are disassembled and the actin cytoskeleton retracts to enable translocation. These processes must occur simultaneously to allow cell movement and a network of regulatory molecules is required to maintain this delicate harmony (for an overview of the cell migration process see (Ridley et al., 2003; Vicente-Manzanares et al., 2005).

Scientists are slowly beginning to build up a picture of the migrating cell and an understanding of many of the molecules that regulate migration. However, much of this knowledge comes from studies carried out *in vitro*: of cells such as fibroblasts migrating across a Petri dish on a 2-dimensional artificial substrate. *In vitro* studies have given us great insights into the cell migration process, but they have a number of limitations, primarily that they do not accurately mimic the environment of normal migrating cells. Cells *in vivo* are surrounded by a 3-dimensional extracellular matrix, as well as by numerous other cells, of many different cell types. They are constantly subjected to an array of signalling molecules from the short-range communications of neighbouring cells to the long-range effects of chemokines. This complexity of environment simply cannot be mimicked *in vitro*. In recent years, attempts have been made to overcome this problem by building 3D matrices (Cukierman et al., 2001; Even-Ram and Yamada, 2005). These kinds of studies have highlighted some important differences between cells migrating in 2 and 3 dimensions, but ideally cell migration needs to be studied *in vivo* in the cell's natural environment. There are of course many potential pitfalls when it comes to studying cell migration *in vivo*. Most obviously perhaps, imaging migrating cells in living tissue presents a problem. One possible solution is to look to cell migration in the embryo. Embryologists have spent decades developing techniques that allow the observation of the behaviour of small groups or even individual cells *in vivo*. Furthermore, the small size of embryos and the fact that some, such as zebrafish, are transparent allow for sophisticated imaging and microscopy techniques to be used.

There are many examples of cell migration during embryogenesis, but one of the most dramatic is the migration of the neural crest (NC). The neural crest is initially a static population of cells located on top of the neural tube, which can later detach from the neural tube and migrate. Neural crest cells travel long distances though the embryos following strictly defined pathways in a migration that is rapid, persistent and highly directional. Here I use the migration of the neural crest in frog (*Xenopus laevis*) and fish (zebrafish) embryos as a model for studying cell migration *in vivo*.

## 1.2. The neural crest

The neural crest is a transient population of cells that exists only for a short period of time during embryonic development. The development of the crest can be broken down into discrete steps (summarized in Figure 1.1). First, the presumptive neural crest cells are specified at the border between the neural plate and the epidermis (Fig 1.1A). As neuralation proceeds, the neural plate folds until eventually the crest comes to lie along the dorsal midline of the neural tube (Fig 1.1B). Upon completion of neurulation, neural crest cells undergo an epithelial to mesenchymal transition (EMT) and detach from the neural tube. Neural crest cells then begin to migrate following strictly defined migratory pathways that eventually allow them to colonize almost the entire embryo (Fig 1.1C). Finally, upon reaching their destination neural crest cells differentiate to ultimately form many different cell types including neurons, glia, cartilage, skeleton and pigment cells (Fig 1.1D).

### *1.2.1. Neural crest specification*

Neural crest cells begin their life as ectodermal cells at the border between the neural plate and the non-neural ectoderm. Their fate is specified during the end of gastrulation and the beginning of neurulation by a combination of extracellular signals, secreted from surrounding tissues. These include various BMP, Wnt, FGF ligands as well as retinoic acid (RA) (LaBonne and Bronner-Fraser, 1998; Marchant et al., 1998; Villanueva et al., 2002). The precise sequence and interaction of these different signals is uncertain and there are some discrepancies between species (Aybar and Mayor, 2002). The current model favours an initial intermediate level of BMP signalling to specify the neural plate border, followed by a second Wnt/FGF/RA signal from the mesoderm, to induce the neural crest (Steventon et al., 2005). What is clear, however, is that this combinatorial signalling specifies the area that will become the neural crest and induces the expression of a network of neural crest-specific transcription factors (reviewed in (Steventon et al., 2005).

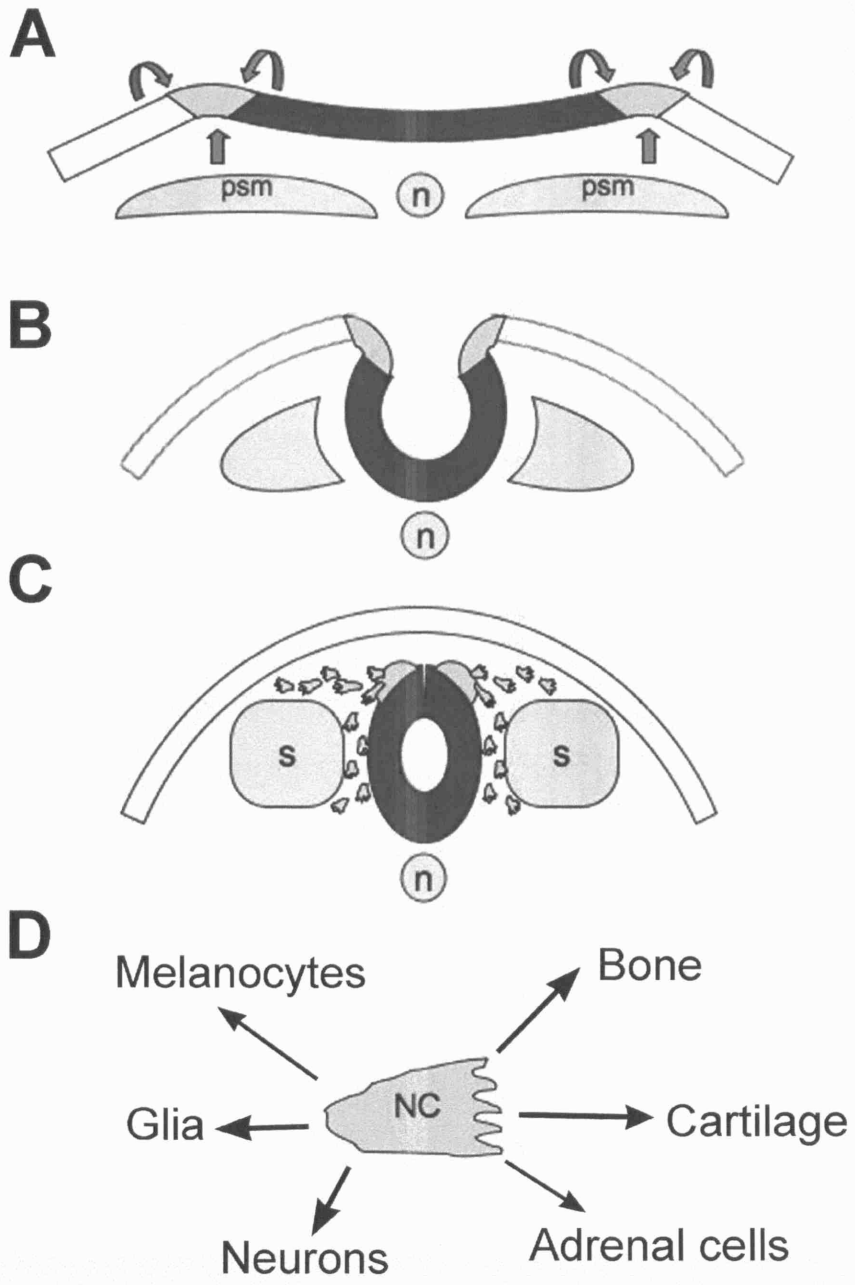


**Figure 1.1. Development of the neural crest**

**(A-C)** Schematic of a transverse section through an embryo with the neural crest shown in pale blue, neural tube in dark blue and epidermis in white. **(A)** Neural crest tissue is specified by signalling from the neural tube, epidermis and underlying mesoderm. **(B)** As the neural plate folds to become the neural tube, the neural crest comes to lie over the dorsal part of the neural tube. **(C)** Neural crest cells detach from the neural tube and migrate through the embryo. **(D)** An individual neural crest cell has the potential to form a variety of derivatives. n, notochord; psm, pre-somitic mesoderm; s, somite; NC, neural crest.

The first transcription factors to appear are the so-called 'early class' that are expressed in a domain slightly wider than the neural crest. These include genes from the *msx* and *dlx* families as well as *pax3* and *c-myc* (Bellmeyer et al., 2003; McLarren et al., 2003; Monsoro-Burq et al., 2005). These are followed by a second class of genes, which are the 'classic' neural crest markers, expressed exclusively in the crest. Many of these genes belong to the *snail* and *sox* gene families, which encode transcriptional repressors (Aybar et al., 2003; Hong and Saint-Jeannet, 2005). Many are anti-apoptotic factors and are believed to play an important role in the survival and proliferation of neural crest cells. Indeed, loss of *snail* or *sox* genes in the crest results in premature death of neural crest cells (Dutton et al., 2001; Vega et al., 2004).

### *1.2.2. Epithelial to mesenchymal transition*

After neurulation is completed, NC cells undergo an epithelial to mesenchymal transition (EMT) and delaminate from the neural tube. EMT involves gross changes in cell morphology, allowing the previously static epithelial cells to become migratory. Cells lose their cuboid shape and apical-basal polarity, and gap junctions replace tight junctions between cells. Occludin, a key component of tight junctions, is down regulated around five hours before neural crest delamination takes place (Aaku-Saraste et al., 1996), while connexin-43, a gap junction protein, starts to be expressed (Lo et al., 1997). Connexin-43 is expressed in migrating neural crest cells and embryos lacking connexin-43 show major defects in neural crest derived tissue such as the heart (Liu et al., 2006).

In chick embryos, EMT in the neural crest can be easily observed, as it is accompanied by a characteristic change in the expression of the cadherins, a class of $Ca^{2+}$-dependent cell-cell adhesion proteins. Prior to migration N-cadherin and cadherin-6B are strongly expressed in the neural crest, but at the onset of migration these cadherins are down-regulated and cadherin-7 begins to be expressed (Nakagawa and Takeichi, 1995; Nakagawa and Takeichi, 1998). It is believed that these changes in cadherin expression allow the neural crest to detach from the epithelial layer, while at the same time strengthening connections between each other, prior to migration. Such a typical cadherin shift at the onset of migration is yet to be observed in other species. In *Xenopus*, no examples of cadherins down-regulated at neural crest migration have been identified, although Cadherin-11 is

expressed specifically in sub-populations of the migrating crest (Borchers et al., 2001; Vallin et al., 1998).

Members of the *snail* superfamily are known to play an important role in regulating EMT. Their function was first elucidated in cancer cells, where activation can increase metastasis and migratory behaviour (Barrallo-Gimeno and Nieto, 2005). Snail gene products function as transcriptional repressors and Snail1 and Snail2 have both been shown to directly repress E-cadherin, a cadherin strongly associated with epithelial cells, during oncogenesis (Bolos et al., 2003; Cano et al., 2000). Furthermore, this role has since been extended to neural crest cells with the discovery that Snail2 binds directly to the promoter region of cadherin-6B and represses it during EMT in chick neural crest cells (Taneyhill et al., 2007).

As well as cell-cell adhesion, another important factor for EMT in the neural crest is the cell cycle. EMT requires careful regulation and synchronisation of the cell cycle, with neural crest cells leaving the neural tube during S phase (Burstyn-Cohen and Kalcheim, 2002). Completing the G1/S transition is crucial for EMT as inhibition of this transition prevents delamination of neural crest cells (Burstyn-Cohen and Kalcheim, 2002). Snail genes are involved in this cell cycle control, by blocking cell cycle progression and maintaining the cells in G1 during EMT (Vega et al., 2004). The G1/S transition signals the end of EMT and delamination from the neural tube and is stimulated by BMP and canonical wnt signalling, which control the timing of the onset of migration (Burstyn-Cohen et al., 2004).

### *1.2.3. Migration and differentiation*

Migration and differentiation are inextricably linked in the neural crest cell, as the path that an individual cell takes determines its eventual fate. Neural crest cells can be classified into two broad populations; the cephalic (or cranial) crest of the head and the trunk neural crest. The onset of neural crest migration proceeds in an anterior to posterior fashion with the cephalic neural crest beginning their migration earliest. Cephalic neural crest cells migrate into the branchial arches in three distinct streams, termed the mandibular, hyoid and branchial streams, and ultimately differentiate to form the skeleton and cartilage of the head (Kontges and Lumsden, 1996). In addition, some cells from the mandibular stream also contribute to the cranial sensory ganglia and the cornea (Sadaghiani and Thiebaud, 1987). Trunk neural crest cells in most animals migrate along two distinct pathways. Some cells

take a ventral pathway between the neural tube and the somites. These give rise to sensory and sympathetic ganglia, Schwann cells and cromaffin cells (Le Douarin and Teillet, 1974).Others choose a lateral pathway between the somites and the ectoderm, eventually colonising the ectoderm to become the pigmented melanocytes (LeDouarin and Kalcheim, 1999). The majority of cells follow the ventral pathway, which can be recognised as streams of migrating cells in a segmented pattern through the somitic mesoderm. These distinct streams are created by migration through only part of each somite. For example, in avian embryos neural crest cells can only enter the rostral half of each somite and are excluded from the caudal half (Bronner-Fraser, 1986a; Rickmann et al., 1985; Teillet et al., 1987).

One of the most notable features of neural crest cells is their ability to differentiate into such a wide range of tissues. Although derived from the ectodermal germ layer, neural crest cells are able to generate both typically ectodermal cells such as neurons as well as mesenchymal tissues like cartilage and muscle. This suggests a high level of pluripotency and it has been suggested that neural crest cells maintain a relatively undifferentiated stem cell-like state for longer than cells in other tissues (see (Delfino-Machin et al., 2007)for review).

### *1.2.4. Neural crest migration in Xenopus and zebrafish*

In the course of this thesis I will present work on the neural crest in *Xenopus* and zebrafish embryos, so it is important to highlight any differences in neural crest migration between these two organisms. Although neural crest migration is relatively conserved between species, there are some subtle differences. Both *Xenopus* and zebrafish have three segmented streams of cranial neural crest and many streams of trunk neural crest, which follow either the ventral or lateral pathway. In *Xenopus*, trunk neural crest cells are offered three additional pathways of migration. As well as the ventral and lateral pathways, cells follow a dorsal pathway into the dorsal fin, a circumferential migration around into the ventral fin and an enteric pathway into the ventral fin via the anus (Collazo et al., 1993). In fish, trunk neural crest cells follow two pathways as in avian embryos, however because of the shape of the zebrafish embryo, both pathways proceed in a ventral direction (Eisen and Weston, 1993; Raible et al., 1992). Also, in contrast to chicks, zebrafish trunk cells migrate through the mid-point of the somites rather than the rostral half (Raible et al., 1992). *Xenopus*

trunk cells on the other hand, migrate through the caudal portion of each somite (Collazo et al., 1993; Krotoski et al., 1988).

Both fish and frogs have a number of unique advantages when it comes to studying neural crest migration. *Xenopus* has a rich history of use as a model organism for embryology (Gurdon and Hopwood, 2000) and many aspects of its development are very well understood. In addition, the large size and general robustness of *Xenopus* embryos makes embryonic manipulations such as the removal and grafting of different tissues relatively straightforward. For example, it is possible to specifically dissect the cranial neural crest intact for culture *in vitro* (Alfandari et al., 2003). Also, targeted injections at the 32-cell stage allow for specific labelling of neural crest cells. Neural crest migration can be easily followed by grafting labelled NC into an unlabelled host, or by DiI injections into the neural tube (Borchers et al., 2000; Collazo et al., 1993; Krotoski et al., 1988). However, the yolky consistency of *Xenopus* embryonic cells makes *in vivo* imaging more than a few layers deep virtually impossible. Zebrafish embryos, by contrast, are almost transparent, meaning that cells deep inside the embryo can be imaged with high resolution. Also, a large number of mutant zebrafish lines have been generated, making them ideal for genetic studies (Amsterdam and Hopkins, 2006). Recently this has led to the development of transgenic lines, including the *sox10:egfp* line, which expresses GFP only in the neural crest and allows individual neural crest cells to be traced throughout their migration (Carney et al., 2006). However, dissection and transplantation experiments are much harder to perform in fragile fish embryos than in frogs. Thus, *Xenopus* and zebrafish provide complimentary approaches that together allow us to study all aspects of neural crest migration.

### 1.3. A Molecular basis for neural crest migration

Neural crest cells follow various convoluted migration pathways throughout the embryo and one of the most interesting questions that remains to be addressed is; what directs them along these intricate routes? In recent years, a number of molecular cues that guide neural crest migration have been identified (Kuriyama and Mayor, 2008). Many of these molecules were initially discovered from studies on axon guidance, where growth cones are guided along strictly defined paths by a combination of short-range and long-range environmental signals, both attractive and

repulsive. The signals regulating axon guidance are mostly well defined, but this is not the case for the neural crest, where the picture still remains very much incomplete. In the remainder of this chapter, I will summarise what is known about the molecular basis of neural crest migration.

### *1.3.1. Extracellular matrix components*

The road on which neural crest cells travel is paved with various extracellular matrix (ECM) components and the distribution of these molecules plays a significant role in guiding neural crest migration. Electron microscope images of migrating neural crest cells *in vivo* show that ECM fibrils tend to align in the direction of migration, providing a physical guide for migration (Newgreen, 1989; Perris and Perissinotto, 2000). However, a polarised ECM is not necessary for neural crest migration, as NC cells are able to migrate *in vitro* where fibril distribution is random (Alfandari et al., 2003). Many different ECM glycoproteins surround the neural crest *in vivo*, but not all are able to support NC cell migration. Indeed, extracellular matrix components can be divided into two groups; those that permit neural crest migration and those that deny it. One of the earliest ECM components to be identified as promoting neural crest migration was fibronectin. Fibronectin is ubiquitously expressed in the neural crest migration pathways, and in some cases the termination of migration corresponds to the disappearance of fibronectin in the ECM (Newgreen and Thiery, 1980; Thiery et al., 1982). Functional experiments show that blocking the interaction of fibronectin with its binding partner, integrin $\alpha5\beta1$, is a powerful method of inhibiting neural crest migration (Alfandari et al., 2003). Other ECM glycoproteins that allow neural crest migration include vitronectin and several members of the laminin and collagen families (Coles et al., 2006; Delannet et al., 1994; Perris and Perissinotto, 2000). However, none of these alone are sufficient for the migration of neural crest cells *in vitro*. Explanted *Xenopus* cranial neural crest cells are only able to migrate when plated on a substrate containing fibronectin (Alfandari et al., 2003).

Conversely, other ECM components actively inhibit neural crest migration, particularly those containing chondroitin 6-sulphate. Tissues rich in those proteoglycans tend to be those such as the notochord, which deny entry to neural crest cells (Oakley et al., 1994).Two examples of proteoglycans with neural crest-repulsive activities are aggrecan and cytotactin-binding proteins, which are expressed

in the notochord and caudal sclerotome respectively, both tissues that neural crest cells are unable to enter (Perissinotto et al., 2000; Tan et al., 1987).The local composition of the extracellular matrix provides both permissive and inhibitory signals that restrict neural crest cells to their correct pathways, however there is no evidence that ECM components are able to actively attract neural crest cells.

### *1.3.2. Inhibitory signals*

As well as ECM components, a number of other repellent molecules are expressed in the tissues that exclude the neural crest. One class of molecules that can repel neural crest cells are the Semaphorins, secreted and membrane bound signalling molecules, initially characterised for their role in axon guidance (Kolodkin, 1998). In zebrafish, Semaphorin-3F and Semaphorin-3G are expressed in neural crest-free regions of the head, while their receptors, Neuropilin-2A and -2B, are expressed in the neural crest. Signalling to these receptors prevents crest cells from straying outside their streams as overexpression of semaphorins can constrict neural crest migration pathways (Yu and Moens, 2005).

Ephrins and Eph receptors also play a role in maintaining the three separate streams of migration in the cranial neural crest. Eph-A4 and Eph-B1 are expressed in the neural crest of the third and fourth branchial arches, while their ligand, ephrin-B2, is expressed in the adjacent second arch, where it repels neural crest cells expressing the receptor, and prevents intermingling of the streams (Smith et al., 1997). Ephrins and semaphorins also play a role in guiding trunk neural crest migration, with expression of ligands of both classes restricting neural crest from the caudal half of the somites in chicks (Gammill et al., 2006; Krull et al., 1997). Another family of molecules that play a role in trunk neural crest guidance is the slit/robo family. Slits are secreted from the dermamyotome, where they prevent robo-expressing, early migratory crest cells from entering the dorsal pathway, directing them instead towards the ventral pathway (Jia et al., 2005).

### *1.3.3. The case for chemoattraction*

The molecules discussed so far are all either permissive signals that allow neural crest migration or negative signals that inhibit it. To date, a distinct lack of positive signals that attract neural crest cells have been identified. In the case of axon guidance, migration is often guided by inhibitory short-range signals such as

semaphorins in conjunction with long-range chemoattractants, which form a diffusion gradient. Examples of chemotaxis can also be found for cells as well as axons. For example, in the zebrafish embryo lateral line cells are guided to their correct position by following a gradient of the chemokine, SDF-1 (David et al., 2002; Valentin et al., 2007). It has been speculated that a similar mechanism may also be operating in the neural crest. There are some examples of chemoattractants that have been found to play a role in the later migration of neural crest derivatives, although not in undifferentiated neural crest cells themselves. For example, DCC, a key mediator of the actions of the netrin family of chemoattractants, is expressed in neural crest-derived enteric neurons and these cells will migrate towards a netrin source *in vitro* (Jiang et al., 2003). Likewise, the chemokine GDNF is expressed in the developing mouse gut and is required for the correct migration of enteric neuronal precursors to their correct destinations (Natarajan et al., 2002; Young et al., 2001). Enteric neural crest cells will cross a filter paper barrier to reach a source of GDNF in organ culture experiments (Young et al., 2001). SDF-1, meanwhile, has been found to play a role in the migration of the NC-derived dorsal root ganglia (DRG), with SDF-1 being expressed in their migratory pathway, while its receptor, CXCR4, is expressed in the DRGs themselves (Belmadani et al., 2005). However, in each of these cases it is not possible to ascribe these effects to true chemotaxis, and they could also be explained by chemokinesis, the process whereby a molecule is able to stimulate increased motility without any kind of directional signal. The best test to distinguish chemokinesis from chemotaxis is to determine whether cells can follow an artificial gradient of the signal using time-lapse analysis in an *in vitro* migration assay (Wells and Ridley, 2005). However, such experiments were performed in only one of the studies of chemotaxis in neural crest derivatives, and in this case no time-lapse analysis was carried out, making it impossible to rule out chemokinesis as a mode of action (Belmadani et al., 2005). In summary, there is some evidence pointing to chemoattraction in the crest but it is limited to specific sub-populations of crest cells late in NC development and the described effects could be explained by chemokinesis rather than true chemoattraction. Certainly a definitive long-range chemoattractant that attracts neural crest cells from the neural tube in the direction of their targets has yet to be identified.

There is, of course, another possibility; that neural crest cells are able to find their way without relying on an external chemoattractant. It is possible that neural

crest cells are intrinsically migratory cells that only travel in one direction because that is the only feasible way open to them. There are repulsive signals in the neural tube that prevent them from going backwards, repulsive semaphorin and ephrin ligands that prevent them from straying from their narrow streams and their migration routes are carpeted with their favoured extracellular matrix components. Could it be that these signals are sufficient to guide the neural crest without chemoattraction? This is an intriguing idea, but raises a number of questions. A system based purely on negative signals would surely be inefficient as randomly migrating cells would travel backwards along their pathways as well as forwards. This is not consistent with the high polarity observed in neural crest cells migrating *in vivo* (Teddy and Kulesa, 2004). It seems likely that there are other signals involved in establishing the polarity and directionality of neural crest cell migration and these could be unidentified chemoattractants, or an entirely different mechanism. One such candidate is the planar cell polarity (PCP) signalling pathway, which has recently been shown to be essential for successful NC migration (De Calisto et al., 2005).

### 1.4. The role of non-canonical Wnt/planar cell polarity signalling

Non-canonical Wnt/planar cell polarity (PCP) signalling refers an alternative branch of the Wnt signalling pathway. In the canonical pathway secreted wnt glycoproteins bind to Frizzled receptors, activating an intracellular cascade that results in the stabilization of β-catenin, which regulates the transcription of a large number of genes (Miller et al., 1999). Canonical wnt signalling controls many embryonic processes, most of which are involved in cell fate determination, and which include playing a vital role in neural crest induction (Garcia-Castro et al., 2002). The PCP pathway uses many of the same components as canonical signalling such as Wnt and Frizzled proteins, but rather than a transcriptional outcome, a β-catenin independent pathway is activated, which acts directly on the cell cytoskeleton (Veeman et al., 2003). So, while canonical wnt signalling often plays a role in controlling cell fate, PCP signalling generally regulates cell shape, morphology and polarity. Figure 1.2 shows three such examples of PCP signalling in controlling cell polarity, shape and motility in the embryo.

### *1.4.1. PCP signalling in Drosophila*

PCP signalling was first described in *Drosophila*, where a number of mutations were identified that disrupt the formation of bristles and hairs on the adult cuticle (Gubb and Garcia-Bellido, 1982). In the *Drosophila* wing, epithelial cells are highly polarized, with a single hair outgrowth forming at the distal end of each cell. Mutations in the genes *frizzled* (*fzd*), *dishevelled* (*dsh*), *prickle, strabismus (stbm), flamingo and diego* cause adherent cellular organisation in this tissue, with hairs forming in a disorganised pattern (Feiguin et al., 2001; Gubb et al., 1999; Theisen et al., 1994; Usui et al., 1999; Vinson and Adler, 1987; Wolff and Rubin, 1998). These genes code for transmembrane or intracellular proteins, which become asymmetrically localised in each cell. Stbm and prickle accumulate at the proximal membrane of each cell, while Fz and Dsh localise solely on the distal side, where they promote the formation of an actin-rich prehair (Axelrod, 2001; Bastock et al., 2003; Strutt, 2001; Tree et al., 2002). Interactions between PCP components on the distal side of one cell and the proximal side of the adjacent cell stabilize the system to give uniform polarity to the entire tissue (Fig 1.2A).

### *1.4.2. PCP signalling in vertebrates*

In vertebrates PCP signalling regulates a number of different developmental processes including neural tube closure, cochlear hair orientation and ciliogenesis (Wang and Nathans, 2007). One of the best characterised examples of PCP signalling in vertebrates is its role during gastrulation in co-ordinating convergent extension (CE) movements in *Xenopus* and zebrafish (Fig 1.2B). CE movements result in the anterior-posterior elongation and mediolateral narrowing of the embryo and are driven by the intercalation of cells in the mesoderm and ectoderm. The intercalating cells are highly polarised with cell protrusions localised at the lateral ends of each cell (Shih and Keller, 1992). Inhibition of PCP ligands Wnt11 or Wnt5a perturb CE movements in *Xenopus* (Moon et al., 1993; Tada and Smith, 2000), while the zebrafish mutants for various PCP elements including *silberblick* (Wnt11), *pipetail* (Wnt5a), and *trilobite* (Strabismus) exhibit a shortened body axis characteristic of defects in CE (Hammerschmidt et al., 1996; Rauch et al., 1997; Solnica-Krezel et al., 1996). Furthermore, inhibition or overexpression of Dsh disrupts the polarity of *Xenopus* mesoderm cells undergoing CE (Wallingford et al., 2000).

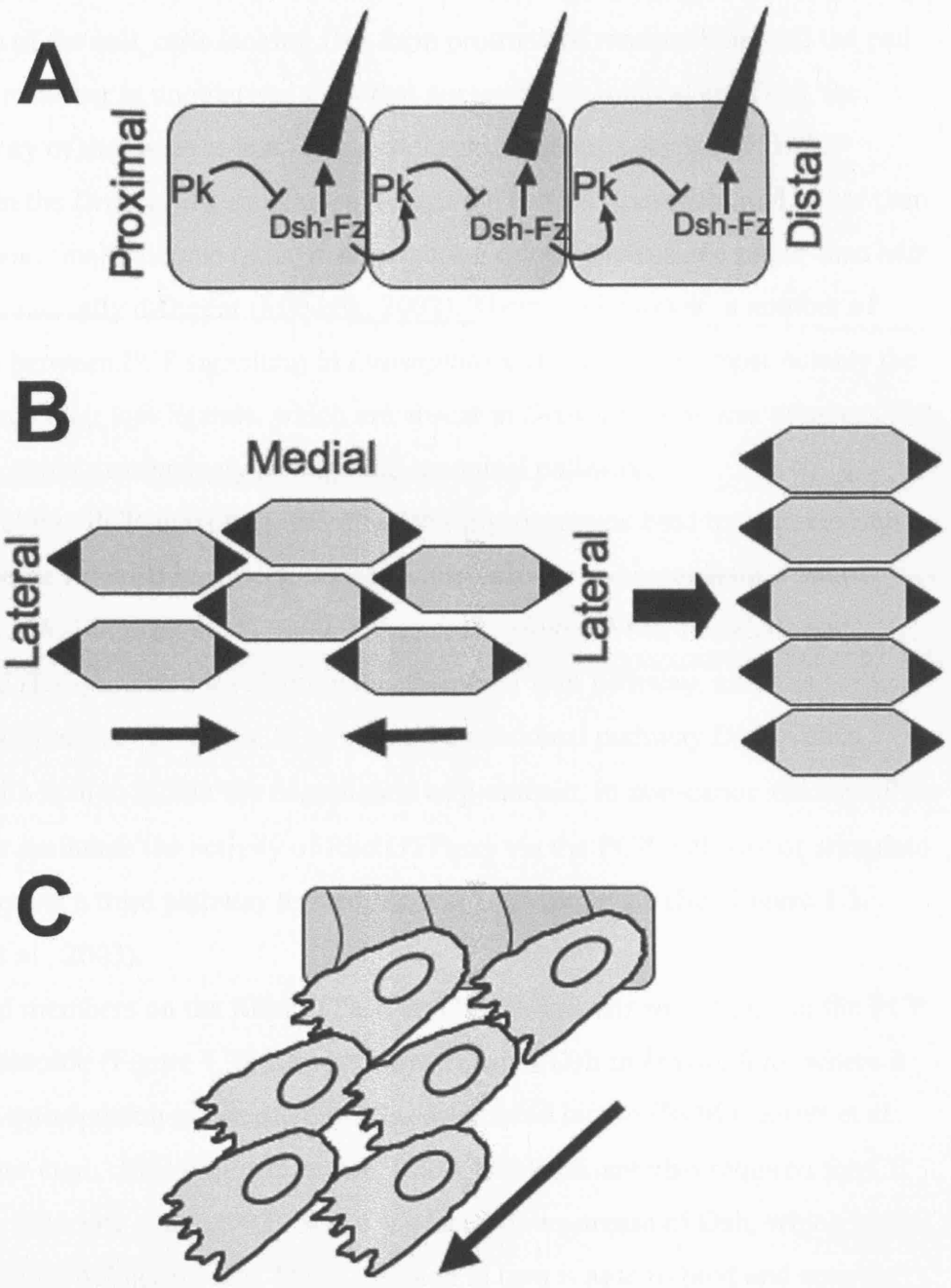


**Figure 1.2 PCP signalling controls diverse developmental processes**

**(A)** PCP signalling regulates epithelial cell polarity in the *Drosophila* wing resulting in hair growth at the Distal side of each cell, Pk, prickle; Dsh, Dishevelled; Fz, Frizzled. **(B)** Convergent extension of the mesoderm. Cells form protrusions at their lateral ends (in black) to allow intercalation and lengthening of the body axis. This process requires PCP signalling. **(C)** PCP signalling is essential for neural crest migration although the mechanism for this is unknown.

Whereas in control embryos lamellipodia in intercalating cells are restricted to the lateral ends of the cell, cells lacking Dsh form protrusions randomly around the cell membrane resulting in unpolarised cells that are unable to intercalate. Thus, the entire polarity of the tissue is lost. This system shares many parallels with PCP signalling in the *Drosophila* wing, even though the tissues (mesenchymal rather than epithelial) and final outcome (polarised formation of cell protrusions rather than hair growth) are radically different (Mlodzik, 2002). There are however, a number of differences between PCP signalling in *Drosophila* and vertebrates, most notably the use of extracellular wnt ligands, which are absent in *Drosophila*, where wingless, the wnt ligand, signals exclusively through the canonical pathway.

In vertebrate PCP signalling, secreted Wnt glycoproteins bind to cysteine rich transmembrane Frizzled receptors, which in turn activate the cytoplasmic factor Dishevelled (Wallingford et al., 2000; Wang et al., 1996). Wnts, Frizzleds and Dishevelled (Dsh) are also involved in the canonical Wnt pathway, and it is at this point that the pathway diverges. Whereas in the canonical pathway Dishevelled interacts with axin to inhibit the degradation of β-catenin, in non-canonical signalling it can either modulate the activity of Rho GTPases via the PCP pathway or stimulate calcium flux via a third pathway termed the wnt/Ca2+ pathway (See Figure 1.3, (Veeman et al., 2003).

Several members on the Rho GTPase family are downstream of Dsh in the PCP signalling cascade (Figure 1.3). Rho is downstream of Dsh in *Drosophila*, where it acts on the cytoskeleton via its effector Rho-associated kinase (ROK) (Strutt et al., 1997; Winter et al., 2001). In vertebrates, RhoA and ROK are also required for CE movements (Marlow et al., 2002). RhoA is placed downstream of Dsh, which binds to the formin homology protein, Daam1, which in turn is able to bind and activate RhoA (Habas et al., 2001). Two other Rho GTPases, Rac and Cdc42 have also been suggested to act as PCP effectors in vertebrates (Choi and Han, 2002; Habas et al., 2003; Penzo-Mendez et al., 2003). RhoA, Rac and Cdc42 are all regulators of the dynamic actin cytoskeleton and regulate many processes involved in cell motility including cell polarity and the formation of cell protrusions (Jaffe and Hall, 2005). It has been proposed that it is through the activities of these small GTPases that cells undergoing CE form protrusions at their lateral sides in a process dependent on PCP signalling. However the mechanism by which this happens is not understood.

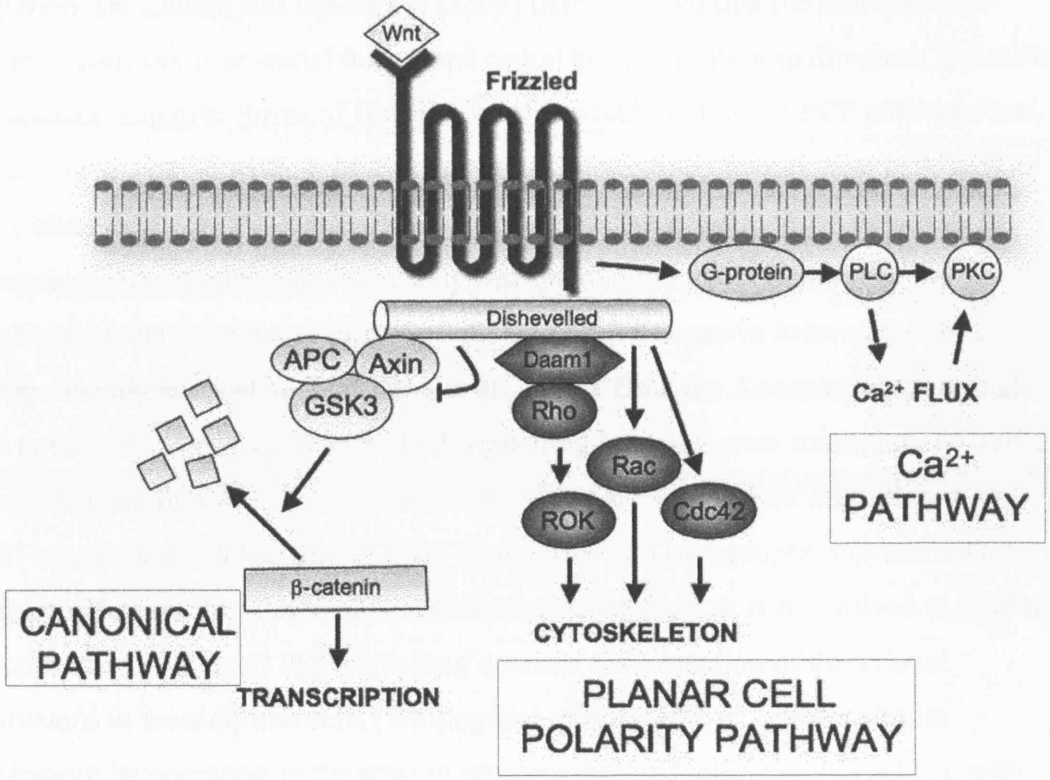


**Figure 1.3 The Wnt signalling pathway in vertebrates**

Three different branches of the Wnt pathway have been identified in vertebrates: i) the canonical/β-catenin pathway, which results in the stabilisation of β-catenin and transcriptional activation, ii) the planar cell polarity (PCP) pathway where small Rho GTPases act on the cytoskeleton to control cell polarity and iii) the Wnt/$Ca^{2+}$ pathway, which stimulates $Ca^{2+}$ flux. All three pathways are activated by the binding of Wnt ligands to Frizzled receptors.

### *1.4.3. PCP signalling in the neural crest*

With PCP signalling playing a key role in cell polarity and motility in many different systems, it comes as no surprise that it also plays a role in neural crest migration. De Calisto and colleagues (2005) demonstrated that the non-canonical wnt/PCP pathway is essential for correct neural crest migration in *Xenopus*. Injection of dominant negative forms of Dsh and Wnt11, which inhibit the PCP pathway, but not canonical wnt signalling, block the migration of cranial neural crest cells *in vivo* (De Calisto et al., 2005). Recently this role has also been extended to zebrafish where neural crest migration is severely disrupted in the PCP mutant *trilobite* (strabismus) and in embryos injected with a dominant negative form of Dsh or a morpholino against *wnt5a* (Matthews et al., 2008). Both the *Xenopus* and zebrafish data point to an important role for PCP signalling in neural crest migration, however the mechanism by which it works remains unknown. Neural crest migration is a multi-step process with an initial EMT stage, followed by a proper migration. Does PCP signalling control the initial delamination of the crest or is it involved in guiding the crest at a later stage? PCP signalling controls the formation of directional protrusions in mesodermal cells (Wallingford et al., 2000), so could a similar mechanism be operating in the crest to promote directed migration? Wnt11, a non-canonical ligand, is expressed laterally to the neural crest prior to migration in the direction in which the crest will eventually migrate (De Calisto et al., 2005). Is it possible that it is working like a chemoattractant, attracting neural crest cells in the right direction? These are some of the questions that I will attempt to address during the course of this thesis.

## 1.5. Syndecan-4: a new element of the PCP pathway

A recently identified component of the PCP pathway, which may shed some light on how PCP regulates cell migration, is Syndecan-4 (Syn4). Syn4 is a member of the heparan sulphate proteoglycan (HSPG) superfamily of transmembrane glycoproteins, which are expressed on the cell surface, where they interact with the extracellular matrix and extracellular soluble factors to modulate a wide range of cell behaviours. Munoz et al (2006) have recently cloned Syndecan-4 in *Xenopus* and find that it plays an essential role in regulating CE movement. Embryos injected with

a morpholino against *syn4* exhibit fail to elongate, as do Keller explants, a classic assay system for CE. Furthermore, Syn4 appears to be signalling via the PCP pathway, as the phenotype observed by inhibiting Syn4 could be rescued by activating the PCP pathway downstream (Munoz et al., 2006).

The involvement of Syn4 in PCP signalling during *Xenopus* gastrulation is a recent observation, but historically Syn4 has been characterised as a key regulator of cell migration. Syn4 knockout mice show defects in wound healing, a process that relies on the migration of fibroblasts, and fibroblasts lacking Syn4 also have impaired motility *in vitro* (Echtermeyer et al., 2001; Longley et al., 1999). Syn4 interacts with fibronectin and is a component of focal contacts, the clusters of proteins that form at the sites at which migratory cells attach to the extracellular matrix (Woods and Couchman, 1994). Regulated adhesion to the ECM is essential for cell migration and is mediated by co-ordinated signalling by members of the integrin and syndecan families (Morgan et al., 2007). On fibronectin, initial attachment is mediated by Integrin-$\alpha 5\beta 1$ binding to the central binding domain (CBD) of fibronectin. However cells fail to form mature focal adhesions or actin stress fibres unless stimulated by a second attachment to the heparin-binding domain of fibronectin (Bloom et al., 1999; Woods et al., 1986). This secondary interaction is mediated by Syndecan-4 (Woods et al., 2000). Cells lacking Syn4 are unable form actin stress fibres or mature focal adhesions in response to the heparin binding domain of fibronectin and show decreased motility (Echtermeyer et al., 1999; Ishiguro et al., 2000; Saoncella et al., 1999). Downstream of Syndecan-4 a number of different signalling pathways have been implicated. Syn4 is able to directly bind to and activate PKC$\alpha$ (Horowitz et al., 1999; Oh et al., 1997b) and to phosphorylate focal adhesion kinase (FAK) (Wilcox-Adelman et al., 2002a). There is also evidence that Syn4 can stimulate the activities of the small GTPases Rac and RhoA, although there is some contradictory evidence in this regard (Bass et al., 2007; Dovas et al., 2006; Saoncella et al., 1999; Tkachenko et al., 2004).

With an important role in controlling both cell migration, through the regulation of attachment to the ECM and in PCP signalling, Syn4 is a potentially interesting target molecule to be involved in neural crest migration. If Syn4 is involved in the migration of the neural crest, it could help shed light on how exactly PCP signalling is functioning to control NC migration.

## 1.6. Summary and aims

The neural crest is a transient embryonic population that transforms from a static epithelial population on top of the neural tube to vigorous migratory cells that travel through the entire embryo and give rise to many different types of cell. Many aspects of the neural crest are of interest: the complex network of signalling molecules involved in its induction, its sudden epithelial to mesenchymal transition and its remarkable pluripotency. However, one of the most intriguing questions about the neural crest is how neural crest cells are able find their way through the embryo. A number of molecules have been implicated including extracellular matrix and secreted repellents, but so far no positive cues to guide neural crest migration have been identified. There is scant evidence for chemoattraction in the neural crest, but in this case, how do neural crest cells establish their polarity? One clue could be in the PCP pathway, a regulator of neural crest migration that is also known to be involved in establishing cell and tissue polarity in other systems. Another could be syndecan-4, a key molecule involved in regulating cell migration, that has recently been implicated in PCP signalling.

The aim of this thesis is to establish whether Syn4 is involved in neural crest migration and, if so, to elucidate the molecular mechanism by which PCP signalling and Syn4 control neural crest migration. First, I present new findings about the role of PCP signalling in neural crest migration, which extends the previously published work by de Calisto et al (2005). Secondly, I demonstrate a vital role for Syn4 in neural crest migration. Then I present a detailed analysis of the effects of PCP signalling and Syn4 on migrating neural crest cells *in vitro* and *in vivo*, looking at cell behaviour, morphology, the actin cytoskeleton and focal adhesions. Then I identify a molecular mechanism for their abnormal cell behaviour, based on the regulation of small Rho GTPases by PCP signalling and Syn4. Finally, I investigate the role of cell-cell contact inhibition in establishing neural crest cell polarity through the activation of PCP signalling. Together these findings allow me to propose a novel mechanism for the control of directional migration of the neural crest *in vivo*.

# 2. MATERIALS & METHODS

## 2.1. Solutions and Media

Alkaline phosphatase (AP) Buffer

100 mM Tris-HCl pH9.5
100 mM NaCl
50 mM $MgCl_2$
0.1% Tween-20

Bleaching Solution

33% $H_2O_2$
5% Formamide
0.5 x SSC

Danilchick's medium

53 mM NaCl
5 mM $Na_2CO_3$
4.5 mM KGluconate
32 mM NaGluconate
1 mM $MgSO_4$
1 mM $CaCl_2$
0.1 % BSA
pH 8.3 (adjusted with 1M Bicine)
50 µg/ml Streptomycin

Egg-laying medium (Ca2+ free)

110 mM NaCl
2 mM KCl
0.6 mM $Na_2HPO_4$
15 mM Tris base
2 mM $NaHCO_3$
0.5 mM $MgSO_4$
pH 7.6 (adjust with acetic acid)

Ficoll

3% Polysucrose
in NAM3/8

Fish water

60 mg "Instant Ocean"
per litre $dH_2O$

Hybridisation Buffer

50% Formamide
5 x SSC
1 x Denhardt's Solution
1 mg/ml Ribonucleic acid
100 µg/ml heparin
0.1% CHAPS
10 mM EDTA
0.1% Tween-20
pH 5.5

Maleic acid buffer (MAB)

100 mM Maleic acid
150 mM NaCl
0.1% Tween-20

MEMFA

4% Formaldehyde
0.1 M MOPS
1 mM $MgSO_4$
2 mM EGTA

Modified Barth's Solution ($Ca^{2+}Mg^{2+}$-free)

88 mM NaCl
1 mM KCl
2.4 mM $NaHCO_3$
15 mM HEPES pH7.6
1 mg/ml BSA

Normal amphibian medium (NAM) 1/10

11 mM NaCl
0.2 mM KCl
0.1 mM $Ca(NO_3)_2$
0.1 mM $MgSO_4$
0.01 mM Disodium EDTA
0.2 mM $Na_2HPO_4$ pH7.5
0.1 mM $NaHCO_3$
50 μg/ml Streptomycin

Normal amphibian medium (NAM) 3/8

41 mM NaCl
0.75 mM KCl
0.36 mM $Ca(NO_3)_2$
0.36 mM $MgSO_4$
0.036 mM Disodium EDTA
0.75 mM $Na_2HPO_4$ pH7.5
0.1 mM $NaHCO_3$
50 μg/ml Streptomycin

PBS (Phosphate buffered saline)

137 mM NaCl
2.7 mM KCl
4.3 mM $Na_2HPO_4$
1.4 mM $KH_2PO_4$
pH 7.3

PBT

137 mM NaCl
2.7 mM KCl
4.3 mM $Na_2HPO_4$
1.4 mM $KH_2PO_4$
pH 7.3
0.1% Tween-20

SSC (20x)
3M NaCl
0.3M Tri-sodium citrate
pH7.0

### 2.2. Obtaining *Xenopus* Embryos

Mature *Xenopus laevis* females were pre-primed by subcutaneous injection of 100 units of Serum Gonadotrophin (Intervet) 4 to 7 days before use. To stimulate ovulation, females were injected with 500 units of choronic gonadotrophin (Intervet) 12-15 hours prior to requirement. Frogs were then placed in Egg-laying medium ($Ca^{2+}$ free), from which naturally laid, mature oocytes could be collected. Adult male *Xenopus* were terminally anaesthetised in a solution of 0.5% Tricaine (3-amino benzoic acid ethylester) and the testes were dissected and stored in Leibovitz L-15 medium (Invitrogen). For *in vitro* fertilisation, a small piece of testis was macerated in $dH_2O$ and the resulting sperm suspension was mixed with the oocytes in a dry Petri dish. After cortical rotation, the dish was flooded with $dH_2O$. At the 2-8 cell stage, the jelly was removed from embryos by vigorous agitation in a solution of 2% L-cysteine (pH8.2) and embryos were raised in normal amphibian media (NAM)1/10. Embryos were staged according to Nieuwkoop and Faber (Nieuwkoop and Faber, 1967).

### 2.3. Obtaining zebrafish Embryos

Zebrafish (*Danio rerio*) strains were maintained and bred according to standard procedures (Westerfield, 2000). Embryos were obtained from natural spawning of an AB wild-type colony. Transgenic *sox10:egfp* embryos were obtained from crosses of identified heterozygous *sox10(-7.2):egfp* carriers (Carney et al., 2006). Embryos were raised in fish water at 28.5 °C and were staged according to (Kimmel et al., 1995).

### 2.4. Synthesis of antisense RNA probes for *in situ* hybridisation

Competent DH5α cells were transformed with plasmid (pCS2+) DNA by heat shock at 37°C for 5 minutes. Cells were then returned to ice for 5 minutes before plating on LB-ampicillin plates. After 24 hours incubation at 37°C, individual colonies were picked and grown up in LB-ampicillin medium for 14-16 hours at 37°C with agitation. Plasmid DNA was purified using a spin midi-prep kit (QIAGEN). 10 μg of plasmid DNA was cut at a 5' restriction site with an appropriate restriction endonuclease (Promega) according to the manufacturer's instructions. The cut DNA was purified by chloroform extraction, ethanol precipitated and re-suspended in molecular biology $H_2O$ (Ambion) to a concentration of 1 μg/μl. *In vitro* transcription of antisense RNA was carried out using T3, T7 or SP6 RNA polymerase (Promega) using conditions suggested by the manufacturer. The NTP mix used for the reaction contained 0.35 mM digoxigenin-labelled UTP, resulting in the production of a digoxigenin-labelled RNA. After transcription 1 μl DNAase (Promega RQ1 DNase) was added to degrade the template DNA and the quality of RNA was checked by gel electrophoresis. RNA was purified using the Chroma-spin-100 kit (Clontech), re-suspended in molecular biology $H_2O$ and diluted in hybridisation buffer to concentrations of 0.5, 1 or 2 ng/μl for use for *in situ* hybridisation. RNA probes for the following genes were used in this thesis: *snail2* (Mayor et al., 1995), *fli* (Meyer et al., 1995), *frizzled7* (Wheeler and Hoppler, 1999), *dishevelled* (Sokol et al., 1995), *daam1*(Nakaya et al., 2004), *wnt11* (Ku and Melton, 1993), *wnt5a* (Moon et al., 1993), *wnt11r* (Garriock et al., 2005) and *syn4* (Munoz et al., 2006).

### 2.5. Whole Mount *in situ* hybridisation

*In situ* hybridisation protocol was adapted from (Harland, 1991). Due to the high risk of RNAase contamination, which can degrade the RNA probe, all solutions (up to

and including post hybridisation washes) were made using diethyl pyrocarbonate (DEPC) treated water. Embryos were fixed in MEMFA for 1hr at room temperature and transferred to 100% methanol for indefinite storage at -20°C. Embryos were re-hydrated with successive washes of: 75% methanol, 50% methanol, 25% methanol and PBT. Embryos were then bleached in bleaching solution under light for 30 minutes, washed thoroughly in PBT and re-fixed for 30 minutes in 4% paraformaldehyde (PFA) in PBS. After further washing in PBT, embryos were transferred to hybridisation buffer and incubated for 3-6 hours at 62°C. The digoxigenin labelled probe was then added and incubated with embryos overnight at 62°C. The following post-hybridisation washes were performed for 10 minutes each at 62°C: 50% formamide/2 x SSC/0.1% Tween-20, 25 formamide/2x SSC/0.1% Tween-20, 12% formamide/2x SSC/0.1% Tween-20, 2x SSC/0.1% Tween-20 followed by one final 30 minute wash with 0.2% SSC/0.1% Tween-20. Embryos were then rinsed with PBT and maleic acid buffer (MAB) and then blocked in 2% BMBR (Boehringer Mannheim blocking reagent; Roche) in MAB for 2 hours at room temperature. Embryos were incubated overnight at 4°C with an anti-digoxigenin-alkaline phosphatase (AP) conjugated antibody (Roche) diluted in 2%BMBR/MAB. Excess antibody was removed by six 30 minute washes with MAB at room temperature with gentle agitation. Embryos were then transferred to AP buffer where the AP colour reaction was developed using 75µg/ml BCIP (5-bromo-4-chloro-3-indoyl-phosphate; Roche) and 150µg/ml NBT (4-nitro blue tetrazolium chloride; Roche) at 37°C. Embryos were then washed with 100% Methanol to remove any background staining and transferred to 4% PFA for storage.

### 2.6. Double *in situ* hybridisation

When it was necessary to visualise the expression of two genes in one embryo, double *in situ* hybridisation was carried out. Double *in situ* hybridisation uses the protocol described above, with a few minor alterations; a mixture of two RNA probes were added, one labelled with digoxigenin as described and one labelled with UTP-fluorescein. After finishing the *in situ* hybridisation, embryos were transferred back to 2% BMBR/MAB and incubated overnight at 4°C with an anti-fluorescein-AP antibody (Roche). Embryos were then washed in MAB and transferred to AP buffer. For the AP colour reaction, BCIP only was added, giving a pale blue colour, which is distinguishable from the dark blue of the first *in situ* hybridisation.

Alternatively, in some cases a BCIP/INT (Roche) reactive was used, with INT acting as an oxidant to yield a red/brown colour.

### 2.7. Synthesis of mRNA/morpholinos for microinjection

Plasmid DNA was linearised with the appropriate restriction endonuclease (Promega), purified by chloroform extraction, ethanol precipitated and re-suspended in molecular biology $H_2O$ to a concentration of 1μg/μl. Synthetic capped mRNA was synthesised using the SP6 mMessage mMachine kit (Ambion) following the manufacturer's instructions. mRNA was purified using the chroma-spin100 kit (Clontech) and re-suspended in molecular biology $H_2O$. The following synthetic mRNAs were used during the course of this thesis: *syn4* (Munoz et al., 2006), *dshΔN* and *dshdep*$^+$ (Tada and Smith, 2000), *dsh-gfp* (Rothbacher et al., 2000), *dsh-yfp* (Witzel et al., 2006) *syn4-gfp* (Kindly donated by J. Larrain), *histone-2B-egfp, histone-2B-cherry, membrane-egfp* and *membrane-cherry* (gifts from S. Megason), *syn4ΔPIP2* and *syn4ΔPDZ* (constructed by S. Kuriyama).

Morpholinos used during this thesis were against *wnt11r* (Garriock et al., 2005), *Xenopus syn4* (Munoz at al, 2006) and zebrafish *syn4*. The *wnt11r* Mo was against the 5'UTR: 5'AATCATCTTCAAACCCAATAACAA3' (Garriock et al., 2005). The morpholino against *Xenopus laevis syn4* consisted of a 1:1 mixture of two translation-blocking Mos against the two *syn4* alleles: *syn4.1* Mo: 5′GCACAAACAGCAGGGTCGGACTCAT3′ and *syn4.2* Mo: 5′CTAAAAGCAGCAGGAGGCGATTCAT3′ (Munoz et al, 2006). The Mo against zebrafish Syndecan-4 was designed over the 5'UTR: 5'CGGACAACTTTATTCACTCGGGCTA3'. A standard control morpholino was used: 5'CCTCTTACCTCAGTTACAATTTATA3'. Injection of this control Mo in wild-type zebrafish or *Xenopus* embryos causes no defective phenotype.

### 2.8. Microinjection in *Xenopus* and zebrafish

Micro-injections were carried out using a Narishige IM300 Microinjector under a Leica MZ6 or a Nikkon SMZ645 dissecting microscope. The needles for injection were constructed from glass capillaries with an internal diameter of 0.5mm (Intrafil) using a Narishige PC-10 needle puller. The needle was filled with mRNA or morpholino solution and calibrated using an eye piece graticule to inject 10nl in *Xenopus* or 4nl in zebrafish. *Xenopus* injections were carried out in a dish of Ficoll.

*Xenopus* embryos were injected at the 2, 8 or 32-cell stage and cultured in Ficoll until the onset of gastrulation, at which point they were transferred to NAM1/10. For injections specifically targeted to the neural crest, embryos were injected in the animal ventral blastomere at the 8-cell stage or into blastomeres A2 or B2 at the 32-cell stage. Zebrafish embryos were injected dry at the 1 or 2-cell stage, with the injection targeted through the yolk and into the cell. Zebrafish embryos were then allowed to develop in fish water at 28.5°C.

### 2.9. *Xenopus* micromanipulation: Animal cap and DLMZ dissection

All *Xenopus* embryo dissections were carried in NAM 3/8 under a dissecting microscope (Leica). The Vitelline membrane was physically removed using No. 5 Watchmakers forceps before dissection. Animal caps were taken from stage 9 embryos and were left to heal in NAM 3/8. They were then cultured until the equivalent of stage 17 before fixation. Dorsal lateral marginal zones (DLMZ) were removed from stage 10.5 embryos, conjugated with animal caps and cultured in NAM3/8 until the equivalent stage 17.

### 2.10. *Xenopus* micromanipulation: Neural crest graft experiment

Neural crest grafts were carried out according to (Borchers et al., 2000). Neural crests from embryos injected with fluorescein-dextran (FDX) were dissected at stage 17 and transferred to wildtype host embryos, which had had their neural crest removed. A fragment of glass coverslip was used to hold the grafted tissue in place until healing was complete. Embryos were then cultured in NAM 3/8 until stage 26, and neural crest migration was followed using fluorescent microscopy (Leica MZFLIII).

### 2.11. Photography of *Xenopus* & zebrafish embryos

Embryos were immobilised in an agarose coated dish and photographed with a Leica DFL420 camera attached to a Leica MZFLIII dissecting microscope using the IM50 software (Leica).

### 2.12. *In vitro* culture of *Xenopus* NC cells

Glass coverslips for neural crest culture were prepared in advance by successive washes in 70% Ethanol, $dH_2O$, and 100% Ethanol and were sterilized under flame.

They were then incubated overnight at 4°C with a solution of 50 μg/ml fibronectin (Sigma) in PBS. Coverslips were then washed with PBS and blocked with 1% bovine serum albumin (BSA)/PBS for 2 hours at room temperature before being transferred to Danilchick's solution. Neural crests were dissected from embryos at stage 17-20 using the technique described in Alfandari et al (Alfandari et al., 2003). Dissection was carried out in NAM 3/8 and once removed, neural crests were transferred to an agarose coated dish containing Danilchick's solution. The neural crests were then transferred to the fibronectin coated coverslips and kept stationary at room temperature until the cells attached to the fibronectin. Cultures were then kept at 18°C. For neural crest culture of dissociated cells, neural crests were initially placed on a coverslip containing a 500 μl drop of Modified Barth's Solution ($Ca^{2+}Mg^{2+}$-free). After the cells had dissociated, the coverslip was flooded with Danilchick's solution and the cells were allowed to attach to the coverslip before transfer to 18°C. For dissociation/re-association experiments, dissociated cells were manually formed into small aggregates using an eyebrow knife before the addition of Danilchick's solution.

### 2.13. Time-lapse analysis of NC cells *in vitro*

Coverslips containing cultured NC cells were mounted on a microscope slide by inverting over a wax chamber filled with Danilchick's medium. Cells were imaged using a Leica DM5500 compound microscope attached to a DFC300 Camera (Leica) using either a 20x (low magnification) or a 40x (high magnification) oil objective. For time-lapse recording images were collected every 1-minute for a period of 1 to 3 hours. Time-lapse movies were collected and edited using the Leica application suite software (v1.7.0). For analysis of cell migration, 1-hour long low magnification movies were analysed using the public domain program ImageJ (developed at the US National Institute of Health, NIH). Individual cells were tracked using the 'Manual tracking' plug-in, with the centre of the cell being taken as its position in each time frame. From this, the velocity (total distance travelled divided by time) and persistence (defined as the ratio between the linear distance between the initial and the final point and the total length of the migratory path) of cells under different conditions could be calculated. For analysis of cell protrusions, high magnification movies were used over a time period of 20 minutes.

## 2.14. Immunostaining of focal contacts *in vitro*

Neural crest cells that had been migrating *in vitro* for several hours were fixed with 4% PFA/4% sucrose in PBS for 30 minutes at room temperature. Cells were then washed thoroughly with PBS and permeabilised by incubation in 0.2% triton-X 100/PBS for 5 minutes at 4°C. After further washing with PBS, cells were blocked with 1% BSA/PBS for 20 minutes, followed by addition of the primary antibody. To visualise focal contacts an antibody against phospho-paxillin (Y118) (Biosource #44-722G) was used at a dilution of 1:200 in 1% BSA/PBS for 30 minutes at 37°C. Cells were thoroughly washed with PBS and incubated with the secondary antibody for 30 minutes at 37°C. The secondary antibody used was anti-rabbit IgG-FITC (Sigma) along with rhodamine-phalloidin (Invitrogen), which stains actin filaments. Both were diluted 1:500 in 1% BSA/PBS. After further washing in PBS, coverslips were mounted in glycerol/PBS mounting medium. Samples were imaged using a Leica SP1-DMRE confocal microscope with a 40 x plan apochromat NA 1.25 Ph3 oil objective. Scanning was performed on a line-by-line basis using a digital zoom of 2. Z-stack images were collected using Leica optimal settings, which results in a z step size of half the z-resolution (167 nm for 40 x objective). Images shown in figures show an average projection for 4 z sections. Focal contact number and size was calculated using ImageJ (NIH), by recording the number and area of particles with fluorescence intensity above an empirically determined threshold. The same threshold was used for all conditions within each experiment.

## 2.15. Time-lapse analysis of zebrafish NC *in vivo*

*Sox10:egfp* (Carney et al., 2006) transgenic zebrafish embryos were used to analyze NC migration *in vivo*. Each embryo was staged according to the number of somites and only embryos with equal numbers were compared. The embryos were dechorionated, inserted into a drop of 0.2 % agarose in fish water (Westerfield, 1995) and mounted in a custom-built chamber, consisting of a glass ring mounted on a microscope slide and sealed with wax. Control and experimental embryos were mounted side to side in the same chamber. A compound (Leica DM5500) or a confocal (Leica SP2-DMRE) microscope was used for time lapse imaging. Digital images were typically collected at 30 to 90 second intervals for a period between 1 and 14 h. A Z-stack was performed in preliminary experiments to establish how deep the NC migrates in the embryo. After 6 to 8 h time lapse of 20 somite embryos I

found that cephalic NC migrate between 500-800 μm in the anterior-posterior axis, between 40-60 μm in the dorso-ventral axis and between 7 and 9 μm in the peripheral-central axis. Therefore, for tracking analysis I assume that most of the cell migration occurs in two dimensions, while the third dimension (in the Z axis when the embryo has a lateral orientation) can be neglected. Sequences of images were quantitatively analyzed using ImageJ (NIH) and Matlab (MathWorks) software. Tracking of individual cells was used to calculate velocity, persistence and angle of migration (with respect to its previous position). For cell protrusion analysis only cells with a clear border were used and the threshold in ImageJ was set in order to visualize only the strongest fluorescence. Cell protrusions were defined as the new positive area between two consecutives frames. Statistical analyses and graphical illustration were performed on Matlab using both built-in functions and customized scripts (Scripts by Carlos Carmona-Fontaine).

### 2.16. Whole mount immunostaining in zebrafish

Zebrafish embryos were fixed at 12 somites in 4% PFA/PBS overnight at 4°C. Embryos were then washed in PBS and blocked in a blocking solution of 2% calf serum/1% BSA/PBT for 2 hours at room temperature. The primary antibody was added and incubated overnight at 4°C. Embryos were then subjected to three thirty minutes washes with PBT before incubation with the secondary antibody for 2 hours at room temperature. After three further half hour washes with PBT at room temperature, embryos were mounted and imaged. For visualisation of focal contacts *in vivo*, the primary antibody used was anti-phospho-paxillin (Y118) (Biosource #44-722G) at a dilution of 1:200 in blocking solution and the secondary antibody was anti-rabbit IgG-FITC, diluted 1:500 in blocking solution. For imaging, the embryonic yolk was removed using a tungsten needle and embryos were flat-mounted under a coverslip in glycerol/PBS. Embryos were imaged using a confocal microscope (Leica SP1-DMRE) with a 40 x plan apochromat NA 1.25 Ph3 oil objective and a digital zoom of 2.5. Focal contact number and size was calculated as with the *in vitro* method, although due to high levels of background, particles less than 0.01$\mu m^2$ in area were discounted.

## 2.17. Cryostat Sections

Embryos for sectioning were fixed in MEMFA for 3-4 hours at room temperature and washed for one hour in 5% sucrose/PBS followed by a further hour in 10% sucrose/PBS at room temperature. They were then transferred to 5% sucrose/ 7.5% gelatine in PBS and incubated for 1-3 hours at 37°C. Embryos were then placed in 15% Gelatine for 1-3 hours at 37°C, before cooling to room temperature. Once solidified, the gelatine block around each embryo was trimmed and they were mounted in OCT medium (Tissue-Tek) and frozen at -80°C. Sections were cut using a Jung CM3000 cryostat to a thickness of either 12μm or 14μm, and mounted on poly-lysine coated slides (VWR). Slides were dried, washed in PBS and mounted using Glycerol/PBS mounting medium. For immunostaining of cryostat sections, samples were permeablised with 0.2% Triton-X/PBS and blocked for 2 hours at room temperature in 4% BSA/PBS. Slides were then incubated overnight at 4°C with the primary antibody, washed in PBS, incubated with the secondary antibody for 2 hours at room temperature, thoroughly washed in PBS and mounted. The primary antibodies used for this technique were anti-p-paxillin(Y118) (Biosource) and the monoclonal antibody 6D9 against *Xenopus* Fibronectin (Hybridoma bank, University of Iowa). Secondary antibodies used were anti-rabbit IgG-FITC (Sigma) and anti-mouse-IgG-Cy5 (Santa Cruz Biotech).

## 2.18. FRET analysis

Plasmid DNA encoding FRET probes; Raichu-Rac, Raichu-Cdc42 (Itoh et al., 2002) and RhoA biosensor (Pertz et al., 2006) were injected directly into *Xenopus* embryos at the 8-cell stage. I was able to achieve suitable levels of expression by directly injecting DNA, as the pRaichu vector (based on pCAGGS) contains the CMV promoter, which is ubiquitously expressed in *Xenopus*. For optimal expression levels 75 pg of RhoA FRET probe or 150 pg of Raichu-Rac or Raichu-Cdc42 was injected. Fluorescence could be detected from stage 14 onwards. Neural crests expressing the FRET probes were dissected at st17 and cultured on fibronectin-coated coverslips for 5-7 hours as previously described. Cells were filmed by time-lapse photography for 10 minutes prior to fixation in order to determine the direction of migration. Cells were then fixed for 30 minutes in 4% PFA/4%sucrose/PBS at room temperature and then mounted in glycerol/PBS for observation.

Analysis of FRET data was carried out by Maddy Parsons as follows: Samples were imaged using a Zeiss lSM 510 META laser scanning confocal microscope and a 63 x Plan Apochromat NA 1.4 Ph3 oil objective. The CFP and YFP channels were excited using the 405 nm blue diode laser and the 514 nm argon line respectively. The two emission channels were split using a 545 nm diachroic mirror, which was followed by a 475-525 nm band pass filter for CFP and a 530 nm long pass filter for YFP. Pinholes were opened to give a depth of focus of 3 mm for each channel. Scanning was performed on a line-by-line basis with zoom level set to two. The gain for each channel was set to approximately 75 % of dynamic range (12-bit, 4096 grey levels) and offsets set such that backgrounds were zero. Time-lapse mode was used to collect one pre-bleach image for each channel followed by bleaching with 50 scans of the 514 nm argon laser line at maximum power (to bleach YFP). A second post-bleach image was then collected for each channel. Pre- and post-bleach CFP and YFP images were then imported into Mathematica 5.2 for processing. Briefly, images were smoothed using a 3 x 3 box mean filter, background subtracted and post-bleach images fade compensated. A FRET efficiency ratio map over the whole cell was calculated using the following formula: $(CFP_{postbleach}-CFP_{prebleach})/CFP_{postbleach}$. Ratio values were then extracted from pixels falling inside the bleach region as well as an equally sized region outside of the bleach region and the mean ratio determined for each region and plotted on a histogram. The non-bleach ratio was then subtracted from the bleach region ratio to give a final value for the FRET efficiency ratio. Data from images were used only if YFP bleaching efficiency was greater than 70 %.

### 2.19. Statistical analysis

Graphs shown in this thesis were constructed using Microsoft Excel. All error bars on graphs represent standard deviation. P values, where shown, were calculated using the two-sample equal variance Student's t-Test.

# 3. Results: The role of PCP Signalling in neural crest migration

## 3.1. Introduction

Wnt signalling plays a role in countless developmental processes and is important throughout the lifetime of neural crest cells. De Calisto et al (2005) elucidated the roles of different branches of the wnt pathway on neural crest development by injection of constructs of Dsh into *Xenopus* embryos. Injection of dd1, a dominant negative form of Dsh that inhibits the canonical pathway, disrupts the expression of early neural crest marker genes, a finding consistent with the much described role of Wnt/β-catenin in neural crest specification (Garcia-Castro et al., 2002; Wu et al., 2003). On the other hand, injection of a form of Dsh that specifically blocks the PCP pathway without affecting the canonical pathway (Tada and Smith, 2000) does not result in neural crest induction defects, but the migration of cranial neural crest cells is impaired (De Calisto et al., 2005). Additional inhibition of the PCP pathway using a dominant negative form of Wnt11 has the same effect. This indicates a vital role for the PCP pathway in controlling neural crest migration in *Xenopus*, a role that has since been extended to zebrafish (Matthews et al., 2008). However, although PCP signalling is indisputably important for neural crest migration, there are many questions that remain unanswered. Firstly, several extracellular wnt/PCP ligands have been identified but it is not certain which ligand is signalling in the neural crest. Wnt11 is likely to be playing a role, but it is not clear if signalling from other wnt ligands is also required, and if so, where these signals might be coming from. Secondly, the localisation of Dsh in neural crest cells has not been investigated. It has been much reported that a membrane localisation of Dsh is a prerequisite to PCP signalling, but is this also the case in the neural crest? Thirdly, it is not obvious how exactly PCP signalling controls migration on a cellular level. Does it prevent the initial delamination of the crest or is it involved in pathfinding at later stages? Finally what are the down-stream effectors of PCP signalling in the neural crest and how are they able to regulate cell migration? These latter two questions require detailed analysis and will be addressed in later chapters of this thesis, but in this chapter I will investigate the first two points; the role of wnt/PCP ligands in the neural crest and the sub-cellular distribution of Dsh.

### *3.1.1. Non-canonical wnt ligands*

So far, 24 different wnt genes have been identified in *Xenopus*, falling into 12 different classes, with Wnts from different classes tending to activate either the canonical or non-canonical pathways (Garriock et al., 2007; Kikuchi et al., 2007). Two of these ligands, Wnt11 and Wnt5a, are known to signal through the PCP pathway. Wnt11 was first isolated due to its role in gastrulation where it is expressed in the marginal zone and is essential for convergent extension movements in fish and frogs (Heisenberg et al., 2000; Tada and Smith, 2000). Wnt5a also regulates morphogenetic movements during gastrulation, through the PCP pathway (Moon et al., 1993; Wallingford et al., 2001).

De Calisto et al (2005) show that overexpression of Wnt11 or inhibition using a dominant negative form inhibits cranial neural crest migration in *Xenopus*, suggesting that Wnt11 could be the extracellular PCP signal required for neural crest migration. However, a novel non-canonical wnt gene in *Xenopus* has been recently identified and named Wnt11-Related (Wnt11R). Sequence alignment reveals greater identity between the *Xenopus* Wnt11R protein and the Wnt11 of mouse and chicken than with *Xenopus* Wnt11, which has prompted its description as the true Wnt11 homologue in *Xenopus* (Garriock et al., 2005). Additionally, like mammalian *wnt11*s, but unlike *Xenopus* and zebrafish *wnt11*, *wnt11r* is expressed in the developing heart (Christiansen et al., 1995; Garriock et al., 2005; Ku and Melton, 1993; Makita et al., 1998). Inhibition of *wnt11r* by morpholino disrupts heart morphogenesis by affecting the contact between cardiac cells (Garriock et al., 2005). Wnt11r has also been implicated in neural crest migration. It is expressed in the sub-population of neural crest cells that migrate into the dorsal fin in *Xenopus* and is required for proper fin development (Garriock and Krieg, 2007). The role of Wnt11r has only been studied at these late developmental stages and it is possible that it also plays a role in the early migration of the cranial neural crest. Here I investigate whether Wnt11R plays a role in controlling cranial neural crest migration.

### *3.1.2. Dishevelled is an important modulator of wnt signalling*

Dishevelled (Dsh) is a key player in wnt signalling, acting at the crossroads between the canonical and non-canonical pathways. Dsh is a vital component for wnt/β-catenin, wnt/calcium and wnt/PCP signalling and its ability to have such wide ranging effects has been the subject of much discussion (Wallingford and Habas,

2005). Domain deletion studies make it clear that different domains of the Dsh protein are required for the activation of different pathways. Dsh has three major conserved domains (Figure 3.1); an N-terminal DIX (Dishevelled/Axin) domain, a central PDZ (PSD-95, DLG, ZO1) domain and a C-terminal DEP (Dishevelled, EGL-10, Pleckstrin) domain (Capelluto et al., 2002; Wong et al., 2003; Wong et al., 2000). The DIX domain is required exclusively for canonical signalling, where it regulates the interaction with axin, whereas the DEP domain is essential for *Drosophila* PCP and vertebrate convergent extension (Axelrod et al., 1998; Heisenberg et al., 2000; Julius et al., 2000; Rothbacher et al., 2000; Tada and Smith, 2000). The PDZ domain, meanwhile, is required for both pathways and facilitates the binding of Dsh to other proteins including the intracellular domain of the frizzled receptors (Wong et al., 2003). The PDZ domain also interacts with downstream elements of the PCP pathway, notably the formin homology protein Daam1, which in turn has been shown to bind and activate RhoA (Habas et al., 2001).

In addition to the domain structure of Dsh, the sub-cellular localisation also appears to play a role in determining whether the canonical or non-canonical pathway is activated. In *Drosophila*, canonical signalling is associated with cytoplasmic Dsh, while PCP signalling requires a membrane localisation (Axelrod et al., 1998) and there is evidence that this is also the case in vertebrates. Dsh can be observed in large discrete puncta in the cytoplasm in Chinese Hamster Ovary (CHO) cells and in *Xenopus* animal caps when canonical signalling is active (Capelluto et al., 2002; Choi and Han, 2005). In contrast, mesodermal cells undergoing CE show a localisation of Dsh at the plasma membrane (Wallingford et al., 2000). This translocation of Dsh to the membrane is thought to be essential for successful PCP signalling and it will be interesting to note whether this also occurs in migrating neural crest cells. The localisation of Dsh and the roles of different wnt ligands will both be addressed in this chapter, but first I will demonstrate the important role of Wnt/PCP signalling in controlling neural crest migration.

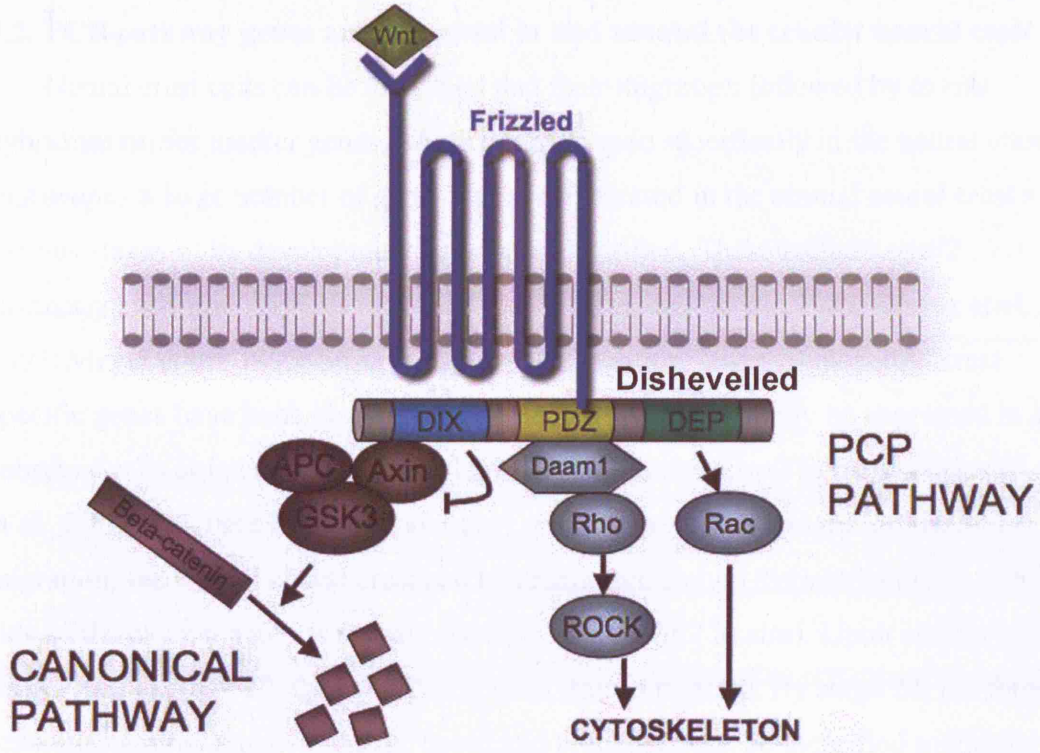


**Figure 3.1. The central role of Dishevelled in wnt signalling**

Dishevelled binds to the Wnt receptor, Frizzled, and is able to activate the canonical/β-catenin pathway (shown in purple) via its DIX domain and the PCP pathway (grey) via its DEP domain. The PDZ domain mediates protein-protein interactions including those with Frizzled7 and Daam1.

### 3.2. PCP pathway genes are expressed in and around the cranial neural crest

Neural crest cells can be identified and their migration followed by *in situ* hybridisation for marker genes, which are expressed specifically in the neural crest. In *Xenopus* a large number of genes that are expressed in the cranial neural crest at various stages of its development have been identified. These include *snail2* (formerly known as *slug*), *foxd3*, *twist* and *fli* (Hopwood et al., 1989; Mayor et al., 1995; Meyer et al., 1995; Sasai et al., 2001). However, fewer trunk neural crest specific genes have been identified and those that have tend only be expressed in a subset of cells at later stages of development, for example *trp2* in melanocytes (Aoki et al., 2003). So, here I will consider only cranial neural crest migration. Before migration, the cranial neural crest can be recognised as two distinct bands on either side of the closing anterior neural tube (Fig 3.2A, *snail2 in situ*). Upon closure of the neural tube at stage 20, the neural crest cells start to migrate. By stage 24, the three separate streams, the mandibular, hyoid and branchial, can be identified migrating through the head (Fig 3.2B arrowheads, labelled by *snail2 in situ*). Later, the crest cells colonise the face region in the area that will become the branchial arches. At this stage, *snail2* is no longer strongly expressed in the crest but cranial neural crest cells can be identified by the expression of other markers such as *fli* (Fig 3.2C).

Intracellular components of the wnt/PCP pathway are also expressed in the cranial neural crest during its development. *In situ* hybridization of *frizzled7*, a wnt receptor implicated in both the canonical and PCP branches of the wnt pathway (Medina et al., 2000; Wheeler and Hoppler, 1999), reveals that it is expressed in a remarkably similar pattern to *snail2* and *fli*. During neural crest induction *frizzled7* is expressed on either side on the neural tube in the neural crest (Fig 3.2D, compare to A). There is also some expression in the neural tube with a particular concentration at the mid-hind brain boundary. At stage 24, it can be seen in the migrating cranial neural crest in streams in the head (Fig 3.2E arrowheads) and at stage 28 it is clearly visible in the branchial arches (Fig 3.2F asterisk). The expression patterns of two intracellular components of the PCP pathway, *dsh* and *daam1* were also analysed. Both show expression in the anterior neural folds in both the neural tube and the crest at stage 17 (Fig 3.2G, J) although the staining is weaker than *snail2* or *fzd7*, which may indicate lower levels of expression. The expression also appears in the deeper rather than superficial layer.

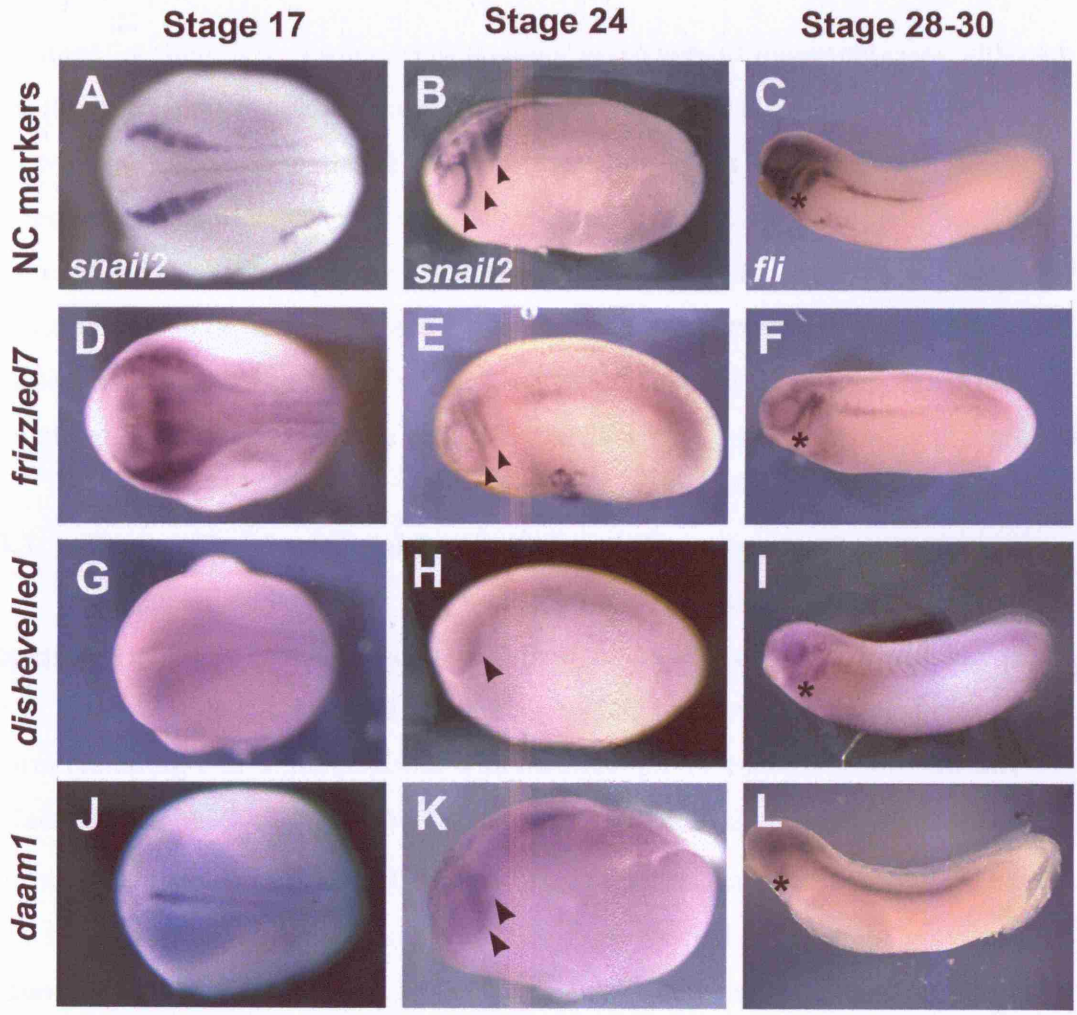


**Figure 3.2. PCP components are expressed in and around the neural crest**

*In situ* hybridisation was carried out for neural crest marker genes *snail2* (A-B), *fli* (C), *frizzled7* (D-F), *dishevelled* (G-I) and *daam1* (J-L). **(A, D, G, J)** Dorsal view of stage 17 *Xenopus* embryos, anterior is to the left. The two stripes of staining in A mark the pre-migratory neural crest. **(B, E, H, K)** Lateral view of stage 24 embryos, anterior to the left. Arrowheads denote streams of migrating cranial neural crest. **(C, F, I, L)** Lateral view of embryos between stage 28 and 30, Anterior to left, *= neural crest cells migrating into the branchial arches.

At stage 24, there is also some weak staining in the area of migrating crest, although the three streams cannot be clearly distinguished (Fig 3.2H, K arrowheads). However, by stage 28, both *dsh* and *daam1* can be seen in the branchial arches, where cranial neural crest cells end their migration (Fig 3.2 I, L asterisk) So, while the expression of *dsh* and *daam1* is not as clearly localised in the crest as that of *fzd7*, some levels can be detected in and around the cranial neural crest. The presence of these important components of the PCP pathway in neural crest cells during their migration is consistent with the vital role of PCP signalling in regulating this process.

### 3.3. PCP signalling is essential for cranial neural crest migration

To demonstrate the role of PCP signalling in neural crest migration, two constructs of Dsh were used, which modulate the activity of the PCP pathway (Fig . 3.3). DshDEP+ consists of the DEP domain of Dsh and acts as a dominant negative form inhibiting PCP signalling, but with no effect on the canonical wnt pathway (Tada and Smith, 2000). DshΔN, on the other hand, acts as a constitutively active form of Dsh, which activates PCP signalling but not the canonical pathway. DshΔN is a truncated form of Dsh, lacking the DIX domain which is the main activator of canonical signalling (Fig 3.3B) (Tada and Smith, 2000). mRNA coding for DshΔN or DshDEP+ was injected into *Xenopus* embryos and the effect on cranial neural crest migration was analysed by *in situ* hybridisation of *snail2*. Injections were carried out at the 8-cell stage in the dorsal animal blastomere, which is fated to become neural crest (Dale and Slack, 1987; Moody, 1987). This is necessary to avoid affecting early developmental processes such as convergent extension, for which PCP signalling is known to be required. Additionally injections were carried out in one side of the embryo only, leaving the other side to develop normally and act as an internal control. After injection, embryos were cultured until stage 24, at which point they were fixed for *in situ* hybridisation. In uninjected embryos, a dorsal view reveals the cranial neural crest migrating ventrally away from the neural tube on both sides of the embryo (Fig 3.3A). However injection of 1ng or 2ng of DshDEP+ inhibits neural crest migration on the injected side of the embryo, while neural crest on the control sides migrate normally (Fig 3.3 C, D). RNA was co-injected with fluorescein dextran (FDX), which allows identification of the injected side of the embryo (Fig 3.3 C',D',E').

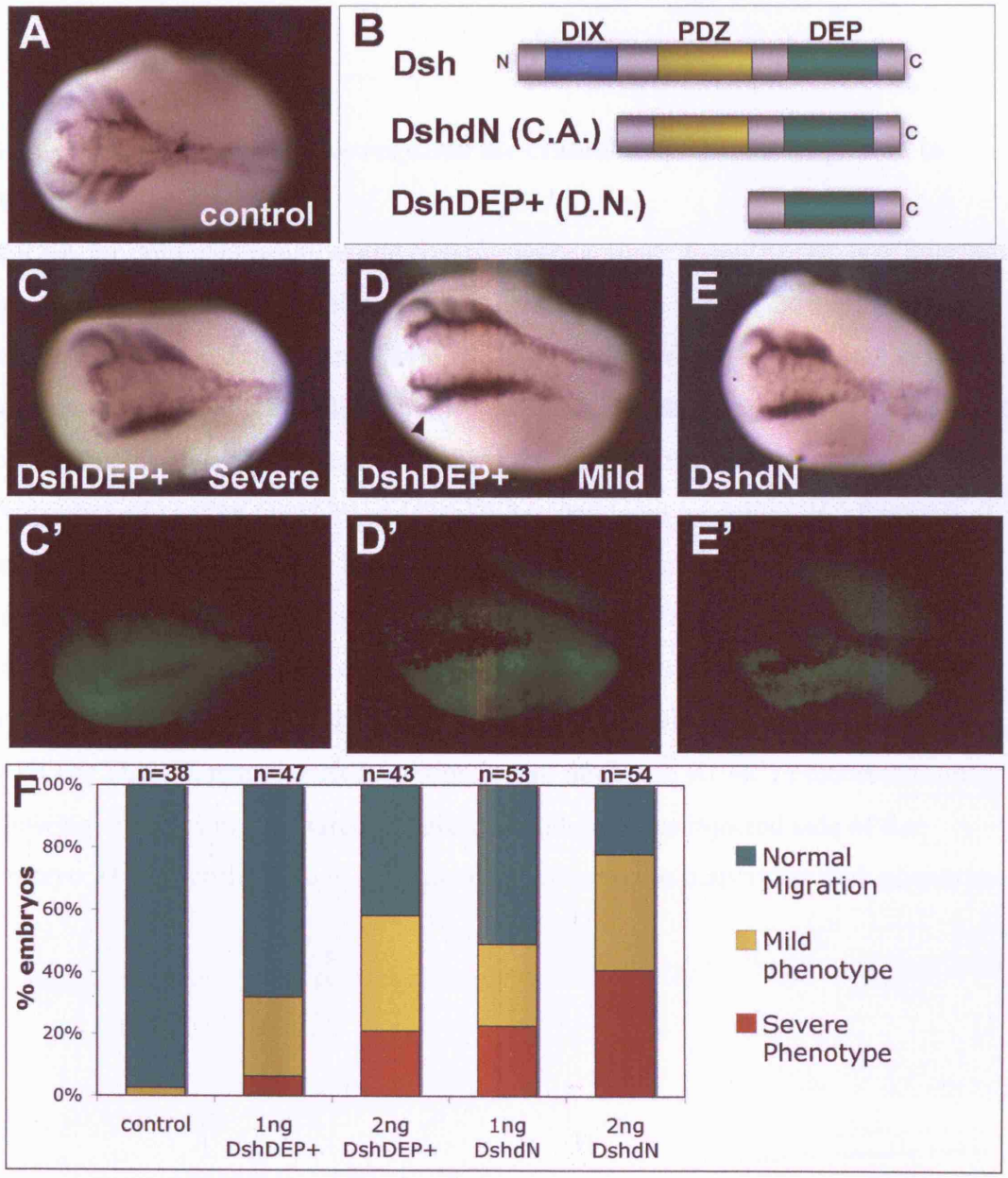
A
control
B
Dsh
DIX
PDZ
DEP
N
C
DshdN (C.A.)
DshDEP+ (D.N.)
C
DshDEP+ Severe
D
DshDEP+ Mild
E
DshdN
C'
D'
E'
F
n=38
n=47
n=43
n=53
n=54
100%
80%
60%
40%
20%
0%
% embryos
control
1ng DshDEP+
2ng DshDEP+
1ng DshdN
2ng DshdN
Normal Migration
Mild phenotype
Severe Phenotype

**Figure 3.3**

**Figure 3.3. PCP signalling is required for cranial neural crest migration in *Xenopus***

mRNA for dominant negative and constitutively activate forms of Dsh was injected into 8-cell stage *Xenopus* embryos. Embryos were fixed at stage 24 and neural crest migration visualised by *in situ* hybridisation of *snail2*. All embryos shown are dorsal view, anterior to the left. **(A)** An uninjected embryo showing normal cranial neural crest on both sides. **(B)** Schematic to show the domain structure of DshΔN (constitutively active for PCP) and DshDEP+ (dominant negative). **(C)** Example of an embryo injected with 1ng DshDEP+ displaying the severe phenotype. Note the lack of neural crest migration on the injected side. **(D)** Example of an embryo injected with 1ng DshDEP+ displaying the mild phenotype. Arrowhead indicates some residual migration on the injected side. **(E)** Example of an embryo injected with 1ng DshΔN, neural crest migration is also inhibited. **(C'-E')** Fluorescent images showing embryos in C-E. Green fluorescent indicates the injected side of the embryo. **(F)** Quantification of the percentage of embryos displaying each phenotype.

Two phenotypes of different severity were identified resulting from inhibition of Dsh with DshDEP+. Embryos were scored as a 'severe migration' phenotype if a total inhibition of cell migration on the injected side was observed (Fig 3.3C). In other embryos, migration was disrupted compared to the uninjected side but not completely blocked. For example, in some embryos a small amount of residual migration was present in one of the streams (Fig 3.3D) or, in others neural crest cells migrated but the patterning of the streams was completely lost. These embryos were classed as 'mild migration phenotype'. Quantification of these phenotypes is shown in figure 3.3F. Activation of Dsh/PCP by injection of 1ng or 2ng of DshΔN also inhibits neural crest migration (Fig 3.3E). Once again, embryos were classified into mild and severe phenotypes and numbers were quantified (Fig 3.3F). Interestingly, the effect of DshΔN is stronger than that of DshDEP+, with up to 80% of embryos displaying a phenotype when 2ng was injected. It is very common to find gain- and loss-of function of PCP signalling producing an identical outcome in both vertebrates and *Drosophila* (Mlodzik, 2002; Wallingford et al., 2002). The fact that both inhibition and activation of Dsh/PCP signalling results in defects in neural crest migration suggests that precise regulation of PCP signalling is required.

### 3.4. Wnt/PCP ligands are expressed around the pre-migratory neural crest

Although intracellular elements of PCP signalling like Dsh are clearly required for neural crest migration, it is less clear where the initial PCP signal is coming from. Therefore, the expression patterns of the PCP ligands, *wnt11* and *wnt5a*, were analysed by *in situ* hybridisation (Fig 3.4). During neurulation, *wnt11* expression can first be detected around stage 14 in two specific locations. At the anterior of the neural tube, wnt11 is present in a narrow band circumventing the edge of the anterior neural folds (Fig 3.4A). Additionally expression is observed in the posterior surrounding the closing blastopore (Fig 3.4B arrow). As neurulation proceeds, expression in the anterior becomes limited to two thin bands lateral to the anterior neural tube, and some expression in the trunk neural tube also appears (Fig 3.4C arrows show two bands of expression) At this stage, the expression in the anterior just is lateral to and closely associated with the cranial neural crest. The restriction of Wnt11 from the most anterior edge of the neural tube also mirrors that of neural crest markers as many early markers are expressed in a wide arc encompassing the

anterior neural plate, which later becomes restricted to two populations lateral to the plate (Carmona-Fontaine et al., 2007). At stage 23, some expression of *wnt11* can be observed in the migrating cranial neural crest around the eye (Fig 3.4D arrow) and also in the somites (Fig 3.4E arrowheads). Later at stage 28, *wnt11* can be identified in the somites and with some expression in the first branchial arch (Fig 3.4F).

In contrast to *wnt11*, the expression of *wnt5a* around the neural crest during neurulation is not so clear. Low levels of *wnt5a* can be distinguished in the entire neural plate at stage 17, with a particular accumulation in the anterior neural plate (Fig 3.4G). This low level expression may also extend to the cranial neural crest. At stage 24, some expression is observed in the branchial arches and also in the extreme posterior of the embryo (Fig 3.4H). However, at stage 28 there is a clear expression in the neural crest derived branchial arches as well as in the tail region (Fig 3.4I).

In addition to Wnt11 and Wnt5a, Wnt11R has recently been identified as a PCP ligand in *Xenopus* (Garriock et al., 2005). *wnt11r* is expressed in the heart and nervous system but its expression in early embryonic development has not been extensively analysed. Thus, the expression of *wnt11r* was analysed by *in situ* hybridisation (Fig 3.5). At stage 17, *in situ* hybridisation reveals a strong localisation of *wnt11r* in the neural tube (Fig 3.5B). This expression does not extend to the outer neural folds and comparison with *snail2* at the same stage (Fig 3.5A) indicates that *wnt11r* is not expressed in the neural crest at this point. However, double *in situ* hybridisation using a mixture of probes against *wnt11r* and *wnt11* leads to an interesting observation. *wnt11r* is present in the neural tube medial to the neural crest, while wnt11 is expressed in a thin band at the crest's lateral edge. When the two genes are shown together in the same embryo (Fig 3.5C) a narrow gap is formed between them. Double *in situ* of *snail2* and *wnt11* (Fig 3.5D) illustrates that this band corresponds exactly to the neural crest. So, at stage 17, just before they start to migrate, neural crest cells are surrounded by PCP ligands, with *wnt11r* medially in the neural tube and wnt11 laterally in the epidermis (Fig 3.5E).

The expression of *wnt11r* was also analysed at later stages of development. At stage 24, *wnt11r* is expressed in the neural tube, but no staining was evident in the migrating neural crest (Fig 3.5F) suggesting that if Wnt11r is involved in neural crest development, it is likely to play a role in the early stages of migration. Later still, at stage 35, *wnt11r* maintains a strong expression in the neural tube (Fig 3.5G), while also appearing in the branchial arches (Fig 3.5H asterisks).

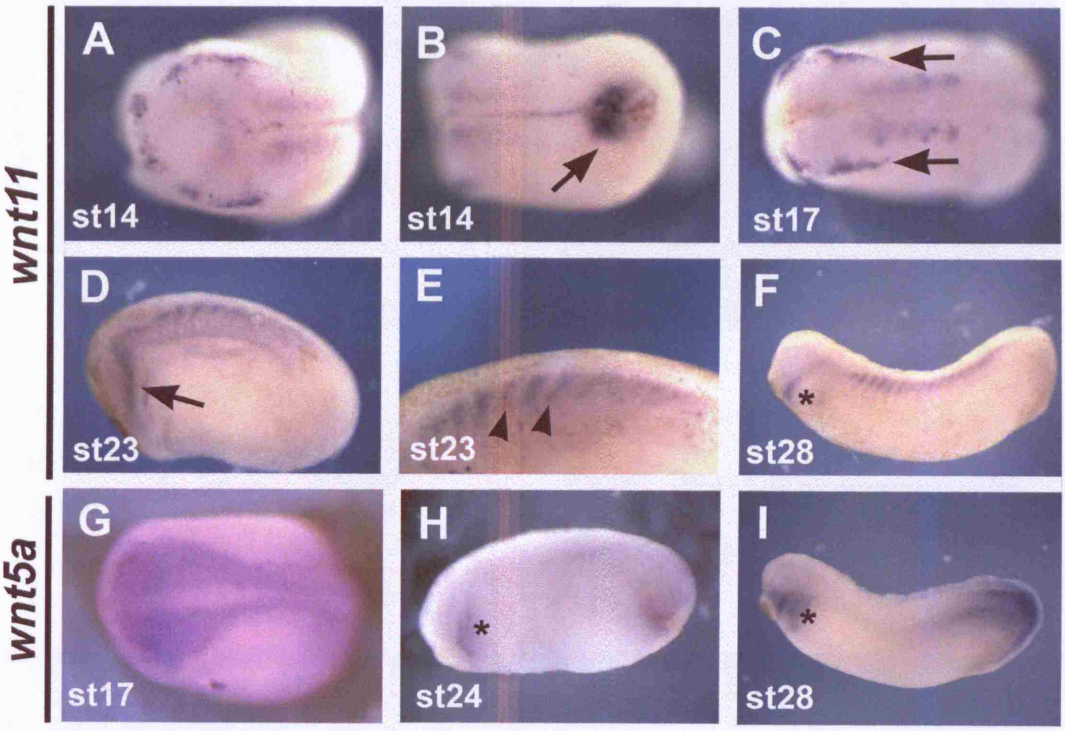


**Figure 3.4. *wnt11* and *wnt5a* are expressed in and around the neural crest**

*In situ* hybridisation was carried out for *wnt11* and *wnt5a* to establish their gene expression patterns in early *Xenopus* embryos. **(A)** Anterior view of a stage 14 embryo, showing the ring of *wnt11* expression around the anterior neural tube. **(B)** Posterior view of a stage 14 embryo, showing *wnt11* at the closing blastopore. **(C)** Dorsal view of stage 17 embryo stained for *wnt11* expression, anterior is to the left, arrows indicate expression adjacent to the neural crest. **(D-F)** Expression of *wnt11* at later stages of development showing expression in the cranial neural crest (arrow in D), somites (arrowheads in E) and branchial arches (asterisk in F), embryos are shown in lateral view with anterior to the left. **(G)** Dorsal view of a stage 17 embryo showing *wnt5a* expression in the neural plate. **(H,I)** Expression of *wnt5a* in later stages, asterisk denotes branchial arches, embryos viewed laterally, anterior to the left.

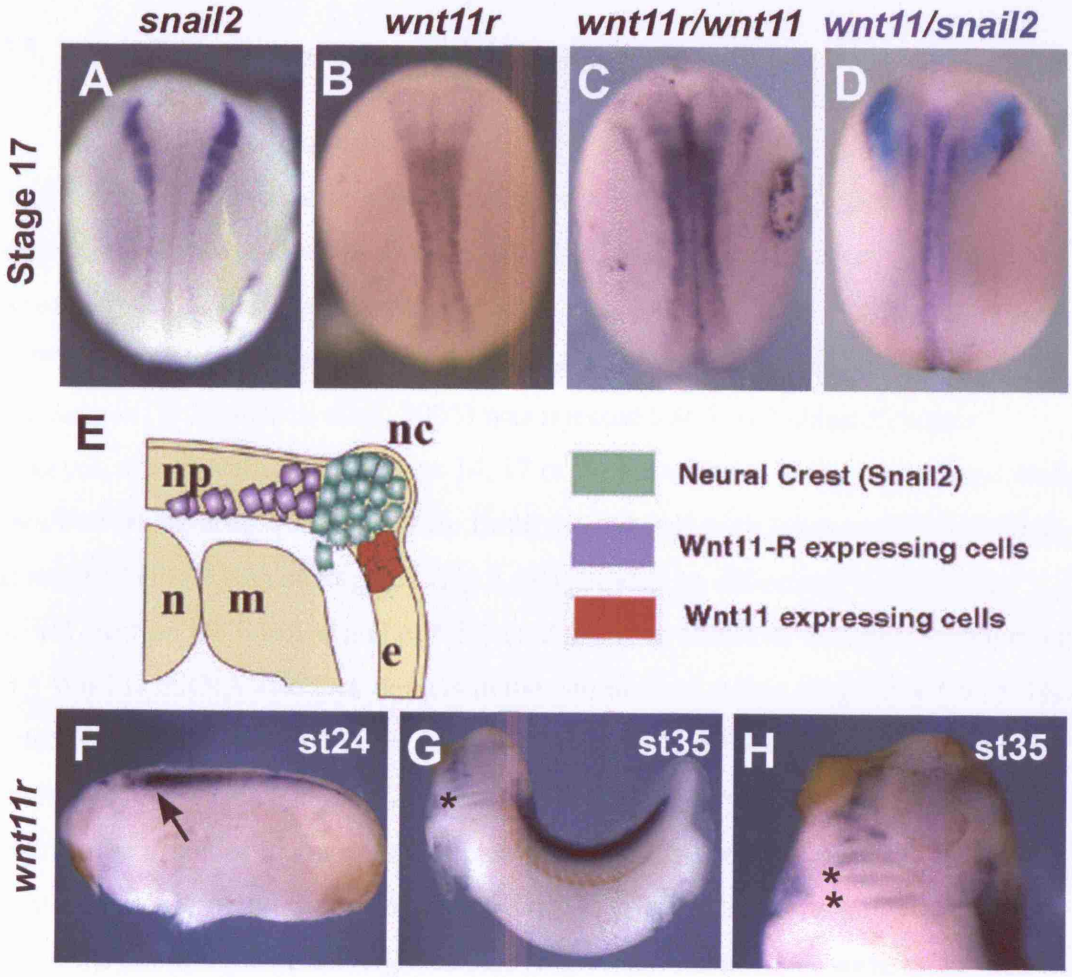


**Figure 3.5. *wnt11* and *wnt11r* surround the neural crest before migration**

*In situ* hybridisation was carried out to compare the expression patterns of *wnt11r*, *wnt11* and *snail2* in the early *Xenopus* embryo. **(A-D)** Dorsal view of stage 17 embryos, anterior is to the top, showing expression patterns of *snail2* (A, D), *wnt11r* (B, C) and *wnt11* (C,D). Note how wnt11 and wnt11r flank the neural crest (marked with snail2) on both sides (C,D). **(E)** Schematic representation of a transverse section through a stage 17 embryo with *wnt11* (red) and *wnt11r* (blue) expressing cells on either side of the neural crest (green); np, neural plate; nc, neural crest; e, epidermis; n, notochord; m, mesoderm. **(F, G)** Lateral view of later stage embryos showing the expression of *wnt11r*, arrow indicates expression in neural tube; asterisk, branchial arches. **(H)** Higher magnification image of *wnt11r* expression in the head of a stage 35 embryo, asterisk denotes branchial arches.

### 3.5. Wnt11R is required for neural crest migration

The co-operative expression of *wnt11* and *wnt11r* around the pre-migratory neural crest prompted me to address the question of whether they play a functional role in neural crest migration. De Calisto et al (2006) have implicated Wnt11 in neural crest migration, but the function of Wnt11R in the neural crest has not been previously explored. To determine the function of Wnt11R, a morpholino (Mo) against *wnt11r* (Garriock et al., 2005) was injected into 8-cell stage *Xenopus* embryos, which were fixed at stage 14, 17 or 24 for analysis of the neural crest using *snail2 in situ* hybridisation (Fig 3.6). Embryos injected with 30ng *wnt11r* Mo fixed at stage 14 (Fig 3.6A) or stage 17 (Fig 3.6B) showed no difference between the neural crest on the injected and non-injected sides. In addition, embryos injected with 1ng Wnt11r mRNA also lack defects in the neural crest at this stage (Fig 3.6C). This demonstrates that Wnt11R is not required for the early induction or maintenance of neural crest genes such as *snail2*. However, once the neural crest cells have started to migrate the effect of the morpholino becomes clear. In stage 24 embryos, the neural crest migrate normally in the uninjected side (Fig 3.6D), but are unable to migrate out of the neural tube on the injected side (Fig 3.6E). Phenotypes were quantified by classification of embryos into 'severe' and 'mild' migration phenotypes using the criteria described previously. When 30ng of morpholino was injected, 60% of embryos showed a neural crest migration phenotype (Fig 3.6H). Use of a morpholino always carries the risk that the morpholino is acting non-specifically on genes other than *wnt11r*. So, to confirm the morpholino's specificity a rescue experiment was carried out, where *wnt11r* Mo was co-injected with *wnt11r* mRNA. Activation of Wnt11R was able to rescue the effect of the morpholino, with the cranial neural crest migrating normally (Fig 3.6F). The percentage of embryos displaying a phenotype was dramatically reduced from 47% when injected with 15ng *wnt11r* Mo, compared to just 22% when 15ng *wnt11r* Mo was co-injected with 1ng *wnt11r* mRNA (Fig 3.6H). This demonstrates that the morpholino is inhibiting *wnt11r* only and therefore that Wnt11R is required for neural crest migration. As Wnt11 is also required for neural crest migration (De Calisto et al., 2004), it is possible that there may be some redundancy between PCP ligands. To test this hypothesis, a rescue experiment was performed to see if Wnt11 could rescue the effects of *wnt11r* Mo. When 15ng *wnt11r* Mo was injected alongside 1ng *wnt11* mRNA, no rescue was obtained and

neural crest migration remained inhibited (Fig 3.6G, H). Thus Wnt11R is affecting neural crest specifically and not by altering global levels of PCP signalling. Furthermore the absence of a rescue by co-injection of Wnt11 suggests that Wnt11R is the primary PCP ligand required for neural crest migration. A dominant negative form of Wnt11 inhibits neural crest migration in *Xenopus* (De Calisto et al., 2005). Although this dominant negative has been shown not to affect Wnt8 signalling (Tada and Smith, 2000), its specificity with regard to non-canonical ligands is unknown and it may also have the ability to inhibit Wnt11r. Therefore, while Wnt11R is clearly required for neural crest migration, Wnt11 may also be involved.

As *wnt11r* is not expressed in the neural crest, we can presume that its requirement during neural crest migration is not in the crest itself but as an extracellular signal from the surrounding tissue. To test this, several graft experiments were carried out (Fig 3.7). The relatively large area and compactness of the *Xenopus* cranial neural crest allows it to be dissected at stage17, removed intact and grafted into other embryos (Borchers et al., 2000). Cranial neural crest from embryos injected with 30ng *wnt11r* Mo and FDX were dissected and grafted into uninjected host embryos. If Wnt11R is acting as an external signal, then grafting neural crests into wildtype embryos expressing *wnt11r* in their neural tube should rescue the effect of the morpholino on neural crest migration. This is indeed the case. When neural crest injected with FDX and 30ng control morpholino are grafted into an uninjected host, they are able to migrate as normal following the migration pathways of the host (Fig 3.6A). The same occurs in *wnt11r* Mo injected neural crest cells (Fig 3.6B), with neural crest migration being effectively rescued by the host embryo. The converse experiment was also performed, with wildtype neural crest, labelled with rhodamine dextran (RDX), being grafted into host embryos injected with *wnt11r* Mo and FDX in both blastomeres at the 2-cell stage. This means that the morpholino is spread throughout the entire embryo except for the grafted neural crest tissue. When RDX containing neural crests were grafted into hosts injected with FDX and the control Mo, migration was able to proceed as normal (Fig 3.6C), but when they were grafted into a host expressing the *wnt11r* Mo, neural crest migration was inhibited (Fig 3.6D). This suggests that the role of Wnt11r in the neural crest is non-cell-autonomous. Thus, neural crest migration requires an extracellular signal from Wnt11r.

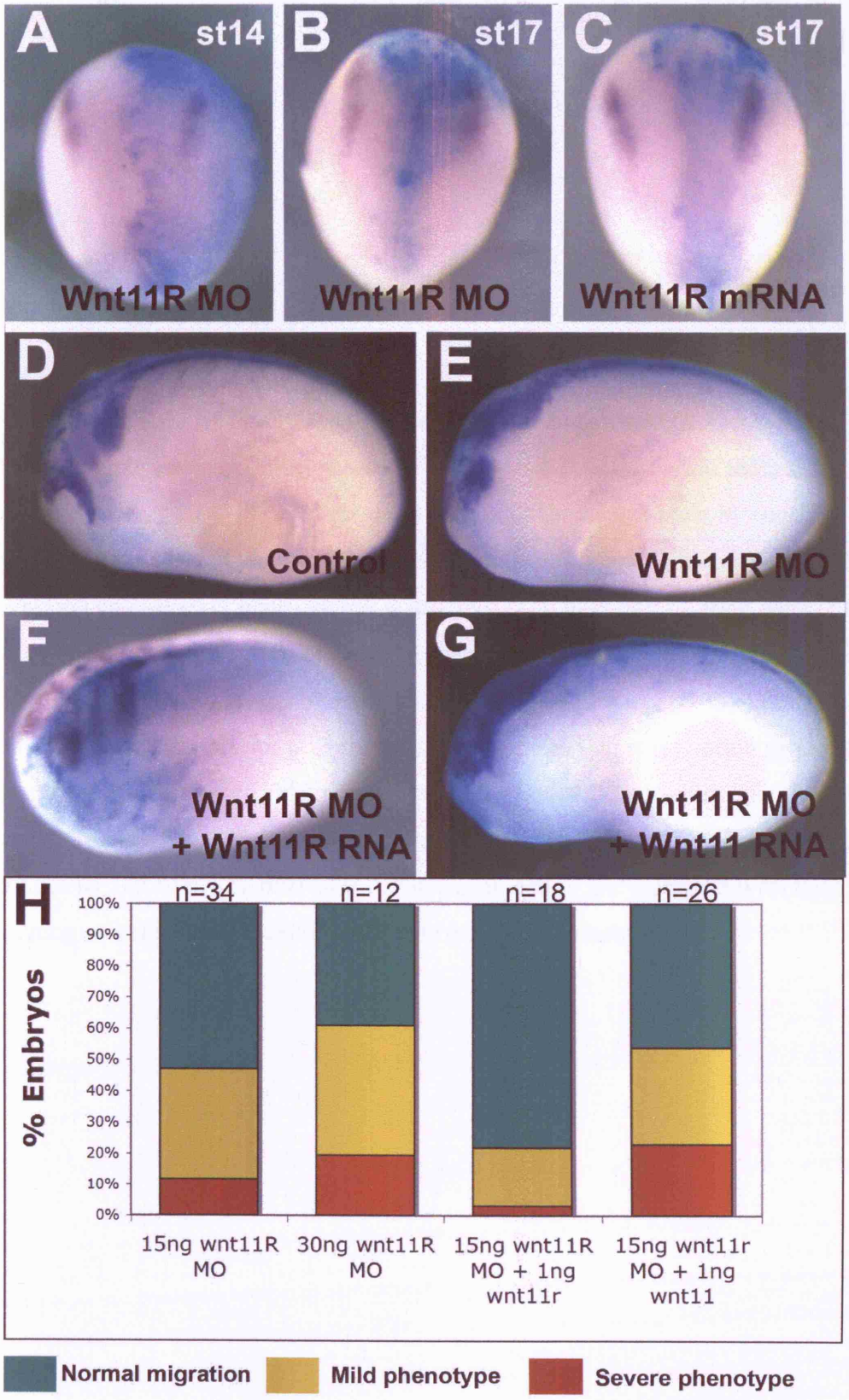
A
st14
Wnt11R MO
B
st17
Wnt11R MO
C
st17
Wnt11R mRNA
D
Control
E
Wnt11R MO
F
Wnt11R MO
+ Wnt11R RNA
G
Wnt11R MO
+ Wnt11 RNA
H
% Embryos
n=34
n=12
n=18
n=26
100%
90%
80%
70%
60%
50%
40%
30%
20%
10%
0%
15ng wnt11R MO
30ng wnt11R MO
15ng wnt11R MO + 1ng wnt11r
15ng wnt11r MO + 1ng wnt11
Normal migration
Mild phenotype
Severe phenotype

**Figure 3.6**

**Figure 3.6. Wnt11R is required for neural crest migration in *Xenopus***

*Xenopus* embryos were injected with Wnt11r Mo and/or mRNA at the 8-cell stage and fixed at stage 14, 17 or 24 for visualisation of the neural crest by *snail2 in situ* hybridisation. **(A-C)** Dorsal view of neurula embryos, anterior is to top. Expression of neural crest marker gene, *snail2,* is unaffected by injection of 30ng *wnt11r* Mo at stage 14 (A) or stage 17 (B) or by over-expression of 1ng of *wnt11r* mRNA (C). The site of injection is indicated by pale blue fluorescein staining. **(D-G)** Lateral view of stage 24 embryos, anterior is to the left. Cranial neural crest migration proceeds as normal in the uninjected side of an embryo (D), but is disrupted by injection of 15ng *wnt11r* Mo (E) This effect can be rescued by co-injection of 1ng *wnt11r* mRNA (F), but not by 1ng of *wnt11* mRNA (G). Sites of injection are indicated with light blue staining as before. **(H)** Quantification of rescue experiment.

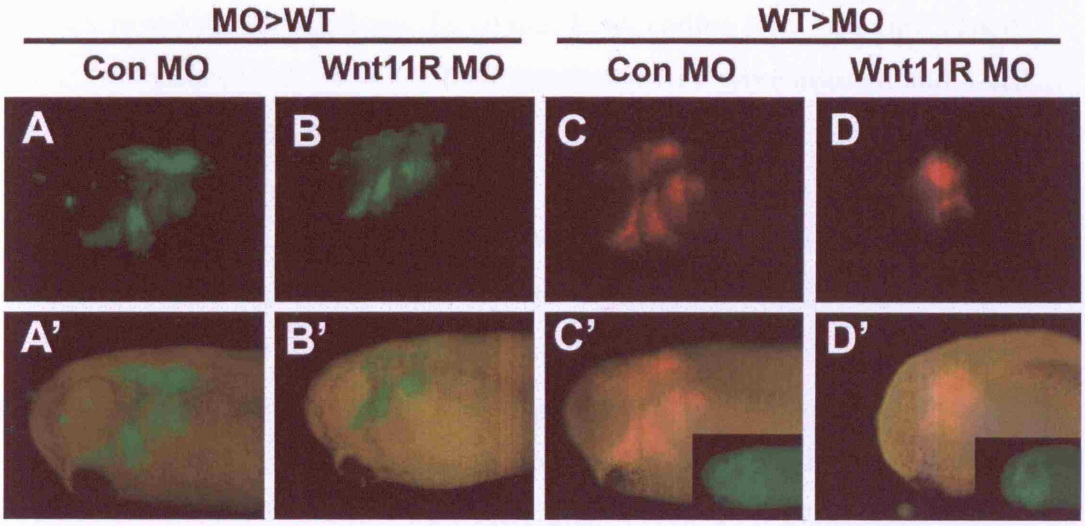


**Figure 3.7. Wnt11R is non cell-autonomous in its control of neural crest migration**

*Xenopus* embryos were injected with FDX or RDX at the 8-cell stage. At stage 17 cranial neural crest explants were removed and grafted into uninjected hosts, so that cell migration can be followed by fluorescent imaging. **(A-D)** Cranial neural crest cells labelled with FDX (A,B) or RDX (C,D) migrating in the head of a stage 28 host embryo. Lateral view, anterior to the left. **(A'-D')** Images from A-D overlaid on brightfield image of the host embryo. Insets in C' and D' show green fluorescence in host embryos co-injected with FDX along with the Mo. Neural crest cells expressing a FDX with a control Mo (A) or *wnt11r* Mo (B) are able to migrate in wildtype hosts. Wildtype neural crest cells labelled with RDX can migrate in an embryo ubiquitously expressing a control Mo (C) but not in a background of *wnt11r* Mo expression (D).

### 3.6. Dsh localises at the cell membrane in migrating neural crest cells

Dishevelled (Dsh) is a key modulator of all Wnt signalling including the PCP pathway, but membrane localisation of Dsh is required for activation of PCP signalling. So I investigated the subcellular localisation of Dsh in neural crest cells, both before and during migration. To do this, RNA coding for a Dsh-GFP fusion protein (Rothbacher et al., 2000) and for membrane-RFP were injected into 8-cell stage embryos and cranial neural crests were dissected as before. However, rather than being grafted into another embryo, the neural crest explants were cultured on fibronectin coated coverslips, which have been shown to support the migration of neural crest cells (Alfandari et al., 2003). The explants were then fixed and the localisation of Dsh-GFP was analysed by confocal microscopy and compared to membrane-RFP (Fig 3.8). Culturing neural crest cells *in vitro* like this allows for the higher resolution imaging that is required to analysis the sub-cellular localisation of a protein. In neural crest cells that were fixed immediately after attachment to the fibronectin, before they have started to migrate, Dsh-GFP can be observed in discrete puncta (Fig 3.8A) of several microns in diameter. These do not co-localise with membrane-RFP (Fig 3.8B, C) and are similar to the localisation of Dsh that has been previously observed in animal caps where canonical Wnt signalling is active (Choi and Han, 2005). In neural crest explants plated on polylysine on which neural crest cells can attach but not migrate (Alfandari et al., 2003), a similar cytoplasmic localisation of Dsh-GFP can be detected (Fig 3.8 D-F). These cells were fixed after 6 hours of culture on polylysine and did not start to migrate, whereas neural crest cells on fibronectin migrated extensively during this time period. In migrating neural crest cells, Dsh-GFP can be observed where it co-localises with membrane-RFP (Fig 3.8G-L). This membrane localisation of Dsh clearly suggests that the PCP pathway is activated in migrating neural crest cells. Interestingly, Dsh does not appear to be uniformly distributed in the cell membrane, but rather has a specific localisation. In groups of cells, Dsh is present in discrete accumulations in the membrane, which are found at the border between two different cells (Fig 3.8G-I). In single cells migrating away from the group, Dsh appears to be enriched in the back of the cell and is notably absent from the leading edge (Fig 3.8J-L). Therefore Dsh not only localises to the plasma membrane, but to specific regions of the membrane in migrating neural crest cells.

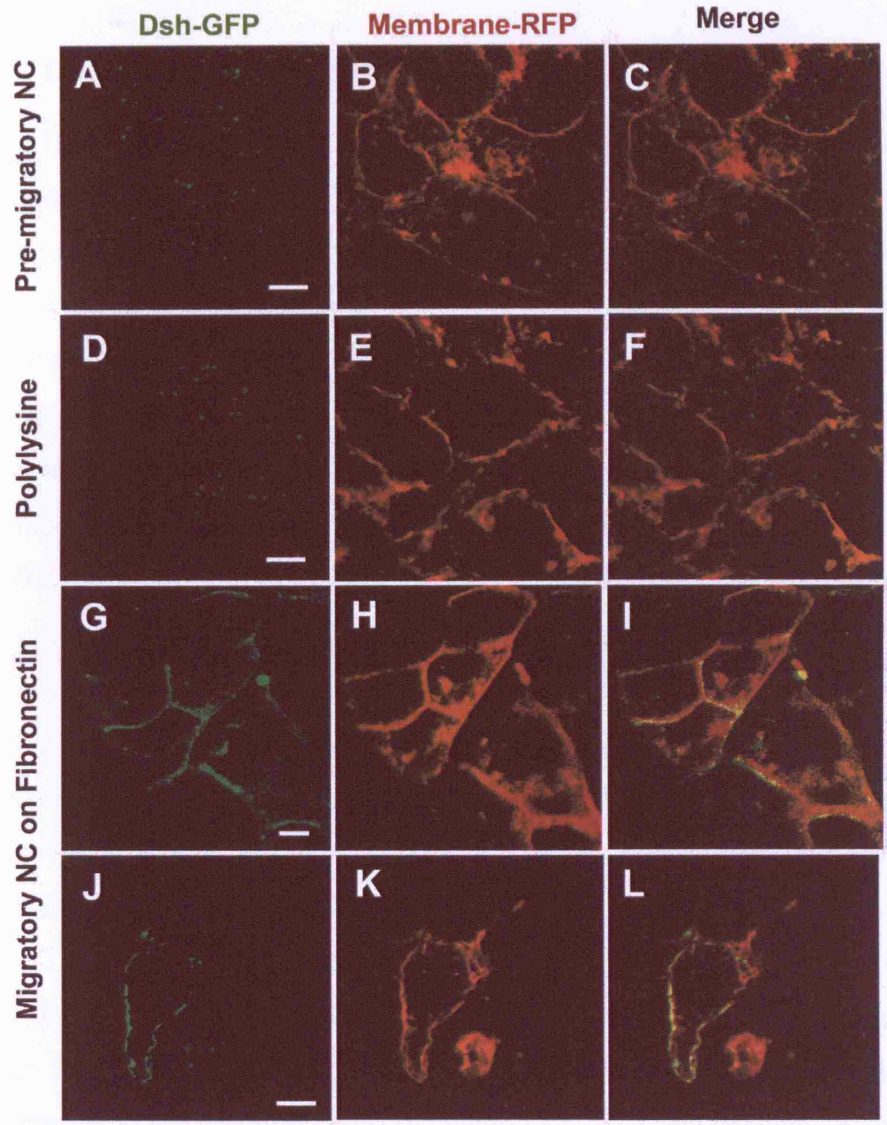


**Figure 3.8. Dishevelled localises to the cell membrane in migrating NC cells**

*Xenopus* embryos were injected with 75pg of Dsh-GFP and 200pg membrane-RFP RNA at the 8-cell stage. Cranial neural crest explants were dissected at stage 17 and crest cells were cultured *in vitro* on glass coverslips. **(A-C)** Images of neural crest cells taken immediately after plating on fibronectin coated coverslips. Note Dsh appears in discrete puncta (A), which do not co-localise with membrane-RFP (C). **(D-F)** Images of neural crest cells cultured on polylysine-coated coverslips for 6 hours. Neural crest cells do not migrate and Dsh is observed in cytoplasmic puncta (D,F). **(G-L)** Neural crest cells that have been migrating on fibronectin coated coverslips for 6 hours. Note co-localisation of Dsh and membrane-RFP (I,L). In groups of cells Dsh can be observed at the contacts between cells (G-I), while in individual migrating cells it can be observed towards the back of the cell (J-L). Scale bar = 20 μm.

### 3.7. Discussion

Here I have re-iterated the vital requirement of the PCP pathway in neural crest migration. Inhibition of PCP signalling using the dominant negative DshDEP+, or over-activation with the constitutively active DshΔN produces disastrous results in terms of neural crest migration. The observation that both inhibition and activation of PCP signalling results in the same phenotype (in this case inhibition of neural crest migration) has been noted previously in mesodermal cells during gastrulation, where the inhibition of PCP signalling using a Dsh mutant or overexpression of the PCP component *strabismus* both cause convergent extension defects (Goto and Keller, 2002; Wallingford et al., 2000). This has been proposed to be a consequence of the role of PCP signalling in regulating polarity in these cells. As Dsh activity controls polarity by limiting cell protrusion formation to the lateral ends of the cell, then either an increase or decrease in activity would result in a subsequent increase or decrease in cell protrusions and hence loss of cell polarity (Wallingford et al., 2002). However, it is not clear whether there is a requirement for spatially restricted PCP signalling, or simply a precise level of activity.

The role of Dishevelled in neural crest migration is clear and is further confirmed by the fact that it is expressed in the neural crest during migration (Fig 3.2). Additionally, I have shown that several other intracellular PCP elements are expressed in the migrating crest including Dsh's binding partner, Daam1, and the Wnt receptor Fzd7. Fzd7 has been implicated in many diverse cellular processes during development including many that require canonical wnt signalling such as dorsal/ventral patterning (Medina et al., 2000; Sumanas et al., 2000), others such as convergent extension that require PCP signalling (Djiane et al., 2000; Medina et al., 2000) and for separation of the ectoderm and mesoderm during gastrulation, where signalling proceeds via the non-canonical Wnt/Calcium pathway (Winklbauer et al., 2001). Thus, Fzd7 is able to act as the receptor for all known branches of the Wnt-signalling pathway. In the neural crest, Fzd7 is expressed as early as stage 13, early enough for it to play a role in the canonical signalling that is required for neural crest induction (Abu-Elmagd et al., 2006). In fact, Fzd7 has been shown to be necessary for neural crest induction, as *snail2* early expression is inhibited by injection of a morpholino against Fzd7 (Abu-Elmagd et al., 2006). Furthermore, neural crest cells can be induced by injection of Fzd7 into noggin-treated animal caps (Abu-Elmagd et

al., 2006). It is interesting to note that the same receptor appears to receive both the canonical wnt signals required for neural crest induction and the non-canonical wnt signals required for neural crest cell migration. At some point during neural crest development there needs to be a switch from the fate-determining canonical Wnt signalling to the PCP signalling required for migration. It is not known how this shift is instigated, but one possibility may be a shift in the expression of Wnt ligands. I have shown that the non-canonical Wnt ligands, Wnt11 and Wnt11r flank the neural crest from stage 17 onwards, and it is possible that their appearance could represent a timing cue that signals the onset of neural crest migration. By the end of neurulation, accumulation of Wnt11/Wnt11R ligands could overwhelm Fzd7, causing the shift from canonical to non-canonical Wnt signalling. Alternatively, instead of offering a temporal signal, non-canonical Wnt ligands could be providing a directional cue to the migrating neural crest. De Calisto et al (2005) postulate that Wnt11 could be acting as an attractant of neural crest cells based on its requirement for neural crest migration and its position in the direction in which the cells will migrate. Furthermore, when tissue expressing *wnt11* was grafted in an inappropriate location, some neural crest cells moved towards the graft and a local increase in motility was observed around the graft (De Calisto et al., 2005). However, this simple hypothesis of Wnt11-based attraction seems unlikely in light of the data shown here regarding Wnt11R. I show that Wnt11R is essential for neural crest migration and that it is independent from Wnt11, as inhibition of Wnt11R cannot be rescued by activation of Wnt11 (Fig 3.6). Wnt11r is acting non-cell autonomously, but it is unlikely that it is acting as an attractant as its expression is restricted to the neural tube, in the opposite direction from the future neural crest migration pathway. It is possible that both signals act in conjunction to convey directionality to the neural crest, with Wnt11 attracting neural crest cells and Wnt11R repelling them. However, this model would suggest that inhibiting Wnt11R alone would not be sufficient to completely block migration and would simply allow 'backwards' migration into the neural tube. From the data presented here, this is clearly not the case. Signalling by Wnt11R plays a fundamental role in controlling neural crest migration, but there is no evidence that it controls the direction of neural crest migration and could be playing a role in regulating the timing of migration or regulating EMT.

Another factor that accompanies the start of neural crest migration is the translocation of Dsh from the cytoplasm to the membrane. In neural crest cells

cultured *in vitro* on fibronectin, Dsh is initially localised in cytoplasmic vesicles but becomes re-localised to the membrane once the cells start to migrate (Fig 3.8). This change mirrors the switch from canonical Wnt signalling, where Dsh is known to have a cytoplasmic localisation to PCP signalling, where a membrane localisation is required (Capelluto et al., 2002; Choi and Han, 2005; Wallingford et al., 2000). Interestingly though, Dsh is not distributed evenly in the membrane of neural crest cells, but rather appears to be enriched in discrete accumulations. These accumulations frequently occur at the border between two cells when cells are in groups and at the rear end of cells that are migrating individually at the point at which the cell was last in contact with its neighbours. Although it has long been known that Dsh has an asymmetrical localisation in *Drosophila* (Axelrod, 2001), recent work by Witzel et al (2006) shows that a specific localisation can also be found in vertebrates. They show that wnt11-YFP, Fzd7-CFP and Dsh-YFP co-localise at discrete areas in the plasma membrane in zebrafish animal pole cells. Furthermore these accumulations are found at the junctions between cells in a manner similar to those observed in migrating neural crest cells. Interestingly these accumulations are only present when PCP signalling has been activated by the addition of Wnt11. They show that these local accumulations are required for the maintenance of cell contacts during movement of the prechordal plate progenitors during gastrulation, which allows the tissue to move persistently as a whole (Ulrich et al., 2005; Witzel et al., 2006). The presence of similar accumulations of Dsh in the neural crest raises the possibility of a role for local cell-cell PCP signalling in guiding neural crest migration and this will be investigated in greater detail in later chapters of this thesis. Here, however, I have shown the essential requirement for PCP signalling for neural crest migration *in vivo*, and demonstrated important roles for Wnt11r and Dishevelled.

# 4. Results: The role of Syndecan-4 in neural crest migration

## 4.1. Introduction

The PCP signalling pathway plays a major role in controlling neural crest migration, and recently a novel co-factor for PCP signalling in *Xenopus* embryos has been identified, the proteoglycan Syndecan-4 (Syn4). Syn4 has been shown to control *Xenopus* gastrulation through Dishevelled (Munoz et al., 2006). In this chapter I will address the role of Syn4 in the neural crest and its interaction with the PCP pathway. Syn4 is an interesting candidate molecule as a regulator of neural crest migration, as it is known to control cell migration in other cell types adherent to fibronectin. Although Syn4 has been much studied in adult migratory cells such as fibroblasts, little is known of its role during embryonic development.

### *4.1.1. The domain structure of Syndecan-4*

The syndecans are a family of transmembrane glycoproteins that act as receptors for the ECM and growth factors. Of the fours syndecans so far identified in vertebrates, *syn4* is the most ubiquitously expressed. Like all syndecans, Syn4 consists of a transmembrane protein core covalently linked to chains of heparan sulphate glycosaminoglycans (GAGs). The basic domain structure of Syn4 is illustrated in figure 4.1A. The extracellular domain of Syn4 contains three GAG attachment sites and it is these GAGs that mediate extracellular interactions with a variety of molecules including growth factors, the extracellular matrix and protease inhibitors (Bernfield et al., 1999). It has been proposed that the GAG chains also facilitate binding with the Heparin-binding domain of fibronectin (Woods et al., 2000). However the extracellular protein core also plays a role, as it is able to stimulate the formation of fibronectin-induced focal adhesions in cells unable to assemble GAG chains (Echtermeyer et al., 1999). The extracellular domain of Syn4 also contains a proteolytic cleavage site, where metalloprotease-mediated shedding of the ectodomain occurs, a process that is required during wound healing (Fitzgerald et al., 2000; Subramanian et al., 1997). The transmembrane domain, along with four conserved membrane-proximal residues of the extracellular domain, mediate Syndecan dimerisation (Asundi and Carey, 1995). Dimerisation is essential for

correct Syn4 function and upon ligand binding clustering of Syn4 induces the formation of multimers (Oh et al., 1997a; Tkachenko and Simons, 2002). The C-terminal domain of Syn4 consists of a short cytoplasmic tail, which mediates intracellular interactions and is made up of two highly conserved sequences (the C1 and C2 domains) linked by a variable (V) region. The C1 domain acts as binding partner for a large number of cytosolic proteins including neurofibromin and the src complex, while the C2 domain contains a conserved EFYA motif, which is a binding site for PDZ domain containing proteins (Bass and Humphries, 2002). Meanwhile, the V domain is rich in basic amino acids, which bind $PIP_2$, which can in turn recruit and activate PKCα (Keum et al., 2004; Oh et al., 1998). Activation of PKCα drives the recruitment of cytoskeletal proteins to focal adhesions, resulting in the maturation and stabilization focal adhesions in a Syn4 dependent manner (Woods and Couchman, 1992; Woods et al., 1986)

Throughout evolution, the syndecan family has shown high levels of conservation with the C1 and C2 domains being conserved between human Syndecans 1-4 and in the Syndecans of *Drosophila* and *C. elegans* (Spring et al., 1994). Syn4 in humans, chick and zebrafish also displays high levels of sequence identity in the cytoplasmic region (Fig 4.1B). In *Xenopus*, however, there are some surprising differences. Two pseudo-alleles have been identified for *syn4* in *Xenopus laevis* (*syn4*.1 and *syn4*.2), with 71% identity between them (Munoz et al., 2006). A single copy of *syn4* has also been cloned *in silico* in *Xenopus tropicalis*, although it has not yet been mapped to a chromosomal location. Although *Xenopus* syndecans1-3 have high identity to their mammalian counterparts in the conserved cytoplasmic domain (Teel and Yost, 1996), the sequence of both *X. Laevis syn4* alleles and *X. tropicalis syn4* reveal some major differences compared to other species (Munoz et al., 2006). Although the GAG attachment sites, proteolytic cleavage site, PIP2 and PKCα binding sites are present, *Xenopus* Syn4 is entirely missing the C1 domain. Also lacking is the characteristic EFYA motif at the extreme C-terminus. However the c-terminal sequence of *Xenopus* Syn4, MEV, has been suggested to be a putative PDZ binding domain (Songyang et al., 1997). Although many important elements of Syndecan structure, such as the PIP2 binding site, are conserved in *Xenopus* Syn4, the differences are great enough to warrant attention. There remains a possibility that the *Xenopus* Syndecan cloned by Munoz et al (2006) may in fact be a novel member of the syndecan family or indeed a novel HSPG.

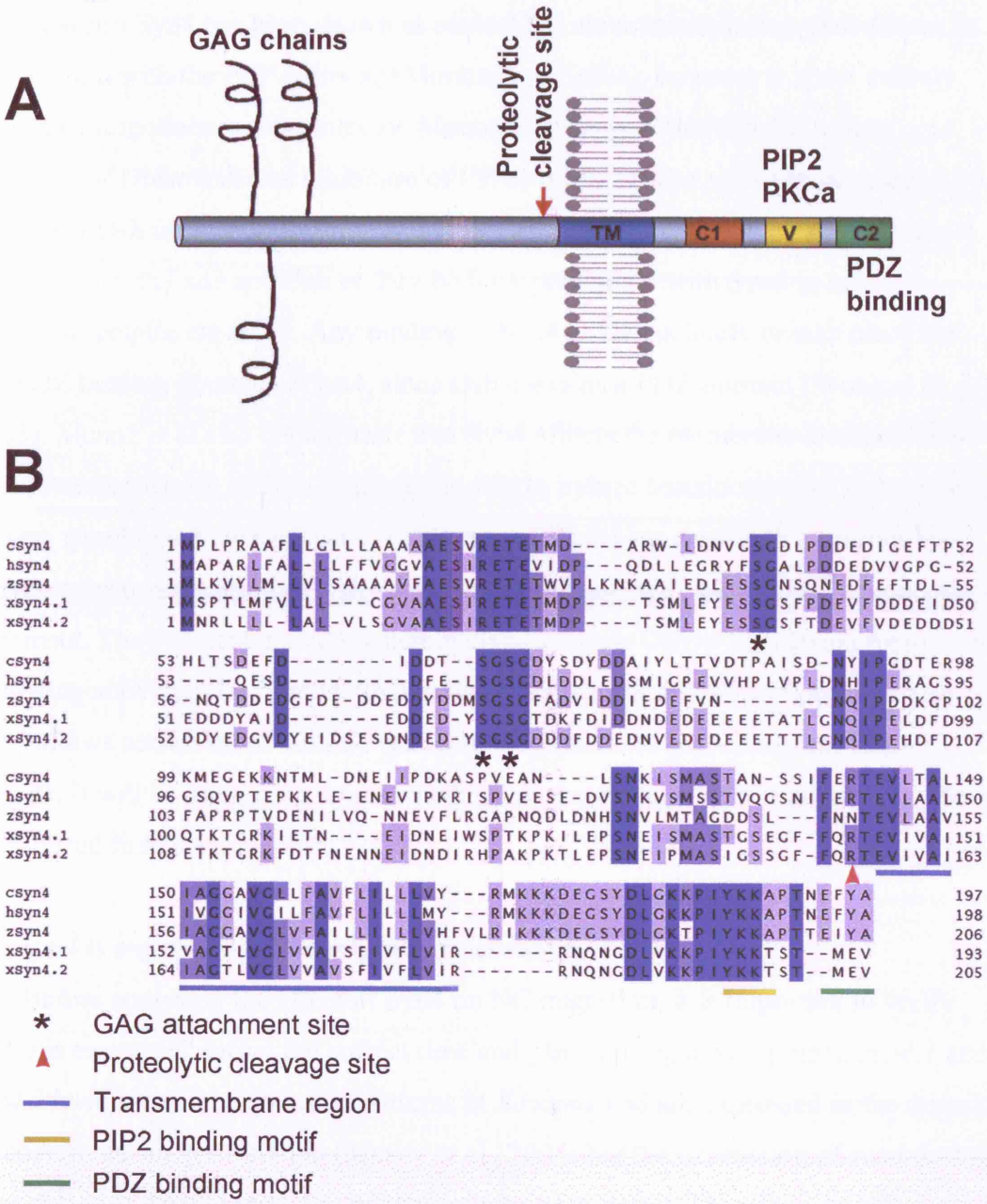


**Figure 4.1. Domain structure and sequence of Syndecan-4**

**(A)** Schematic illustrating the domain structure of Syn4. Syn4 consists of a large extracellular domain with three GAG chain attachment sites, a single span transmembrane region (TM) and a short cytoplasmic tail with two conserved (C1,C2) regions and a variable (V) region. **(B)** Comparison of the protein sequences of the two *Xenopus laevis* Syn4 pseudoalleles (xSyn4.1, xSyn4.2) with those from other species. c, *Gallus gallus*; h, *Homo sapiens*; z, *Danio rerio*.

### *4.1.2. Interaction with the PCP pathway*

*Xenopus* Syn4 has been shown to control CE movements during gastrulation in conjunction with the PCP pathway (Munoz et al., 2006), however it is not entirely clear how it modulates this pathway. Munoz et al suggest that Syn4 is acting upstream of Dishevelled as inhibition of CE by a Mo against *syn4* can be rescued by activating Dsh using a constitutively active form. Additionally they suggest a direct interaction with Fzd7 and Dsh as they both co-precipitate with Syn4 in an immunoprecipitation assay. Any binding of Syn4 to Dsh is likely to take place via the PDZ binding domain of Syn4, since Dsh contains a PDZ domain (Wong et al., 2003). Munoz et al also demonstrate that Syn4 affects the membrane localisation of Dsh. Overexpression of *syn4* mRNA was able to induce translocation of Dsh to the plasma membrane in animal caps. Furthermore, inhibiting *syn4* with a morpholino prevents the translocation of Dsh to the membrane normally induced by fibronectin treatment. They present a model whereby Syn4 recruits Dsh to the plasma membrane following activation by fibronectin binding. Recruitment of Dsh and possibly also Fzd7 allows activation of the PCP pathway in response to non-canonical Wnt ligands. It will be interesting to see whether the observations of Munoz et al can be reproduced in the neural crest.

## 4.2. *syn4* is expressed in the migrating neural crest

Before analysing the effect of Syn4 on NC migration, it is important to verify that it is expressed during the correct time and place during development. *syn4.1* and *syn4.2* have identical expression patterns in *Xenopus* and are expressed in the dorsal mesoderm during gastrulation (Munoz et al., 2006) but the expression of *syn4* during later stages of development has not been analysed in detail. Therefore, *in situ* hybridisation was carried out to determine the spatial and temporal expression pattern of *syn4.1* during embryonic development (Fig 4.2). As gastrulation ends, *syn4* expression can be observed in a ring around the closing blastopore (Fig 4.2A). Later, this expression disappears and *syn4* is expressed in the neural tube and is particularly enriched at the mid-hindbrain boundary (Fig 4.2B). At this stage, neural crest tissue has been specified as illustrated by the expression of *snail2* (Fig 4.2C), however there is no overlap between the two genes and it appears that *syn4* is absent from the neural crest.

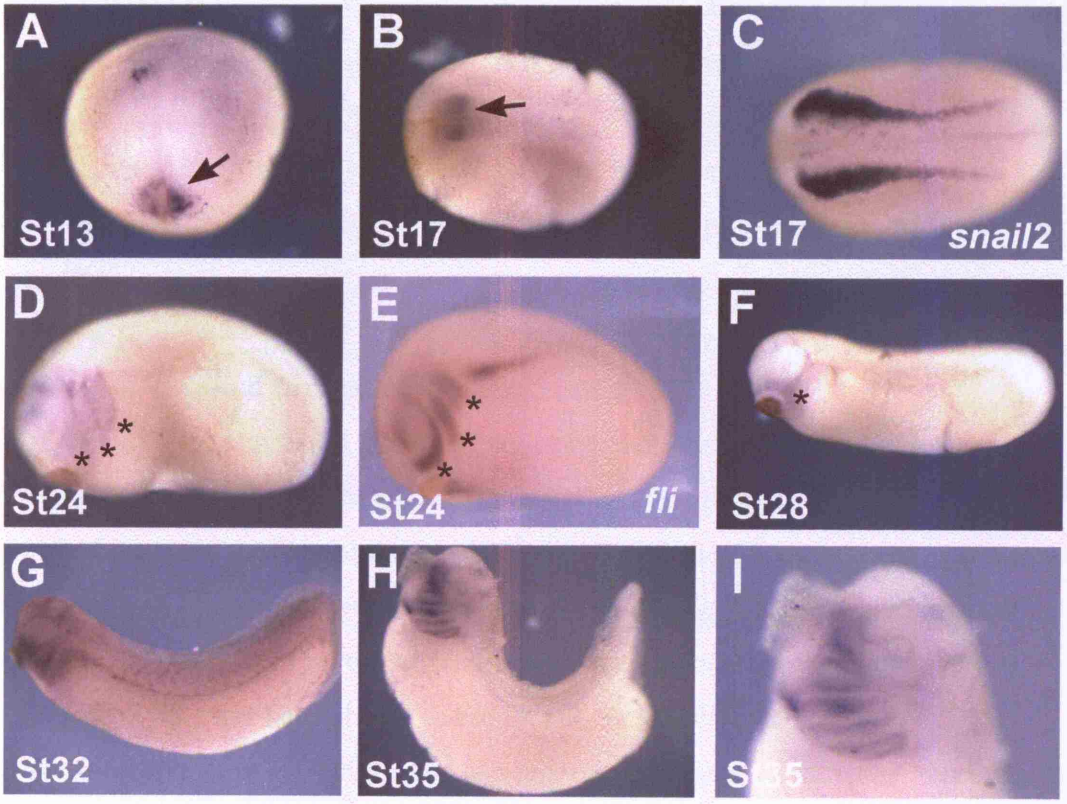


**Figure 4.2. Syndecan-4 is expressed in the migrating neural crest**

*In situ* hybridisation of *syn4* at various stages of development (A,B, E-I) and neural crest marker *snail2* (C) and *fli* (E) for comparison. **(A)** Dorsal view of stage 13 embryo. Anterior is to the top. Arrow shows expression around the blastopore. **(B,C)** Dorsal view of stage 13 embryos. Anterior is to the left. Note the difference in expression patterns between *syn4* and *snail2*. Arrow in B indicates midbrain-hindbrain boundary. **(D,E)** lateral view of embryos at stage 2. Anterior is to the left. Asterisks indicate three streams of migrating cranial neural crest. **(F-H)** Expression of *syn4* at later stages of development. Lateral view, anterior to the left. **(I)** Close-up of head region of st35 embryo. Note Syn4 expression in the NC-derived branchial arches.

Once the neural crest starts to migrate at stage 24 however, *syn4* expression can clearly be observed in the three streams of cranial neural crest (Fig 4.2D) in a similar pattern to the neural crest marker *fli* (Fig 4.2E). *syn4* can still be observed in the cranial neural crest as late as stage 28, when the neural crest cells enter the branchial arches (Fig 4.2F). At later stages, *syn4* is expressed in the brain and the pronephros (Fig 4.2G) and continues to be expressed at high levels in the branchial arches (Fig 4.2G-I). This highly localised expression of *syn4* in the migrating neural crest demonstrates that it is present at the right time to play a potential role in neural crest migration.

### 4.3. Syn4 is required for neural crest migration

Since Syn4 is expressed in the migrating cranial neural crest in *Xenopus*, I investigated a possible functional role for Syn4 in controlling NC migration. Morpholinos were used to inhibit *syn4* translation and the effect on the neural crest was visualised by *in situ* hybridisation against *snail2* (Fig 4.3). An equal mixture of two morpholinos that target the translation initiation sites of x*syn4*.1 and x*syn4*.2 were used, which has been shown to completely knock down Syn4 protein expression (Munoz et al., 2006). The Mo mixture was injected into *Xenopus* embryos at the 8-cell stage into blastomeres fated to become neural crest to avoid effects on gastrulation. Injection of 8ng and 16ng of Mo produced an effect on neural crest migration with some embryos exhibiting a severe phenotype with a complete inhibition of migration on the injected side (Fig 4.3C). Others showed a milder phenotype with a decreased distance of migration or migration inhibited only in some streams (Fig 4.3B). In total when 8ng Mo was injected 74% of embryos showed some defect in NC migration, while 16ng affected 86% of embryos (Fig 4.3F). These high percentages indicate an important requirement for Syn4 for cranial NC migration. In order to show that the Mo was specifically inhibiting *syn4*, a rescue experiment was carried out. The *syn4* Mo was co-injected with *syn4* mRNA, which contains a mutated translation start site that cannot be recognised by the Mo. Injection of 250pg of *syn4* mRNA was able to significantly reduce the number of affected embryos and in many cases completely restore NC migration (Fig 4.3E-F; 8ngMo + 250pg mRNA 34% show defects in migration).

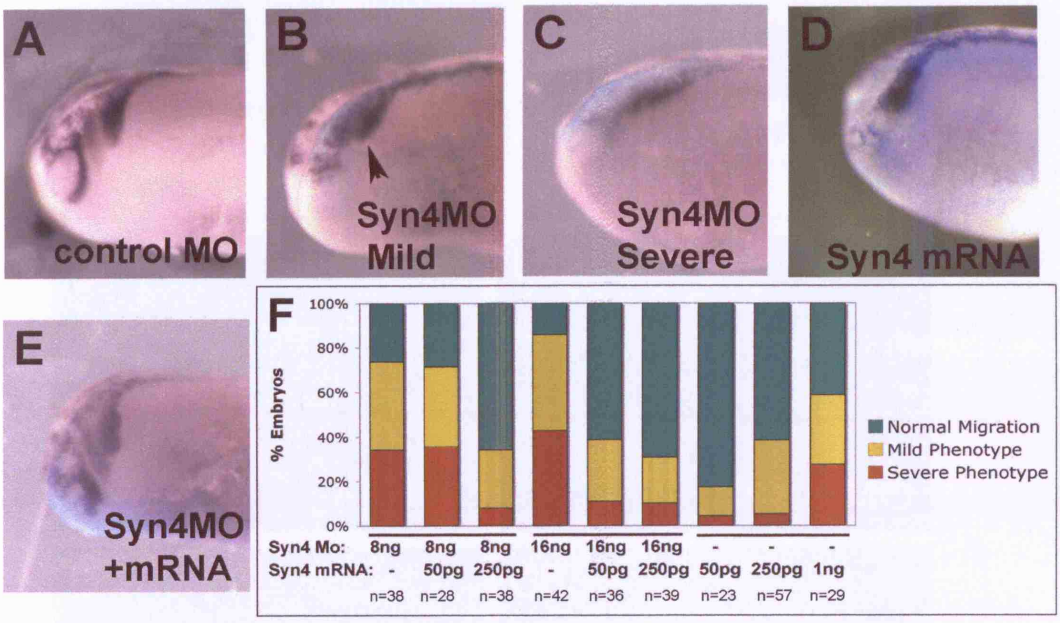


**Figure 4.3. Inhibition or overexpression of Syn4 inhibits cranial NC migration**

**(A-E)** Lateral view of stage 24 embryos with neural crest migration visualised by *in situ* hybridisation of *snail2*. Lateral view, anterior to left, head only is shown. Pale blue staining indicates FDX localisation and thus, site of injection. Representative embryos are shown for each phenotype. 8ng of Control Mo shows no effect on NC migration (A), while injection of 8ng of Syn4 Mo produces two NC phenotypes: mild (B) and severe (C). Arrowhead indicates residual migration in mild phenotype. Injection of 1ng Syn4 mRNA inhibits NC migration (D). Mo phenotype can be rescued by co-injection of 250pg Syn4 mRNA (E). **(F)** Graph showing the percentage of Embryos affected in each condition.

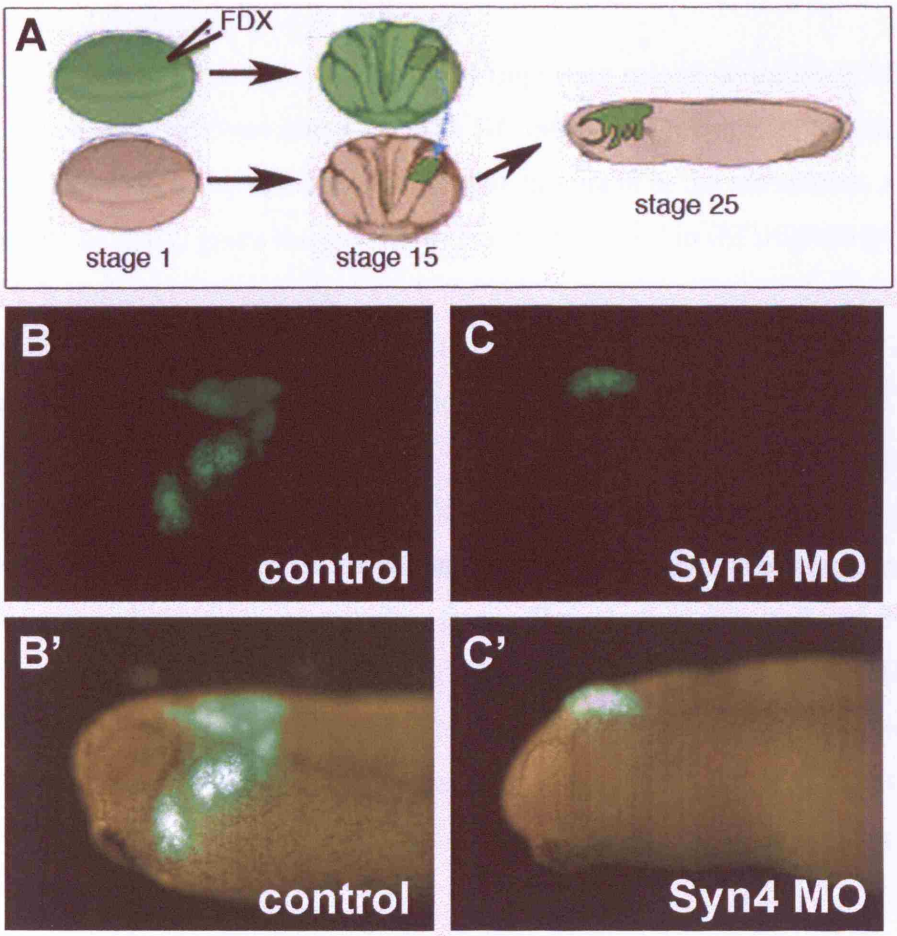


**Figure 4.4. The effect of Syn4 is cell autonomous**

**(A)** Embryos were injected with FDX and 8ng control or *syn4 Mo*; at stage 17 neural crests were dissected and grafted into an uninjected host embryo. NC migration was analysed at stage 25 by looking at FDX fluorescence. **(B)** Head region of a control embryo showing normal neural crest migration. Lateral view, anterior to left. Migration observed in 90% of embryos, n=10. **(C)** Head region of Syn4 Mo injected embryo where NC migration is inhibited. Migration observed in 0% of embryos, n=12.

Over-expression of *syn4* mRNA alone also produces a neural crest phenotype with injection of 1ng *syn4* mRNA able to completely inhibit neural crest migration in 58% of cases (Fig 4.3D, F). So, modulating Syn4 levels by either Mo knockdown or over-expression disrupts neural crest migration.

These data indicate that Syn4 plays an important role in neural crest migration, but it is possible that Syn4 interferes with NC migration in a non-cell autonomous manner, for example by affecting convergent extension in the mesoderm. Although this seems unlikely, given the specific expression of *syn4* in the migrating neural crest, it is nonetheless important to rule out this possibility. To test the cell-autonomy of Syn4 for NC migration, a neural crest graft experiment was performed (Fig 4.4). Embryos were injected with the *syn4* Mo alongside fluoroscein dextran (FDX) at the 2-cell stage in one blastomere. At stage 17, the cranial neural crest on the injected side was removed and grafted into a wildtype host embryo, which had had its neural crest removed (Fig 4.4A). This technique ensures that the Mo is only present in the neural crest and not in any surrounding tissue. Neural crests injected with FDX only are able to migrate in the host following the characteristic three pathways (Fig4.4B, 90% migrated n=10). However, neural crest injected with the *syn4* Mo were completely unable to migrate even in the control host (Fig 4.4C, 0% migrated n=12). This indicates that Syn4 is required in the neural crest cells themselves to control their migration.

### 4.4. Syn4 is not involved in NC specification

Syn4 is required for proper migration of the cranial neural crest in *Xenopus*, but it is necessary to eliminate the possibility that these effects are due to an earlier role that Syn4 may be playing in neural crest induction. To address this question, embryos were observed at stage 17 before neural crest migration has begun (Fig 4.5). Injection of 16ng *syn4* Mo was not able to elicit any effect on neural crest induction, with the expression of *snail2* appearing identical on the injected and uninjected sides of the embryo (Fig 4.5A). The same was true with injection of *syn4* mRNA (Fig 4.5B), although in some cases the crest was shifted slightly laterally. This can be explained by an expansion of the neural tube, as Syn4 is involved in neural induction in *Xenopus* and overexpression of *syn4* has been shown to promote neural fates (S. Kuriyama, unpublished data). However this is not at the expense of the neural crest, which remains present. To further demonstrate that Syn4 is not involved in NC

induction, an animal cap induction assay was carried out. Naïve ectoderm in the form of animal caps from stage 9 embryos was dissected and conjugated with dorsal lateral marginal zone (DLMZ) from stage 11 embryos (Fig 4.5C). When cultured alone until the equivalent of stage 20, animal caps do not differentiate to form neural crest tissue (Fig 4.5D, E). However, DLMZ acts as a powerful neural crest inducer and when cultured together with animal caps, neural crest tissue is specified and can be visualised by the expression of *snail2* (Fig 4.5F). In the presence of the *syn4* Mo this induction still occurs (Fig 4.5G), indicating that Syn4 is not required for cell fate specification in the neural crest.

### 4.5. Syn4 interacts with the PCP pathway in the neural crest

I have demonstrated an important requirement for both PCP signalling and Syn4 in neural crest migration. As Syn4 has been shown to interact with PCP signalling in the mesoderm (Munoz et al., 2006) it is likely that this interaction is also occurring in the neural crest. To test this hypothesis, two rescue experiments were performed (Fig 4.6). *syn4* Mo was co-injected with different concentrations of the constitutively active Dsh, DshΔN, into 8-cell stage embryos and neural crest migration was analysed by *snail2* expression at stage 24. Embryos were scored as normal migration, mild defects in migration and severe defects in migration as before (Fig 4.6 A-C). Injection of 8ng or 16ng of *syn4* Mo or 100pg of DshΔN alone all caused defects in migration in a high percentage of embryos (Fig 4.6 D 1$^{st}$, 5$^{th}$ and 10$^{th}$ bars). However when *syn4* Mo and DshΔN were injected together the percentage of affected embryos greatly decreased (Fig 4.6D). For example, 16ng *syn4* Mo causes migration defects in 96% of embryos (Fig 4.6D 5$^{th}$ bar), while injection of 100pg of DshΔN affects 66% of embryos (Fig 4.6D 10$^{th}$ bar) but when they are injected together this dramatically reduces to only 21% (Fig 4.6D 8$^{th}$ bar). Thus, the effect of *syn4* Mo can be rescued by activating the PCP pathway, suggesting that they are indeed acting in the same pathway to control NC migration. Furthermore, this suggests that Dsh is acting downstream of Syn4. To test this further, the reverse rescue experiment was also attempted. DshDEP+, which inhibits neural crest migration by inhibiting PCP, was co-injected with *syn4* mRNA (Fig 4.6E). Overexpression of *syn4* mRNA was not able to rescue the effect of DshDEP+ in the neural crest. When 1ng of DshDEP+ is injected 32% of embryos show NC migration defects (Fig 4.6E 1$^{st}$ bar) compared to 62% when DshDEP+ is co-injected with 350pg *syn4* mRNA (Fig 4.5E 4$^{th}$ bar).

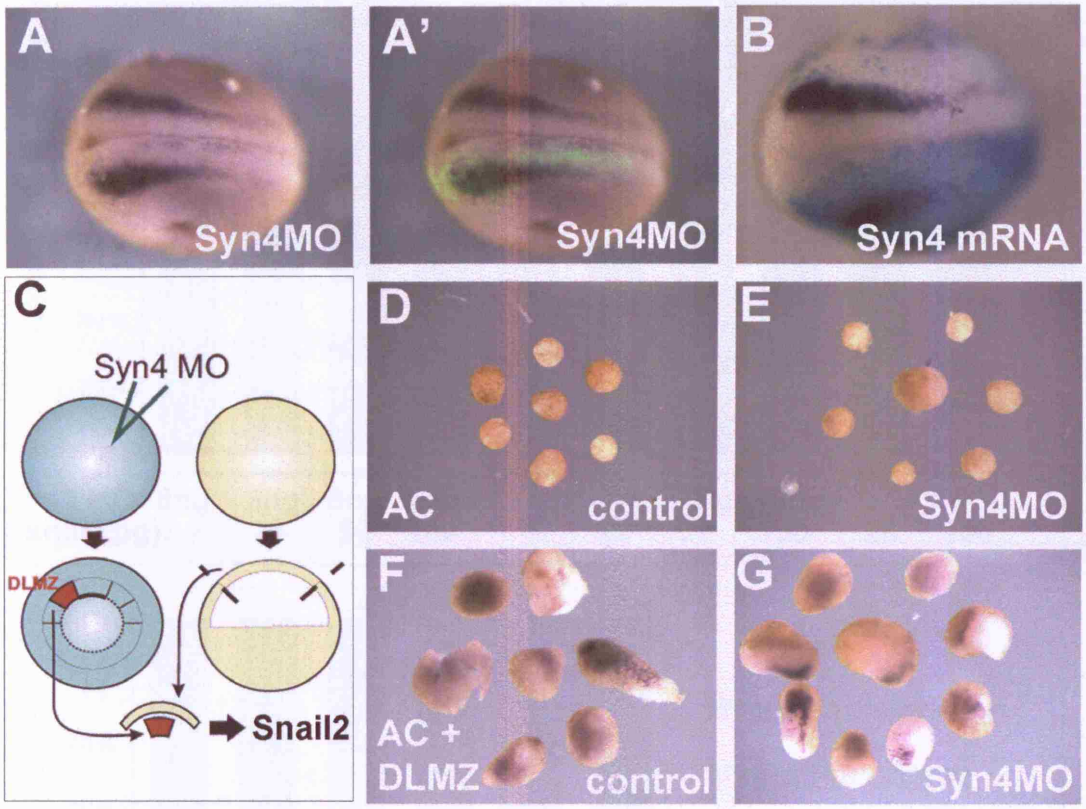


**Figure 4.5. Syndecan-4 does not affect neural crest induction**

**(A,B)** Dorsal view of stage 17 embryos with neural crest labelled by *snail2 in situ* hybridisation. Anterior is to left. Injection of 8ng *syn4* Mo (A, 95% n=42) or Syn4 mRNA (B, 89% n=27) do not affect *snail2* expression. The site of injection is indicated by green fluorescent overlay (A') or blue anti-FDX staining (B). **(C-G)** Neural crest induction assay. (C) 8ng of *syn4* Mo was injected into 1-cell stage *Xenopus* embryos and animal caps were dissected at the blastula stage and conjugated with dorsal lateral mesoderm, which is known to induce NC. The expression of *snail2* was analysed at the equivalent of stage 18. (D, E) Animal caps cultured alone do not express *snail2* (F) Conjugates of animal caps with DLMZ show a strong expression of *snail2*. 100% n=15. (G) Conjugates of *syn4* Mo injected animal caps with DLMZ also show a strong *snail2* induction. 100%, n=10.

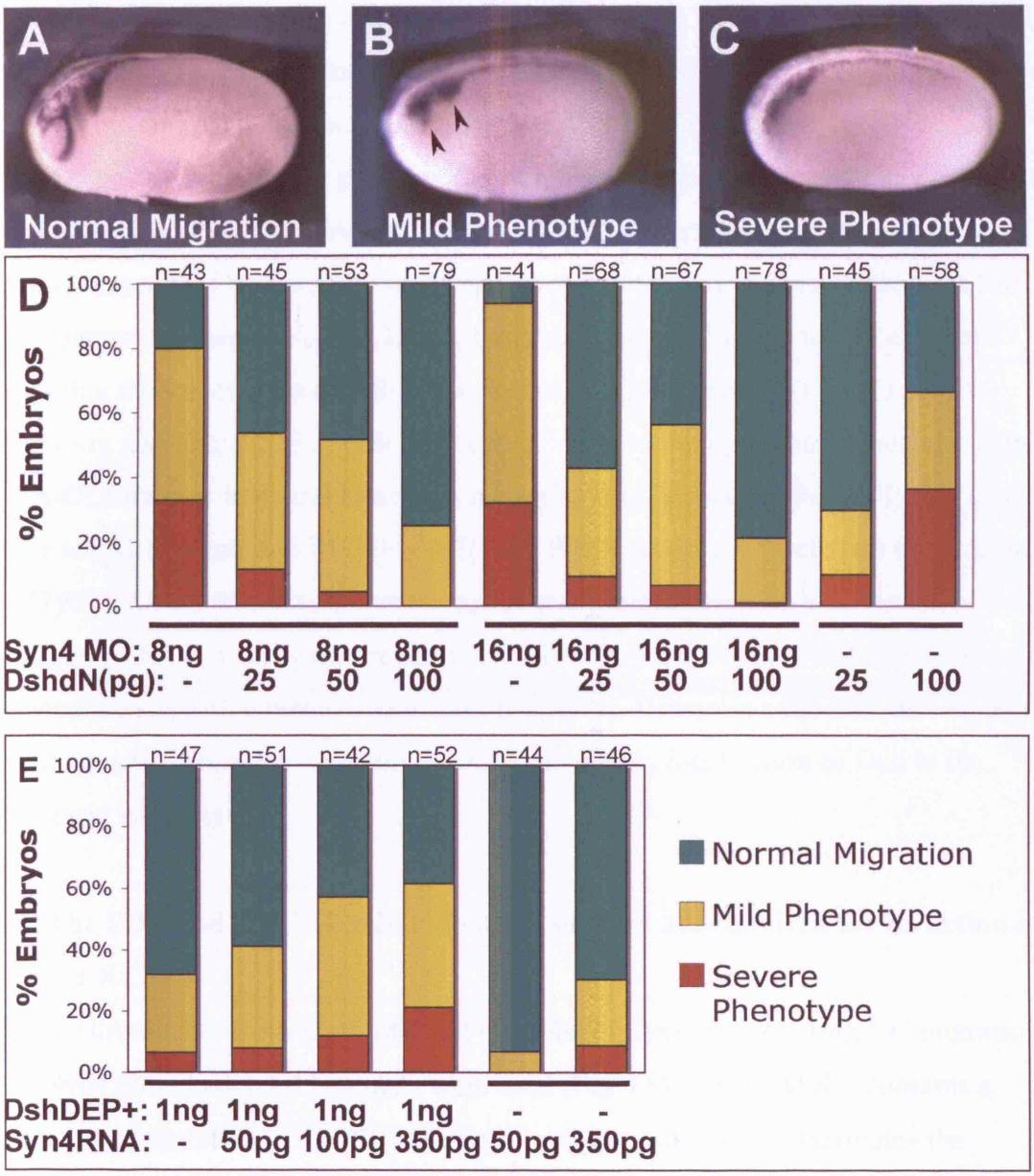


**Figure 4.6. The effect of Syn4 Mo can be rescued by activation of Dsh**

**(A-C)** Examples of the three neural crest phenotypes used to score embryos. Neural crest migration can be recognised by *snail2 in situ* hybrisation in stage 24 embryos. Lateral view, anterior is to the left. Arrowheads in B show residual migration in mild phenotype. **(D)** Graph showing phenotypes obtained by co-injection of different concentrations of *syn4* Mo and DshΔN. Note DshΔN is able to rescue *syn4* Mo phenotype e.g.compare 1st and 4th bars. **(E)** Graph showing phenotypes obtained by co-injection of different concentrations of Syn4 mRNA and DshDEP+. Note that activation of Syn4 is is unable to rescue DshDEP+ phenotype e.g.compare 1st and 4th bars.

The fact that activating Dsh can rescue the phenotype of inhibiting Syn4, but activating Syn4 cannot rescue dominant negative Dsh places Dsh downstream of Syn4 in the signalling cascade that controls neural crest migration.

As we have seen in the previous chapter, Dsh localises to the plasma membrane in migrating neural crest cells and this localisation is important for the activation of the PCP branch of Wnt signalling. Munoz et al (2006) have suggested that it is this localisation that requires Syn4. This hypothesis was tested in the neural crest by analysing the localisation of Dsh in the absence of Syn4 protein (Fig4.7). In pre-migratory neural crest cells, Dsh-GFP can be observed in cytoplasmic vesicles (Fig 4.7A-C), however in neural crest cells migrating on fibronectin Dsh-GFP co-localises with membrane-RFP (Fig 4.7D-F). When neural crest cells are taken from embryos injected with 8ng of *syn4* Mo, however, this membrane localisation is abolished. Dsh is once again visible in cytoplasmic puncta (Fig 4.7G) and shows no co-localisation with a membrane marker (Fig 4.7H, I) even in cells that are migrating on fibronectin. So, Syn4 is required for the membrane localisation of Dsh in the migrating neural crest.

## 4.6. The PDZ and PKCα binding domains of Syn4 are required for its action in the NC

To investigate the role of different domains of Syn4 in regulating NC migration, two Syn4 domain deletion mutants were used (Fig 4.8). xSyn4ΔPKC contains a YKK>LQQ mutation in the PIP2 binding site (Fig 4.8A), which facilitates the binding of PKCα (Horowitz et al., 1999).This mutation has been shown to prevent PIP2 recruitment and thus interaction with PKCα. A second mutant contains a C-terminal truncation, which results in the deletion of the final three amino acids, MEV, which have been suggested to act as a putative PDZ binding domain and potential binding site for Dsh (Fig 4.8A). Mutants were injected into *Xenopus* embryos at the 8-cell stage alongside the *syn4* Mo to test their ability to rescue the effects of the Mo. As before, 8ng *syn4* Mo has a strong effect on NC migration (Fig 4.8B 1$^{st}$ bar) that can be rescued by co-injection of 250pg *syn4* mRNA (Fig 4.8B 2$^{nd}$ bar, Fig 4.3F). However, co-injection of 250pg xSynΔPDZ (Fig 4.8B 3$^{rd}$ bar) or 250pg xSynΔPDZ (Fig 4.8B 4$^{th}$ bar) was not sufficient to rescue the effects of the Mo. This indicates that both of these domains are required for the activity of Syn4 in the neural crest.

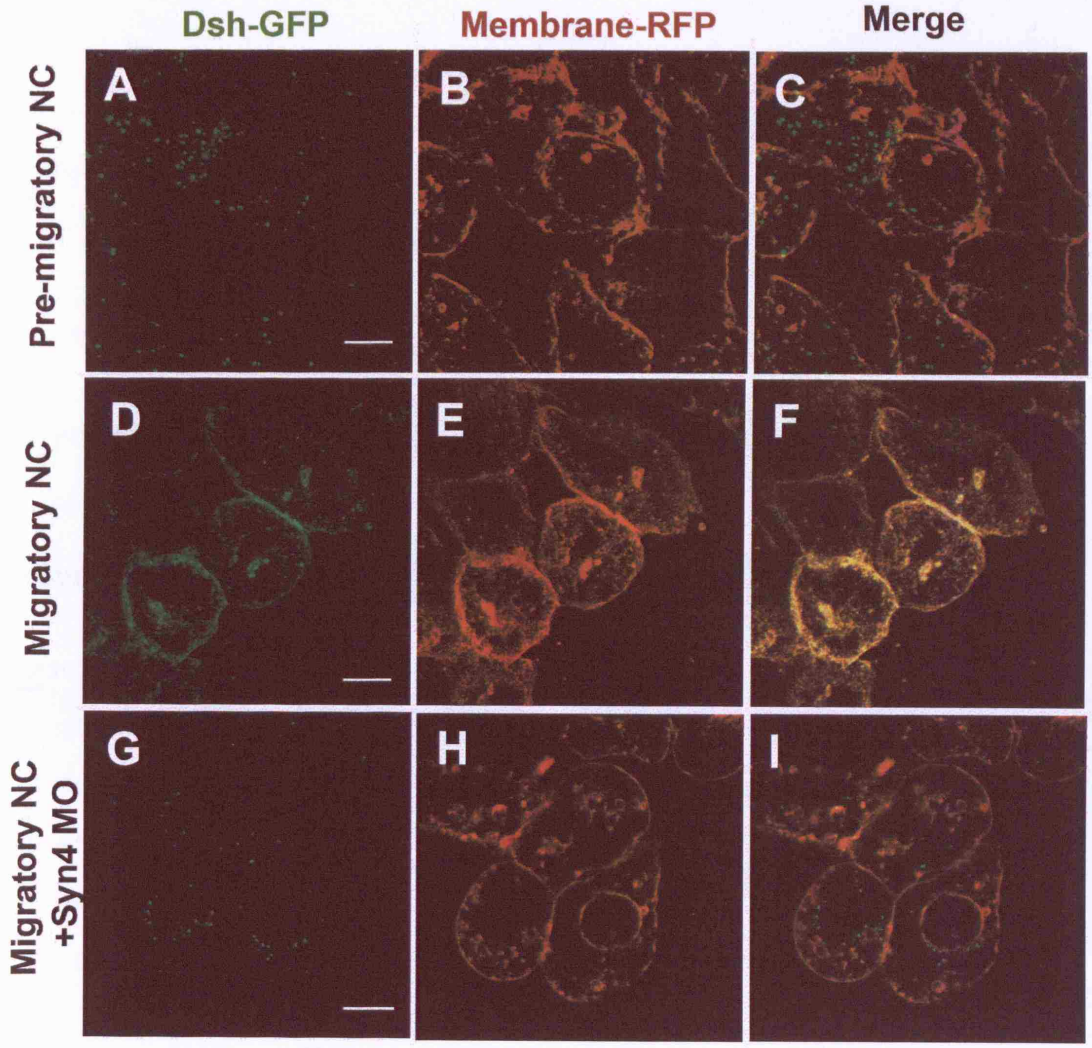


**Figure 4.7. Syn4 is required for translocation of Dsh to the membrane in migrating NC cells**

Embryos were injected with 75pg Dsh-GFP and 200pg membrane-RFP at the 8-cell stage. Neural crests were removed at stage 17 and cultured *in vitro*. NC explants were fixed and the localisation of Dsh (A,D,G) and membraneRFP (B,E,H) was observed by confocal microscopy. **(A-C)** Cells fixed immediately after attachment show no co-localisation of Dsh-GFP and membrane-RFP. **(D-F)** Cells allowed to migrate and fixed 3 hours after attachment have a clear co-localisation between Dsh and the membrane. **(G-I)** In NC cells co-injected with 8ng *syn4* Mo and cultured under the same conditions this membrane localisation was lost. Scale bars = 50 μm.

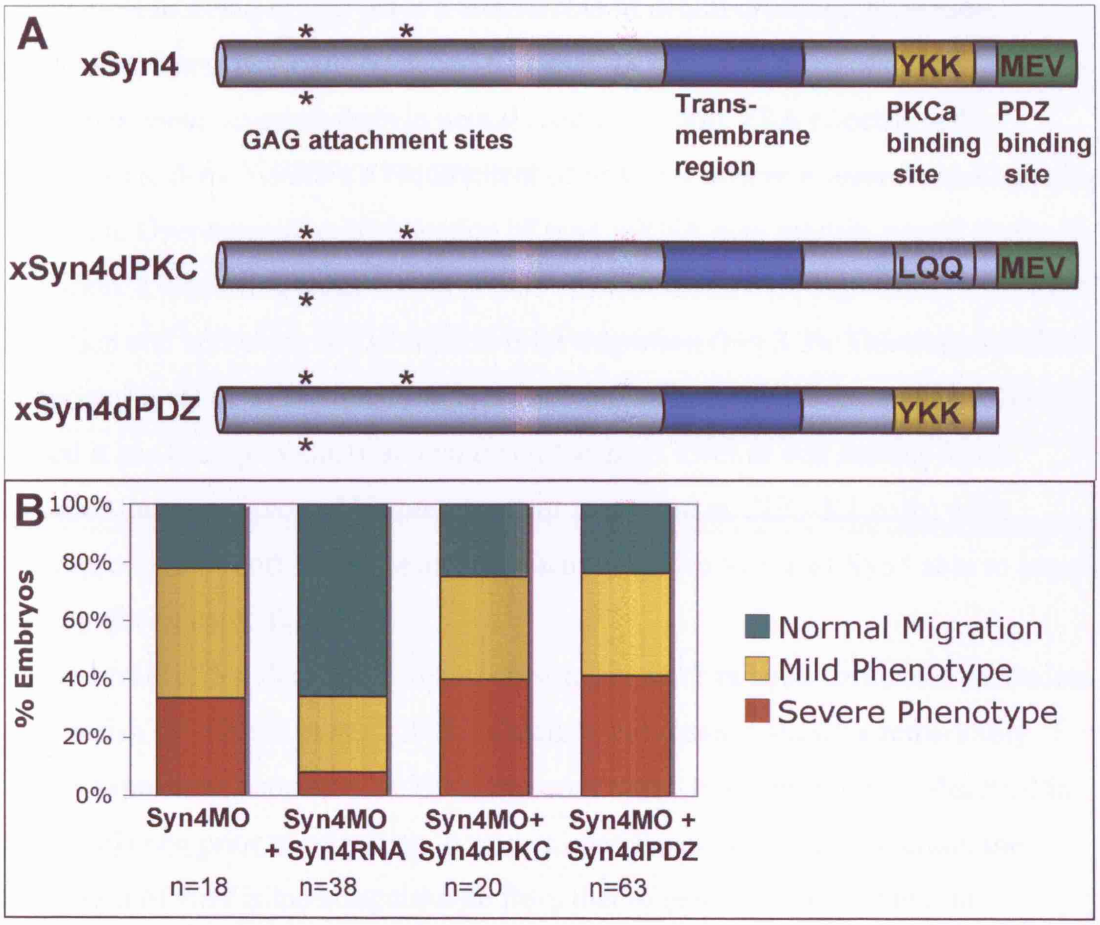


**Figure 4.8. The $PIP_2$ and PDZ binding domains of Syn4 are required for its action in the neural crest.**

**(A)** Domain structure of two Syn4 mutants. Syn4dPKC contains a YKK>LQQ mutation in the $PIP_2$ binding site. Syn4dPDZ is terminally truncated resulting in the removal of the PDZ binding site. **(B)** 250pg of full length Syn4, Syn4dPDZ and Syn4dPDZ were co-injected with 8ng *syn4* Mo. Neural crest migration was visualised by *snail2 in situ* hybridisation and phenotypes were scored as before (refer to Fig 4.6A-C for examples). Full length Syn4 mRNA was able to rescue the phenotype of *syn4* Mo (compare 1st and 2nd bar) but neither mutant was able to reproduce this effect (3rd and 4th bars).

## 4.7. Discussion

In this chapter I have shown that Syndecan-4 is expressed in the migrating neural crest in *Xenopus* and plays a crucial role in neural crest cell migration. Morpholino knockdown of Syndecan-4 does not affect neural crest induction, but morphants show severe defects in neural crest migration. This effect is cell-autonomous, demonstrating a requirement of Syn4 signalling in neural crest cells for migration. Overexpression by injection of *syn4* mRNA also inhibits neural crest migration, a result that parallels the effects of modulating PCP signalling, where both inhibition and activation of Dsh inhibit crest migration (Fig 3.3). This suggests that an optimal level of Syn4 signalling is required to achieve neural crest migration. Indeed it has been previously shown that a 'normal' level of cell surface Syn4 produces the most favourable conditions for migration in CHO-K1 cells, with overexpression of both wildtype and dominant negative forms of Syn4 able to impair motility (Longley et al., 1999).

This role of Syndecan-4 in neural crest migration has been confirmed in studies in zebrafish (Matthews et al., 2008). Zebrafish Syndecan-4 shows a remarkably similar expression pattern to its *Xenopus* counterpart. No expression is observed in the neural crest prior to migration, however once the crest starts to migrate, the expression of *syn4* is indistinguishable from that of neural crest markers. In zebrafish, *syn4* is expressed in both the migrating cranial and trunk neural crest, unlike in *Xenopus*, where it appears to be restricted to the cranial crest. However, low levels of expression in trunk neural crest cells cannot be entirely ruled out in *Xenopus* as trunk cells are difficult to identify and there are no good markers available. Inhibition of Syn4 in zebrafish by morpholino injection disrupts both cranial and trunk neural crest migration, as can be seen by *in situ* hybridisation against the zebrafish neural crest marker, *crestin* (Matthews et al., 2008). Additionally, over-expression of *syn4* by mRNA injection also inhibits neural crest migration. These zebrafish data strongly support those from *Xenopus*, which indicate a vital role for Syn4 in neural crest migration. The functional conservation of Syn4 in frogs and fish suggests that despite its structural differences in the cytoplasmic domain, it is likely to be the *Xenopus* Syn4 orthologue.

It has been suggested that Syn4 plays no real role in embryological development as the *syn4* knock-out mouse survives to adulthood and only shows relatively minor

defects in wound healing (Echtermeyer et al., 2001). However, the data presented here demonstrates that Syn4 plays an important role in the embryo, as it is required for neural crest migration, an essential process for the development of many tissues including the PNS and craniofacial skeleton. Indeed, zebrafish embryos lacking Syn4 allowed to develop to later stages show major defects in the cartilage of the head and jaw as well as an almost total lack of NC-derived melanocytes (Matthews et al., 2008). Studies in *Xenopus* have also shown a requirement for Syn4 during gastrulation and neural tube closure, two early and fundamental steps of development (Munoz and Larrain, 2006). Therefore it would be expected that inhibition of *syn4* would disrupt many aspects of development. This inconsistency highlights a possible difference in the role of Syn4 between mice and lower vertebrates such as fish and frogs. It could be that redundancy with other heparan sulphate proteoglycans in mice is able to compensate for the loss of Syn4. Individual knockouts for many HSPGs, including Syn1, Syn3 and Syn4, develop to adulthood with relatively subtle phenotypes (Alexander et al., 2000; Echtermeyer et al., 2001; Kaksonen et al., 2002; Reizes et al., 2001), however mice carrying a homozygous null-mutation in the gene EXT1, which codes for an enzyme that catalyses the construction of heperan sulphate chains show severe developmental defects and die at gastrulation (Lin et al., 2000). This demonstrates an important role for HSPGs during development, but in mice at least there is clearly some redundancy.

The effect of *syn4* morpholino on neural crest migration can be rescued by activation of PCP signalling, as has been previously demonstrated during *Xenopus* gastrulation (Munoz et al., 2006). This supports a clear involvement of Syn4 in PCP signalling. Syndecan-4 is not the first proteoglycan to be implicated in Wnt signalling and a number of proteoglycans have been described as acting as co-receptors in both the canonical and non-canonical pathways. For example, in *Drosophila* two members of the glypican family, dally and dally-like, facilitate canonical signalling by binding and stabilising wingless at the cell surface, thus regulating the range of wingless diffusion and the production of a gradient (Baeg et al., 2001; Lin and Perrimon, 1999; Strigini and Cohen, 2000). Syndecan-1 has also been implicated in canonical signalling and is required for Wnt-1 induced tumorigenesis in mice (Alexander et al., 2000). HSPGs have also been identified that act specifically in the PCP pathway including *knypek*/Glypican-4, which is required for PCP-dependent CE movements in zebrafish and *Xenopus* (Ohkawara et al., 2003;

Topczewski et al., 2001). It is not known how Glypican-4 interacts with the PCP pathway, although it does bind to both Wnt11 and Fzd7 in immunoprecipitation assays and therefore may be involved in presentation of non-canonical wnt ligands to their receptors (Ohkawara et al., 2003). It is possible that Syndecan-4 may also be acting in this way as a co-receptor for soluble PCP ligands such as Wnt11 or Wnt11R. However, Munoz et al (2006) have suggested an alternative mechanism whereby Syn4 is required upstream of PCP signalling for the recruitment of Dsh to the plasma membrane, which allows the activation of the PCP pathway in response to Wnt ligand binding to their receptors. The results presented here are consistent with this hypothesis as the *syn4* morpholino was able to inhibit the membrane translocation of Dsh normally observed when neural crest cells start to migrate (Fig 4.7). It is also likely that binding of Syn4 to fibronectin plays a role in this process as I have previously shown that plating on fibronectin is sufficient to induce Dsh translocation (Fig 3.8) in neural crest cells. Culture on fibronectin is also sufficient to induce membrane translocation of Dsh in *Xenopus* dorsal marginal zone explants (Marsden and DeSimone, 2001). In fact, several studies point to an important role for fibronectin in co-ordinating CE movements, where correctly aligned fibrils are required to polarize cells along the mediolateral axis (Goto et al., 2005; Marsden and DeSimone, 2001; Marsden and DeSimone, 2003). A similar mechanism could also be operating in the neural crest, with cells responding to signals from the polarised extracellular matrix, resulting in the recruitment of Dsh to the membrane and the activation of the PCP pathway required for migration. With interactions with both fibronectin and PCP elements, Syn4 is a good candidate to mediate this interaction.

An interaction between Syn4 and Dsh is supported by the rescue experiments described in this chapter, as Syn4 lacking the PDZ binding domain, the potential binding site of Dsh, is unable to rescue the effect of *syn4* Mo (Fig 4.8). In addition, my results also point to a requirement for PKCα activation downstream of Syn4 in the neural crest, as Syn4 mutated in the PKCα binding site was also unable to compensate for the effect of the morpholino. Signalling through PKCα is a well-established consequence of Syn4 activation *in vitro* and contributes to the Syn4-dependent stabilisation of focal adhesions. The Syn4 cytoplasmic domain forms oligomeric complexes, which bind the catalytic domain of PKCα, resulting in hyper-activation of the enzyme (Koo et al., 2006; Lim et al., 2003). Both Syn4 and PKCα localise to the substrate contacts of cells migrating *in vitro* and stabilise focal

adhesion complexes (Hyatt et al., 1990; Oh et al., 1997b; Woods and Couchman, 1994). In the neural crest also, it would seem that the downstream response to Syn4 signalling requires activation of PKCα.

In conclusion, Syn4 working via the PCP pathway is essential for neural crest migration in the embryo. Cell migration *in vivo* is, however, a complex process involving the co-ordination of many different cellular mechanisms. In the next chapter, I will address in further detail exactly how Syn4 and Dsh affect neural crest cell migration.

# 5. Results: A cellular basis for the effect of Syn4 and PCP Signalling in neural crest migration.

## 5.1. Introduction

In previous chapters I have shown that both Syn4 and PCP signalling are required for neural crest migration, however it is not clear how exactly they influence cell migration. Neural crest migration is a multi-step process beginning with an initial delamination from the neural tube, followed by the onset of cell migration, a process that requires constant guidance to keep neural crest cell to their correct pathways. Which stage of this migration is affected by Syn4 and the PCP pathway? Furthermore, how do individual neural crest cells behave when Syn4 or Dsh signalling is inhibited? In this chapter I attempt to address these questions by carrying out an in-depth analysis of neural crest cell behaviour under different conditions of Syn4 and PCP signalling. For this, I employ two different but complementary methods. Firstly, cranial neural crest cells will be dissected from *Xenopus* embryos and observed migrating *in vitro* on a fibronectin substrate. This allows high-resolution imaging and the characterisation of cell morphology. However, as Syn4 and PCP signalling modulate migration in the embryo, it is also important to gain an *in vivo* perspective. Additionally, some reports suggest that there may be some significant differences between the mechanisms of cell migration on a flat substrate and in a three dimensional matrix (Even-Ram and Yamada, 2005). For the *in vivo* analysis, I use a transgenic *sox-10:egfp* zebrafish line (Carney et al., 2006), which expresses GFP in neural crest cells. The aim of this chapter is to analyse changes in cell behaviour and morphology when Syn4 or Dsh signalling is modulated both *in vitro* and *in vivo*, with a particular emphasis on two physical aspects of cell migration; the formation of cell protrusions and the attachment to the substrate at focal contacts.

### *5.1.1. Cell protrusions and the actin cytoskeleton*

Directional cell migration requires a highly polarised actin cytoskeleton (Ridley et al., 2003). At the front of the cell, actin filaments form new protrusions to extend the membrane forwards, while thick actin bundles known as stress fibres take the strain under the cell body. Extension of protrusions at the leading edge is driven by

polymerisation of actin monomers to form actin filaments. Inherently polarised actin filaments are orientated with their faster growing 'barbed' ends towards the cell edge, where their extension drives membrane protrusion (Pollard and Borisy, 2003). The organisation of actin filaments at the leading edge differs to form two different types of cell protrusion. Broad, thin lamellipodia are formed by a branching network of cross-linked filaments, whereas spiky filopodia are composed of densely packed parallel bundles (Welch and Mullins, 2002). A number of protein complexes control the polymerization of actin at the leading edge. In lamellipodia, the main regulator of actin polymerization is the Arp2/3 complex, which binds to the sides of pre-existing actin filaments to promote the formation of a new branched daughter filament (Goley and Welch, 2006). The activity of Arp2/3 complex is dependent on various nucleation promotion factors, mostly members of the WASP/WAVE family, which are activated at the cell membrane (Takenawa and Suetsugu, 2007). Numerous other factors help to regulate actin polymerization in lamellipodia including profilin, which promotes self-nucleation, capping proteins that restrict polymerization close to the membrane to promote branching and filamin A and α-actinin, which serve to stabilize the entire network (See (Welch and Mullins, 2002) for review). Filopodia also have their own array of scaffold proteins, many of which are localized at their tips. For example, the Ena/VASP proteins bind the barbed ends of filopodial bundles to inhibit both capping and branching and therefore promote elongation of the filaments (Bear et al., 2002). The formation of both filopodia and lamellipodia at the front of the cell is a tightly controlled process, which requires co-ordination of a large number of structural and regulatory proteins.

### *5.1.2. Attachment to the substrate*

In addition to forming membrane protrusions, a migrating cell needs to attach to its surrounding substrate. Early interference reflection microscopy studies of cells migrating *in vitro* showed that attachment is not uniform, but that cells bind to the extra-cellular matrix at discrete foci (Curtis, 1964). These points of attachment, known as focal contacts or focal adhesions (FAs) have since been shown to be large protein complexes containing more than 50 different constituents (Zamir and Geiger, 2001), which play a key role in cell migration. Focal contacts act not only as transmembrane anchorage sites, physically linking the extracellular matrix to the actin cytoskeleton and allowing the cell to exert traction against its surroundings

(Beningo et al., 2001; Galbraith et al., 2002), but also transduce information about the state of the ECM into the cell (Wozniak et al., 2004). Focal adhesion formation begins with the engagement of Integrins in the membrane with the extracellular matrix, which is rapidly followed by the recruitment of a large number of other proteins. These include scaffold proteins that link to the actin cytoskeleton such as paxillin, vinculin, α-actinin and tensin, as well as enzymes including many tyrosine kinases such as focal adhesion kinase (FAK) and members of the src family (reviewed in (Zamir and Geiger, 2001). Focal contacts can be generally grouped into three categories depending on their size, sub-cellular location and component parts (Webb et al., 2002). The smallest, known as focal complexes, are found immediately behind the leading edge of the cell (Nobes and Hall, 1995b). These quickly mature to form larger focal adhesions, which are found at the periphery as well as more centrally and are often associated with the tips of actin protrusions (Ridley and Hall, 1992; Sastry and Burridge, 2000). Finally, fibriller adhesions are larger, elongated focal adhesions, which are enriched along the length of stress fibres under the cell body (Pankov et al., 2000). Different proteins are recruited at different stages of focal adhesion maturation. For example paxillin is rapidly recruited to nascent focal complexes at the leading edge, shortly followed by α-actinin (Laukaitis et al., 2001) while tensin and α5β1-integrin are found in the most mature fibriller adhesions (Pankov et al., 2000). For a cell to move forward, focal contacts also need to be disassembled. This occurs as both a rapid turnover and cycling of FA components in the lamella and by dismantling focal adhesions at the rear of the cell to facilitate detachment from the substrate (Webb et al., 2002).The assembly, disassembly and turnover of focal adhesions is a tightly co-ordinated process, which is crucial for cell migration.

Syn4 localises to focal adhesions and promotes their formation and maturation in fibroblasts (Echtermeyer et al., 1999; Saoncella et al., 1999; Woods and Couchman, 1994). Therefore, it may be playing a similar role in the neural crest. Focal adhesion formation has not been previously studied in *Xenopus* or zebrafish embryology. Several FA components have been cloned in fish and frogs and have been shown to play important roles in morphogenesis and tissue separation. For example, paxillin and phosphorylated FAK co-localise with fibronectin at the boundaries between the forming somites and in the notochord of zebrafish embryos (Crawford et al., 2003; Henry et al., 2001). FAK, along with vinculin and β-integrin,

is also found at the intersomitic junctions in *Xenopus* embryos and inhibition of FAK in *Xenopus* results in defects in somite formation and fibronectin matrix deposition (Hens and DeSimone, 1995; Kragtorp and Miller, 2006). However these studies have been confined to epithelial tissues and any role in cell migration during embryonic development has not been described. In fact, some controversy exists about the nature of focal adhesions *in vivo*. FAs have been characterised almost exclusively during *in vitro* migration and it has been suggested they may be an artefact of cells migration in 2 dimensions. Recent studies in artificial 3D matrices have found accumulations of focal adhesion proteins that appear very different in structure from the FAs observed *in vitro* (Cukierman et al., 2001; Even-Ram and Yamada, 2005). Therefore the study of focal adhesions in neural crest cells *in vivo* is of particular interest.

## 5.2. Syn4/PCP signalling affects the persistence but not the speed of neural crest cell migration

To observe the behaviour of neural crest cells under different conditions, cranial neural crest explants were taken from stage 17 *Xenopus* embryos, cultured on fibronectin and monitored by time-lapse photography (Fig 5.1). Figure 5.1A shows four frames of a one hour long time-lapse film of a cranial neural crest explant on fibronectin. After attachment to fibronectin, the mass of cells in the explant initially starts to spread out as a coherent sheet, moving away from the centre of the explant. By 60 minutes, cells on the edge of the sheet begin to break away from their neighbours and migrate away from the explant as individual cells. A similar pattern can be observed in neural crest explants taken from embryos injected with 8ng *syn4* Mo (Fig 5.1B). *syn4* Mo cells are able to attach to fibronectin and are highly motile. However, tracking of individual cell movements reveals a significant difference between the behaviour of cells expressing the control and *syn4* morpholinos. Cell trajectories were tracked by marking the nucleus of the cell at each one-minute time point over the 60-minute period and the paths taken by individual cells were plotted using ImageJ software (NIH). Cells migrating at the edge of the sheet and as individual cells were included in the analysis. Control Mo cells move persistently away from the centre of the explant to produce relatively straight trajectories (Fig 5.1 C, D, G). In contrast, *syn4* Mo cells move randomly and frequently change their direction of migration (Fig 5.1 E,F). This results in cell tracks that are curly and

frequently cross over themselves (Fig 5.1H). Cells over-expressing *syn4* mRNA were also analysed in this way (Fig 5.2). Interestingly, compared to controls (Fig 5.2 A-C), *syn4* mRNA cells showed a decreased motility. Although they were able to attach to the fibronectin-coated coverslip and migrate, their movement was severely impaired and once again the direction of migration appeared random with frequent changes of migration (Fig 5.2D-F). To quantify these difference in cell behaviour two different parameters were calculated; the average speed of cell migration (Fig 5.2G) and the persistence (Fig 5.2H). Neural crest cells expressing the control morpholino migrate with an average speed of 1.9μm/min. This is relatively fast compared to other cell types plated on fibronectin. Fibroblasts travel between 0.5 to 1μm/min on a similar concentration of fibronectin, although some cell types such as keratocytes can reach speeds of up to 10μm/min (Lauffenburger and Horwitz, 1996). Neural crest cells expressing the *syn4* Mo do not show any impairment of motility compared to controls, in fact they travel marginally faster with an average speed of 2.2μm/min. On the other hand, cells over-expressing *syn4* mRNA had a significant decrease in velocity with their average speed being 1.4μm/min. Both increasing and decreasing Syn4 levels has a significant effect on the persistence of cell migration (Fig 5.2H). Persistence gives an indication of a cell's commitment to continue moving in the same direction and is calculated by dividing the vectoral distance between the start and end position of a cell over a given time by the length of the actual path taken. Thus, persistence close to 1 indicates a straight migration pathway. Control neural crest cells have an average persistence of 0.65, while in the presence of the *syn4* Mo this is reduced to 0.36. This reflects the increase of random movement observed in *syn4* Mo cells. So, inhibiting Syn4 does not affect the intrinsic ability of cells to migrate, but rather they are unable to maintain a directional movement. Cells expressing *syn4* mRNA also saw a significant decrease in persistence compared to controls, with an average of 0.27. Thus, increasing Syn4 activity also results in a decrease in persistent migration as well as a decrease in speed, suggesting a more general impairment of motility.

Since Syn4 interacts with the PCP pathway to control neural crest migration, the effect of modulating PCP signalling on cell behaviour was also tested *in vitro* (Fig 5.3). Uninjected explants (Fig 5.3A-C) were compared to explants taken from embryos injected with DshDEP+ (a dominant negative of Dsh/PCP; Fig 5.3 D-F) or DshΔN (an activated form of Dsh/PCP; Fig 5.3 G-I).

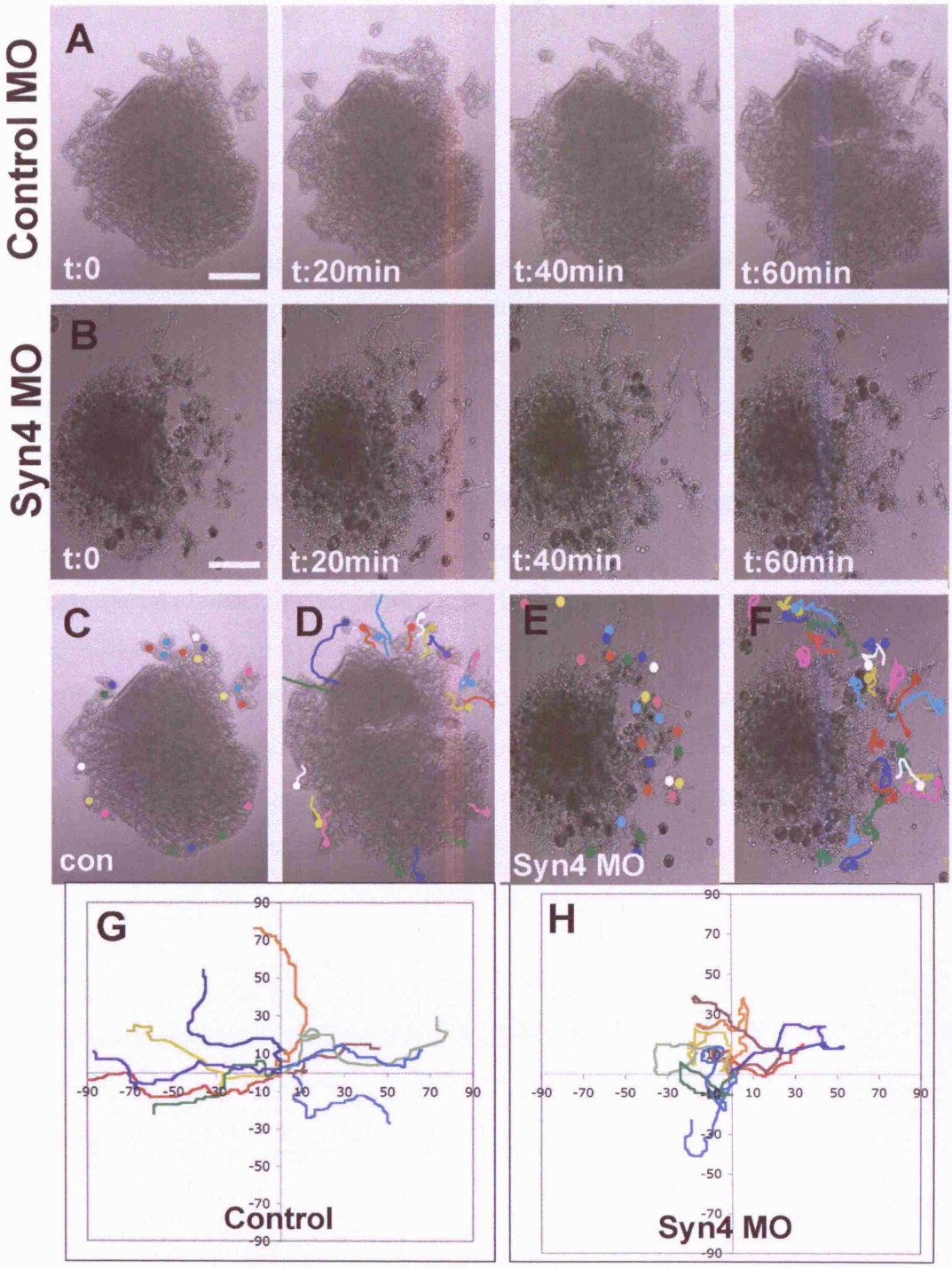
Control MO
Syn4 MO
A
B
C
D
E
F
G
H
t:0
t:20min
t:40min
t:60min
con
Syn4 MO
Control
Syn4 MO

**Figure 5.1**

**Figure 5.1. Syn4 is required for persistent migration of neural crest cells *in vitro***
Xenopus cranial neural crest explants were cultured *in vitro* on fibronectin coated coverslips and their migration was filmed over a 1 hour period. **(A)** Four frames of a 60-minute time-lapse film of a neural crest explant migrating on fibronectin, taken from an embryo injected with 8ng control Mo. **(B)** Four frames of a 60-minute time-lapse film of a neural crest explant migrating on fibronectin, taken from an embryo injected with 8ng *syn4* Mo. Scale bars = 200μm. **(C-F)** Manual tracking of individual cell migration pathways of control Mo cells (C,D) and *syn4* Mo cells (E,F). The first frame (A,E) and last frame (D,F, $60^{th}$ frame) of each 60-minute film is shown. **(G,H)** Individual cell tracks were plotted on a graph. Axis show distance travelled in X and Y in μm. Tracks appear different to D and F as they have been rotated 90° and have all been plotted from a common origin. Note the relatively straight persistent tracks of control Mo cells (G) compared to *syn4* Mo cells (H).

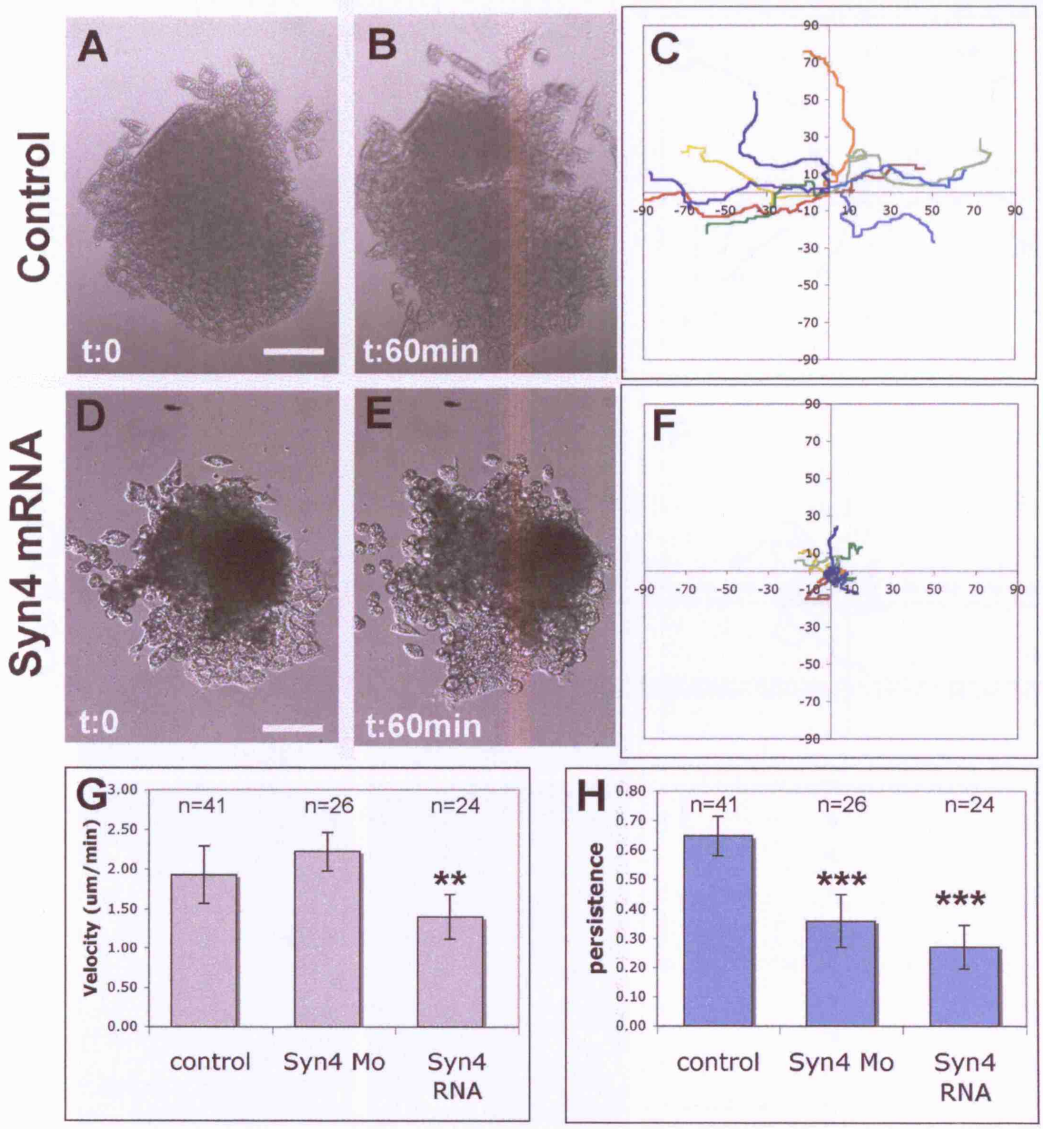


**Figure 5.2. Syn4 mRNA affects the persistence and velocity of neural crest migration *in vitro*.**

Cranial neural crest explants were cultured on fibronectin as before and individual cell trajectories were tracked. **(A,B)** Images from a timelapse film of control Mo neural crest cells as in figure 5.1. **(C)** Graph showing tracks of control neural crest cells as in Fig 5.1G. **(D,E)** A neural crest explant taken from an embryo injected with 1ng *syn4* mRNA. Images show two timepoints taken 60 minutes apart. **(F)** Individual cell tracks of *syn4* mRNA cells. Note the lack of migration compared to control cells. **(G)** Graph showing the average speed of neural crest cell migration in control, syn4 Mo and *syn4* mRNA expressing cells. **(H)** Graph showing the average persistence of neural crest cell migration in control, *syn4* Mo and *syn4* mRNA expressing cells. ***p<0.005 ; **p<0.01; scale bars = 200μm. n indicates number of cells, 3 (controls) or 2 (Syn4 Mo/mRNA) explants were analysed in each case.

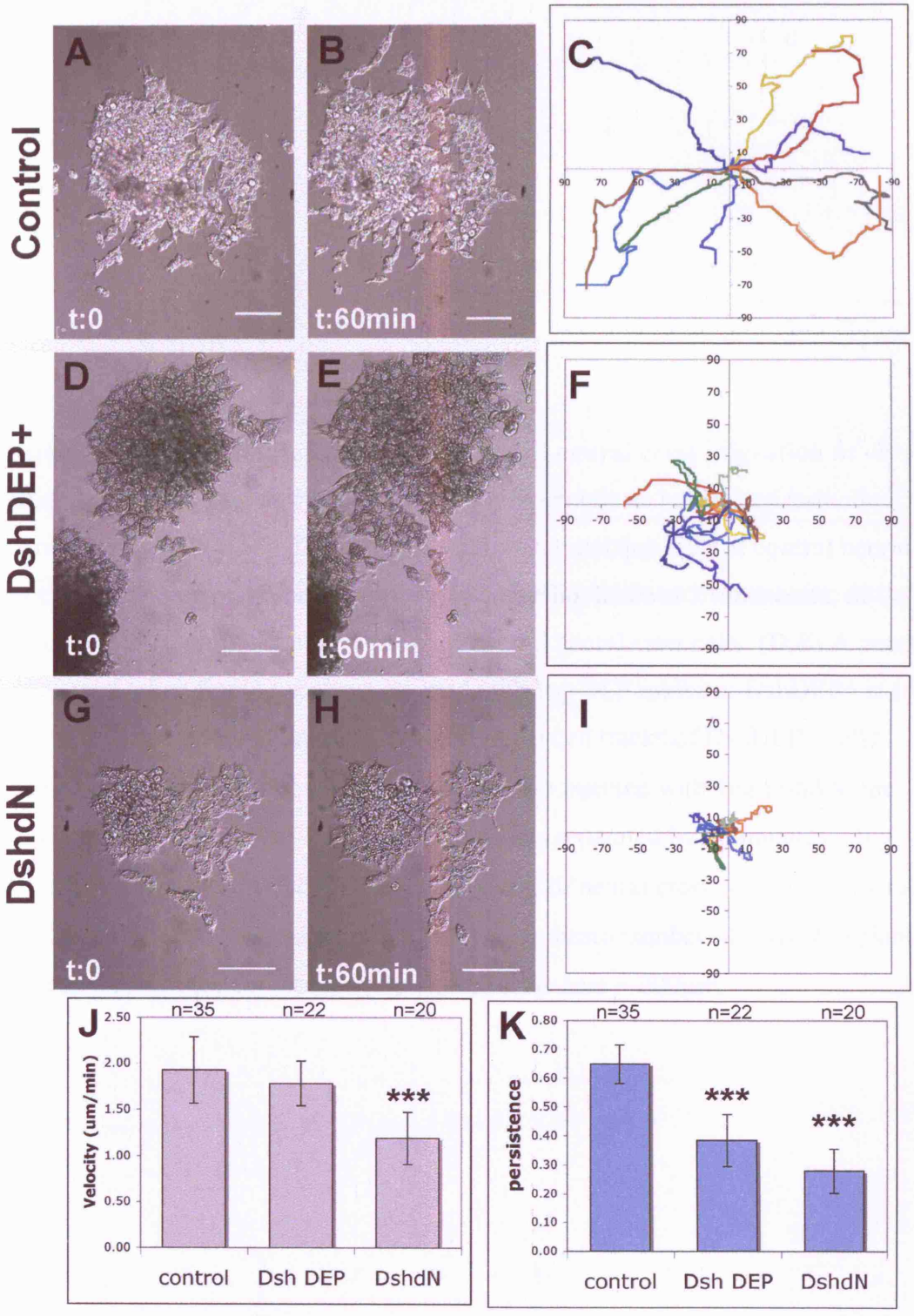
Control
DshDEP+
DshdN
A
B
C
D
E
F
G
H
I
t:0
t:60min
J
K
n=35
n=22
n=20
Velocity (um/min)
persistence
***
control
Dsh DEP
DshdN

**Figure5.3**

**Figure 5.3. Dishevelled affects the persistence of neural crest migration *in vitro***
Cranial neural crest explants were cultured on fibronectin as before and individual cell trajectories were tracked. **(A,B)** Images from a timelapse film of control neural crest cells migrating on a fibronectin-coated coverslip, taken at 2 timepoints, 60-minutes apart. **(C)** Individual cell tracks of control neural crest cells. **(D,E)** A neural crest explant taken from an embryo injected with 1ng PCP inhibitor DshDEP+ at two timepoints separated by 60 minutes. **(F)** Individual cell tracks of DshDEP+ cells. **(G,H)** A neural crest explant taken from an embryo injected with 1ng DshΔN, the constitutively active form of Dsh at two timepoints separated by 60 minutes. **(I)** Individual cell tracks of DshΔN cells. **(J)** Velocity of neural crest cell migration. **(K)** Persistence of neural crest migration. n numbers indicate number of cells, 2 explants were analysed in each condition. ***$p<0.005$; scale bars = 200μm.

Uninjected cells migrated persistently as those previously shown in cells expressing the control Mo (Fig 5.3 C). Inhibiting PCP signalling using DshDEP+ resulted in cell behaviour reminiscent of that observed when Syn4 is inhibited (Fig 5.3F). Once again the cells were able to attach to the fibronectin and migrate with no significant difference in speed compared to the controls (Fig 5.3J) but they did display a greatly reduced persistence (Fig 5.3K) of 0.38 compared to 0.64 in uninjected cells. Likewise, over-activating PCP signalling using DshΔN (Fig 5.3I) produced a phenotype similar to that resulting from over-expression of *syn4*. DshΔN cells were considerably less motile with a significant decrease in speed compared to control cells (Fig 5.3J). Additionally the directionality of migration was also affected with cells expressing DshΔN having an average persistence of only 0.28 (Fig 5.3K). In summary, the phenotypes observed by modulating the activity of Dsh closely mirrors that observed when Syn4 levels are altered. As with Syn4, the correct level of PCP signalling is required for persistent and directional migration of neural crest cells *in vitro*.

Neural crest cells migrating *in vivo* face a completely different environment to a fibronectin-coated coverslip and therefore it is important to ascertain whether these observations also hold true *in vivo*. *In vivo* imaging in *Xenopus* presents many technical difficulties with high levels of background fluorescence from the dense yolky particles making it impossible to image more than a few cells deep. Therefore, zebrafish embryos were used for *in vivo* analysis. A single copy of *syn4* has been identified in zebrafish, which has not yet been mapped to a chromosome (Whiteford and Couchman, 2006). Zebrafish Syn4 retains the conserved regions of the C1 domain, which are lacking in *Xenopus* (See Fig 4.1 for sequence alignment), however like *Xenopus* Syn4, it is also required for neural crest migration (Matthews et al., 2008). To analyse neural crest migration in zebrafish, I utilized a *sox10:egfp* transgenic line, which expresses GFP only in the neural crest (Carney et al., 2006). The movement of individual cephalic neural crest cells was followed over a time period of 4 hours and their migration pathways were tracked (Fig 5.4). It is worth noting that only cranial neural crest cells were used for this analysis although similar effects were also observed in the trunk neural crest. This is because the *in vitro* analysis used only cephalic crest, as the trunk cells in *Xenopus* form a more disperse population and are not easily separated from the surrounding tissue. Furthermore, the

effect of *syn4* Mo has only been analysed in the cranial neural crest (Fig 4.3). Fig 5.4 A-D shows a time-lapse sequence of cranial neural crest migration in a control Mo injected embryo covering 4 hours of development, while figure5.4F-I shows the equivalent *syn4* Mo injected embryo. Over this time period, control neural crest cells disperse over a significant area (Fig 5.4D) and their tracks reveal a highly directional migration away from the neural tube (Fig 5.4E). The cells travel at an average speed of 2μm/min, a similar speed to *Xenopus* neural crest cell migrating *in vitro*. In the *syn4* morphant neural crest cells are highly motile and are clearly able to delaminate from the neural tube epithelium as cells can frequently be observed outside the neural tube (Fig 5.4I). However most cells fail to travel any distance away from the neural tube and tracking of individual cell pathways shows a random migration with frequent changes of direction (Fig 5.4J). As with the *in vitro* system, *syn4* morphant cells show no significant difference in speed compared to control cells (Fig 5.4K), but their persistence of migration is reduced (Fig 5.4L). This confirms that *in vivo* as well as *in vitro* Syn4 does not interfere with the intrinsic ability of neural crest cells to migrate but instead is involved in regulating the directionality of migration. To further assess the directionality of migration, the angle of migration was measured for each individual cell at each time point. The distribution of angles showed a significant difference between controls (Fig 5.4M) and *syn4* Mo expressing cells (Fig 5.4N), with *syn4* Mo cells showing a much wider distribution of angles reflecting their movement in many different directions.

### 5.3. Syn4 and PCP signalling control the directionality of cell protrusions.

As persistence of migration usually depends on the directional formation of cell protrusions, I analysed the effect of modulating Syn4 and Dsh on cell protrusion formation. Higher magnification images and time-lapse movies were used to analyse the shape of *Xenopus* neural crest cells migrating on fibronectin under different condition (Fig 5.5). Control cells show a highly polarised morphology reminiscent of typical migratory cell types such as fibroblasts, with extensive lamellipodia forming at the leading edge and a lagging edge devoid of cell protrusions. Time lapse analysis over a 20 minute interval (with frames taken every one minute) shows that extension of cell protrusions occurs only at the leading edge while retraction occurs at the very back of the cell with very little change along the lateral edges (Fig 5.5 A-C). In contrast, *syn4* Mo cells are much more dynamic and lack any clear polarity.

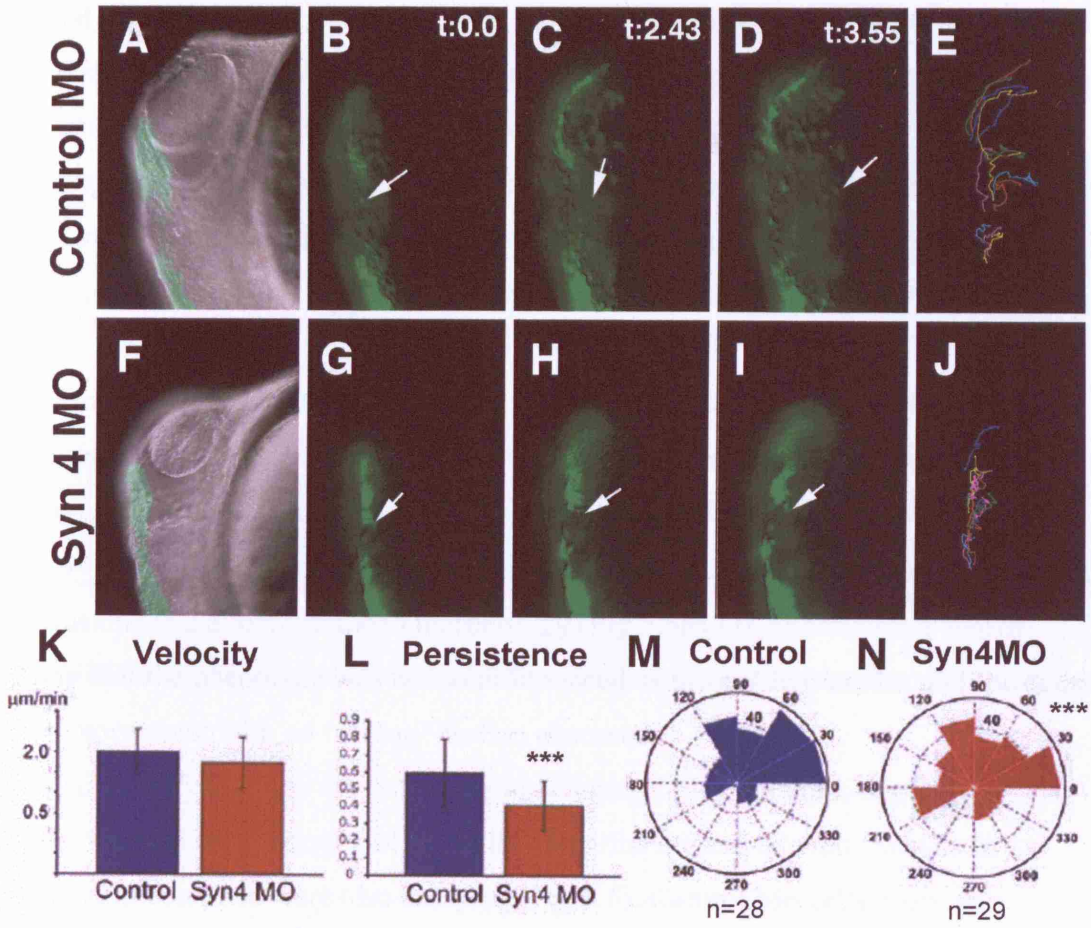


**Figure 5.4. Syn4 is required for persistent migration *in vivo*.**

A *sox10:egfp* zebrafish transgenic line was used to analyse neural crest migration *in vivo*. **(A-D, F-I)** Timelapse sequence showing cranial neural crest migration in embryos at 16hpf for 4hours, three frames are shown (t= 0 hours, t=2h43, t=3h55). A and F show the first frame overlapped with a DIC image, dorsal is to left, anterior to top. Arrow indicates an individual cell as an example. (A-D) An embryo injected with 6ng control Mo (F-I) An embryo injected with 6ng *syn4* Mo. **(E)** Trajectories of control Mo cells over 4 hours of migration. **(J)** Trajectories of *syn4* Mo cells over 4 hours of migration. **(K)** Velocity of migration **(L)** Persistence of migration. **(M,N)** Roseplot showing the distribution of angles at each time point during the 4 hours of migration. The area of each bin represents the number of cells moving in each direction. (M) Control Mo (N) *syn4* Mo. At least two embryos were analysed in each condition. ***p<0.005

Over a 20-minute period lamellipodia and filopodia are extended in all directions around the cell periphery (Fig 5.5 D-F). While *syn4* Mo cells have an increase in cell protrusions, cells over-expressing *syn4* mRNA have a marked lack of cell protrusion formation. These cells have a smooth, rounded morphology with no identifiable lamellipodia or filopodia (Fig 5.5G-I). The cells are alive and can be observed to constantly move, but with a rolling rather than crawling movement. However, although the peripheral regions of the cell are fairly dynamic, the body remains static.

Once again, modulating Dsh signalling has a similar effect to Syn4. Inhibiting PCP signalling using DshDEP+ results in depolarised cells that produce many cell protrusions around the entire membrane (Fig 5.5J-L), similar to what was observed in *syn4* Mo cells. Likewise, DshΔN expressing cells have a decreased number of cell protrusions and a more rounded morphology (Fig 5.5M-O), although it is worth noting that the phenotype was not so pronounced as in *syn4* RNA cells, and the cells were more static with no 'rolling' motion observed.

To identify whether these changes in cell morphology are also apparent *in vivo*, higher magnification images of NC cells migrating around the optic vesicle in *sox10:egfp* zebrafish were also analysed (Fig 5.6). Control Mo cells show an elongated morphology and are uniformly aligned along the axis of migration (Fig 5.6A, B). However when Syn4 is inhibited, the cells appear more rounded with no obvious alignment (Fig 5.6D, E). Likewise, cells lacking Dsh activity also appear more rounded with no clear polarity (Fig 5.6G-H). To quantify the effect on cell protrusions, the 'cell extension area' was calculated for each of these treatments. I define cell extension as the new positive area of a cell formed between two consecutive frames (separated by 1 min). During this time the body of a cell (and centroid) does not move significantly, which suggests that these cell extensions mostly correspond to cell protrusions such as lamellipodia. It is unlikely that filopodia can be observed, however, as their rapid movement and small area mean that the intensity of fluorescence would be much weaker. In control cells most cell extension can be observed at the anterior of the cell at the 'leading edge', the direction in which the neural crest is migrating (red area in Fig 5.6C). However cells lacking Syn4 (Fig 5.6F) or Dsh (Fig 5.6I) produce extensions in all directions around the cell.

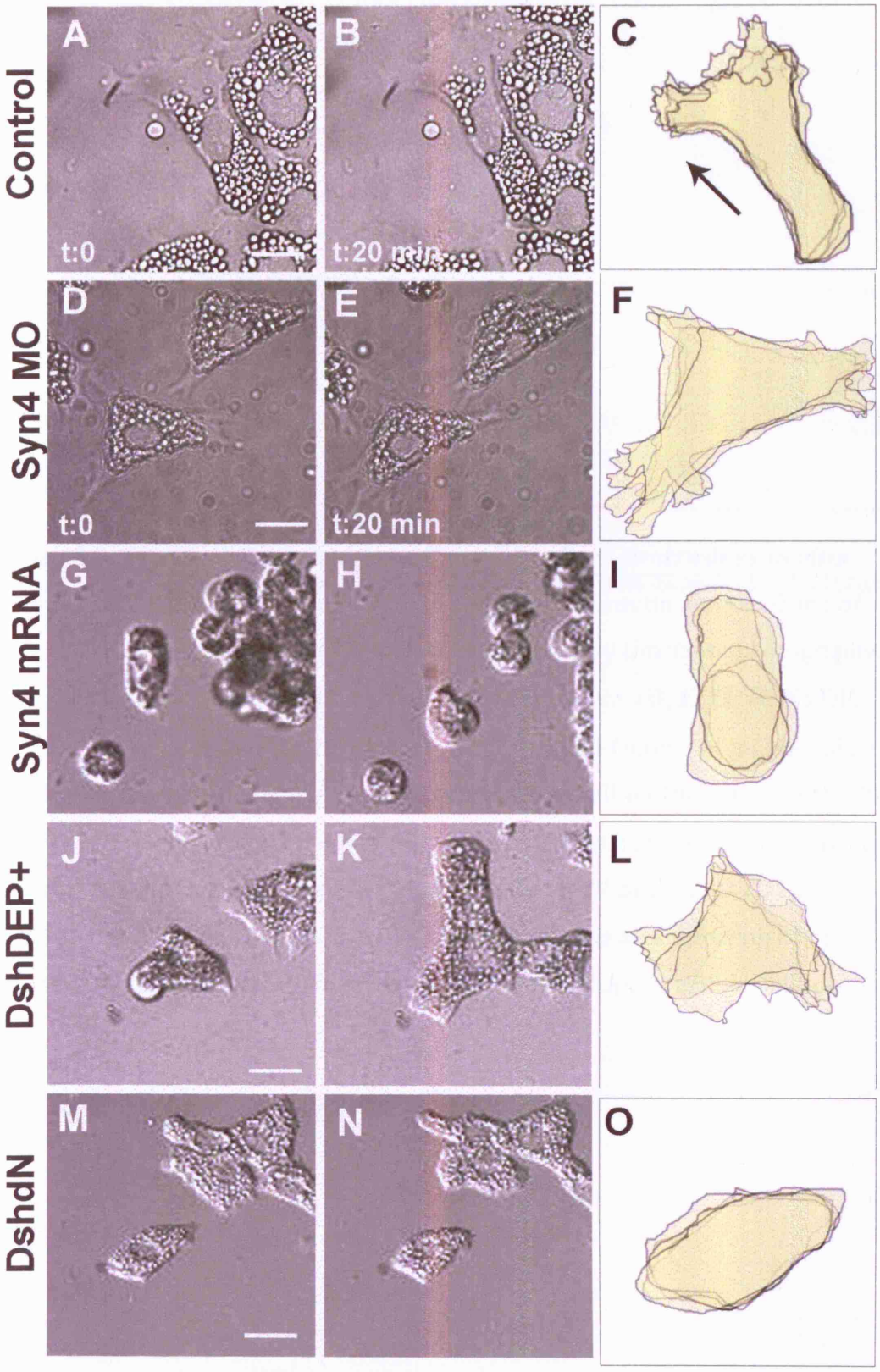
Control
A
t:0
B
t:20 min
C
Syn4 MO
D
t:0
E
t:20 min
F
Syn4 mRNA
G
H
I
DshDEP+
J
K
L
DshdN
M
N
O

**Figure 5.5**

**Figure 5.5. Syn4 and Dsh control the formation of cell protrusions *in vitro***

*Xenopus* cranial neural crest cells were cultured on fibronectin and the shape of individual cells was observed over a 20-minute period by timelapse photography. **(A, D, G, J, M)** DIC image of cells at t=0. Scale bars = 20μm. **(B, E, H, K, N)** DIC image of the same field after 20 minutes. **(C, F, I, L, O)** Outline of individual cell shapes plotted every 5 minutes to show the change in cell protrusions over the 20-minute time period. Images not to scale. Cell were taken from control embryos (A) and embryos injected with 8ng *syn4* Mo (D-F), 1ng syn4 mRNA (G-I), 1ng DshDEP+ (J-L) and 1ng DshΔN (M-O). Arrow in C indicates direction of cell migration. Examples shown are representative of cell shape in each condition.

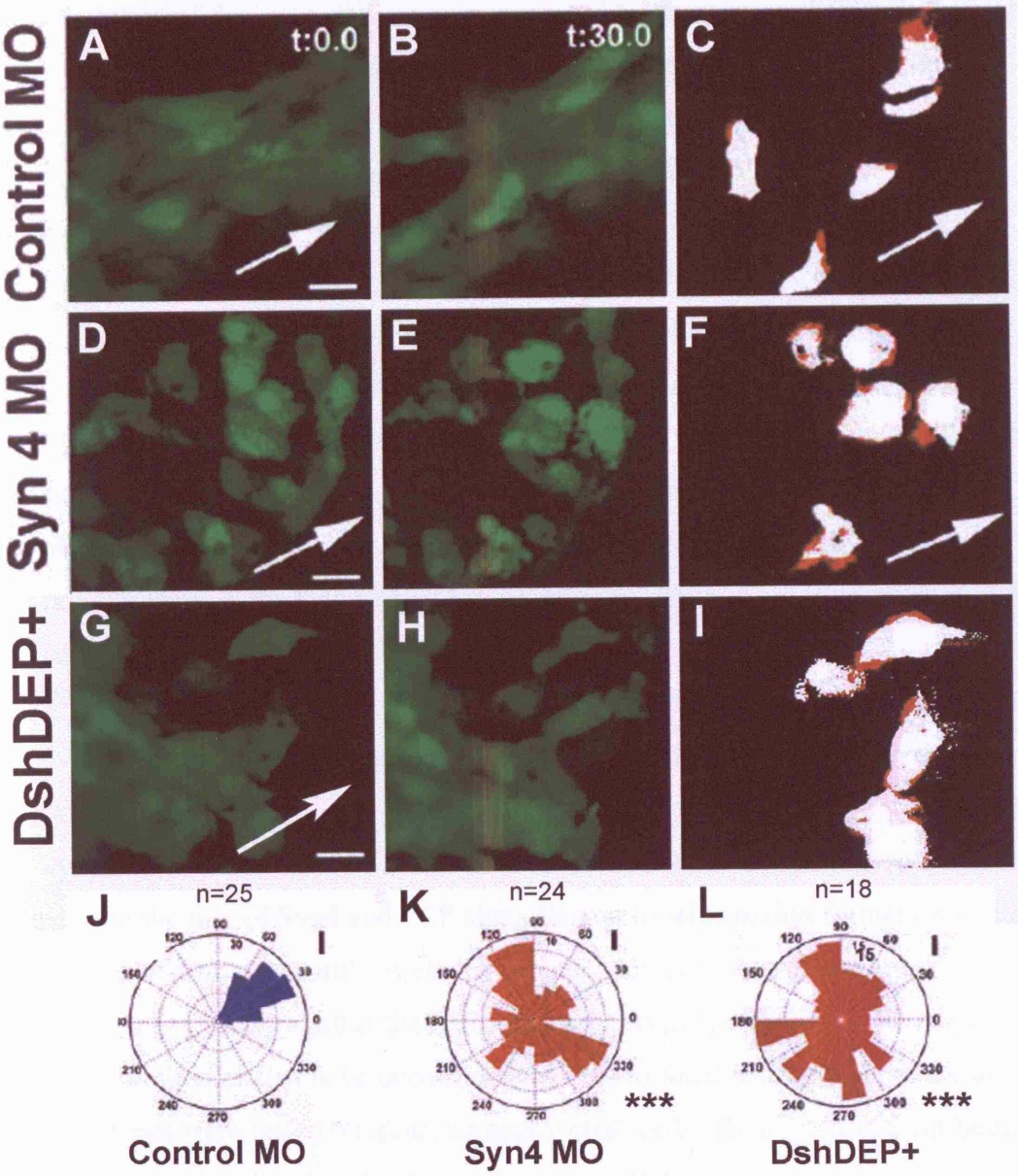


**Figure 5.6. Syn4 and Dsh control the formation of cell protrusions *in vivo***

**(A, B, D, E, G, H)** Time-lapse analysis of the mandibular neural crest stream of a *sox10:egfp* zebrafish embryo at 18hpf for 30 minutes. The initial and final frames are shown. Arrows indicate the expected direction of migration based on the orientation of the embryo, scale bars = 25μm. **(C, F ,I)** Outlines of individual cells taken from time-lapse analysis. Red area indicates the new cell extensions formed over the 30-minute period. (A-C) Embryo injected with 6ng control Mo (D-F) Embryo injected with 6ng *syn4* Mo (G-I) Embryo injected with 300pg DshDEP+. (J-L) Rose plots showing the orientation of cell extension over 30 minutes in control Mo (J), *syn4* Mo (K) and DshDEP+(L) injected embryos. At least three embryos were analysed in each condition. ***p<0.005.

The orientation of the cell extension was measured by calculating the direction of the vector that goes from the centroid of the cell to the centre of the new cell extension area. A significant difference in the orientation was observed between control Mo cells (Fig 5.6J) and *syn4* Mo (Fig 5.6K) or DshDEP+ (Fig 5.6L) cells.

Taken together, these results indicate that both Syn4 and Dsh regulate the polarized formation of cell protrusions *in vitro* and *in vivo*. These changes in cell morphology underlie the differences observed in cell behaviour. Cells that form protrusions in all directions such as those where Syn4 or Dsh is inhibited will be unable to maintain a persistent migration as protrusions in new directions will result in frequent changes of direction. On the other hand, cells where formation of protrusions is inhibited, such as Syn4 or Dsh over-expression, will also lack directional migration through lack of cell protrusions required to move in the 'correct' direction.

## 5.4. Syn4 and Dsh signalling control the formation of paxillin-containing focal contacts *in vitro*

Syndecan-4 is known to be a regulator of focal adhesion formation, so I investigated the role of Syn4 and PCP signalling on focal adhesion formation in the neural crest. Although several FA elements have been cloned in *Xenopus* and zebrafish, no antibodies against these proteins are currently available. Therefore, a number of antibodies that have been shown to bind to focal adhesion elements in other cell types were tested on *Xenopus* neural crest cells. These included antibodies against β1-integrin, vinculin, focal adhesion kinase (FAK), phospho-FAK, paxillin and phospho-paxillin. Out of these, only phospho(Y118)-paxillin (Biosource) revealed any specific staining in *Xenopus* neural crest cells (Fig 5.7). In control neural crest cells, p-paxillin accumulates in discrete puncta (Fig 5.7A) as has been described in many other cell types. Co-staining with rhodamine-phalloidin, which binds to filamentous actin, reveals co-localisation with the ends of actin filaments in cell protrusions (Fig 5.7B, C) suggesting that these are focal adhesions rather than smaller focal complexes. Focal complexes can be too small to recognise in some fast moving cell types (Webb et al., 2002) and this could be the case in the neural crest. It is not possible to distinguish for certain between focal complexes and focal adhesions, so for ease of reference I shall simply refer to these paxillin accumulations as focal contacts (FC). Cells from embryos injected with the *syn4* Mo

and nuclear-GFP (used so that injected cells could be easily identified *in vitro*) show a decrease in phospho-paxillin (ppax) staining with very few focal contacts visible under the same conditions (Fig 5.7 D-F). Phalloidin staining (Fig 5.7E) also illustrates the increase of cell protrusions in *syn4* Mo cells compared to controls (Fig 5.7B). In contrast, cells over-expressing *syn4* mRNA showed an increase in the number of paxillin-containing focal contacts (Fig 5.7G-I) compared to controls. Furthermore, many of the focal contacts appeared much larger, with some elongated along the length of the actin bundles, resembling mature fibriller adhesions. To accurately compare different conditions, the number of focal contacts per cell was counted (Fig 5.7J, expressed as no. FCs per $\mu m^2$ to allow for variety in cell size). The size of individual focal contacts was also measured and averaged over a number of cells (Fig 5.7K). *syn4* Mo cells showed a significant decrease in both FC number and size while *syn4* mRNA cells had a significant increase in both parameters. Therefore, an increase in Syn4 activity correlates with an increase in focal contact size and number, suggesting that Syn4 may contribute to focal contact stability and maturation in the neural crest.

The effect of modulating PCP signalling on focal contacts was also investigated in the same way (Fig 5.8). Inhibition of PCP using DshDEP+ resulted in a decrease in ppax staining (Fig 5.8D-F) compared to controls (Fig 5.8A-C), with many DshDEP+ cells completely lacking any visible ppax staining. On the other hand activation of PCP signalling with DshΔN resulted in an increase in p-paxillin staining (Fig 5.8G-I) with many focal contacts in the interior of the cell as well as in the lamella. Once again, the average number of focal contacts per cell (Fig 5.8J) was calculated as well as the average size (Fig 5.8K). DshDEP+ cells showed a significant decrease in both the number and size of focal contacts compared to controls, while DshΔN cells had a significantly larger number of focal contacts than controls, although curiously the average size of focal contacts was unaffected. As with Syn4, the level of PCP signalling in neural crest cells has a positive correlation with the formation of focal contacts.

### 5.5. Syn4 and Dsh signalling affect p-paxillin distribution *in vivo*.

Focal contacts have been well characterised *in vitro*, however they are much less well defined *in vivo*, therefore it is of interest to analyse focal contact formation in the embryo.

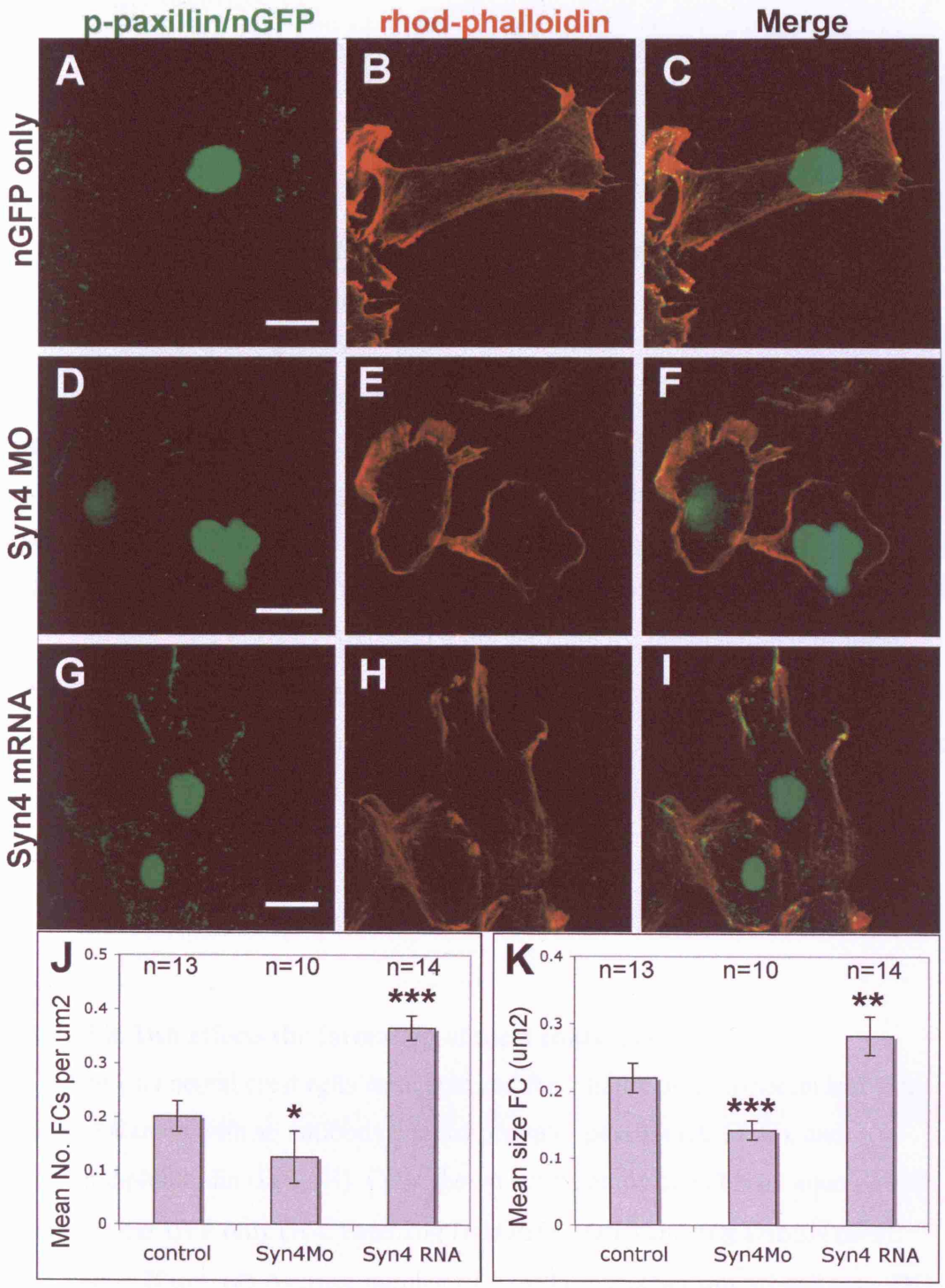
p-paxillin/nGFP
rhod-phalloidin
Merge
nGFP only
Syn4 MO
Syn4 mRNA
A
B
C
D
E
F
G
H
I
J
Mean No. FCs per um2
0.5
0.4
0.3
0.2
0.1
0
n=13
n=10
n=14
*
***
control
Syn4Mo
Syn4 RNA
K
Mean size FC (um2)
0.4
0.3
0.2
0.1
0
n=13
n=10
n=14
***
**
control
Syn4Mo
Syn4 RNA

**Figure 5.7**

**Figure 5.7. Syn4 affects the formation of focal contacts *in vitro***

**(A-I)** *Xenopus* neural crest cells were cultured for 5 hours on fibronectin and then fixed and stained with an antibody against phospho-paxillin (small green puncta in A, D, G) and rhodamine-phalloidin (shown in red in B, E ,H). Embryos were also co-injected with nuclear-GFP (Large green circles in A, D, G) to identify injected cells *in vitro*. (C,F,I) show merged green and red channels. Note paxillin accumulations that co-localise with actin protrusions. Scale bars = 20 μm. Cells shown are taken from embryos injected with 300pg nuclear GFP only (A-C) and with 8ng *syn4* Mo (D-F) and 1ng syn4 mRNA (G-I). **(J)** Graph showing the mean number of focal contacts per $\mu m^2$ of cell area. **(K)** Graph showing the mean size of each paxillin accumulation (in $\mu m^2$). N numbers indicate the number of cells analysed, taken from at least two experiments. Only individually migrating cells were analysed. ***p<0.005 ; **p<0.01; *p<0.05.

**Figure 5.8. Dsh affects the formation of focal contacts *in vitro***

**(A-I)** *Xenopus* neural crest cells were cultured for 5 hours on fibronectin and then fixed and stained with an antibody against phospho-paxillin (A, D, G), and rhodamine-phalloidin (B, E, H). Cells shown are taken from embryos injected with 300pg nuclear GFP only (A-C) and 1ng DshDEP+ (D-F) and 1ng DshΔN (G-I). Scale bars = 20μm. **(J)** Average number of focal contacts per $\mu m^2$ of cell area. **(K)** Average size of focal contacts (in $\mu m^2$). N numbers indicate the number of cells analysed, taken from at least two experiments. Only individually migrating cells were analysed. ***p<0.005 ; **p<0.01.

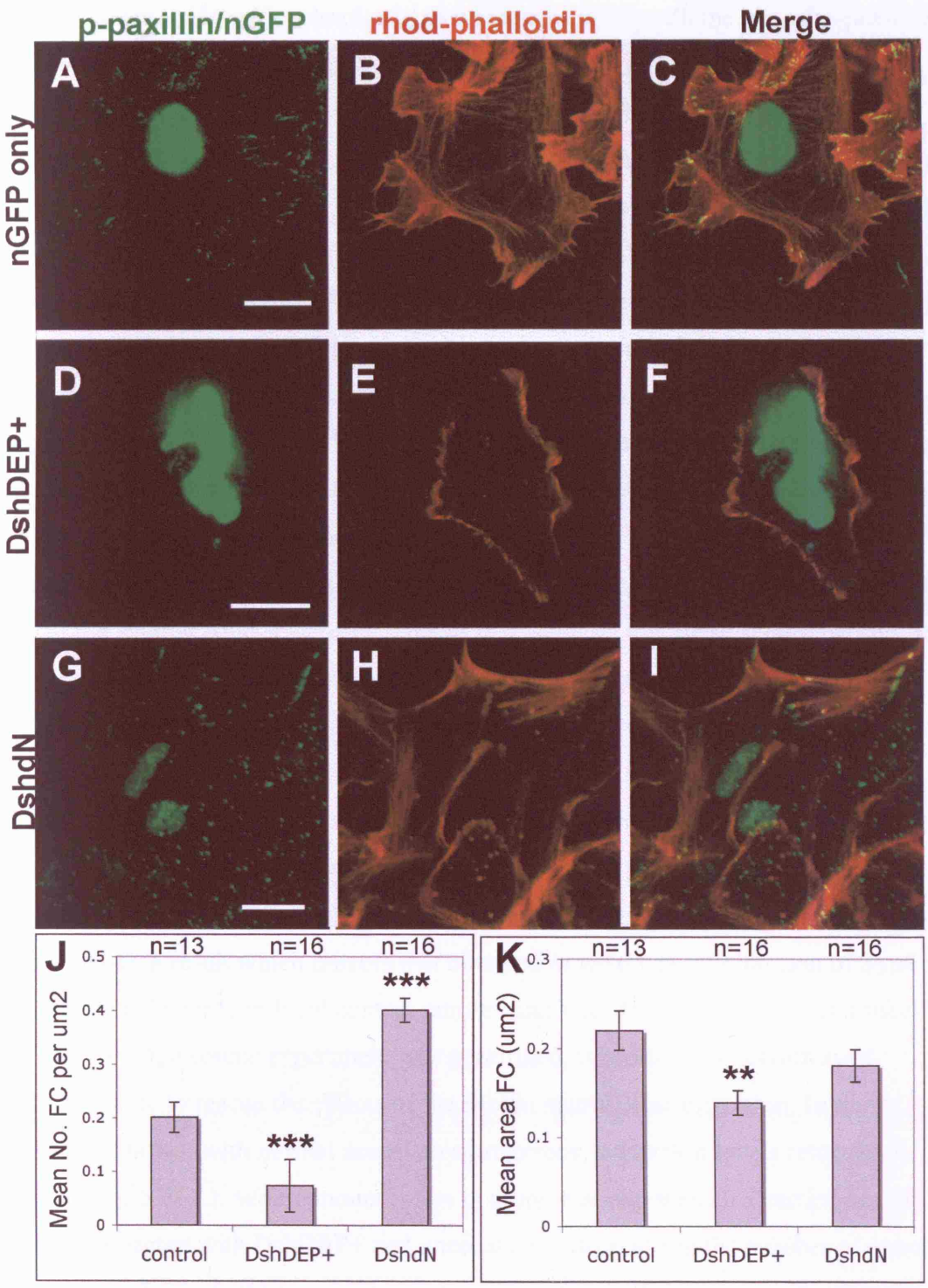
p-paxillin/nGFP
rhod-phalloidin
Merge
nGFP only
DshDEP+
DshdN
A
B
C
D
E
F
G
H
I
J
n=13
n=16
n=16
Mean No. FC per um2
0.5
0.4
0.3
0.2
0.1
0
***
***
control
DshDEP+
DshdN
K
n=13
n=16
n=16
Mean area FC (um2)
0.3
0.2
0.1
0
**
control
DshDEP+
DshdN

**Figure 5.8**

Whole mount *sox10:egfp* zebrafish embryos were stained with the phospho-paxillin antibody (Fig 5.9). Specific ppax staining was observed in zebrafish embryos, compared to embryos incubated without the primary antibody. Accumulation of activated paxillin can be observed around the edges of the neural tube (Fig 5.9A) and between the forming somites (Fig 5.9B) as has been previously described (Crawford et al., 2003). Interestingly, the neural crest cells identifiable by their GFP fluorescence, appear to have less p-paxillin staining than the surrounding tissue, such as the neural tube (Fig 5.9C). However, closer analysis reveals there is significant paxillin in and around neural crest cells (Fig 5.9 D,E). Furthermore, the staining appears in discrete clusters, which could be equivalent to the puncta of paxillin staining observed in focal contacts *in vitro*. By looking at the co-localisation between GFP and p-paxillin fluorescence it is possible to see that many of the puncta are clearly within neural crest cells and are particularly enriched at the border of the cells and at the leading edge (Fig 5.9F). This further suggests that these accumulations do correspond to focal contacts, although it is not possible to state this with certainty without looking for co-localisation with other FA proteins, the actin cytoskeleton or fibronectin. Embryos injected with *syn4* Mo were also stained with p-paxillin to assess the effect of Syn4 on FA formation *in vivo*. As before, neural crest cells in *syn4* Mo embryos were more rounded and did not move persistently away from the neural tube (Fig 5.9G). p-paxillin staining is dramatically decreased in *syn4* Mo cells (Fig 5.9H-I), a result which mirrors that obtained *in vitro* where inhibition of Syn4 resulted in a decrease in focal contact number and size. To show that this is a specific effect of Syn4, a rescue experiment was performed, whereby co-injection *syn4* mRNA is able to rescue the effects of the Mo on neural crest migration. In these rescued embryos, with normal neural crest migration, p-paxillin levels returned to normal (Fig 5.9J-L). Whole mount p-pax immuno-staining was also carried out in embryos injected with DshDEP+ and once again, a decrease in the number of puncta was observed (Fig 5.9M-O), similar to the effect of DshDEP+ *in vitro*. To quantify these differences, the average percentage of GFP-positive area per cell that co-localises with p-paxillin staining was calculated. A significant decrease was observed in embryos injected with *syn4* Mo and DshDEP+ compared to control Mo injected embryos (Fig 5.9P). So, the observed effect of Syn4 and Dsh on focal contact formation *in vitro* also hold true in an *in vivo* environment.

It is difficult to conclude whether the paxillin puncta in zebrafish neural crest cells truly represent focal contacts *in vivo*, so I attempted to see whether paxillin staining in the neural crest co-localises with fibronectin in the extracellular matrix. For this *Xenopus* embryos were used (Fig 5.10). Graft experiments were carried out where cranial neural crests were taken from embryos injected with membrane-RFP and grafted into uninjected control embryos. After the grafted cells had started to migrate, embryos were fixed and sectioned into 12μm slices using a cryostat. In these sections, the migrating neural crest cells are clearly visible and as the membrane is labelled, it is possible to see the shape of the migrating cells and identify cell protrusions (Fig 5.10A'). Staining with an antibody against fibronectin (mAb 6D9, Hybridoma Bank, Iowa) shows that fibronectin is distributed primarily between the different tissue layers in particular around the neural tube, underneath the epidermis and around the somites (Fig 5.10B). However closer magnification reveals that there are also substantial deposits of fibronectin around the neural crest cells (Fig 5.10B', B''). Co-staining with phospho-paxillin reveals that it co-localises with fibronectin surrounding the somites and the neural tube (Fig 5.10C,D). Paxillin and fibronectin also co-localise in the neural crest, although not fully as both fibronectin and ppax staining can be observed separately (Fig 5.10C',D'). In general the fibronectin staining takes up a greater area around neural crest cells while p-paxillin appears in discrete puncta, similar to what was observed in zebrafish (Fig 5.10 C'',D''). Both, ppax and fibronectin staining frequently overlaps with the membrane of neural crest cells, with ppax being found almost exclusively in the membrane (Fig 5.10E). Thus we have a picture where fibronectin is distributed around migrating neural crest cells, with specific points of paxillin activation that co-localise with membrane-RFP and in many cases, with fibronectin. This co-localisation suggests that the paxillin accumulations observed *in vivo* are involved in attachment of neural crest cells to fibronectin, which would correspond to the focal adhesion complexes described *in vitro*.

Graft experiments using explants from embryos that had been injected with *syn4* Mo or DshDEP+ were also carried out and sections were stained with p-paxillin. Both *syn4* Mo cells (Fig 5.10G) and DshDEP+ cells (Fig 5.10H) showed a decrease in ppax staining compared to control cells (Fig 5.10F). The percentage of neural crest cell membrane that stains positive for p-paxillin was calculated and once again *syn4* Mo cells and DshDEP+ cells showed a significant decrease (Fig 5.10I).

# SPECIAL NOTE

## ITEM SCANNED AS SUPPLIED
## PAGINATION IS AS SEEN

Whole mount *sox10:egfp* zebrafish embryos were stained with the phospho-paxillin antibody (Fig 5.9). Specific ppax staining was observed in zebrafish embryos, compared to embryos incubated without the primary antibody. Accumulation of activated paxillin can be observed around the edges of the neural tube (Fig 5.9A) and between the forming somites (Fig 5.9B) as has been previously described (Crawford et al., 2003). Interestingly, the neural crest cells identifiable by their GFP fluorescence, appear to have less p-paxillin staining than the surrounding tissue, such as the neural tube (Fig 5.9C). However, closer analysis reveals there is significant paxillin in and around neural crest cells (Fig 5.9 D,E). Furthermore, the staining appears in discrete clusters, which could be equivalent to the puncta of paxillin staining observed in focal contacts *in vitro*. By looking at the co-localisation between GFP and p-paxillin fluorescence it is possible to see that many of the puncta are clearly within neural crest cells and are particularly enriched at the border of the cells and at the leading edge (Fig 5.9F). This further suggests that these accumulations do correspond to focal contacts, although it is not possible to state this with certainty without looking for co-localisation with other FA proteins, the actin cytoskeleton or fibronectin. Embryos injected with *syn4* Mo were also stained with p-paxillin to assess the effect of Syn4 on FA formation *in vivo*. As before, neural crest cells in *syn4* Mo embryos were more rounded and did not move persistently away from the neural tube (Fig 5.9G). p-paxillin staining is dramatically decreased in *syn4* Mo cells (Fig 5.9H-I), a result which mirrors that obtained *in vitro* where inhibition of Syn4 resulted in a decrease in focal contact number and size. To show that this is a specific effect of Syn4, a rescue experiment was performed, whereby co-injection *syn4* mRNA is able to rescue the effects of the Mo on neural crest migration. In these rescued embryos, with normal neural crest migration, p-paxillin levels returned to normal (Fig 5.9J-L). Whole mount p-pax immuno-staining was also carried out in embryos injected with DshDEP+ and once again, a decrease in the number of puncta was observed (Fig 5.9M-O), similar to the effect of DshDEP+ *in vitro*. To quantify these differences, the average percentage of GFP-positive area per cell that co-localises with p-paxillin staining was calculated. A significant decrease was observed in embryos injected with *syn4* Mo and DshDEP+ compared to control Mo injected embryos (Fig 5.9P). So, the observed effect of Syn4 and Dsh on focal contact formation *in vitro* also hold true in an *in vivo* environment.

It is difficult to conclude whether the paxillin puncta in zebrafish neural crest cells truly represent focal contacts *in vivo*, so I attempted to see whether paxillin staining in the neural crest co-localises with fibronectin in the extracellular matrix. For this *Xenopus* embryos were used (Fig 5.10). Graft experiments were carried out where cranial neural crests were taken from embryos injected with membrane-RFP and grafted into uninjected control embryos. After the grafted cells had started to migrate, embryos were fixed and sectioned into 12μm slices using a cryostat. In these sections, the migrating neural crest cells are clearly visible and as the membrane is labelled, it is possible to see the shape of the migrating cells and identify cell protrusions (Fig 5.10A'). Staining with an antibody against fibronectin (mAb 6D9, Hybridoma Bank, Iowa) shows that fibronectin is distributed primarily between the different tissue layers in particular around the neural tube, underneath the epidermis and around the somites (Fig 5.10B). However closer magnification reveals that there are also substantial deposits of fibronectin around the neural crest cells (Fig 5.10B', B''). Co-staining with phospho-paxillin reveals that it co-localises with fibronectin surrounding the somites and the neural tube (Fig 5.10C,D). Paxillin and fibronectin also co-localise in the neural crest, although not fully as both fibronectin and ppax staining can be observed separately (Fig 5.10C',D'). In general the fibronectin staining takes up a greater area around neural crest cells while p-paxillin appears in discrete puncta, similar to what was observed in zebrafish (Fig 5.10 C'',D''). Both, ppax and fibronectin staining frequently overlaps with the membrane of neural crest cells, with ppax being found almost exclusively in the membrane (Fig 5.10E). Thus we have a picture where fibronectin is distributed around migrating neural crest cells, with specific points of paxillin activation that co-localise with membrane-RFP and in many cases, with fibronectin. This co-localisation suggests that the paxillin accumulations observed *in vivo* are involved in attachment of neural crest cells to fibronectin, which would correspond to the focal adhesion complexes described *in vitro*.

Graft experiments using explants from embryos that had been injected with *syn4* Mo or DshDEP+ were also carried out and sections were stained with p-paxillin. Both *syn4* Mo cells (Fig 5.10G) and DshDEP+ cells (Fig 5.10H) showed a decrease in ppax staining compared to control cells (Fig 5.10F). The percentage of neural crest cell membrane that stains positive for p-paxillin was calculated and once again *syn4* Mo cells and DshDEP+ cells showed a significant decrease (Fig 5.10I).

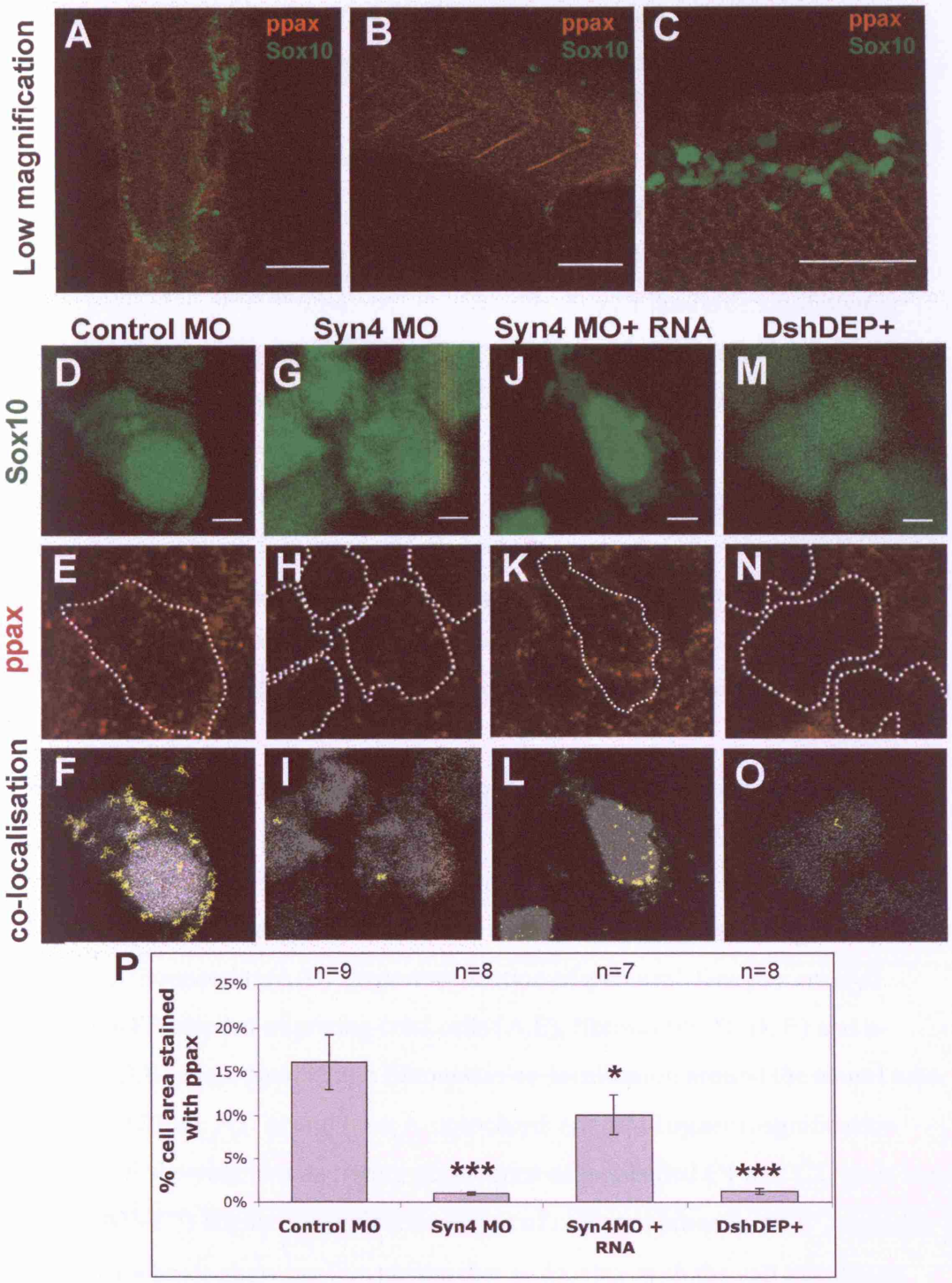
Low magnification
A
ppax
Sox10
B
ppax
Sox10
C
ppax
Sox10
Control MO
Syn4 MO
Syn4 MO+ RNA
DshDEP+
Sox10
D
G
J
M
ppax
E
H
K
N
co-localisation
F
I
L
O
P
n=9
n=8
n=7
n=8
% cell area stained with ppax
25%
20%
15%
10%
5%
0%
*
***
***
Control MO
Syn4 MO
Syn4MO + RNA
DshDEP+

**Figure 5.9**

**Figure 5.9. Syn4 and Dsh control focal contact formation *in vivo* in Zebrafish**
Wholemount *sox10:egfp* transgenic zebrafish embryos were fixed at 12 somites and stained with phospho-paxillin. **(A)** Dorsal view, anterior to top, of a 12 somite control embryo showing p-pax staining at the edges of the neural tube **(B,C)** Two different magnifications of p-pax staining between the somites in control embryos, lateral view, anterior to right. Scale bars in A-C=120μm. **(D-O)** Higher magnification view of individual neural crest cells (Sox10 fluorescence shown in green in D,G,JM) showing paxillin staining (red dots in E, H, K, N). F, I, L & O show sox10-GFP in grey and area of paxillin/sox10 co-localisation in yellow. Scale bars= 5μm. (D-F) Embryo injected with 6ng control Mo. (G-I) Embryo injected with 6ng *syn4* Mo. (J-L) Embryo injected with 6ng *syn4* Mo and 200pg *syn4* mRNA. Note the *syn4* Mo phenotype is rescued. (M-O) Embryo injected with 300pg DshDEP+. **(P)** Quantification of rescue experiment, graph shows average percentage of cell area (sox10-GFP positive area) that co-localises with p-pax staining. n indicates number of cells analysed, taken from at least 2 embryos. ***p<0.005 ; *p<0.05.

**Figure 5.10. Syn4 and Dsh control focal contact formation *in vivo* in *Xenopus***
Xenopus embryos were injected with 300pg membrane-RFP, and cranial neural crests were dissected and grafted into wildtype host embryos and allowed to migrate. Embryos were fixed at stage 28, sectioned and stained with antibodies against p-paxillin and fibronectin. **(A-E)** Transverse section of a control *Xenopus* embryo showing mRFP labelled migrating crest cells (A,E), fibronectin (B, D, E) and p-paxillin (C,D,E). Note paxillin and fibronectin co-localisation around the neural tube. Scale bar = 120μm. NT, neural tube; n, notochord. **(A'-E')** Higher magnification image of A-E showing two migrating neural crest cells labelled C1 and C2, scale bar = 10μm. **(A''-E'')** Higher magnification image of cell membrane in A'-E', scale bar = 2μm. Arrowheads show paxillin puncta that co-localise with the cell membrane and fibronectin. C1, cell 1; C2, cell 2. **(F-H)** Neural crest cells from a control embryo (F) compared to cells from an embryo injected with 8ng syn4 Mo (G) or 1ng DshDEP+ (H). P-paxillin (F-H) and membrane-RFP (F'-H') are shown, scale bars = 20μm. **(I)** Graph showing the average percentage of cell membrane (mRFP positive area) that co-stains with p-pax. n indicates number of cells analysed, taken from at least 3 embryos. ***p<0.005.

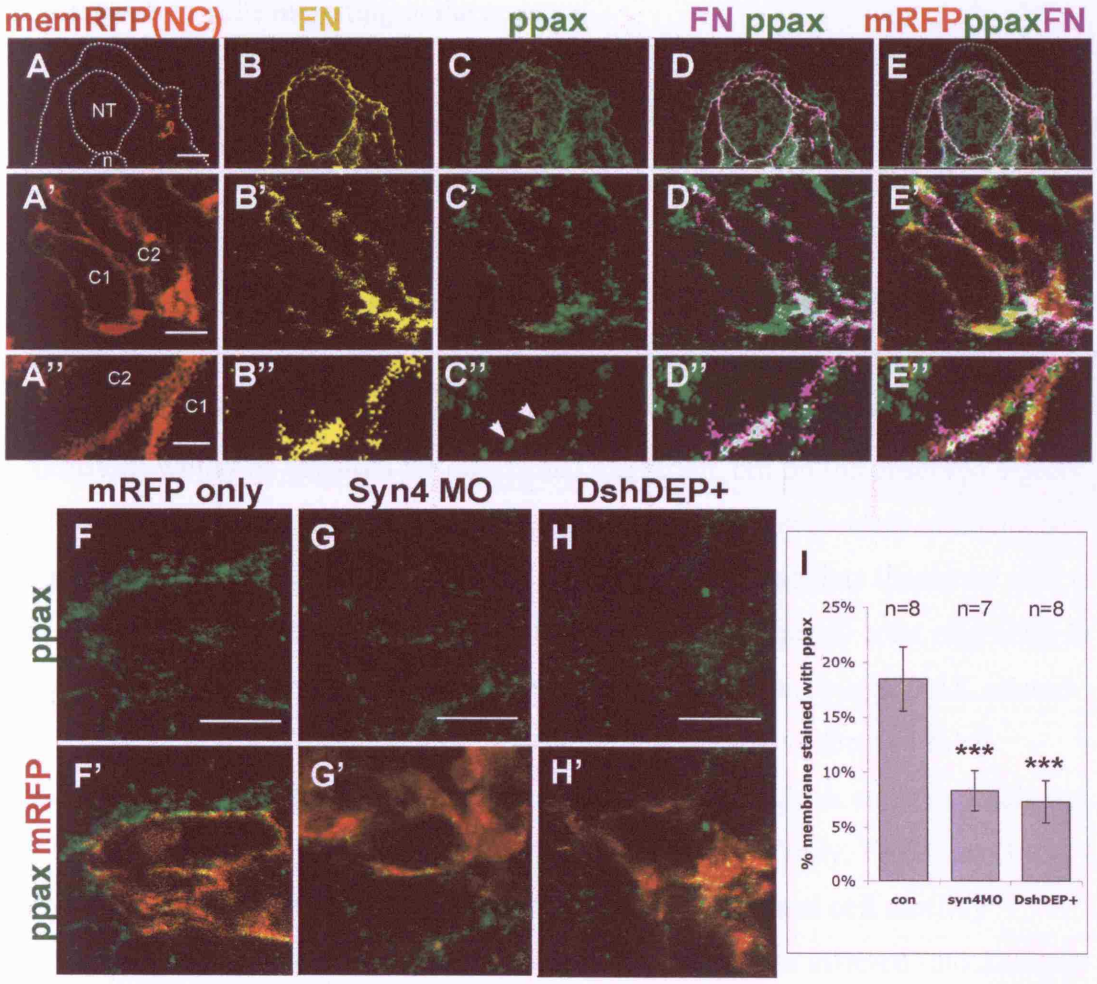
memRFP(NC)
FN
ppax
FN ppax
mRFPppaxFN
A
B
C
D
E
NT
A'
B'
C'
D'
E'
C2
C1
A''
B''
C''
D''
E''
mRFP only
Syn4 MO
DshDEP+
F
G
H
ppax
F'
G'
H'
ppax mRFP
I
% membrane stained with ppax
25%
20%
15%
10%
5%
0%
n=8
n=7
n=8
***
***
con
syn4MO
DshDEP+

**Figure 5.10**

So, as in zebrafish there appears to be a correlation between Syn4/PCP levels and the amount of activated paxillin-containing puncta. These puncta may well be the *in vivo* equivalent to focal contacts, as they co-localise with fibronectin. It is clear that Syn4 and Dsh both play a role in focal contact regulation *in vitro* and it is likely that this also extends to cells migrating in the embryo.

### 5.6. Focal adhesion kinase (FAK) is required for NC migration *in vivo* but not *in vitro*

Syndecan-4 and PCP signalling regulate directional migration of neural crest cells by controlling the polarised formation of cell protrusions, but they also play a role in regulating focal contact number and size. Which of these two functions is required for the migration of neural crest cells in the embryo, or do they both equally contribute to neural crest migration? It is clear how the formation of polarised cell protrusions would be essential for directional migration, but do the observed effects on focal contacts also affect directionality, or are they just a secondary consequence of inhibition of Syn4 or PCP signalling? In an attempt to dissociate these two effects and also to further investigate the role of focal adhesions in neural crest migration *in vivo*, an independent method for disrupting focal contacts was sought. FAK related non-kinase (FRNK) is a naturally occurring dominant negative form of focal adhesion kinase (FAK), which was originally isolated from chick embryos (Schaller et al., 1993). Consisting of the non-catalytic domain of FAK only, FRNK has been shown to be a potent inhibitor of FAK autophosphorylation and cell motility (Richardson and Parsons, 1996; Sieg et al., 1999). FRNK was injected into *Xenopus* embryos at the 8-cell stage and any effect on neural crest migration were analysed by *in situ* hybridisation against *snail2* (Fig 5.11). Two different concentrations were injected resulting in embryos expressing 400pg or 800pg of FRNK mRNA. The 800pg amount proved toxic, although embryos gastrulated normally and survived to around stage 20, whereupon they started to disintegrate. Embryos injected with 400pg FRNK survived long enough to allow analysis of neural crest migration, although they too perished around stage 35. FRNK had no effect on neural crest induction (Fig 5.11A), but did have a strong effect on neural crest migration with no migration observed in the injected side (Fig 5.11C), compared to the control side (Fig 5.11B). Strikingly, a very high proportion of embryos displayed this phenotype with 92% (n=60) of embryos having neural crest migration defects. This is much

higher even than the percentage affected by *syn4* Mo or DshDEP+. Graft experiments reveal that the effect of FRNK on neural crest migration is cell autonomous, as FRNK injected neural crest cells are unable to migrate even in a control host embryo (Fig 5.11E,F). To understand the cellular mechanism underlying this extreme phenotype, *sox10:egfp* zebrafish embryos were also injected with FRNK and their neural crest migration was followed by time-lapse analysis as before (Fig 5.12). While control neural crest cells migrate extensively as before (Fig 5.12 A,B), FRNK injected neural crest cells hardly move any distance and most remain static in the neural tube (Fig 5.12C,D). Tracking of individual cell movements reveal the contrast between FRNK expressing NC cells (Fig 5.12F) and controls (Fig 5.12E). Unlike *syn4* Mo or DshDEP+ cells, the speed of migration is greatly reduced in FRNK neural crest cells (Fig 5.12G). Whereas inhibition of Syn4 or Dsh results in motile neural crest cells that have lost directionality, cells lacking FAK appear unable to move at all. This could point to an underlying defect in neural crest delamination.

FRNK injected neural crest explants were also dissected and cultured *in vitro* (Fig 5.13). Surprisingly, cells were able to attach to the fibronectin and migrate. Tracking of individual neural crest cells illustrates that FRNK cells are able to migrate fairly persistently (Fig 5.13B). However the distance that they travel is reduced compared to controls over the same time period (Fig 5.13A). Once again, the speed at which the cells travel is significantly reduced (Fig 5.13C) but there is no difference in persistence (Fig 5.13D). However, unlike *in vivo*, cells are able to move forwards. Higher magnification images show that like control cells (Fig 5.13E-G) FRNK expressing cells are polarised, with cell protrusions being found mostly at the leading edge. However an interesting cell 'elongation phenotype' is sometimes observed, whereby cells move their leading edge forward without retracting their rear, resulting in thin elongated cells (Fig 5.13H-J). This phenotype was only observed in 30% of cells and many cells were observed successfully retracting at the rear. Thus, the only defect in cell migration *in vitro* when FAK is inhibited is a reduction in speed, a relatively minor phenotype compared to *in vivo*. This suggests that *in vivo*, FAK is playing an additional role to the regulation of migration, perhaps being involved in the earlier process of delamination.

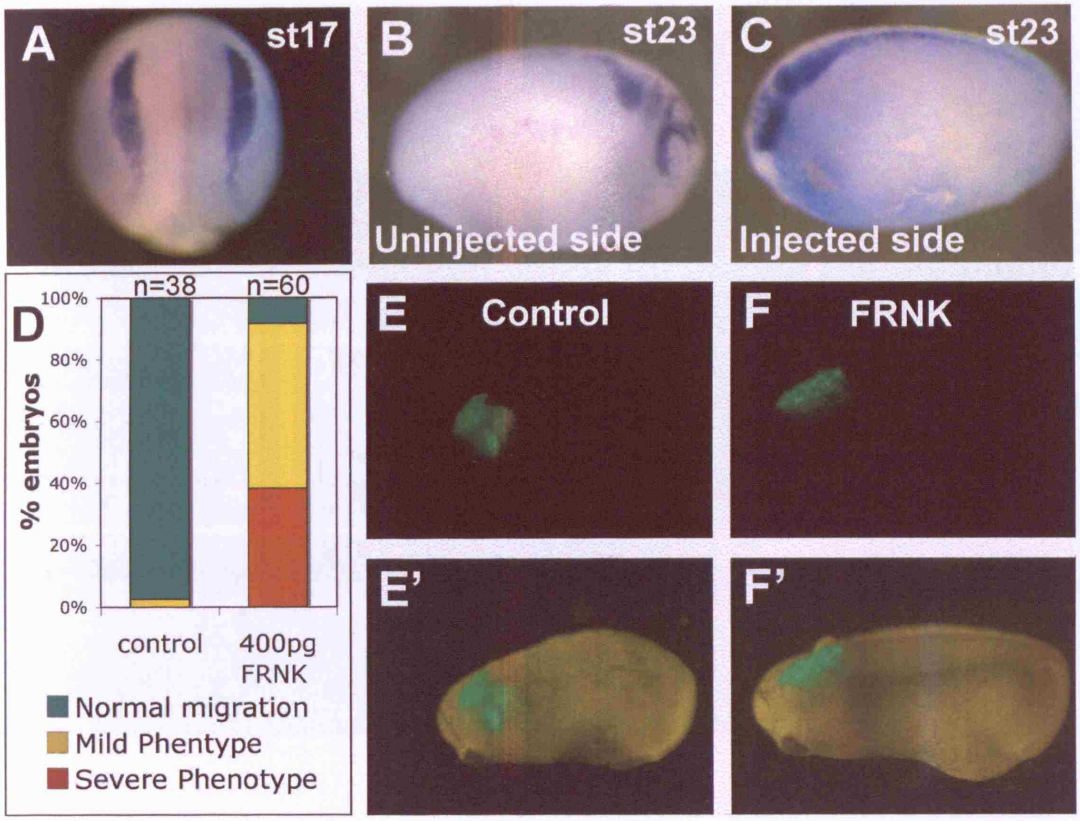


**Figure 5.11. FAK is required for neural crest migration in *Xenopus* embryos**
Focal adhesion kinase was inhibited in *Xenopus* embryos by injection of 400pg FRNK at the 8-cell stage. **(A)** In hybridisation of *snail2* in a stage 17, FRNK injected embryo, dorsal view, anterior to top. Injected side is shown in pale blue. Note that FRNK has no effect on the neural crest at this stage. **(B,C)** Lateral view of a stage 23 FRNK-injected *Xenopus* embryo with neural crest visualised by *snail2 in situ* hybridisation. Site of injection is shown in pale blue. Compare uninjected side (B) to injected side where no migration is observed (C). **(D)** Quantification of the FRNK phenotype. **(E,F)** FDX-labelled neural crests were grafted into wildtype hosts. (E) Neural crest taken from an embryo injected with FDX only, (F) Neural crest taken from an embryo injected with FDX and 400pg FRNK. Inhibition of migration indicates a cell autonomous effect.

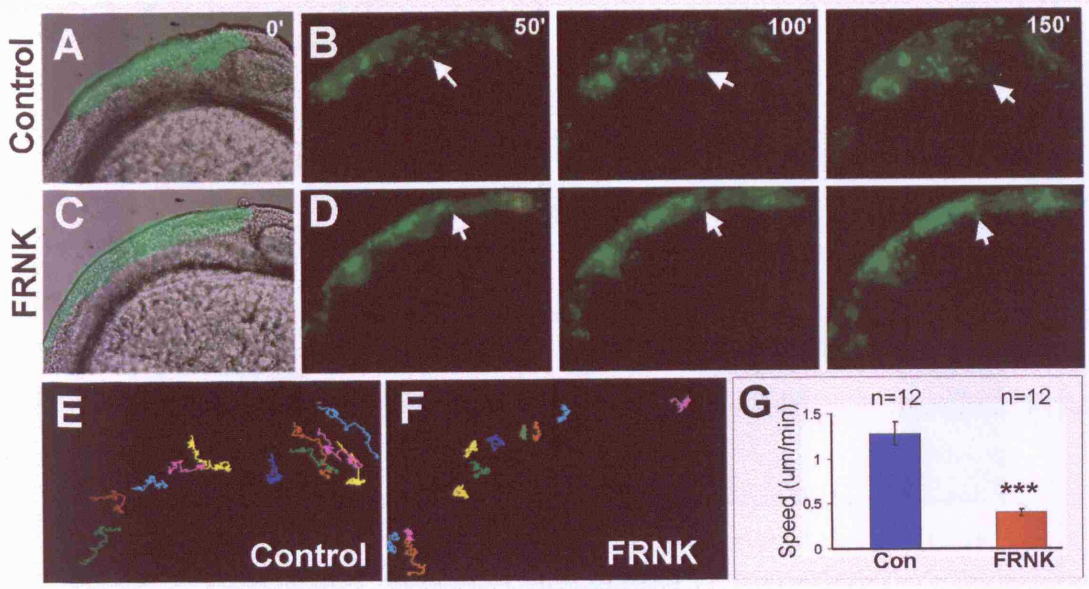


**Figure 5.12. FRNK affects the speed of neural crest cell migration in zebrafish embryos**

A *sox10:egfp* zebrafish transgenic line was used to analyse neural crest migration *in vivo*. **(A-D)** Time-lapse sequences showing cranial neural crest migration in embryos at 16hpf for 150 minutes, four frames are shown (t= 0 mins, t= 50 mins, t=100 mins, t=150 mins). A and C show the first frame overlapped on a DIC image, dorsal is to top, anterior to right. Arrow indicates the position of individual neural crest cells as examples. (A-B) control embryo. (C-D) Embryo injected with 100pg FRNK. **(E)** Trajectories of control cells over 150 minutes of migration. **(F)** Trajectories of FRNK Mo cells over 150 miutes of migration. **(G)** Velocity of migration ***p<0.005.

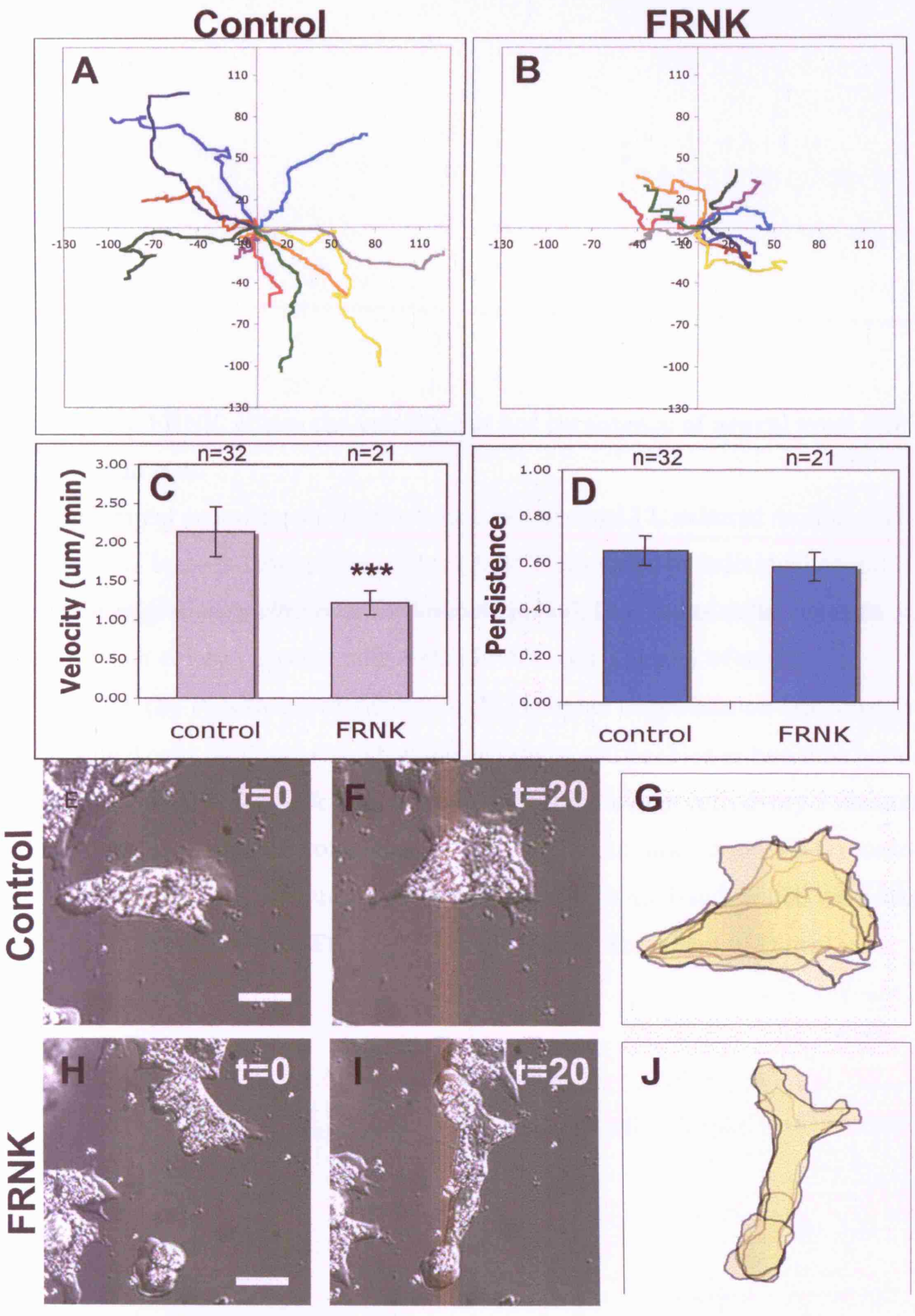
Control
FRNK
A
B
C
D
n=32
n=21
Velocity (um/min)
***
control
FRNK
Persistence
Control
FRNK
t=0
t=20
E
F
G
H
I
J

**Figure 5.13**

**Figure 5.13. FRNK affects the velocity but not persistence of neural crest cell migration *in vitro***

*Xenopus* cranial neural crest cells were dissected at stage 17, cultured on fibronectin and observed by time-lapse photography. **(A,B)** Trajectories of individual neural crest cells migrating *in vitro* over a 60-minute period, (A) control cells, (B) cells taken from an embryo injected with 400pg FRNK. **(C)** Velocity of migration, ***$p<0.005$. **(D)** Persistence of migration. **(E-J)** Higher magnification DIC images of individual cells on fibronectin showing cell shape and position at two time periods separated by 20 minutes. G & J show the outline of individual cells every 5 minutes to show the change in cell protrusions over the 20-minute time period. (E-G) control cells (H-J) FRNK cells. n numbers show number of cells analysed, which were taken from three (control) or two (FRNK) different explants. Scale bars = 20 μm.

## 5.7. FRNK treatment results in the stabilisation of focal contacts *in vitro* and *in vivo*

In order to assess how exactly FRNK affects focal contacts in the neural crest, FRNK expressing cells were stained with an antibody against phospho-paxillin and rhodamine phalloidin (Fig 5.14). Once again, focal contacts can be observed in control cells migrating *in vitro* (Fig 5.14A-C). However in cells taken from embryos injected with FRNK, the amount of p-paxillin staining was greatly increased. In particular some very large fibriller adhesions could be observed arranged along the entire length of the actin stress fibres (Fig 5.14D-F). In the FRNK cells, the number of focal contacts was increased (Fig 5.14G), but more significantly the area of each paxillin particle was very much larger than in controls (Fig 5.14H). Thus it appears that FRNK treatment results in the stabilisation and maturation of focal adhesions *in vitro*. These large focal contacts explain the slower speed of FRNK cells, as too strong an attachment to the matrix is likely to slow the cells down. This could also account for the strange morphology in FRNK cells where they have difficulty retracting their rears, as these large focal adhesions may prove difficult to disassemble.

Paxillin was also analysed *in vivo* in zebrafish and *Xenopus* embryos injected with FRNK (Fig 5.15). In FRNK-injected zebrafish, it is difficult to identify individual neural crest cells as they remain in the neural tube, however some rounded neural crest cells can be observed on the periphery of the tube (Fig 5.15D-F). The Paxillin deposits in and around these cells do appear much larger than in control cells (Fig 5.15A-C). Similarly in *Xenopus* embryos, paxillin accumulations also appear much larger in FRNK injected embryos (Fig 5.15J-L) compared to controls (Fig 5.15G-I). Furthermore, some of these accumulations appear to run the whole length of one side of a neural crest cell (Fig 5.15L), in a similar manner to the fibriller adhesions observed *in vitro*. In both embryos the percentage of sox10-GFP /membrane-RFP, which co-stains with ppax is significantly higher in FRNK cells than in controls (Fig 5.15M, N). Thus, the increase of FA size observed *in vitro* is reproducible *in vivo*. However, it is difficult to attribute this purely to the effects of FRNK as the neural crest cells in FRNK injected embryos stay in the neural tube, an area that is surrounded by a layer of activated paxillin with much higher levels of staining than migrating neural crest cells (See Fig 5.10).

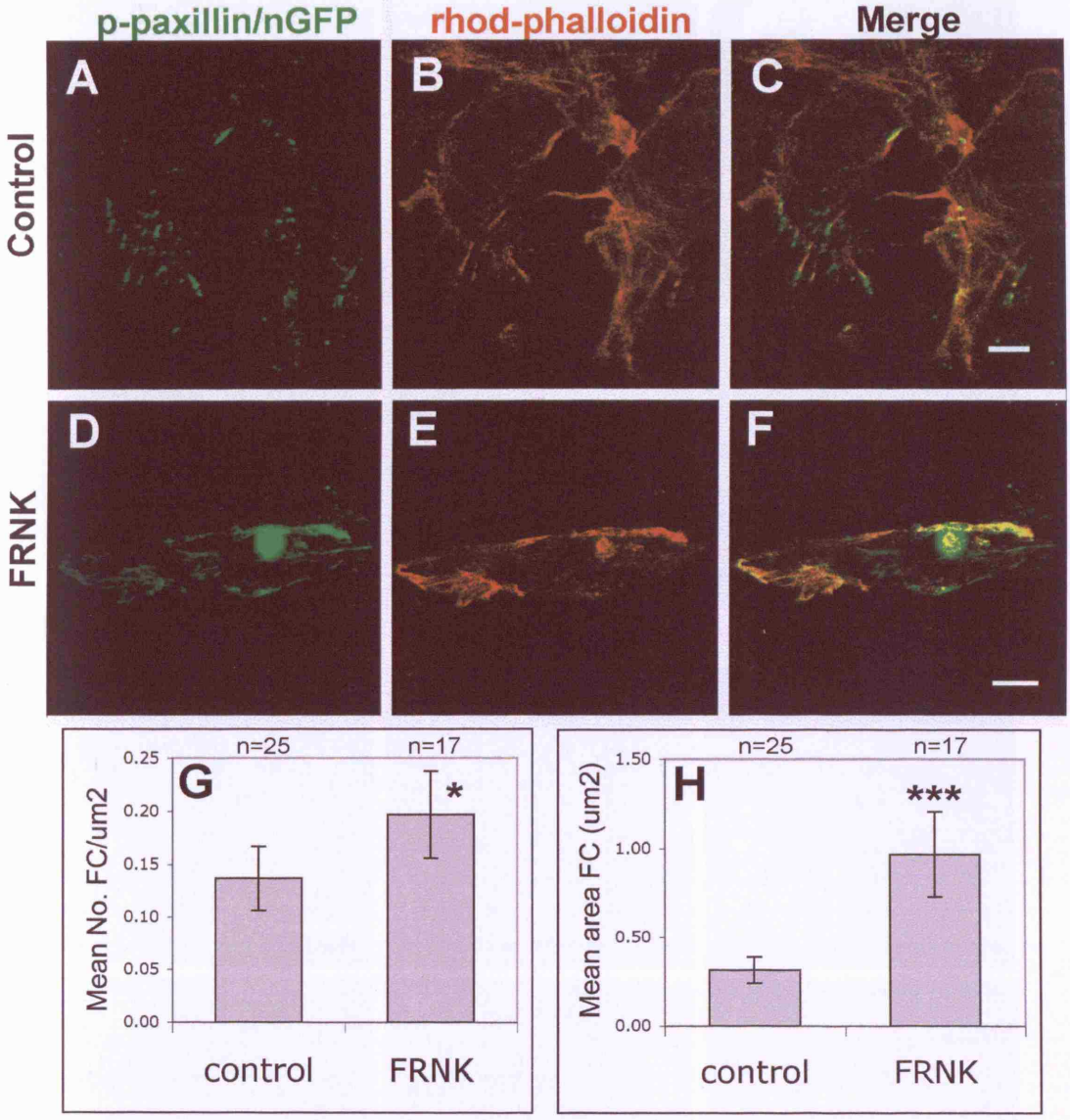


**Figure 5.14. FRNK stabilises focal contacts in neural crest cells *in vitro***

**(A-F)** *Xenopus* neural crest cells were cultured for 5 hours on fibronectin and then fixed and stained with an antibody against phospho-paxillin (A, D), and rhodamine-phalloidin (B, E). (A-C) Control neural crest cells. (D-F) Neural crest cells taken from an embryo injected with 400pg FRNK and 200pg nuclear-GFP. Scale bars = 20μm. **(G)** Average number of focal contacts per $\mu m^2$ of cell area. **(H)** Average size of focal contacts (in $\mu m^2$). n numbers show number of cells analysed, taken from at least 3 explants. ***p<0.005 ; *p<0.05.

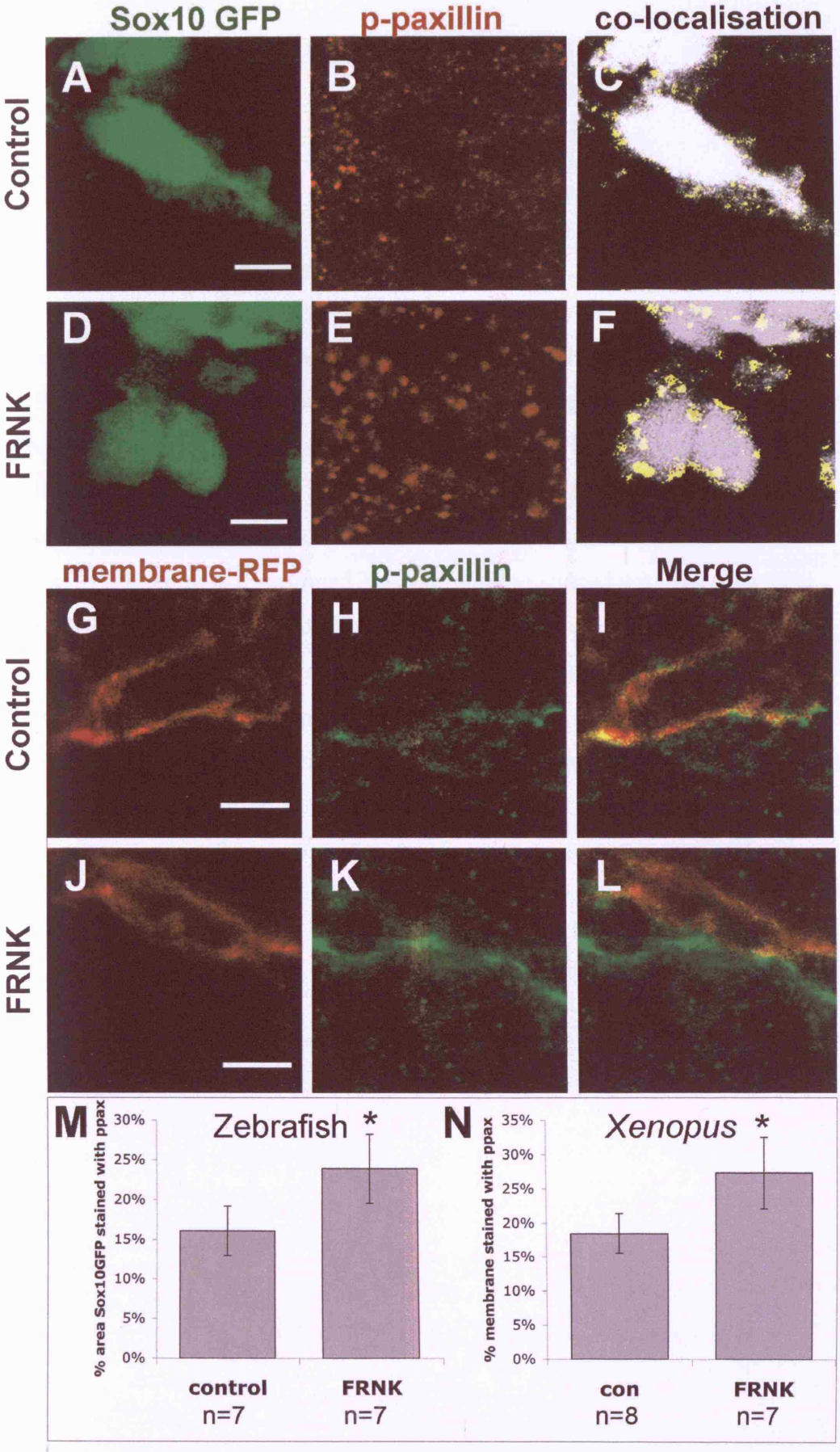
Sox10 GFP
p-paxillin
co-localisation
Control
FRNK
A
B
C
D
E
F
membrane-RFP
p-paxillin
Merge
G
H
I
J
K
L
M
Zebrafish *
% area Sox10GFP stained with ppax
30%
25%
20%
15%
10%
5%
0%
control
n=7
FRNK
n=7
N
Xenopus *
% membrane stained with ppax
35%
30%
25%
20%
15%
10%
5%
0%
con
n=8
FRNK
n=7

**Figure 5.15**

**Figure 5.15. FRNK stabilises focal contacts in neural crest cells *in vivo***

**(A-F)** Neural crest cells migrating in a *sox10:egfp* transgenic zebrafish (sox10-GFP in A,D) stained with p-paxillin (B,E). D & F show sox10-GFP in grey and area of paxillin/sox10 co-localisation in yellow. (A-C) Control embryo (D-F) Embryo injected with 100pg FRNK. Scale bars= 5μm. **(G-L)** Images of individual neural crest cells migrating in a sectioned *Xenopus* embryo stained with the p-paxillin antibody (H,K). Crest cells are labelled with membrane-RFP (G, J), scale bar = 10μm. **(M)** Graph showing average percentage of cell area (sox10-GFP positive area) that co-localises with p-paxillin staining in zebrafish neural crest cells. **(N)** Graph showing the average percentage of cell membrane (mRFP positive area) that co-stains with p-paxillin in *Xenopus* neural crest cells. n numbers show number of cells analysed, taken from at least 2 embryos for each condition. *$p<0.05$.

## 5.8. Discussion

The effects of modulating Syn4 and Dsh signalling on neural crest cell behaviour are remarkably similar, perhaps unsurprisingly so, since I have shown that they are working in the same pathway. Inhibition of both Syn4 and Dsh results in motile cells that are unable to migrate persistently *in vitro* and *in vivo*. Increasing Syn4 and PCP activity also causes a loss of persistent migration, but this is also coupled with a decrease in speed. It is well known that persistent, directional migration requires the formation of polarised cell protrusions (Ridley et al., 2003) and in neural crest cells too, the lack of persistence observed in cells where Syn4/PCP signalling is disrupted correlates with a disorganisation of cell protrusions. When either Syn4 or Dsh is inhibited, an increase in the number of protrusions is seen, with cells producing many peripheral protrusions all around the cell, which explains the lack of persistent migration. Conversely, over-expression of Syn4 or Dsh suppresses protrusion formation. These cells have a very unusual rounded appearance and any protrusions they do form have a more rippled, circular formation quite unlike a classical lamellipodium. This is more reminiscent of other types of migratory cell such as fish keratocytes, which migrate using a rapid rolling motion (Anderson et al., 1996). However unlike keratocytes, which are amongst the fastest known migratory cells, the *syn4* RNA/DshΔN neural crest cells' movement is severely limited. There is a clear correlation between Syn4/PCP signalling and cell protrusion formation, with both Syn4 and Dsh appearing to act as general inhibitors of protrusion formation. Furthermore, a balanced level of Syn4/PCP signalling is required for the production of polarised protrusions at the front of the cell, with either too much or too little signalling disrupting cell polarity and thus preventing directional migration. This explains why the embryonic phenotypes of inhibiting or activating Syn4 or Dsh are so similar, as neural crest cells are unable to maintain a directional migration under either condition.

Little has been previously published about the effect of Syndecan-4 on the actin cytoskeleton and protrusion formation. However, recent work from Bass et al (2007) have shown that Syn4 can control persistence of migration in fibroblasts through regulation of the small GTPase Rac1, although they do not specifically examine the formation of cell protrusions. PCP signalling, on the other hand, is a known regulator of the actin cytoskeleton and its earliest identified role in hair formation in the

*Drosophila* wing requires the polarised formation of an actin pre-hair structure (Adler, 2002; Mlodzik, 2002). During *Xenopus* gastrulation PCP signalling regulates the formation of polarised cell protrusions in *Xenopus* mesodermal cells undergoing CE (Wallingford et al., 2002). However the mechanism underlying this must be subtly different from the neural crest, as intercalating cells produce cell protrusions at both lateral ends of the cell, with a suppression of protrusions at the medial sides. Finally, de Calisto et al (2005) also show that inhibition of Dsh in neural crest cells cultured *in vitro* affects the formation of cell protrusions, with cells lacking Dsh forming a large number of filopodia around the cell periphery.

As well as regulating directional migration through the production of polarised protrusions, I have also shown a role for Syn4 and PCP signalling in the control of focal contact formation. Despite some limitations in this analysis, such as the use of only one antibody (against paxillin) and the fact that no turnover was studied, a clear correlation was observed between Syn4/Dsh levels and the number and size of paxillin-containing focal contacts *in vitro* and *in vivo*. Increased levels of Syn4/Dsh result in an increase in focal contacts, while decreased levels decrease the number of observable focal contacts, suggesting that Syn4/Dsh signalling may be playing a role in the maturation or stabilisation of focal contacts. Overexpression of Syn4 in CHO-K1 cells increases focal contact formation, whilst at the same time decreasing motility while expression of a truncated, dominant negative form inhibits the formation of mature focal contacts (Longley et al., 1999). Furthermore, fibroblasts plated on the cell binding domain of fibronectin (which binds integrin-β1 only) can be stimulated to form focal adhesions only after engagement of Syndecan-4 (Mostafavi-Pour et al., 2003; Saoncella et al., 1999). This has led to a 2-step model of focal adhesion formation, whereby integrin engagement mediates an initial attachment and drives the formation of focal complexes at the cell periphery, while Syndecan-4 is required for the maturation and stabilisation of focal adhesions (Morgan et al., 2007; Wilcox-Adelman et al., 2002b). The results presented here in the neural crest clearly fit with this model. Several downstream pathways have been proposed by which Syn4 may modulate focal adhesion formation. Syndecan-4 binds directly to an adaptor protein Syndesmos, which itself binds to paxillin, indicating a possible mechanism to physically link Syn4 to focal adhesions (Baciu et al., 2000; Denhez et al., 2002). This interaction requires the activity of PKCα (Denhez et al., 2002), and as I have demonstrated previously, an intact PKCα binding site is

essential for Syndecan-4 to control neural crest migration. Additionally, Syn4 activity has also been shown to promote phosphorylation of FAK at tyrosine-397, a role that is dependent on the activity of RhoA (Wilcox-Adelman et al., 2002a).

Until recently, the role of PCP signalling in controlling focal contacts has remained unknown, but a recent study by Iioka and colleagues (2007) firmly links Dsh activity with focal adhesion formation. They show that paxillin, like PCP signalling, is required for cell intercalation during gastrulation in *Xenopus*. Furthermore, they suggest that Dsh/PCP regulates the stability of paxillin by two mechanisms; firstly, using pull-down assays, they demonstrate that non-canonical Wnt signalling promotes paxillin ubiquitination. Secondly they show that PCP signalling stabilises a novel ring finger protein, XRNF185, which physically binds to both paxillin and the proteosome, thus targeting paxillin for degradation (Iioka et al., 2007). This appears to be in direct contradiction to what I have shown here, where an increase in Dsh signalling results in an increase in active paxillin. However it is worth noting that Iioka et al do not directly examine the effect of modulating Dsh levels on paxillin-containing focal contacts, but rather show that XRNF185 promotes the turnover of focal adhesions.

The fact that inhibition of FAK results in such a strong neural crest migration phenotype highlights the need for proper focal adhesion regulation during neural crest migration. FAK is a 125kDa tyrosine kinase, which was originally identified to localise to focal adhesions and has since emerged as a key modulator of focal adhesion dynamics (Schaller et al., 1992; Schlaepfer et al., 2004). Many focal adhesion components are phosphorylated in response to integrin engagement and FAK is thought to be responsible for much of this phosphorylation especially of its binding partners paxillin and p130Cas (Tachibana et al., 1997). However it is also likely to be important as a FA scaffold protein, as kinase dead FAK retains much of its activity (Schaller et al., 1999). FAK itself requires auto-phosphorylation of its tyrosine 395 residue to be active, and clustering of FAK to focal adhesion sites enhances this auto-phosphorylation (Kwong et al., 2003; Schaller et al., 1994). In focal adhesions the main function of FAK is as a regulator of focal adhesion turnover and disassembly. Thus, focal adhesion kinase null fibroblasts exhibit larger focal adhesions and impaired migration (Ilic et al., 1995). This is very similar to what is observed in neural crest cells. More recently live imaging experiments reveal that FAK promotes the turnover and disassembly of adhesion complexes (Ren et al.,

2000; Webb et al., 2004). Since the rate of attachment/detachment from the extracellular matrix also governs the speed of cell movement (Palecek et al., 1997), FAK null cells also move slower (Ilic et al., 1995). In neural crest cells, too, inhibition of FAK results in a greatly reduced speed of migration. Interestingly, a difference in severity is observed between the effect of FRNK on neural crest cells migrating *in vitro* versus *in vivo*. This hints at an additional role for FAK *in vivo*, which may not be directly related to regulation of focal adhesions. As neural crest cells remain in the neural tube in FRNK embryos, this additional role may be in controlling delamination from the neural tube epithelium. FAK has been linked to invasive behaviour in cancer cells and FAK expression levels is often elevated in metastatic tumours (McLean et al., 2005). FAK -/- fibroblasts cannot permeate a 3D matrix, and more importantly, neither can v-src transformed FAK null cells, despite the fact that v-src transformation fully rescues the ability of these cells to migrate in 2D (Hsia et al., 2003). This indicates that FAK may be playing quite a different role in 3-dimensions than in two. FAK may be regulating invasion through the control of matrix metalloproteases (MMP), which are required for degradation of the extracellular matrix. FAK activity is required for the expression and secretion of matrix metalloproteases in an number of cancer cell lines as well as in fibroblasts (Hsia et al., 2003; Hu et al., 2006; Shibata et al., 1998; Zhang et al., 2002). In addition, expression of FRNK in thyroid carcinoma cells results in a reduction of the transcription and secretion of MMP-9 and a decrease in invasiveness (Rothhut et al., 2007). Matrix-metalloproteases also play a role in cranial neural crest migration (Alfandari et al., 2001; Kuriyama and Mayor, 2008), therefore it is not unreasonable to imagine that FAK is playing a similar role in delamination in cancer cells and the neural crest. Thus FRNK cells are unable to leave the neural tube *in vivo*, while *in vitro* neural crest cells do not face this problem, having been already forcibly removed from the neural tube. Another possible explanation for the difference observed *in vitro* and *in vivo* is that FAK affects cell matrix deposition. FRNK has been shown to inhibit the deposition of fibronectin during *Xenopus* somitogenesis (Kragtorp and Miller, 2006). FAK may also be required for the proper organisation of fibronectin in the ECM, as FAK-deficient endothelial cells lack a fibriller, organised fibronectin matrix in the E8.5 mice (Ilic et al., 2004). So, FAK may also be required to regulate polarised fibronectin matrix deposition around the neural crest.

One of my original aims in studying FAK was to assess the effect of focal adhesions on neural crest migration, in an attempt to dissociate the two observed effects of Syn4 and Dsh signalling. However, as its effects on delamination and the ECM illustrate, the role of FAK is more complex than the simple regulation of focal adhesion formation and turnover. Furthermore, focal adhesion mediated-attachment to the extracellular matrix has been postulated to be a key regulator of persistent cell migration (Moissoglu and Schwartz, 2006) and indeed overexpression of FAK causes a loss of persistence and directionality in cell migration (Gu et al., 1999). FAK has also shown to be an upstream regulator of Rac and RhoA, both of which control cell protrusion formation (Chen et al., 2002; Moissoglu and Schwartz, 2006; Zhai et al., 2003). However here I show that, unlike Syn4 or Dsh, inhibition of FAK *in vitro* affects neither the persistence of migration nor cell polarity (Fig5.13). This indicates that focal adhesion size and number is not important for directional migration of neural crest cells. Thus, the effects of Syn4 and PCP signalling on directional migration are likely to be independent of their capacity to regulate focal adhesions. While the effects on directed protrusion formation are likely to underlie the loss of persistent migration, the effect on focal adhesions may be more important in regulating speed. Inhibition of FAK and overexpression of Syn4 and DshΔN all result in increased focal adhesion size and a reduction of velocity.

In summary, both Syn4 and PCP signalling are having wide ranging effects on the global migration machinery, affecting the formation of polarised cell protrusions to control directional migration, as well as regulating focal contacts. One family of molecule that are known to be similar global regulators of cell migration are the small Rho GTPases, and in the next chapter I will address the role of the Syndecan-4 and Dsh as regulators of these molecules.

# 6. Results: Syndecan-4 and PCP signalling control Small GTPase activity

## 6.1. Introduction

Syndecan-4 and PCP signalling regulate neural crest migration by similar cellular mechanisms: both are required for directional, persistent migration of crest cells *in vitro* and *in vivo* by controlling the directed formation of cell protrusions as well as by modulating focal adhesion dynamics. In this chapter I investigate the down-stream signalling responsible for these effects.

Both Syn4 and the PCP pathway have been suggested to modulate the activity of Rac1 and RhoA (Bass et al., 2007; Dovas et al., 2006; Habas et al., 2003), members of the Rho family of small GTPases. The Rho GTPases are a highly conserved protein family that regulate many aspects of eukaryotic cell biology including the cell cycle, morphogenesis, and cell polarity, but are especially well known as regulators of cell migration (Jaffe and Hall, 2005). In particular three well-studied members of the family; Rac, RhoA & Cdc42, regulate different aspects of cell migration.

### *6.1.1. Rac, RhoA and Cdc42 in cell migration*

Rac, RhoA and Cdc42 are pivotal regulators of the actin cytoskeleton during migration. Rac and Cdc42 promote actin polymerisation at the leading edge and are associated with lamellipodia and filopodia respectively, while RhoA promotes stress fibre formation (Kozma et al., 1995; Nobes and Hall, 1995b; Ridley and Hall, 1992; Ridley et al., 1992). Although Rac and Cdc42 promote different types of protrusions at the cell membrane, both are thought to initiate actin polarisation through the Arp2/3 complex. Activated Cdc42 can bind directly to N-WASP, relieving an inhibition and allowing N-WASP to bind and activate the Arp2/3 complex (Rohatgi et al., 2000; Rohatgi et al., 1999). Rac activates Arp2/3 via an indirect interaction with the WAVE complex (Soderling and Scott, 2006; Steffen et al., 2004). RhoA, on the other hand, stimulates actin polymerisation during stress fibre formation through several members of the formin family, including mDia, which is a direct binding partner of RhoA (Watanabe et al., 1999; Zigmond, 2004). RhoA also stimulates formation and contraction of stress fibres through its downstream effectors Rho kinases (ROKs), serine/threonine kinases, which phosphorylate myosin light chain

(Riento and Ridley, 2003). As well as modulating the actin cytoskeleton, Rho GTPases also regulate focal adhesion dynamics. Focal complex formation at the front of the cell is driven by the activity of Rac and Cdc42 (Nobes and Hall, 1995b), while RhoA promotes the formation of the more mature focal adhesions (Chrzanowska-Wodnicka and Burridge, 1996; Nobes and Hall, 1995a; Ridley and Hall, 1992).

Thus Rac and Cdc42 play complementary roles to RhoA during cell migration, with Rac and Cdc42 acting at the leading edge to regulate both actin polymerisation and the production of new focal complexes, while RhoA works under the cell body to stabilise focal adhesions and promote the formation of stress fibres. In addition, RhoA inhibits the formation of cell protrusions away from the leading edge (Worthylake and Burridge, 2003). A fine balance between Rac/Cdc42 and RhoA signalling enables a cell to remain polarised and promotes directional migration and the perturbation of either RhoA or Rac is characterised by defects in persistent migration (Bass et al., 2007; Pankov et al., 2005; Worthylake and Burridge, 2003). Naturally then, the activities of the Rho GTPases during cell migration require tight regulation. Like all small G proteins, Rho GTPases exist in two different conformations: an active GTP-bound state and an inactive GDP-bound state. Switching between these two states is regulated by guanine nucleotide exchange factors (GEFs) that activate GTPases by catalysing the GDP to GTP exchange, and GTPase activating proteins (GAPs), which stimulate GTPase activity and thus the return to the GDP-bound inactive form (Bos et al., 2007). This switch allows many different signalling inputs to feed into regulation of Rho GTPases through the control of GAPs and GEFs. A diverse array of upstream signalling pathways affect Rho GTPase activity including inputs from growth factors, ECM/integrin interactions, Ephrins and Semaphorin ligands and lysophosphatidic acid (Bernards and Settleman, 2005; Klein, 2004; Moolenaar et al., 2004; Puschel, 2007) . In addition there is considerable crosstalk between Rac, Cdc42 and RhoA themselves as well as with other members of the Rho GTPase family (Burridge and Wennerberg, 2004). Rac antagonizes RhoA in fibroblasts, as expression of a constitutively active form of Rac results in the down-regulation of RhoA (Sander et al., 1999). This repression may be the result of Rac-mediated production of reactive oxygen species, which leads to the activation of a RhoGAP (Nimnual et al., 2003). Activation of Cdc42 has also been shown to suppress RhoA activity (Sander et al.,

1999). RhoA has been shown to limit protrusion formation and may do this by repression of Rac away from the leading edge (Tsuji et al., 2002; Worthylake and Burridge, 2003). Activation of RhoA using a constitutively active form suppresses Rac activity, while inhibition of ROK using the small molecule inhibitor Y27632 results in an increase in GTP-bound Rac (Tsuji et al., 2002; Yamaguchi et al., 2001). ROK has also been shown to phosphorylate and activate FilGAP, a GAP specific for Rac, providing a mechanism for RhoA antagonism of Rac (Ohta et al., 2006). This mutual repression of Rac and RhoA is likely to contribute to the polarised GTPase activity that is required for directional migration.

### *6.1.2. Using FRET to measure small GTPase activity*

The current model for Rho GTPase control of cell migration relies on activation of discrete Rho GTPases in specific locations within the cell and there have been many attempts to visualise both the localisation and activity of Rho GTPases. Previously Rho GTPase localisation has been imaged in live cells cultured *in vitro* using GFP-Rho GTPase fusion proteins, but although these can show the location within the cell, they do not show whether the protein is in the GTP-bound, active form. Alternatively pull-down assays, which utilise the effecter domains of Rho GTPase binding partners that bind only the GTP-loaded form, can be used to measure levels of Rho GTPase activity in cell lysates. Recently, however, a new generation of fluorescent probes have been developed that allow the simultaneous measurement of Rho GTPase activity levels and live imaging of their sub-cellular localisation, by utilizing fluorescent resonance energy transfer (FRET) technology (reviewed in (Kiyokawa et al., 2006; Kurokawa et al., 2005; Pertz and Hahn, 2004). FRET is based on the principle that when two fluorophores with the appropriate excitation and emission spectra come into close proximity (10-100Å apart), non-radioactive energy transfer will take place from an excited donor fluorophore to an acceptor fluorophore, which will then emit at its characteristic wavelength. Initial Rho GTPase FRET probes consisted of two components: for example, Kraynov et at (2000) measured Rac activation using a GFP-Rac fusion protein which acts as a donor and the CRIB-domain of Rac effector PAK fused to Alexa-546, which acts as the acceptor fluorophore. Only when Rac is loaded with GTP, will it bind the CRIB domain, bringing the two fluorophores into close enough proximity to allow FRET to occur, resulting in a shift from GFP to Alexa-546 fluorescence. They showed a gradient of Rac activation at the leading edge in migrating cells, with specific

activity in membrane ruffles. (Kraynov et al., 2000). More recently, unimolecular FRET reporters have been developed. These are single fusion proteins consisting of the Rho GTPase/donor-fluorophore physically joined by a small linker domain to the effector domain/acceptor-fluorophore. Activation of the GTPase results in binding to its effector, changing the conformation of the molecule and bringing two fluorophores together to allow FRET to occur. These unimolecular FRET probes allow direct measurement of the levels of interaction from the FRET/donor emission ratio, and eliminate some of the previous problems associated with the two protein system such as donor bleed through and direct acceptor excitation, which result from the different distribution of donor and acceptor fluorophores (Pertz and Hahn, 2004). Unimolecular FRET probes, using cyan fluorescent protein (CFP) and yellow fluorescent protein (YFP) have confirmed specific localisations of active Cdc42 and Rac. Cdc42 activity is strongest at the tip of the cell protrusions, while Rac is concentrated slightly behind the leading edge (Itoh et al., 2002). RhoA has also been analysed in this manner and its activity is found to be highest away from the leading edge but at the base of the cell protrusions and in the retracting tail of the cell (Pertz et al., 2006). Here I use these FRET probes; raichu-Rac (YFP-PAK CRIB domain-Rac-CFP) raichu-cdc42 (YFP-PAK CRIB domain-cdc42-CFP)(Itoh et al., 2002) and the RhoA unimolecular FRET probe (RhoA-YFP-CFP-RhoA binding domain of Rhotekin)(Pertz et al., 2006) to analyse the activity of small GTPases in neural crest cells and the effects of Dishevelled and Syndecan-4 on this activity.

### 6.2. Syn4 controls Rac activity but not RhoA or Cdc42

Plasmid DNA coding for the FRET probes for Rac, RhoA and Cdc42 (150pg DNA was injected for Rac and Cdc42, 75pg for RhoA) was injected into 8-cell *Xenopus* embryos and neural crest cells were removed at stage 17 and cultured on fibronectin. Plasmid DNA diffuses slower than mRNA, resulting in a mosaic expression pattern with not all cells expressing the FRET probes. Nevertheless, between 5 and 10 cells in each neural crest explant expressed the probes and this was sufficient to measure FRET efficiency in individual cells. Initially, live imaging of moving cells was attempted, but the rapid dynamics of neural crest cell movement quickly ruled this out, as the position of the cells was shifted between the pre-bleach and post-bleach scans. Thereafter only fixed cells were analysed. To avoid losing vital information about the directionality of the fixed cells, cells were filmed before and during fixation so that it was possible to tell the direction of movement for each

cell prior to fixation. The FRET efficiency of each probe was compared in cells from embryos injected with the control morpholino and those from a *syn4* morpholino embryo (Fig 6.1). No difference was observed in the levels of Cdc42 or RhoA activity with or without *syn4* morpholino (Fig 6.1A), however a significant difference in Rac levels was observed. In *syn4* Mo cells, the FRET efficiency was increased four-fold compared to controls (Fig 6.1A). This indicates that Syn4 plays a role in the repression of Rac in the neural crest, as removal of Syn4 results in an up-regulation of Rac activity. Analysis of the distribution of Rac activity in individual cells reveals a difference in spatial distribution between *syn4* Mo cells and controls. In control Mo cells, Rac activity is concentrated at the leading edge of the cell (Fig 6.1B), as has been described in other cell types (Itoh et al., 2002). However, in *syn4* Mo cells elevated levels of Rac are visible around the entirety of the cell membrane (Fig 6.1C). As Rac activity is associated with cell protrusion formation, this explains why *syn4* Mo cells produce protrusions all around the cell.

### 6.3. Dishevelled controls RhoA activity but not Rac or Cdc42

The effect of modulating Dsh signalling on small GTPase activity was also addressed. FRET efficiencies were measured for all three FRET probes in NC cells taken from embryos injected with 1ng DshDEP+ or 1ng DshΔN (Fig 6.2). Once again, no difference was observed in the levels of Cdc42 activity in the presence of DshDEP+ or DshΔN (Fig 6.2A). However, surprisingly given the effect of *syn4* Mo on Rac, no difference was observed in the levels of Rac activity (Fig 6.2A). Instead, Dsh appears to be regulating the activity of RhoA. In DshΔN cells, RhoA activity was doubled, while inhibition of Dsh via DshDEP+ resulted in a significant decrease in RhoA activity (Fig 6.2A). No specific localisation of RhoA was observed in control neural crest cells, with RhoA enriched around the entire membrane, although in a few cells there was a visible accumulation of RhoA at the retracting edge of the cell (Fig 6.2B). In Dsh ΔN cells, RhoA activity was increased around the entire membrane (Fig 6.2C), while DshDEP+ treatment resulted in a general decrease in RhoA activity all over the cell (Fig 6.2D). This suggests that Dsh is promoting RhoA activity in the neural crest. Thus Syn4 and Dsh are affecting different GTPases, with Syn4 regulating Rac activity, while Dsh controls RhoA.

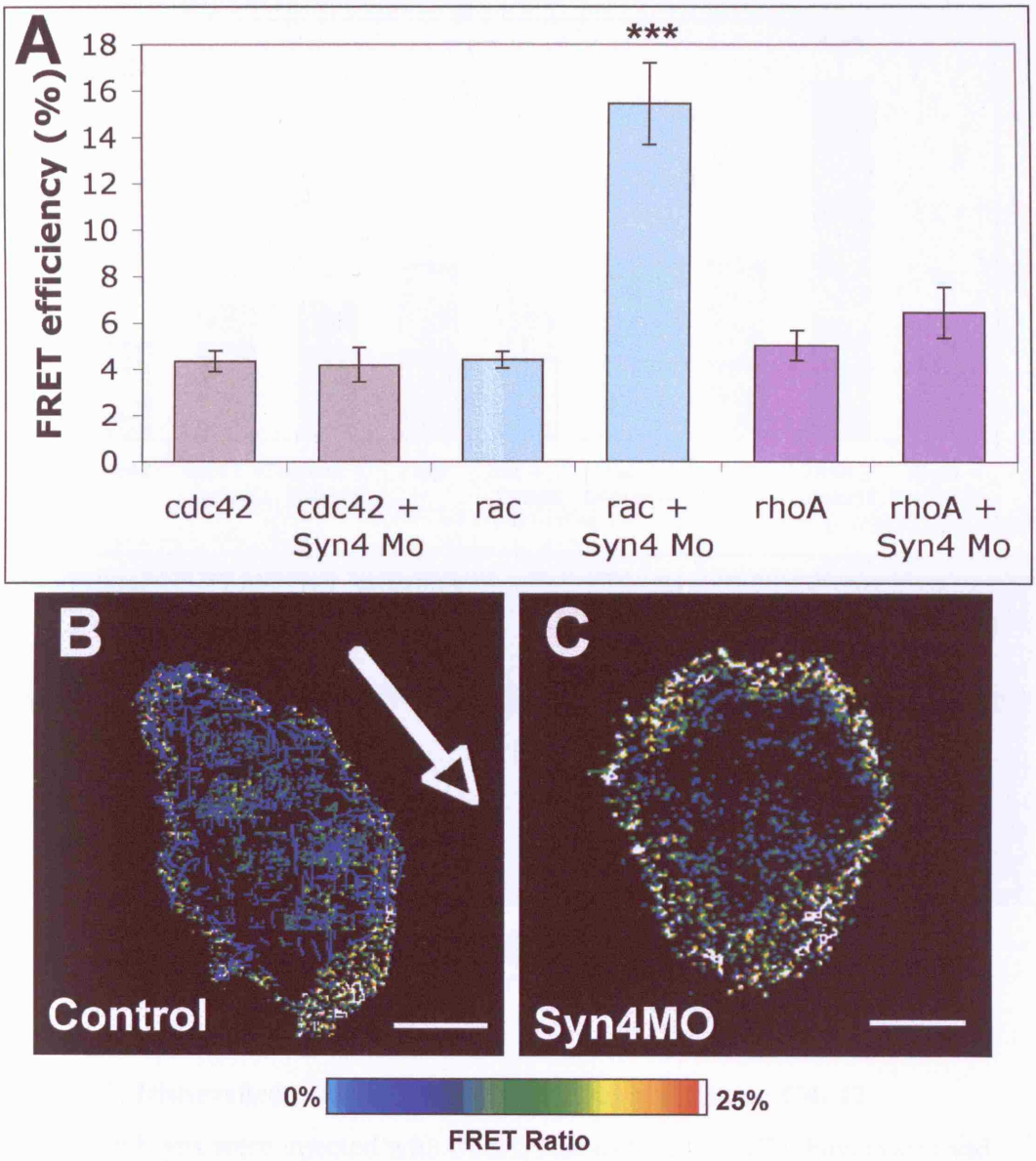


**Figure 6.1. *syn4* Mo affects Rac activity but not RhoA or Cdc42**

*Xenopus* embryos were injected with 75pg RhoA, or 150pg Rac or Cdc42 FRET biosensor plasmid DNA and cranial neural crest explants were cultured on fibronectin for 4 hours. Explants were then fixed and the FRET efficiency measured in individually migrating cells. n= 5 cells for each condition, taken from at least 2 coverslips, ***p<0.005. **(A)** Graph of average FRET efficiency for Cdc42, Rac and RhoA in control Mo and *syn4* Mo injected cells. **(B)** Rac FRET efficiency for a control Mo cell. Arrow indicates direction of migration determined by time-lapse analysis of cell behaviour immediately before fixation. **(C)** Rac FRET efficiency for a *syn4* Mo cell. Scale bars = 10 μm

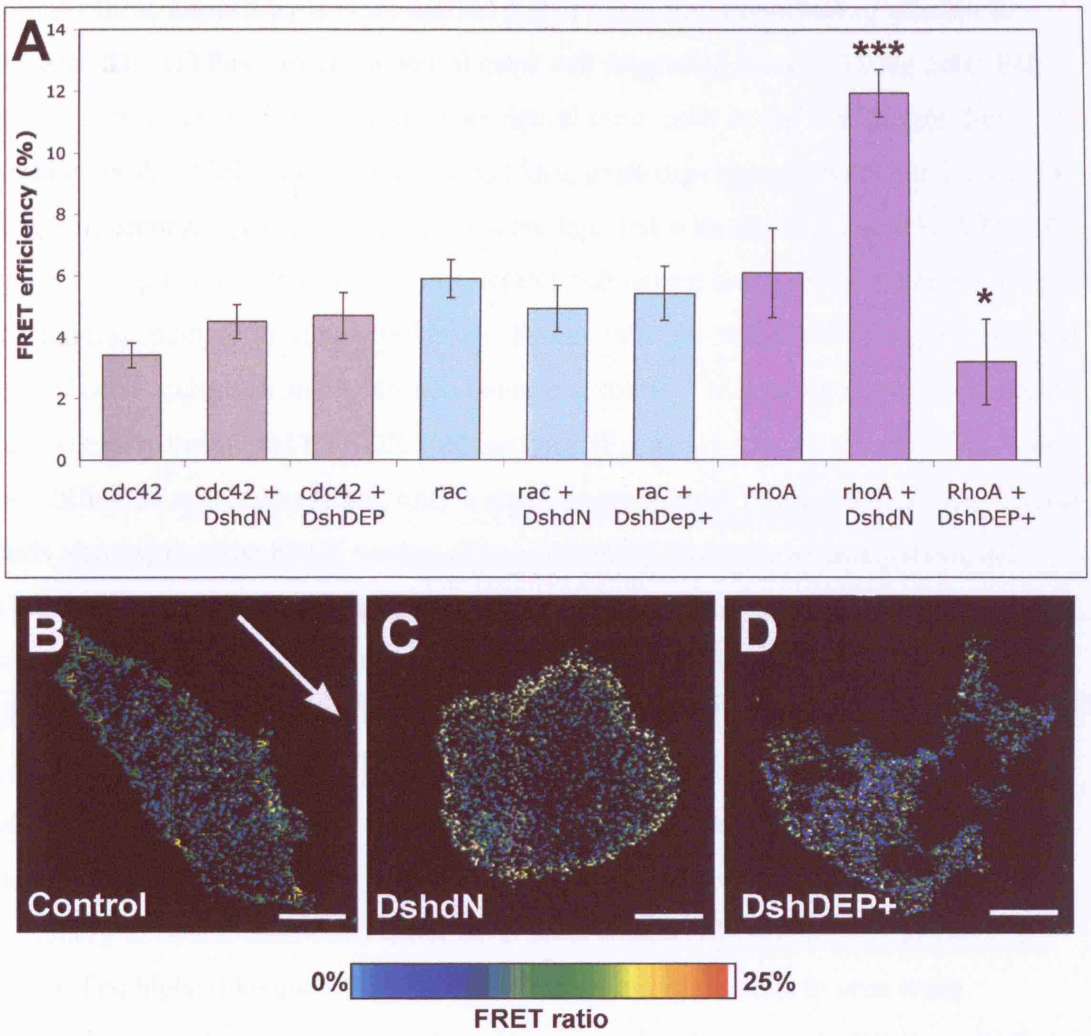


**Figure 6.2. Dishevelled affects RhoA activity but not Rac or Cdc42**

*Xenopus* embryos were injected with RhoA, Rac or Cdc42 FRET biosensors and cranial neural crest explants were cultured on fibronectin for 4 hours. Explants were then fixed and the FRET efficiency measured in individually migrating cells. **(A)** Graph of average FRET efficiency for Cdc42, Rac and RhoA in cells taken from control embryos, and embryos injected with 1ng DshDEP+ or 1ng DshΔN. n= 6 cells for each condition, taken from at least 2 coverslips, ***$p<0.005$; *$p<0.05$. **(B)** RhoA FRET efficiency for a control cell. Arrow indicates direction of migration determined by time-lapse analysis of cell behaviour immediately before fixation. **(C)** RhoA FRET efficiency for a DshΔN cell. **(D)** RhoA FRET efficiency for a DshDEP+ cell. Scale bars = 10 μm.

As these experiments were carried out *in vitro*, it is important to attempt to observe Rho GTPase levels in neural crest cell migrating *in vivo*. Using zebrafish embryos in this case is not possible, as neural crest cells in the *sox10:egfp* line already exhibit GFP fluorescence. Therefore, graft experiments were carried out in *Xenopus* embryos (Fig 6.3). Embryos were injected with the Rac and RhoA FRET probes alongside rhodamine dextran (RDX) and neural crests were dissected at stage 17 and transplanted to uninjected hosts. Embryos were then fixed at stage 25 during neural crest migration and sectioned using a cryostat. Migrating neural crest cells can be easily visualised by RDX fluorescence (Fig 6.3 A-D). As plasmid DNA does not diffuse as quickly as RDX, only a small proportion of RDX positive neural crest cells also express the FRET probes (Fig 6.3 A'-D'). This allows analysis of the FRET efficiency of individual migrating neural crest cells (Fig 6.3E-H). The resolution is significantly lower than for neural crest cells *in vitro*, but it was still possible to observe localised Rac and RhoA activation. In some, although not all cases, Rac activity is clearly localised at the front of migrating neural crest cells *in vivo* (Fig 6.3E). This was particularly clear for leading cells in a group of migrating neural crest. As with *in vitro*, Rac activity was enriched around the entire cell periphery in neural crest cells taken from embryos co-injected with *syn4* Mo (Fig 6.3F). The highest levels of RhoA activity in neural crest cells *in vivo* were concentrated at the edges of the cell, with some cells showing a particular enrichment at the back (Fig 6.3G). In cells taken from embryos injected with Dsh-DEP+, this was significantly reduced (Fig 6.3H). Most importantly, measurement of the overall FRET efficiency for a number of cells in each condition, reveals a clear difference when Syn4 or Dsh is inhibited. Rac levels were greatly increased in *syn4* Mo cells compared to controls (Fig 6.3I), while RhoA levels suffered a significant reduction in the presence of DshDEP+ (Fig 6.3J). Therefore, the effects observed *in vitro* can be reproduced *in vivo*.

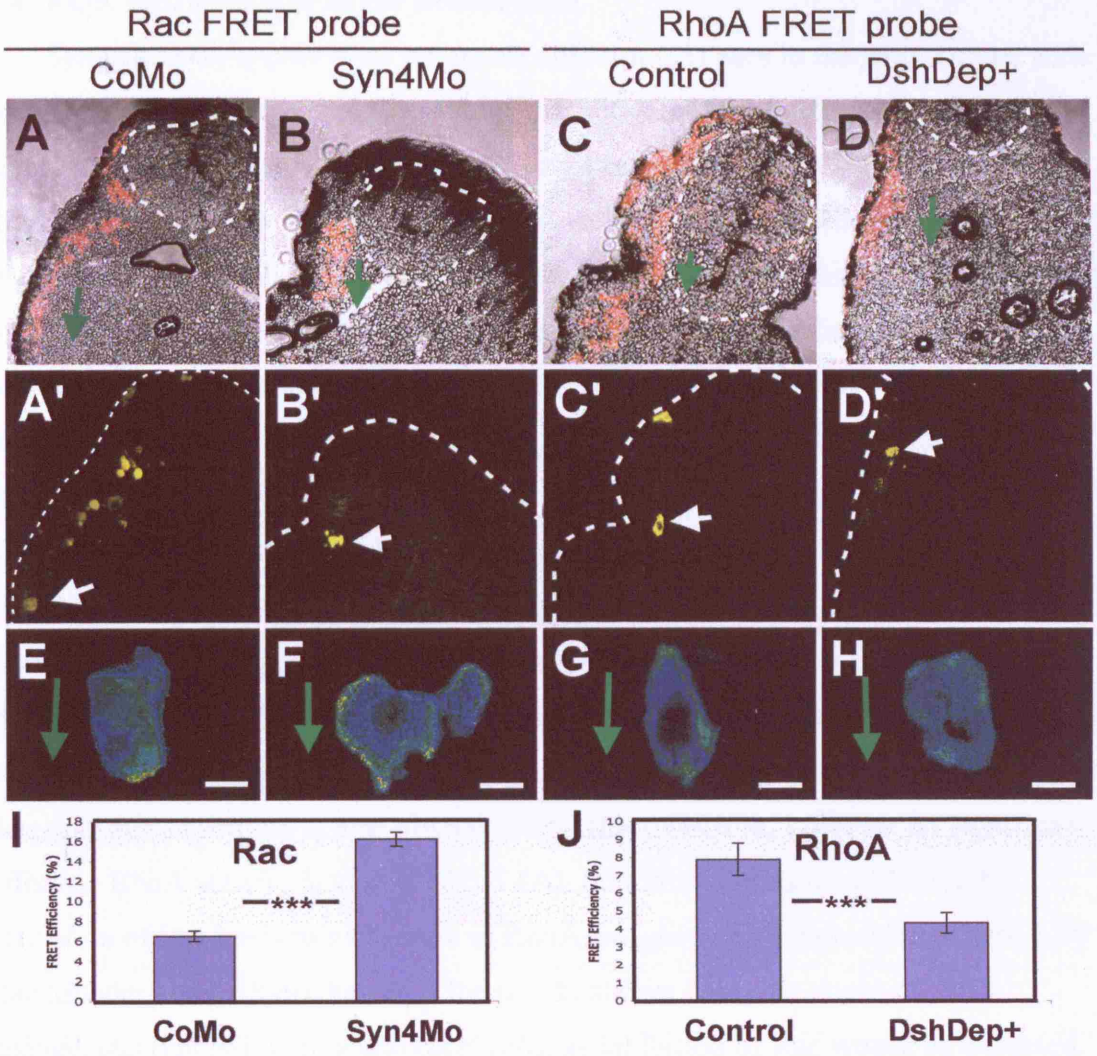


**Figure 6.3. Syn4 affects Rac while Dsh affects RhoA *in vivo***

Embryos were injected with the FRET probes for Rac and RhoA and membrane-RFP. Before migration the injected neural crests were grafted into wildtype host embryos. NC migration was observed *in vivo* and then the embryos were fixed, sectioned and processed for FRET analysis. **(A-D)** Transverse section of stage 28 *Xenopus* embryos, overlay of membrane-RFP (NC cells) and bright field images. Dotted circle indicates the neural tube. Green arrow: direction of migration. **(A'-D')** The embryos from A-D showing fluorescence from the FRET probes. Arrows indicate the selected cells shown in E-H. **(E-H)** Examples of FRET efficiency in individual migrating cells *in vivo*. (A, A' E) Rac probe in cells injected with the control Mo. (B, B', F) Rac probe in cells injected with *syn4* Mo. (C, C', G) RhoA probe in cells injected with control Mo. (D, D', H) RhoA probe in cells injected with DshDep+. **(I)** Average FRET efficiency for Rac *in vivo*. **(J)** Average FRET efficiency for RhoA *in vivo*. ***: $p < 0.005$, scale bars=10μm.

### 6.4. ROK represses Rac in the neural crest

Syn4 and Dsh appear to be acting on different GTPases in the neural crest, with Syn4 acting as a repressor of Rac, while Dsh activates RhoA. However, neither GTPase exists as an isolated entity and many example of crosstalk between the different GTPases has been described. To investigate the possibility of cross regulation between RhoA and Rac in the neural crest, small molecule inhibitors were used to modulate Rac and RhoA signalling. Y-27632 is a specific inhibitor of ROK, RhoA's downstream effector, (Uehata et al., 1997) while the inhibitor NSC-23766 has been specifically designed to inhibit Rac1 by interfering with the Rac-GEF interaction (Gao et al., 2004). Neural crest cells taken from embryos injected with the FRET reporters for Rac, RhoA or Cdc42 were cultured *in vitro* in a medium containing either 50 μM Y-27632 or 100 μM NSC-23766 (Fig 6.4). The results reveal crosstalk between all three GTPases. Treatment with the specific Rac inhibitor, NSC-23766, results in an increase in Cdc42 activity, suggesting possible competitive roles of Rac and Cdc42 at the leading edge (Fig 6.4A). Naturally, a decrease in Rac activity is also observed with this treatment, however no significant effect on RhoA activity is visible (Fig 6.4A). Previous studies have shown that activation of Rac leads to a decrease in RhoA, suggesting a suppression of RhoA by Rac (Sander et al., 1999), however the results shown here cast doubt on an endogenous repression in neural crest cells, as inhibition of Rac would be expected to relieve such repression resulting in an activation of RhoA.

Treatment with the ROK inhibitor, Y-27632, also results in an increase in Cdc42 levels and a small decrease in RhoA activity, likely to be due to positive feedback between ROK and RhoA. Most significantly, though, a large increase in Rac activity is observed in the presence of the ROK inhibitor (Fig 6.4A). This suggests that ROK is acting as a potent inhibitor of Rac in the neural crest, an interaction which has been well described in other cell types (Ohta et al., 2006; Tsuji et al., 2002; Yamaguchi et al., 2001) Images of the FRET efficiency of individual migrating cells demonstrate that while Rac activity is confined to the leading edge in control cells as before (Fig 6.4B), Y-27632 treatment results in high levels of Rac activity around the cell membrane (Fig 6.4C). This is very similar to what is observed in cells expressing the *syn4* Mo. So like Syn4, RhoA may be acting as a repressor of Rac in the neural crest.

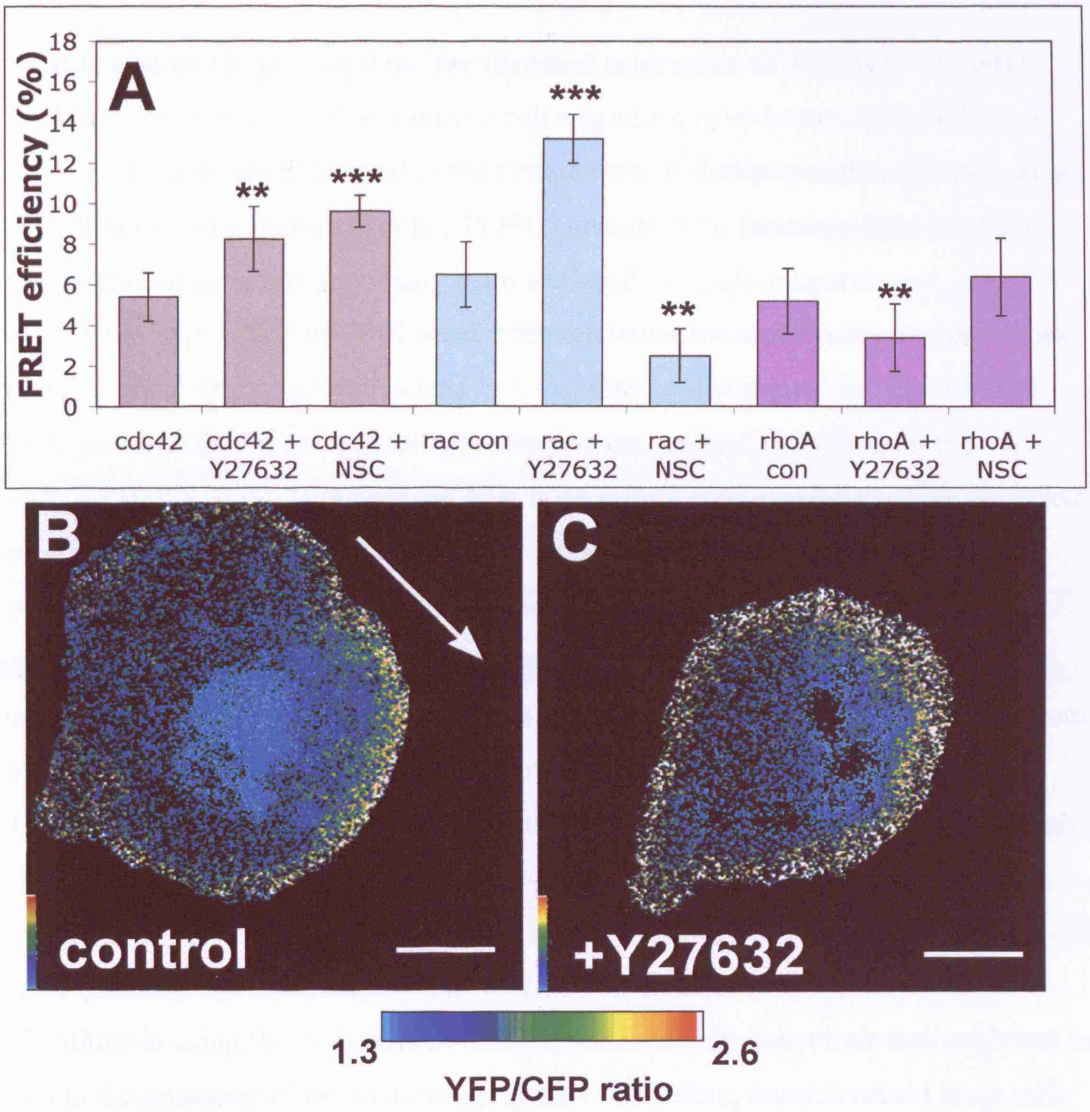


**Figure 6.4. ROK represses Rac in neural crest cells migrating *in vitro***

*Xenopus* embryos were injected with DNA coding for RhoA, Rac or Cdc42 FRET biosensors and cranial neural crest explants were cultured for 4 hours on fibronectin. Explants were then fixed and the FRET efficiency measured in individually migrating cells. **(A)** Graph of average FRET efficiency for Cdc42, Rac and RhoA in cells cultured in a control medium or in a medium containing 50 μM Y-27632 or 100 μM NSC-23766 (NSC). n= 5 cells for each condition, taken from at least 2 coverslips, ***$p<0.005$; **$p<0.01$. **(B)** Rac FRET efficiency for a control cell. Arrow indicates direction of migration determined by time-lapse analysis of cell behaviour immediately before fixation. **(C)** Rac FRET efficiency for a cell treated with the ROK inhibitor, Y-27632. Scale bars = 10 μm.

### 6.5. Rac and ROK are required for directed migration of neural crest cells

The roles of Rac and RhoA during cell migration have been widely described, and both GTPases are expressed in the neural crest in *Xenopus* embryos(Lucas et al., 2002; Wunnenberg-Stapleton et al., 1999), however their functions during neural crest migration have not previously been analysed. Therefore neural crest behaviour was analysed when Rac or ROK were inhibited using the small molecule inhibitors. Initially, whole embryos were placed in a medium containing up to 100 μM of Y-27632 or NSC-23766, and *in situ* hybridisation was carried out to examine *in vivo* neural crest migration. However, no effects on neural crest migration were observed nor any other developmental defects. It is not known whether Y-27632 or NSC-23766 are able to cross the outer epithelium of the embryo, and since Rac and ROK are known to be vital for many developmental processes, it would seem likely that they are not. Additionally beads soaked in Y-27632 or NSC-23766 were grafted into the neural crest of *Xenopus* embryos, but no effect on neural crest migration was observed. Once again, it is not known whether the inhibitors would in fact be caught up in the porous beads and whether they would be able to diffuse freely out. Also, the small size of Y-27632 or NSC-23766 means that any diffusion would likely to be rapid, resulting in a rapid dispersal away from the neural crest. Due to these difficulties in using the inhibitors *in vivo*, neural crest cell behaviour was analysed *in vitro* in the presence of the inhibitors (Fig 6.5). As before, control neural crest cells migrated persistently away from the centre of the neural crest explant with an average speed of 1.9μm/min (Fig 6.5A-C). When neural crest cells were cultured in a medium containing 50 μM Y-27632, their behaviour was markedly different from controls and they rapidly dispersed away from the centre of the explant (Fig 6.5D,E). Tracking of individual cell trajectories reveals that in the presence of Y-27632 cells lose persistent migration and frequently change direction (Fig 6.5F, compare to 6.5C). On the other hand, cells cultured in medium containing 100 μM NSC-23766 show a decrease in migratory behaviour and travel very little distance over 60 minutes (Fig 6.5G-H). Cell tracking shows a loss of persistence and as well as a shortening of track length indicating a decrease in migration speed (Fig 6.5I). Measurement of the velocity of individual cells shows that in the presence of the Rac inhibitor, cells do have a significantly decreased mean speed of 1.55μm/min. The speed of cells treated with the ROK inhibitor is unaffected. So, an increase in Dsh

signalling, which correlates with an increase in RhoA levels results in a decrease in migration speed (Fig 6.5J). Meanwhile, the higher levels of Rac activity associated with *syn4* Mo or with the ROK inhibitor treatment have no significant effect on migration speed (Fig 6.5J). The average persistence of individual neural crest cells was also calculated. Treatment with either the Rac or ROK inhibitors resulted in a decrease with cells having an average of 0.26 and 0.45 respectively (compared to 0.65 in control neural crest cells). All of the treatments result in a significant decrease in persistence of migration (Fig 6.5K), suggesting that a fine balance of Syn4 and Dsh signalling is required to precisely regulate Rac and RhoA to allow persistent migration.

### 6.6. Rac and ROK control the formation of cell protrusions and focal contacts in neural crest cells

As Syn4 and Dsh both control the formation of cell protrusions and focal contacts and modulate Rho GTPase levels, it is likely that Rac and RhoA are also playing a role in these processes. Cells treated with the Rac and ROK inhibitors were imaged at higher magnification to observe the effects on cell protrusion formation (Fig 6.6). As previously, control cells have a polarised morphology with new protrusions forming only at the leading edge (Fig 6.6A-C). By contrast cells cultured with the ROK inhibitor are anything but polarised with filopodium-like protrusions forming all around the cell (Fig 6.6D-E). Analysis of protrusions over a 20-minute period reveals that these small protrusions form and collapse very rapidly (Fig 6.6F). As Rac activity is increased in these cells, this is consistent with the well-established role of Rac in promoting protrusion at the leading edge. Additionally, RhoA has been described to limit the production of cell protrusions possibly through repression of Rac (Worthylake and Burridge, 2003). In cells cultured in the presence of the Rac inhibitor, polarity is also lost (Fig 6.6G, H). Furthermore these cells exhibit a rounded morphology and lack cell protrusions. In fact over a 20minute period, no protrusive activity was observed (Fig 6.6I), although the cells moved constantly and were clearly alive. Again, this is consistent with an essential role for Rac in protrusion formation.

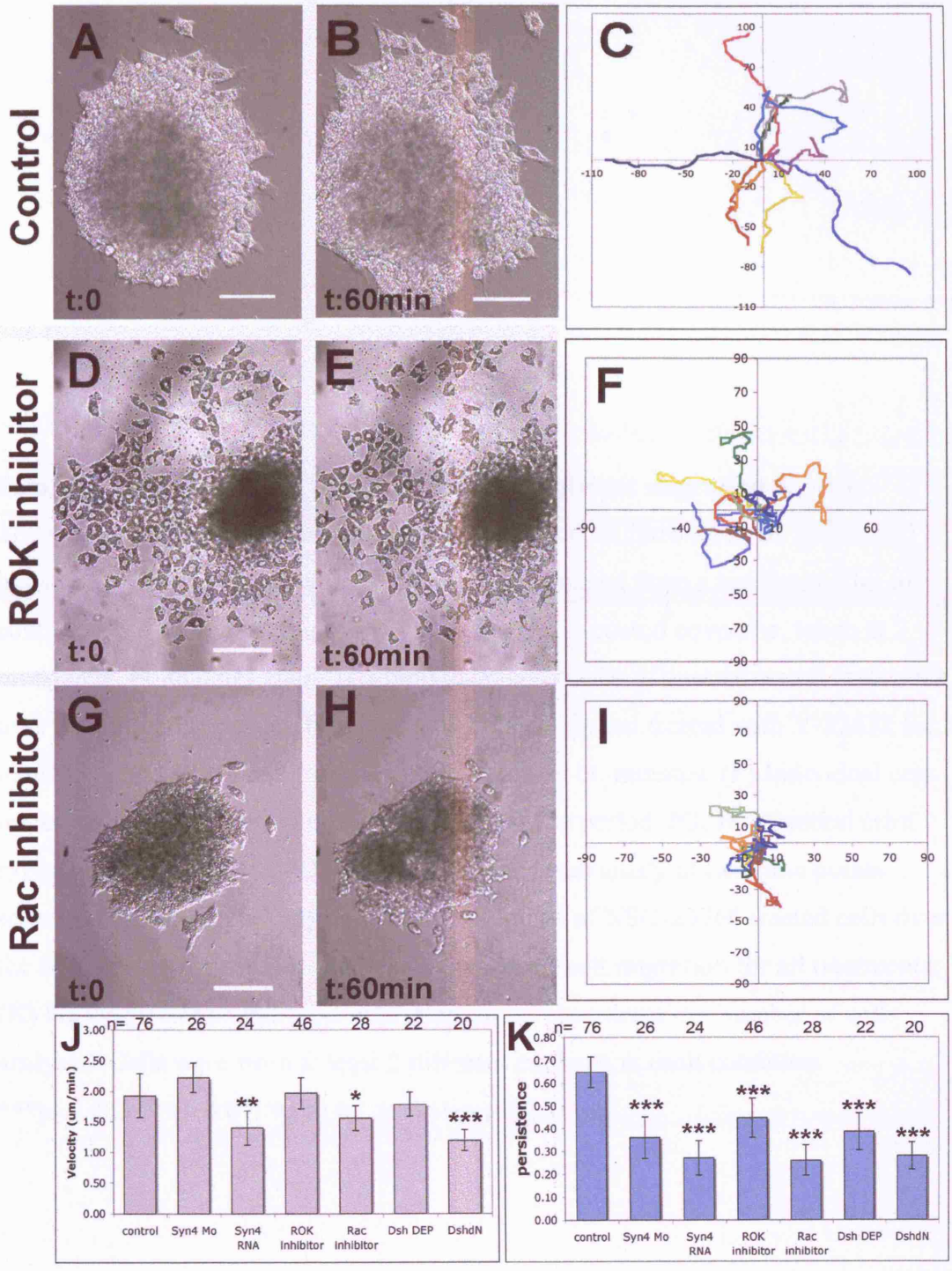
Control
ROK inhibitor
Rac inhibitor
A
B
C
D
E
F
G
H
I
t:0
t:60min
J
K
n= 76 26 24 46 28 22 20
Velocity (um/min)
persistence
control
Syn4 Mo
Syn4 RNA
ROK inhibitor
Rac inhibitor
Dsh DEP
DshdN

**Figure 6.5**

**Figure 6.5. Rac and ROK are required for persistent migration *in vitro*.**
*Xenopus* cranial neural crest explants were cultured on fibronectin as before and individual cell trajectories were tracked. **(A, B)** Images from a timelapse film of control neural crest cells migrating on a fibronectin-coated coverslip, taken at 2 timepoints, 60-minutes apart. **(C)** Individual cell tracks of control neural crest cells over the 60-minute period. **(D, E)** A neural crest explant treated with Y-27632 for 30 minutes previously at two timepoints separated by 60 minutes. **(F)** Individual cell tracks of Y-27632 treated cells over the 60-minute period. **(G, H)** A neural crest explant treated with NSC-23766 for 30 minutes previously at two time points separated by 60 minutes. **(I)** Individual cell tracks of NSC-23766 treated cells over the 60-minute period. **(J)** Velocity of neural crest cell migration for all treatments. **(K)** Persistence of neural crest migration for all treatments. n= number of cells analysed. Cells were from at least 2 different explants in each condition. ***p<0.005; **p<0.01; *p<0.05, scale bars = 200 μm.

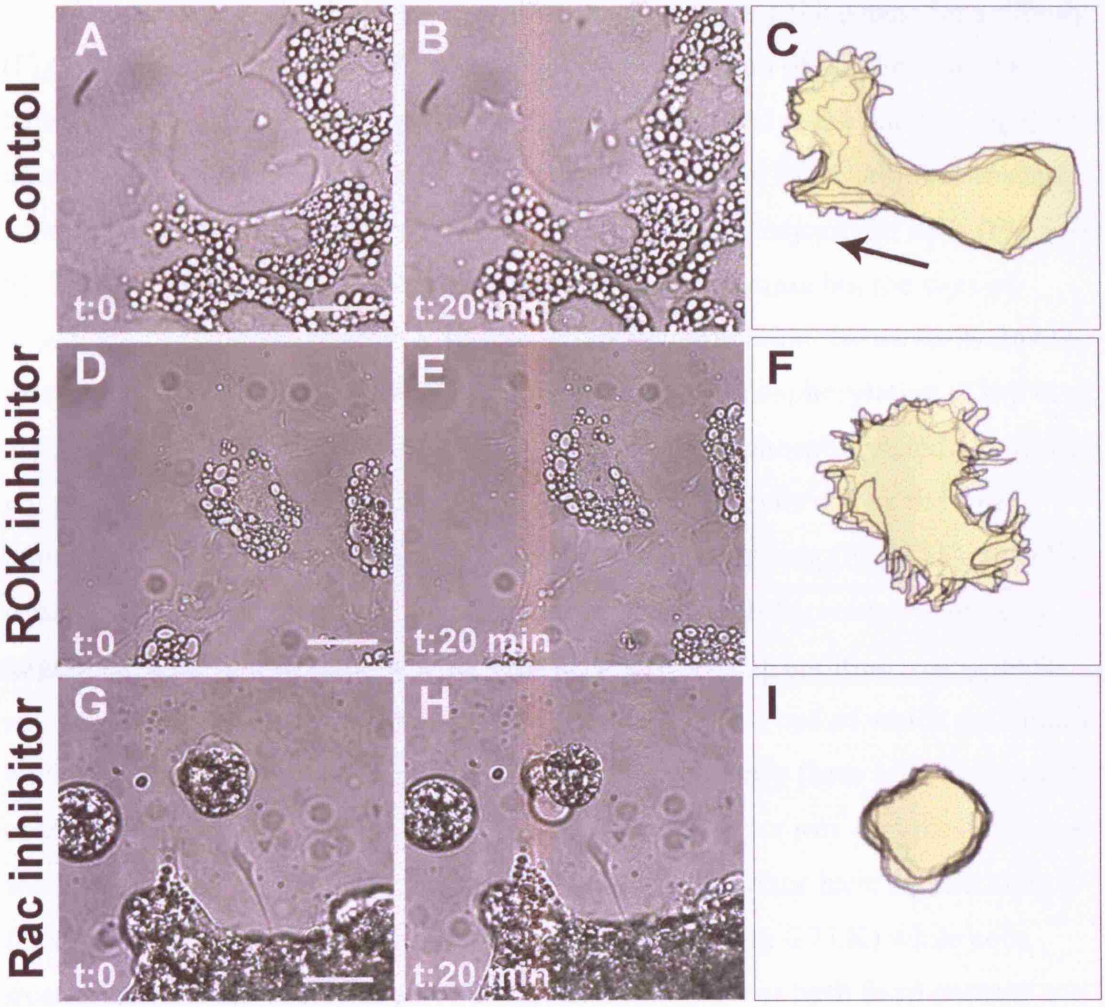


**Figure 6.6. Rac and ROK control the formation of cell protrusions *in vitro***

*Xenopus* cranial neural crest cells were cultured on fibronectin and the shape of individual cells was observed over a 20-minute period by timelapse photography. **(A, D, G)** DIC image of cells at t=0. **(B, E, H)** DIC image of the same field after 20 minutes. **(C, F, I)** Outline of individual cell shapes plotted every 5 minutes to show the change in cell protrusions over the 20-minute time period. Images not to scale. (A-C) Control neural crest cells. Arrow in C indicates direction of cell migration. (D-F) Cells treated with Y-27632. (G-I) Cells treated with NSC-23766. Scale bars = 20μm.

Cells were also fixed and focal contacts analysed using the p-paxillin antibody (Fig 6.7). Polarised control cells have a similar distribution of focal contacts as before, with paxillin containing adhesions mostly localised at the leading edge, often associated with the tips of actin filaments (Fig 6.7A-C). In ROK inhibitor treated cells, no paxillin accumulations could be observed in the majority of cells (Fig 6.7D-F). These cells are clearly attached to the underlying substrate but the sites of attachment may be too small to visualise at this magnification. However Y-26732 treatment has been shown to decrease paxillin tyrosine phosphorylation (Tsuji et al., 2002), so it is likely that adhesion structures containing phosphorylated paxillin are not present. Staining with rhodamine phalloidin in these cells shows the large number of small actin protrusions all around the cell periphery (Fig 6.7F). In cells treated with the Rac inhibitor, p-paxillin staining is greatly increased with many large focal adhesion structures being visible (Fig 6.7G). In addition, many thick actin stress fibres can be observed under the cell body, the tips of which co-localise with paxillin containing adhesions (Fig 6.7H,I). To quantify these effects on focal contact formation, the average number of focal contacts per $\mu m^2$ and the average size was measured as before. Cells treated with the ROK inhibitor have significantly fewer and smaller focal contacts compared to controls (Fig 6.7J,K) while cells treated with the Rac inhibitor show a significant increase in both focal contact number and size (Fig 6.7J.K). Once again, these results confirm the previously well-described roles of Rac and RhoA in cell migration in neural crest cells. Inhibition of Rac gives rise to cells lacking in cell protrusions, but containing many mature focal adhesions and stress fibres, confirming a role for Rac in protrusion formation and focal contact turnover. Meanwhile, inhibition of ROK, which I have shown corresponds to a general increase in Rac activity (Fig 6.4), results in an increase in cell protrusions and decrease in focal contacts (presumably due to increased turnover and promotion of new focal complex formation driven by Rac), as well as a decrease in stress fibres, which are typically associated with RhoA activity.

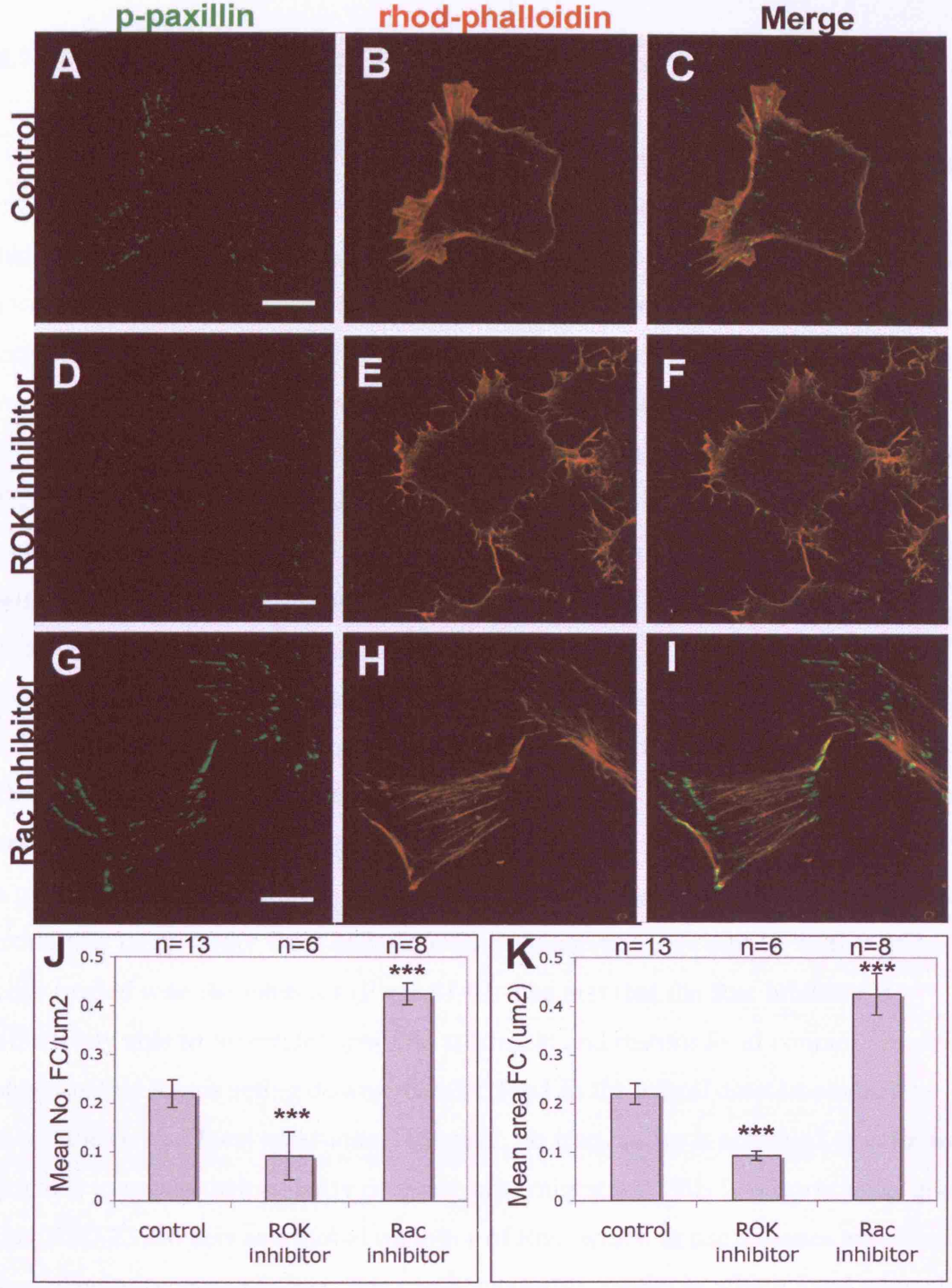


**Figure 6.7. Rac and ROK control focal contacts *in vitro***

**(A-I)** *Xenopus* neural crest cells were cultured for 5 hours on fibronectin, fixed and stained with an antibody against phospho-paxillin (A, D, G), and rhodamine-phalloidin (B, E, H). (A-C) Control neural crest cells. (D-F) Cells treated with Y-27632. (G-I) Cells treated with NSC-23766. Scale bars = 20μm. **(J)** Average number of focal contacts per $\mu m^2$ of cell area. **(K)** Average size of focal contacts (in $\mu m^2$). n= no. cells analysed, takend from at least two experiments. ***p<0.005.

## 6.7. Inhibition of Rac is able to rescue the effect of *syn4* Mo on focal contact formation.

FRET analysis indicates that Syn4 is acting as a repressor of Rac in the neural crest, as injection of *syn4* Mo results in an increase in Rac activity (Fig 6.1). It is likely to be through this inhibition of Rac that Syn4 modulates cell polarity and the formation of cell protrusions and focal contacts. To test this hypothesis, a rescue experiment was carried to see if inhibition of Rac using NSC-23766 was able to reverse the effect on focal contact formation observed with *syn4* Mo (Fig 6.8). Neural crest cells were dissected from stage 17 *Xenopus* embryos, cultured *in vitro* for 5 hours and then fixed and stained with the p-paxillin antibody and rhodamine-phalloidin. As before, control neural crest cells have a polarised actin cytoskeleton with medium sized focal contacts visible at the front of the cell (Fig 6.8A-C). Treatment of control cells with the Rac inhibiter once again greatly increases the number and size of focal contacts and results in increased stress fibre formation (Fig 6.8D-F). Cells taken from *syn4* Mo injected embryos, when cultured in a normal Danilchick medium, show a decrease in focal contact formation compared to controls and also lose cell polarity (Fig 6.8G-I). However when *syn4* Mo cells are cultured in a medium containing the Rac inhibitor, the opposite phenotype is observed with cells exhibiting much larger focal adhesions in a phenotype more similar to that of control cells treated with the inhibitor (Fig 6.8J-L). The fact that the Rac inhibitor is effectively able to 'override' *syn4* Mo treatment and restore focal contact formation, suggests that Rac is acting downstream of Syn4 in the neural crest to control the cytoskeleton and focal adhesions. However, no true rescue is achieved as cells are not able to regain their polarity or directional migration. This is unsurprising, given that NSC-23766 acts as a global inhibitor of Rac, which in itself causes an inherent loss of polarity. Nevertheless, this result supports a model in which Syn4 controls neural crest migration through repression of Rac.

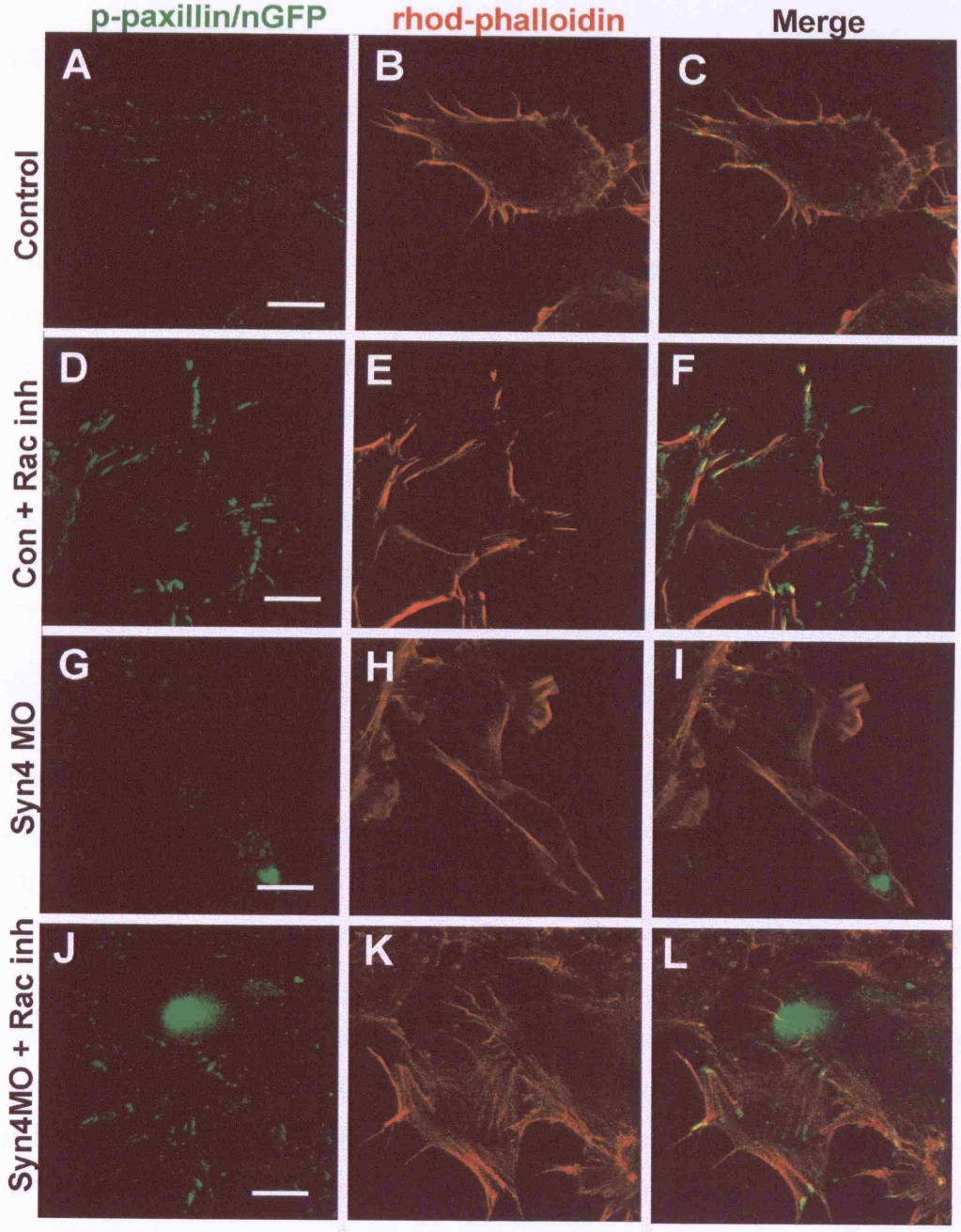


**Figure 6.8. The effect of *syn4* Mo on focal contacts can be rescued by inhibition of Rac.**

*Xenopus* neural crest cells were cultured for 5 hours on fibronectin and then fixed and stained with an antibody against phospho-paxillin (A, D, G, J), and rhodamine-phalloidin (B, E, H, K). **(A-C)** Control neural crest cells. **(D-F)** Cells cultured in a medium containing 100 μM NSC-23766 **(G-I)** Cell taken from an embryo injected with 8ng *syn4* Mo and nuclear-GFP. **(J-L)** Cell taken from an embryo injected with 8ng *syn4* Mo and nuclear-GFP, cultured in a medium containing 100 μM NSC-23766. Note how the decrease in focal contacts normally observed with *syn4* Mo is reversed. Scale bars = 20μm.

## 6.8. Discussion

Rac and RhoA are pivotal regulators of cell migration in many different cell types and the data presented here, using small molecules to inhibit Rac and ROK activity, confirms that this is also the case in neural crest cells. Cells with reduced Rac or ROK activity lose polarised morphology and are unable to undertake directional migration (Figs 6.5, 6.6). Furthermore, the roles of Rac and RhoA in regulating membrane protrusion and substrate attachment in the neural crest correlate with those that have been previously described in other cell types. It comes as no surprise that small GTPases act downstream of Syn4 and Dsh in the neural crest, however it appears that Syn4 and the PCP pathway are primarily affecting the activities of different GTPases.

Cdc42 is involved in the regulation of cell polarity in a number of migratory cell types (Reviewed in (Etienne-Manneville and Hall, 2002). Expression of dominant negative forms of Cdc42 results in cell depolarisation and inhibits directional migration in fibroblasts and astrocytes (Etienne-Manneville and Hall, 2001; Nobes and Hall, 1999). Cdc42 also regulates polarity during migration by contributing to formation of filopodia at the leading edge and by re-orientating the microtubule organising centre and Golgi apparatus to form a polarised network (Etienne-Manneville and Hall, 2003; Nobes and Hall, 1995b; Nobes and Hall, 1999; Palazzo et al., 2001). However, more recent studies have shown little effect of Cdc42 upon cell polarity. Pankov et al (2005) used siRNA to inhibit Cdc42 in fibroblasts and found no effect on directional migration. Likewise, genetic ablation of Cdc42 in fibroblastoid ES cells, unlike expression of a dominant negative form, has been shown to have no effect on directional migration, cell polarity or the formation of filopodia in a wound healing assay (Czuchra et al., 2005). One possible explanation for these differences is that dominant negative forms of Cdc42 may bind GEFs that are not specific for Cdc42, and therefore could disrupt the activity of other Rho GTPases such as Rac or RhoA. Here I show that inhibition of Syn4 or PCP signalling have no effect on the activation status of Cdc42, despite the fact that these treatments have a profound effect upon cell polarity and directed migration. This would suggest that in NC migration Cdc42 is not the primary GTPase regulating cell polarisation and protrusion formation. However a role for Cdc42 cannot be ruled out as inhibition of Cdc42 in neural crest cells has not been attempted here.

There is much evidence that Syndecan-4 regulates Rho GTPases, and it was initially proposed to be an activator of RhoA, based upon the rapid formation of stress fibres observed when Syn4 is artificially activated by antibody binding. This effect can be blocked by addition of a Rho inhibitor, C3 transferase from Clostridium botulinum, suggesting a direct link between Syn4 and Rho activation (Saoncella et al., 1999). Syn4-dependent phosphorylation of focal adhesion kinase may also involve RhoA, as activation of RhoA with LPA treatment can rescue the decrease in phosphorylation observed in Syn4 null fibroblasts (Wilcox-Adelman et al., 2002a). More recent work places PKCα in this pathway, with Syn4 activating PKCα, which in turn activates RhoA to control FAK phosphorylation (Dovas et al., 2006). However none of these studies directly measured GTPase activity in the presence or absence of Syn4 and most conclusions are inferred from the use of RhoA activators or inhibitors to rescue cell morphologies. Here, by directly measuring RhoA activity using FRET, I have shown that in neural crest cells at least, the effect of Syn4 on RhoA is negligible. Instead, an antisense Mo against *syn4* increases the levels of Rac in the entire cell, suggesting that Syn4 contributes to the inhibition of Rac. Several recent publications have supported the idea that Rac, rather than RhoA may be the principal small GTPase acting downstream of Syn4. Saoncella et al, using both a Rac-GTP pull-down assay and immunostaining of Rac in fixed cells, show that Rac activity is elevated in Syn4-null fibroblasts and that its sub-cellular distribution is disrupted (Saoncella et al., 2004). However work by Tkachenko and colleagues has shown that Rac is activated at the leading edge in response to Syn4 engagement and clustering (Tkachenko et al., 2006; Tkachenko et al., 2004). Some clarification has come from the recent study by Bass et al (2007). They used FRET to measure Rac activity in migrating fibroblasts and found that while wildtype cells showed Rac activity localised at the leading edge, Syn4-null cells had an increase in Rac activity all around the membrane. RhoA, however, was unresponsive to changes in Syn4 signalling. Furthermore, they show that regulation of Rac by Syn4 contributes to persistent migration. I have shown here that this is also the case in the neural crest. However, Bass et al also propose that Syn4 stimulates an initial wave of Rac activation upon cell spreading. They suggest that this early activation of Rac, induced by engagement of Syn4 with the extracellular matrix, is responsible for localised Rac activity and hence membrane protrusion at the leading edge (Bass et al., 2007). In neural crest cells only antagonism of Rac by Syn4 was observed, a

result that conflicts with the hypothesis presented by Bass and colleagues. Their model is based on the finding that *syn4-/-* fibroblasts lack the early wave of Rac activation that is normally observed in wildtype cells plated on fibronectin. However they also show that Rac levels are consistently higher in Syn4-null cells, so it is possible that any initial increase in Rac could simply be masked by a background of high Rac activity, and is therefore not necessarily dependent on Syn4. Alternatively, an initial Syn4-based activation of Rac may occur in the neural crest, but may not have been observable in the conditions used here. As live FRET imaging proved impractical, analysis of neural crest cells was carried out on fixed cells that had been migrating for several hours and Rho GTPase activity was not analysed during initial attachment and onset of migration. Thus, it is possible that any initial peak in Rac activity could have been missed during this analysis. Either way, the data presented here are consistent with the conclusions of Bass et al that Syn4 controls directional migration through the regulation of Rac, but not RhoA.

While Syn4 appears to be affecting Rac but not RhoA in the neural crest, PCP signalling is principally acting on RhoA. Inhibition of Dsh using DshDEP+ decreases RhoA activity levels, while overexpression of DshΔN results in higher RhoA levels, suggesting that Dsh is acting as an activator of RhoA in the neural crest. In the literature Rac, RhoA and Cdc42 have all been placed downstream of the PCP signalling cascade, as direct links to the actin cytoskeleton. Cdc42 has been implicated in PCP signalling in both the *Drosophila* wing and during vertebrate gastrulation (Choi and Han, 2002; Eaton et al., 1996; Penzo-Mendez et al., 2003). However other reports suggest that RhoA and Rac are the main PCP effectors. Rac and RhoA are both required for cell intercalation during convergent extension movement and appear to play complimentary roles, with RhoA controlling cell shape while Rac is responsible for protrusive activity and filopodium formation (Tahinci and Symes, 2003). Biochemical assays measuring Rho GTPase activity in *Xenopus* cells after modification of PCP signalling have indicated that Rac and RhoA, but not Cdc42, are activated in response to PCP signalling (Habas et al., 2003). However, a triple deletion of the three *rac* genes in *Drosophila*, *rac1, rac2* and *mtl*, fails to cause PCP defects (Adler, 2002; Hakeda-Suzuki et al., 2002) suggesting that Rac signalling is not essential for the PCP pathway. The body of evidence for RhoA playing a role in PCP signalling is more compelling. RhoA can bind to Dishevelled, albeit indirectly through their common interaction with the Formin homology protein,

Daam1 (Habas et al., 2001). RhoA and ROK have both been shown to act downstream of dishevelled in *Drosophila* PCP signalling (Strutt et al., 1997; Winter et al., 2001) and overexpression of ROK also disrupts convergent extension in zebrafish (Marlow et al., 2002). RhoA zebrafish morphants phenocopy PCP mutants and furthermore, activation of RhoA is able to rescue the convergent extension defects normally associated with Wnt11 or Wnt5 mutants (Zhu et al., 2005), suggesting that PCP signalling is responsible for an activation of RhoA during gastrulation. Cells undergoing convergent extension with their elongated morphology and lateral cell protrusions present a different prospect to individually migrating neural crest cells, which form protrusions only at the leading edge. However the effect of PCP signalling on RhoA in the neural crest appears to be conserved. This is the first study in which the levels of Rac, RhoA and Cdc42 have been directly measured using FRET in response to changes in PCP signalling and it points to a clear role for PCP signalling in activating RhoA, but not Rac and Cdc42.

These results indicate that Syn4 and Dsh activate two parallel pathways that lead to the inhibition of Rac and activation of RhoA respectively. However I also show that ROK inhibits Rac in the neural crest. So activation of RhoA by PCP signalling is also likely to lead to Rac inhibition. Thus both pathways ultimately have the same effect of decreasing the overall levels of Rac either directly, or indirectly. Activation of Rac at the front of a cell is a key event during directional migration. Several factors control the localized activity of Rac, such as specific guanine nucleotide exchange factors (GEFs) that are delivered at the front of the cell in a $PI_3K$ dependent manner (Welch et al., 2003), and the formation of lipid rafts (del Pozo et al., 2004). Once Rac is active, numerous feedback loops help maintain directional protrusions. It has been shown that maintaining precise levels of Rac activation at the leading edge is enough to promote persistent migration *in vitro*. Pankov et al (2005) found that modulating Rac levels using RNAi was sufficient to switch cell migration from persistent directional migration to random walk. At very low levels of Rac migration of fibroblasts was inhibited, while at higher levels cells migrated with a high persistence. If levels were increased further, cells lost their persistence and migrated randomly with frequent changes of direction (Pankov et al., 2005). I propose that something similar is happening in neural crest cells. Signalling via Syn4 and the PCP pathway contribute to the inhibition of Rac in the neural crest, thus forming part of the mechanism by which highly localised Rac activity and

directional migration is maintained. Bass et al (2007) have proposed a similar Syn4-based mechanism for the maintenance of directional migration in fibroblasts migrating *in vitro*. This model is able to explain the effects of modulating Syn4 and Dsh on cell migration and morphology described in the previous chapter: Inhibition of Syn4 or Dsh results in an increase in Rac levels and loss of cell polarity. Increased Rac activity also causes an increase in cell protrusions and a decrease in paxillin-containing focal contacts. Conversely, over-activation of Syn4 or Dsh results in a decrease in Rac signalling. This also gives loss of polarity as no cell protrusions are produced in any direction. Additionally, inceased Dsh activity results in higher RhoA levels and the associated increase in stress fibres and mature focal adhesions. This model however throws up a somewhat paradoxical result. If Dsh activates RhoA, which then represses Rac, why is it that no effect on Rac FRET is observed when Dsh is inhibited in neural crest cells? One possible explanation is that a residual amount of RhoA after Dsh inhibition is sufficient to maintain the normal Rac level.

This model explains how Syn4 and PCP signalling allow neural crest cells to maintain a balance of small GTPase activity and thus a directional, persistent migration. However it does not address how neural crest cells establish this polarity in the first place. Additionally, are Syn4 and PCP signalling functioning purely by modulating the overall levels of Rac and RhoA in the cell or are they able to transmit some kind of directional cue that limits Rac activity to the front of the cell? If the latter is the case, then Syn4 and Dsh activity would be expected to be confined to the body of the cell, away from the leading edge, where Rac is not active. In fact, this is indeed the case for PCP signalling as I have shown in chapter 3 that Dsh localises to the back of individual migrating crest cells. Interestingly, this localisation is different in groups of cells where Dsh is localised at the point of contact between two cells. In fact, the localisation of Dsh at the rear of individually migrating cells may result from the fact that the back of the cell was probably the last portion to be in contact with other neural crest cells. This raises the possibility that cell-cell interactions may be involved in the establishment of cell polarity and it is this possibility that will be explored in the following chapter.

# 7. Results: PCP Signalling controls 'Contact inhibition of locomotion' in neural crest cells

## 7.1. Introduction

The sub-cellular localisation of Dsh has often been suggested to be an essential factor in Wnt signalling and I have shown that Dsh accumulates at the back of individually migrating neural crest cells. This is consistent with a role for Dsh in activating RhoA and thus inhibiting cell protrusion formation away from the leading edge. However I have also shown that in groups of neural crest cells Dsh localises to the points of contact between cells (Fig 3.8), a localisation which has also been described in other cell types such as mesoderm (Witzel et al., 2006). This infers a potential role for cell-cell signalling in establishing Dsh localisation in the neural crest and hence in controlling cell polarity.

It is well established that physical contact between two migrating cells can determine cell polarity and the direction of migration. The effect of cell-cell contact on migratory cell behaviour was first described by Abercrombie and Heaysman in the early 1950s (Abercrombie and Heaysman, 1953; Abercrombie and Heaysman, 1954b). They filmed fibroblasts migrating on glass and examined the pathways taken by individual migrating cells upon contact with each other. They found that individual fibroblasts initially migrated randomly but after touching another cell, they cease movement in the previous direction and are diverted away from the point of cell contact. This phenomenon has been termed 'contact inhibition of locomotion' (Abercrombie and Ambrose, 1958). Since then, contact inhibition of locomotion has been show to occur in other cell types including epithelial cells (Brown and Middleton, 1981) and the failure of contact inhibition has been suggested to underlie malignant invasion (Abercrombie, 1979; Abercrombie and Heaysman, 1954a; Paddock and Dunn, 1986). Abercrombie also proposed that contact inhibition of locomotion could account for embryonic cell movements such as gastrulation (Abercrombie, 1967), but to date no *in vivo* examples of contact inhibition have been described. Neural crest cells migrating *in vivo* maintain many short and long range contacts with other neural crest cells (Teddy and Kulesa, 2004), so it is possible that this kind of interaction may also be guiding neural crest migration. In this chapter I will examine the hypothesis that contact inhibition of locomotion occurs in the neural crest and that this process is controlled by Dsh/PCP signalling.

### 7.2. Leading neural crest cells behave differently to non-leading cells *in vitro*

*Xenopus* neural crest explants cultured on fibronectin will rapidly disperse with cells moving persistently away from the centre of the explant (see Figs 5.1, 5.3, 6.4 and also (Alfandari et al., 2003; De Calisto et al., 2005). To analyse a possible role for cell-cell contact in this behaviour, a detailed analysis of *Xenopus* neural crest explants on fibronectin was carried out (Fig 7.1). Scanning Electron Microscopy (SEM) images of migrating neural crest explants illustrate this behaviour, with cells in the centre of the explant forming a tight group, while cells at the edge start to disperse (Fig 7.1A, SEM images thanks to Chaudhary Riaz). Higher magnification SEM reveals that it is only the cells at the very edge of the explant that show any clear polarity, with large lamellipodia protruding away from the bulk of the explant (Fig 7.1B, C). Behind these leading cells, the 'trailing' cells are clearly attached to the substrate and although they possess many thin filopodia-like membrane protrusions, these are distributed all around the cell body and often form connections with the neighbouring cells (Fig 7.1B,C). 95% of leading cells show lamellipodia at the front and only 10% of non-leading cells have lamellipodia. These differences can also be observed using time-lapse analysis of neural crest cells expressing membrane-GFP. Cell at the leading edge are highly polarised in the direction away from the centre of the explant and cells never over-lap with each other (Fig 7.1D, D'). The behaviour of leading cells (i.e. the cells at the front of migration) versus non-leading cells (i.e. cells behind the leading cells) was analysed by tracking their individual migration pathways. Leading cells showed a persistent directional migration (blue lines in Fig 7.1F) with no changes in their angle of migration (blue dots in Fig 7.1G close to 0°). On the contrary, non-leading cells exhibited a low persistence (red lines in Fig 7.1F) and the angles of migration were randomly distributed between -180° and +180° (red dots in Fig 7.1G). These differences in behaviour indicate that two populations of neural crest cells exist *in vitro*; those at the leading edge of migration that exhibit high polarisation and persistent migration (Note it is this population that has been analysed in previous cell tracking experiments, e.g. Fig 5.1) and those behind, which are surrounded by other cells and show much more random movement. This difference could be due to intrinsic cell differences inherited from two populations of cells in the embryo. To test this, neural crest explants were dissected and dissociated in a $Ca^{2+}$ $Mg^{2+}$ free medium (Modified Barth's Solution) and then randomly re-aggregated into groups. A similar cell

behaviour was observed between the re-associated cells and the intact NC explants cultured *in vitro*. Cells re-associated into small groups become rapidly polarized and migrate away from each other (Fig 7.1E). This suggests that the difference between leading and non-leading neural crest cells is not due to intrinsic cell differences, but rather that any cell is able to become polarised if it reaches the leading edge. As non-leading cells are surrounded by other neural crest cells on all sides, the suppression of lamellipodia in these cells could be due to a mechanism like contact inhibition.

### 7.3. Contact inhibition of locomotion occurs between neural crest cells *in vitro* and *in vivo*

To test whether cell contact is sufficient to polarise a cell and interfere with the direction of migration, an explant confrontation assay was developed (Fig7.2A). Two neural crest explants were cultured on a fibronectin-coated coverslip in close proximity, so that soon after the beginning of migration the leading cells from one explant would confront leading cells from the other explant migrating in the opposite direction. This allows the direct observation of a collision between two individual cells. When a neural crest cell encounters a cell from the opposite group, it ceases migration and rapidly collapses its lamellipodium (Fig 7.2A, time of collapse 7.8±3 min) and changes direction to migrate away from the other cell. This behaviour is exactly what was observed by Abercrombie and colleagues in migrating fibroblasts and for which the term 'contact inhibition of locomotion' was coined (Abercrombie, 1970). Analysis of several collisions demonstrates that this behaviour is highly reproducible (Fig 7.2B, 100% cells changed direction, total n=18).

Contact inhibition has been well described *in vitro*, but it is not known if it also occurs *in vivo*. Therefore, the behaviour of individual neural crest cells migrating in the head of *sox10:egfp* transgenic zebrafish was analysed (Fig 7.2D). Cell collision events are rare *in vivo* but do increase in the later stages of development when neural crest cells are more dispersed. Cell behaviour observed at these events mimics that which is observed *in vitro*. When a neural crest cell makes contact with another cell, it rapidly collapses its protrusion and changes direction, migrating in the opposite direction away from the other cell (Fig 7.2E-F). This behaviour was observed in a number of individual cell collision events (Fig 7.2C) and in total 30% of cell collisions *in vivo* resulted in cells separating and moving away from each other (n=60 individual cells). This indicates that contact inhibition is also occurring between neural crest cells *in vivo*.

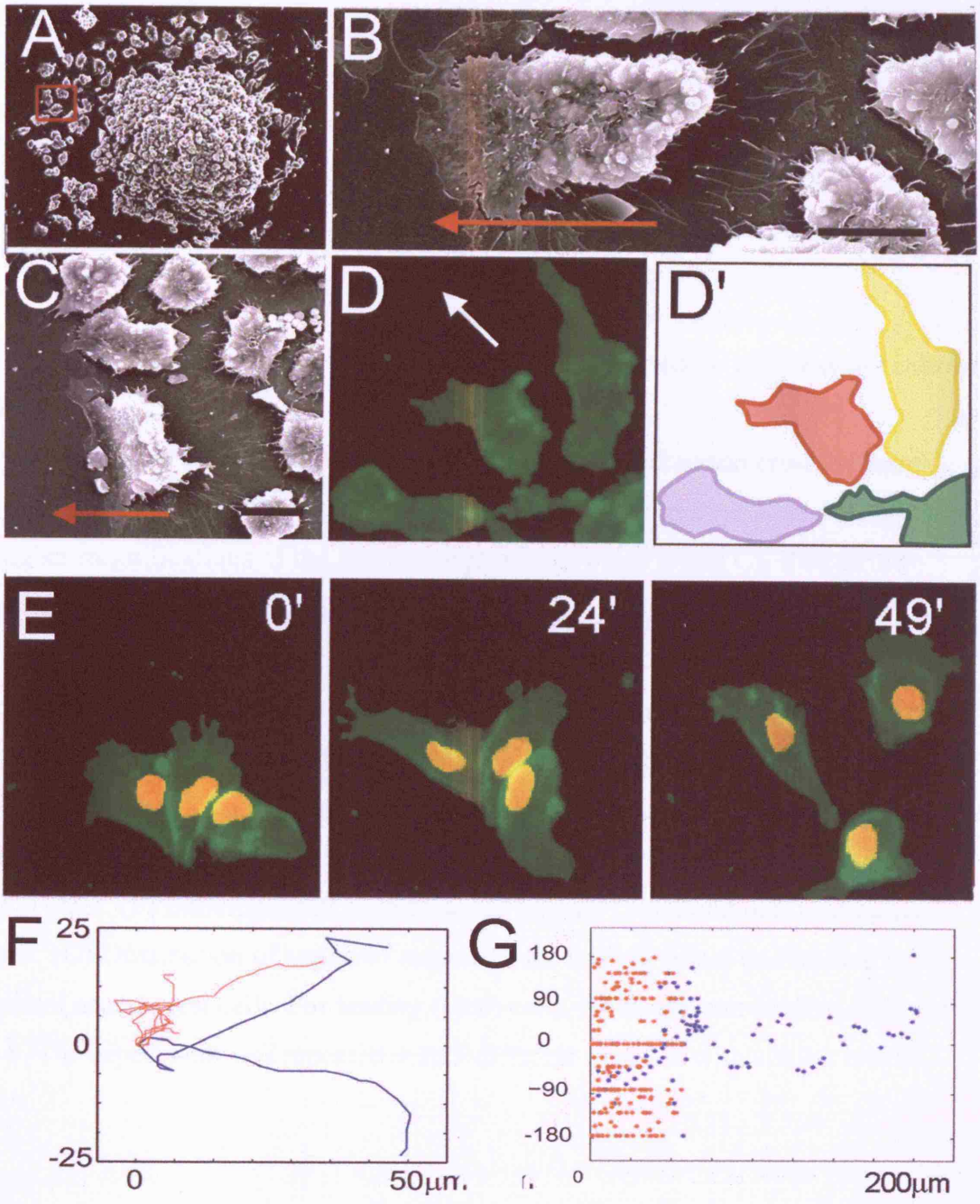


**Figure 7.1**

**Figure 7.1. Leading neural crest cells behave differently to non-leading cells *in vitro***

**(A-C)** Scanning electron micrographs of *Xenopus* cranial neural crest explants migrating *in vitro*. Red square in A indicates cells at the leading edge of migration (higher magnifications of the leading edge are shown in B and C). Red arrow indicates direction of migration. Note extensive lamellipodium in leading cell in B. Scale bars = 50μm. **(D)** Fluorescent microscope image of neural crest cells expressing membrane-GFP at the edge of a cranial neural crest explant. D' shows schematic of D, note how cells do not overlap. Arrow shows direction of migration. **(E)** Three frames of a time-lapse movie of dissociated and re-aggregated neural crest cells expressing membrane-GFP and nuclear-RFP. Cell rapidly move away from each other. **(F)** Individual cell trajectories of leading (blue) and non-leading (red) cells. **(G)** Distribution of angles of migration for leading (blue) and trailing (red) control neural crest cells. For leading (blue) cells, n = 3, for non-leading (red) cells, n = 8. The experiment was repeated with 3 different explants with similar results.

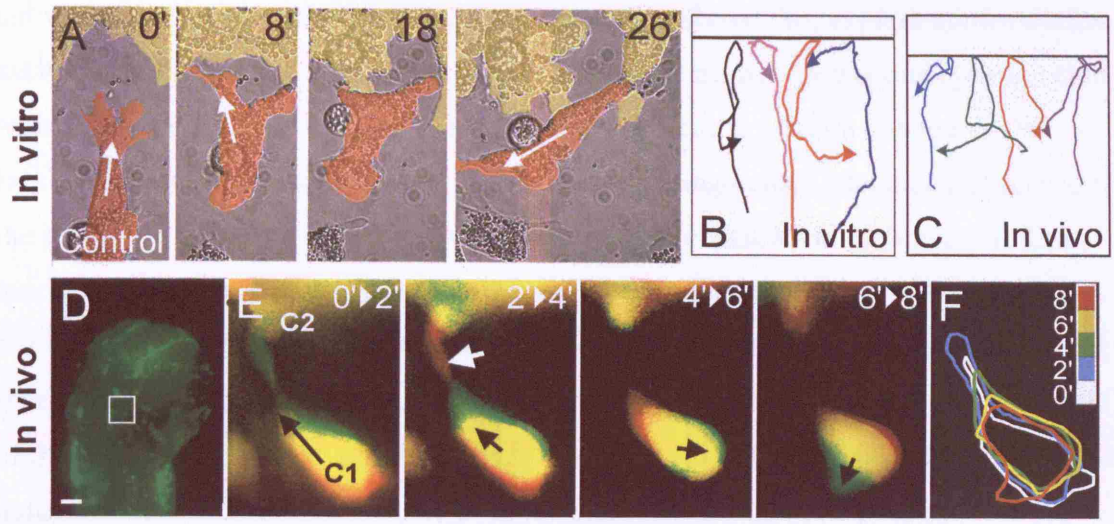


**Figure 7.2. Contact inhibition of locomotion occurs in the neural crest**

**(A)** Four frames of a time-lapse film (t= 0mins, 8mins, 18mins and 26mins) of a collision between two neural crest cells migrating on fibronectin in an explant confrontation assay. Cells from different explants are artificially coloured in orange or yellow. White arrow indicates direction of migration, note change of direction in orange cell after contact with yellow cell. **(B)** Trajectories of individual neural crest cells *in vitro* over a 30 minute period during which a collision occurred, horizontal black line represents point of contact. **(C)** Trajectories of individual neural crest cells at collision events in zebrafish embryos, horizontal black line represents point of contact. **(D)** The cephalic region of a *sox10:egfp* zebrafish embryo, dorsal view, anterior to top. Box indicates region shown in E. **(E)** Time-lapse film of the collision collision between two NC cells (C1 and C2) *in vivo*. Each panel corresponds to the difference between two consecutive two-minute frames. Green: new area; red: collapsing area; black arrow: direction of migration; white arrow: collapsing protrusion. **(F)** Outline of C1 at different times (minutes).

### 7.4. Dsh spontaneously localises to cell contacts upon a collision

Dishevelled localises to the cell contacts in groups of neural crest cells migrating on fibronectin (Fig 3.8), however its localisation has not been analysed during individual cell collision events like those described above. So, explant confrontation assays were carried out with neural crest cells taken from *Xenopus* embryos injected with Dsh-GFP (Fig 7.3A-D). Time-lapse analysis demonstrates a change in Dsh localisation upon cell collision. In individual migrating cells, Dsh can by observed in the entire cell membrane (Fig 7.3A), however upon contact with another cell, Dsh quickly accumulates at the point of contact between the cells (Fig 7.3B, C, red arrowhead). The cells depolarise and migrate away from each other and Dsh can be seen once again in the membrane, with a slight accumulation observable at the back of the cell, which was the point at which the cell contact was formed (Fig 7.3D). This dynamic localisation of Dsh at the point of cell contact hints at a possible role for Dsh and PCP signalling in controlling contact inhibition in the neural crest.

So far, Dsh localisation at cell contacts has only been analysed *in vitro*, so its position in neural crest cells migrating *in vivo* was also assessed using a Dsh-RFP construct expressed in *sox10:egfp* transgenic zebrafish (Fig 7.3E-J). Once again Dsh can be clearly observed at the points of contact between cells in both large groups of cells (Fig 7.3E-G) and in leading cells, where it can be observed at the back of the cell, the only point at which it is in contact with another neural crest cell (Fig 7.3H-J). Taken together, these data point to a role for Dsh in contact inhibition of neural crest cells both *in vitro* and *in vivo*.

### 7.5. Syn4 does not show specific localisation at cell contacts

As I have shown Syn4 to be involved in PCP signalling, the localisation of Syn4 in migrating neural crest cells was also analysed (Fig 7.4). *Xenopus* embryos were injected with 20pg syn-GFP alongside membrane-RFP and neural crests were dissected and cultured *in vitro*. These levels of Syn4-GFP are too low to observe directly, however immunostaining using an anti-GFP antibody allows a specific localisation to be observed (Fig 7.4A-C). Syn4 has been previously described to localise to focal adhesions, however no such puncta could be observed in neural crest cells. Instead Syn4 can be observed localised in discrete points around the edge of the cell (Fig 7.4A), which co-localise with membrane-RFP (Fig 7.4B,C).

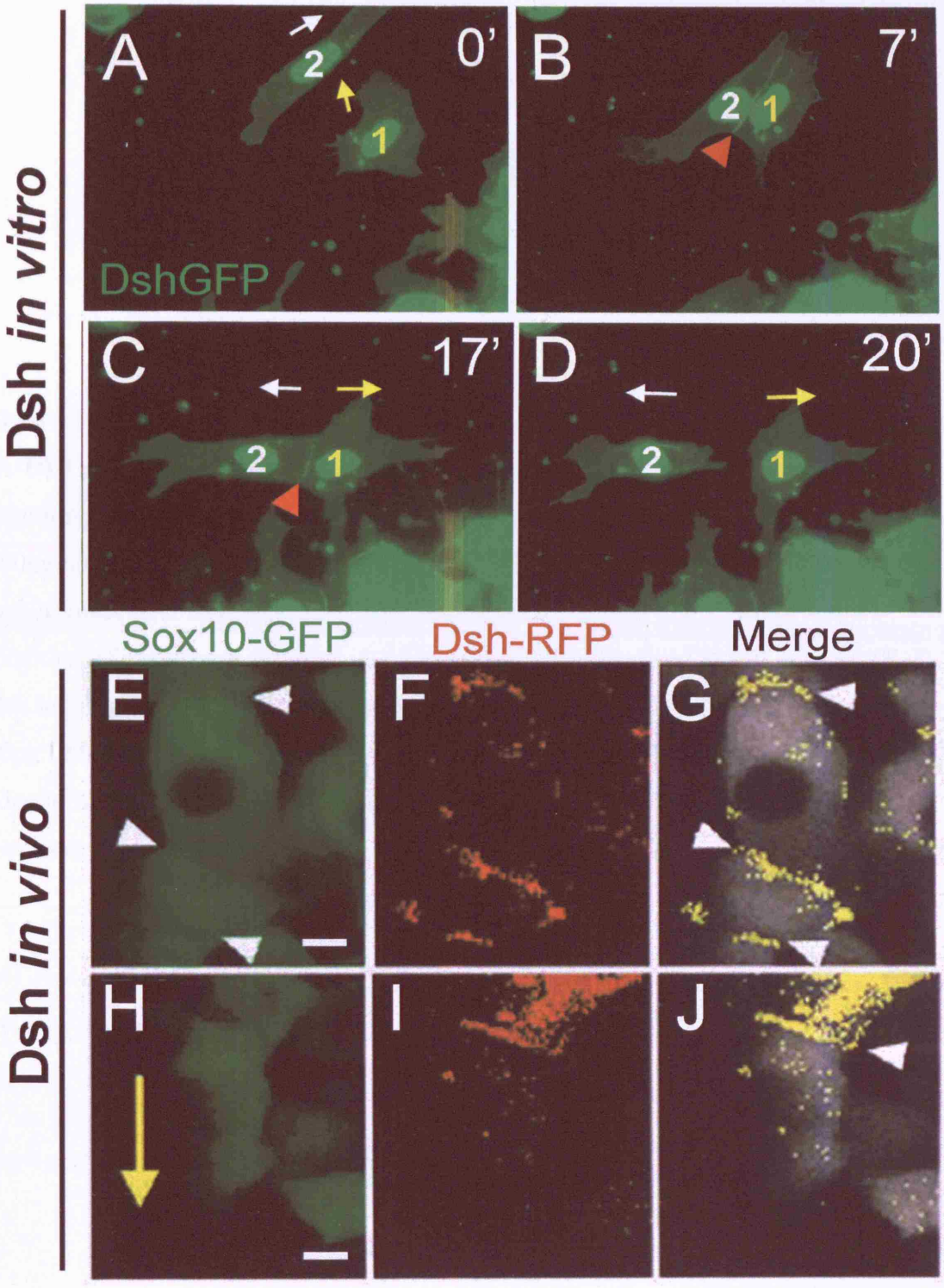
Dsh in vitro
A
0'
2
1
DshGFP
B
7'
2
1
C
17'
2
1
D
20'
2
1
Sox10-GFP
Dsh-RFP
Merge
Dsh in vivo
E
F
G
H
I
J

**Figure 7.3**

**Figure 7.3. Dishevelled localises to points of contact between neural crest cells** **(A-D)** Time-lapse series of a collision between two neural crest cells (cells 1 and 2) migrating on fibronectin, taken from embryos injected with 75pg Dsg-GFP and 300pg nuclear-GFP. Four frames are shown at 0 mins (A), 7 mins (B), 17mins (C) and 20 mina (D). Yellow arrow: direction of movement of cell 1, white arrow: direction of movement of cell 2, red arrowhead: Dsh localised at cell contact. **(E-J)** Dsh localisation was observed in sox10:egfp (sox10 in E,H) zebrafish by injection of 50pg Dsh-RFP (F,I). (E-G) A group of migrating cells (H-J) A cell at the leading edge of migration, yellow arrow: direction of migration, white arrowheads: Dsh localisation at cell contacts. Scale bars = 5 μm.

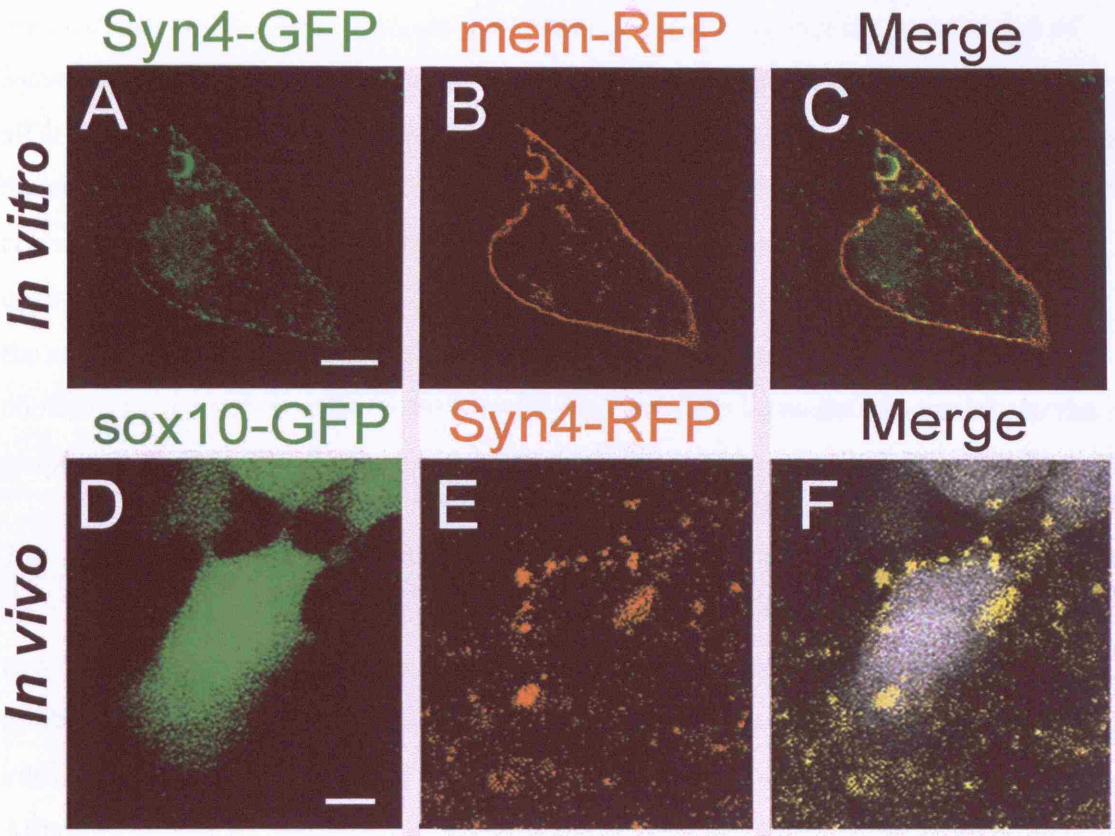


**Figure 7.4 Localisation of Syndecan-4 in neural crest cells**

**(A-C)** *Xenopus* cranial neural crest cell migrating on fibronectin showing the expression of a syn4-GFP fusion protein (A,C) and membrane-RFP (B,C). Scale bar = 10μm. **(D-F)** Zebrafish neural crest cell migrating in a *sox10:egfp* zebrafish embryo showing the expression of Syn4-RFP (E) and co-localisation with sox10-GFP in the neural crest (D,F). Scale bar = 5μm.

They are distributed all around the cell and do not show any specificity to the leading edge or cell body and do not localise at cell-cell contacts in groups of cells. The localisation of Syn4 was also analysed *in vivo* using a Syn4-RFP fusion protein injected into *sox10:egfp* zebrafish (Fig 7.4D-F). Again, no specific localisation of Syn4 was observed at cell-cell contacts. Syn4 is distributed in small accumulations all around the cell (Fig 7.4E), with many of these being localised towards the edge of the cell, possibly in the cell membrane as *in vitro* (Fig 7.4F). The lack of Syn4 at cell contacts suggests that Syn4 may not be involved in cell-cell signalling, although it does not rule out this possibility altogether. The endogenous localisation of Syn4 in the neural crest was not analysed and unlike Dsh-GFP, the Syn4-GFP and RFP constructs have not been previously tested and may not be targeted correctly to the proper sub-cellular localisation.

### 7.6. Inhibition of Dsh/PCP limits contact inhibition in the neural crest.

The specific and dynamic localisation of Dsh at the points of contact between two cells during a collision, prompted me to address its role in modulating contact inhibition in neural crest cells. Neural crest cells in which Dsh/PCP has been inhibited using DshDEP+ were observed migrating on fibronectin (Fig 7.5). Although DshDEP+ explants cultured on fibronectin do disperse, SEM imaging reveals significant differences between these cells and control neural crest cells. In control explants, the leading cells are highly polarised while there is an absence of cell protrusions in the non-leading cells (Fig 7.1A-C). In contrast, all cells in DshDEP+ explants have a large number of cell protrusions and cells at the edge of the explant have not obvious polarity (Fig 7.5A-C). I have previously shown that inhibition of Dsh leads to an increase in cell protrusion formation in leading and individually migrating cells (See Figs 5.5, 5.6), however SEM imaging makes it clear that this phenotype also extends to trailing cells within the explant, with cells generating a large number of overlapping protrusions giving a 'messy' appearance (Fig 7.5B, compare to fig 7.1B). Live imaging using cells expressing membrane GFP reveals that DshDEP+ cells frequently crawl on top of each other (Fig 7.5D,D'), something that is never observed in control neural cells (Fig 7.1D). Furthermore, time-lapse imaging of groups of DshDEP+ cells, artificially created from dissociated cells, reveals significant differences in behaviour compared to controls. The re-aggregated cells expressing DshDEP+ extend their protrusions over the top of adjacent cells (Fig 7.5E), and in consequence they do not migrate away of each

other as control cells do, but remain formed in small clusters of cells. Unlike control neural crest cells, where there is a clear difference in both the persistence and the angle of migration between leading and non-leading cells in an explant (Fig 7.5F,G), DshDEP+ cells showed no difference between leading and trailing cells. All DshDEP+ expressing cells behaved as if they were trailing neural crest cells with a low persistence of migration(Fig 7.5H) and wide variety of migration angles (Fig 7.5I). So, DshDEP+ transforms both cell populations with the leading cells lacking persistence and polarity (as described in chapter 5) while the trailing cells lose the cell-contact mediated suppression of protrusions.

DshDEP+ cells were also analysed in an explant confrontation assay *in vitro*. When a DshDEP+ cell touches a cell from the opposing explant, it does not retract its protrusion even after almost an hour of cell contact (Fig 7.6A). Furthermore, it does not halt migration or change direction but instead carries on migrating until it joins the confronting explant (Fig 7.6A). This kind of behaviour is never observed in control neural crest cells. Tracking of cell trajectories at individual collisions reveals that DshDEP+ cells seldom change direction upon contact with another cell and their migration is often slowed by repeated attempts to pass over the physical bulk of the opposing cell (Fig 7.6B, 0% cells changed direction, n=12). DshDEP+ cells were also analysed migrating *in vivo* in the head of *sox10:egfp* transgenic zebrafish embryos (Fig 7.6D). Analysis of cell collisions in embryos lacking Dsh is very difficult as neural crest cells do not migrate extensively and cells tend to form clusters, making collision events between individual cells extremely rare. Nevertheless, on the few occasions that I was able to observe individual cell collisions, cell behaviour proved very different to that in control embryos. Cells that extended their protrusions to touch another neural crest cell, did not collapse the protrusion and change their direction of migration as in control embryos, but rather continued migrating towards the other cell, eventually forming an aggregate (Fig 7.6E, F). Tracking of cell trajectories in individual cell collisions (Fig 7.6C, 0% cell changed direction, total n= 23 individual cells) shows that the situation for DshDEP+ cells *in vivo* is similar to that *in vitro*, with cells continuing towards the point of contact rather than turning away from it.

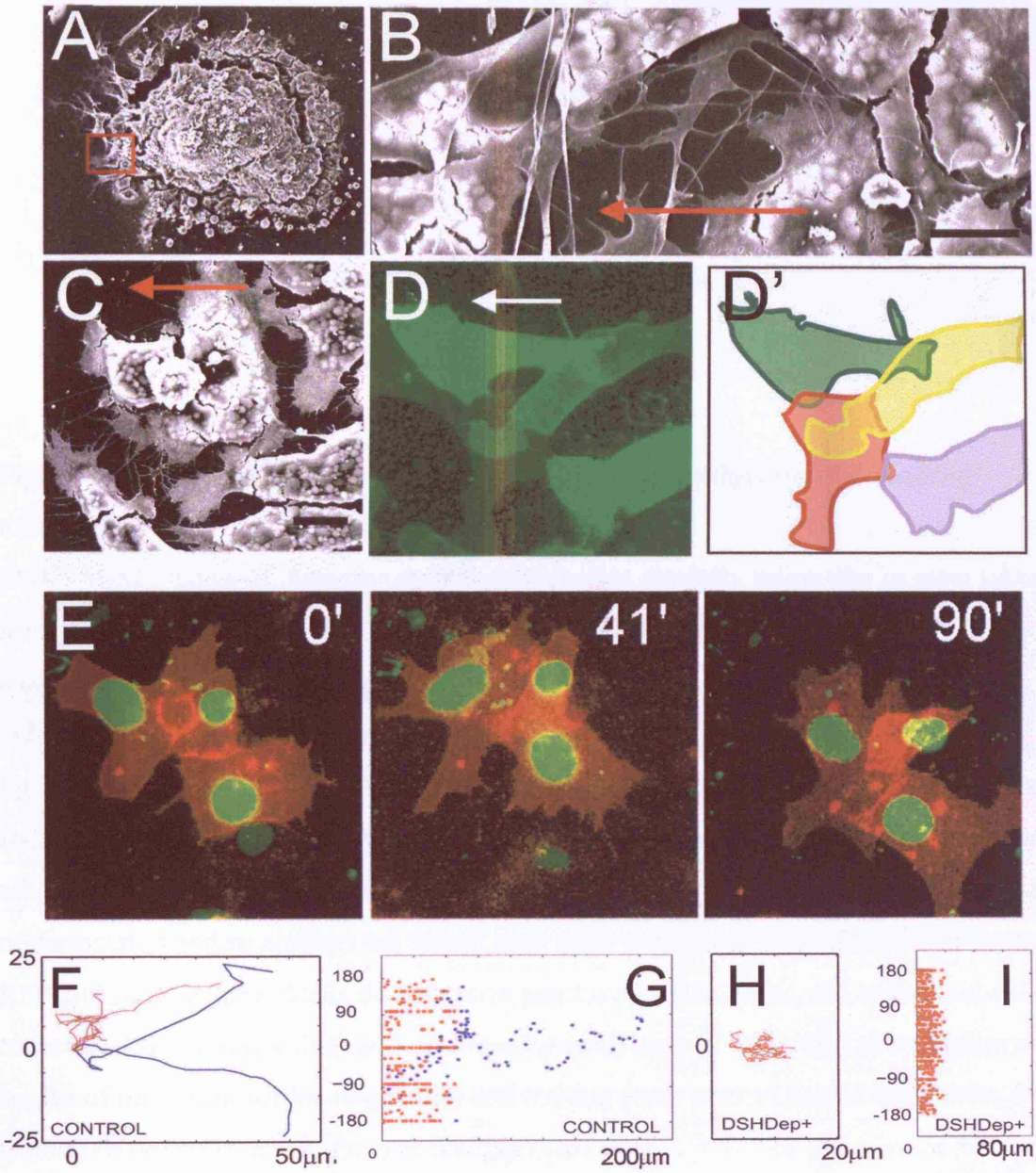
A
B
C
D
D'
E
0'
41'
90'
F
CONTROL
25
0
-25
0
50µm
G
CONTROL
180
90
0
-90
-180
0
200µm
H
DSHDep+
0
20µm
I
DSHDep+
180
90
0
-90
-180
0
80µm

**Figure 7.5. Dishevelled is required for the persistent migration of 'leading' neural crest cells**

**(A-C)** SEM images of *Xenopus* cranial neural crest explants migrating *in vitro* taken from an embryo injected with 1ng DshDEP+. Red square in A indicates cells at the leading edge of migration (higher magnifications shown in B and C). Red arrow indicates direction of migration. Note extensive protrusions in all cells, compare to fig 7.1A-C. Scale bars= 50μm. **(D)** Fluorescent image of neural crest cells expressing DshDEP+ and membrane-GFP at the edge of a cranial neural crest explant. D' shows schematic of D, note overlap between cells. **(E)** Three frames of a time-lapse movie of dissociated and re-aggregated neural crest cells expressing DshDEP+, membrane-RFP and nuclear-GFP. Cells do not move apart over 90 minutes. **(F)** Individual cell trajectories of leading (blue) and non-leading (red) control cells. **(G)** Distribution of angles of migration for leading (blue) and trailing (red) control neural crest cells. For leading (blue) cells, n = 3, for non-leading (red) cells, n = 8. The experiment was repeated with 3 different explants with similar results. **(H)** Individual cell trajectories DshDEP+ cells. **(I)** Distribution of angles of migration for DshDEP+ cells (n = 15. The experiment was repeated with 3 different explants with similar results). Note how DshDEP+ cells all behave as non-leading (red) cells.

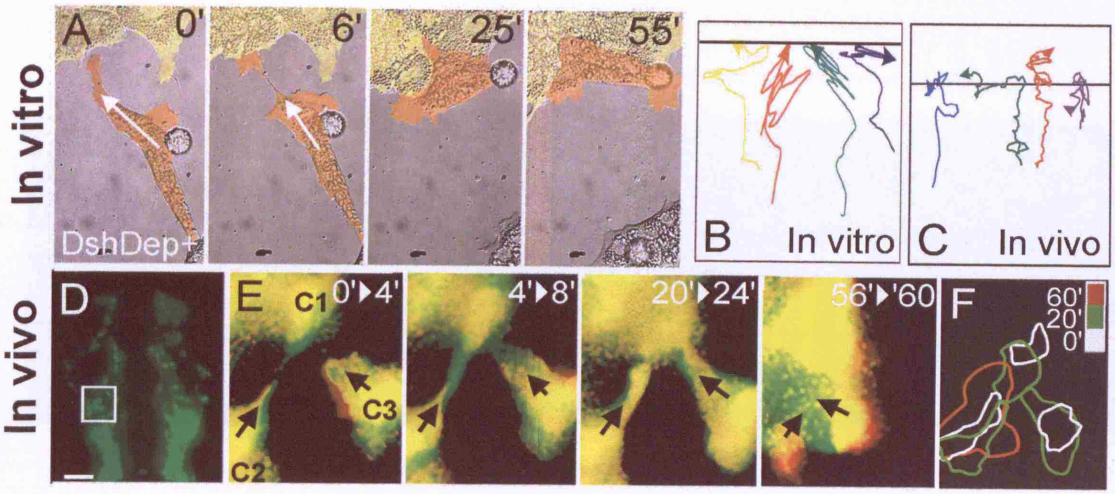


**Figure 7.6. PCP signalling is required for contact inhibition of locomotion**

**(A)** Four frames of a time-lapse film (t= 0mins, 6mins, 25mins and 55mins) of a collision between two DshDEP+ neural crest cells migrating on fibronectin in an explant confrontation assay. Cells from different explants are artificially coloured in orange or yellow. White arrow indicates direction of migration. Note orange cell does not change direction, compare to fig 7.2A. **(B)** Trajectories of individual DshDEP+ neural crest cells at collision events *in vitro*, horizontal black line represents point of contact. **(C)** Trajectories of individual DshDEP+ cells at collision events in zebrafish embryos, horizontal black line represents point of contact. **(D)** The cephalic region of a *sox10:egfp* zebrafish embryo, dorsal view, anterior to top. Box indicates region shown in E. **(E)** Time-lapse film of the collision between DshDEP+ NC cells (C1, C2 and C3) *in vivo*. Each panel corresponds to the difference between two consecutive two-minute frames. Green: new area; red: collapsing area; black arrow: direction of migration; Compare to control cells in Fig 7.2E. **(F)** Outlines of cells in E at different times (minutes).

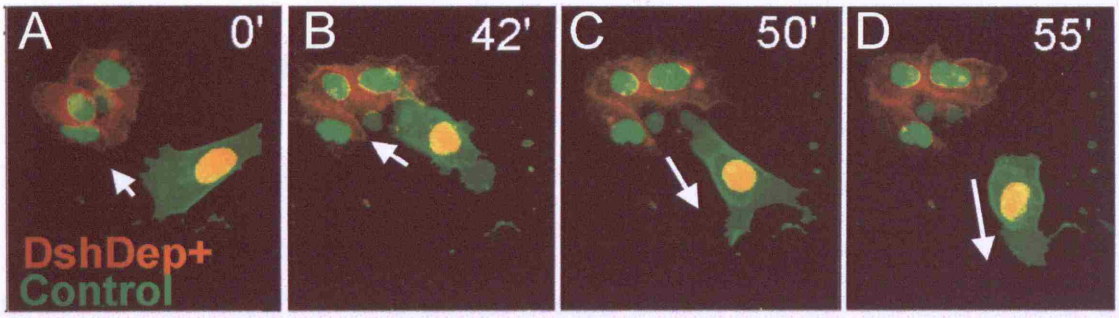


**Figure 7.7. Dishevelled is required cell-autonomously for contact inhibition**
A mixture of control *Xenopus* neural crest cells (also expressing membrane-GFP and nuclear-RFP) and cells taken embryos injected with 1ng DshDEP+ (alongside membrane-RFP and nuclear-GFP) were cultured together on fibronectin-coated coverslips. **(A-D)** A collision between a control and DshDEP+ cell. Four frames of a time-lapse film are shown; 0 mins (A), 42 mins (B), 50mins (C) and 55mins (D). Arrow indicates direction of migration of control cell. Note how contact inhibition occurs in the control cell but not DshDEP+ cells.

An explant confrontation assay was also carried using a mixture of DshDEP+ and control cells (Fig 7.7) to investigate whether the PCP signal has to be present in both colliding cells for contact inhibition to occur. In this assay, a control cell, upon extending its lamellipodia to touch a DshDEP+ cell (Fig 7.7A, B) quickly collapses its protrusion (Fig 7.7C) and changes direction to migrate away from the cell contact (Fig 7.7D). Meanwhile, the DshDEP+ cells do not visibly respond to the confrontation. Taken together, these results demonstrate that neural crest cells exhibit contact inhibition of locomotion both *in vitro* and *in vivo* and that this process requires functional Wnt/PCP signalling in the responding cell.

### 7.7. Discussion

Contact inhibition of locomotion is a well-described phenomenon, but the molecular mechanism that controls this process has not been previously identified. In fact Abercrombie once speculated that contact inhibition could be a purely mechanical reaction, with one cell physically obstructing the movement of another (Abercrombie, 1970). However here I show that contact inhibition of locomotion in neural crest cells requires the activity of a cell signalling pathway, the non-canonical Wnt/PCP pathway. Neural crest cells in which the PCP pathway is inhibited frequently overlap and fail to form a strict monolayer (Fig 7.5). Furthermore, cells expressing DshDEP+ do not cease movement and change direction upon contact with other neural crest cells (Fig 7.6), unlike control neural crest cells (Fig 7.2). I have previously shown that Dsh controls persistence during neural crest migration (Fig 5.3) by limiting cell protrusion formation (Fig 5.6), a process that is controlled by Dsh-mediated activation of RhoA. This provides a possible mechanism for contact inhibition of locomotion in the neural crest. Contact between two cells leads to a transient localisation and activation of Dsh at the point of contact, which is likely activate RhoA and halt protrusion formation, and hence movement in that direction. Syn4 also contributes to cell polarity through the inhibition of Rac, and it remains a possibility that Syn4 may also be involved in mediating contact inhibition of locomotion. This possibility has not been addressed here, but it certainly cannot be ruled out. Two different mechanisms have been hypothesized to underlie contact inhibition: The first involves a sequence of cell contact followed by paralysis of lamellipodial activity, temporary adhesion between the cells and then retraction and

movement away from each other. The alternative does not involve paralysis of the migratory machinery and rather postulates that contact inhibition is a consequence of preferential adhesion of a cell to the substrate than to other cells (Heaysman, 1978). Given the known involvement of Syn4 in cell-matrix adhesion, it is possible that it may be involved in mediating this second type of contact inhibition. In this study, it is not possible to distinguish between the two types of contact inhibition, although the localisation of Dsh at the cell contacts and it's role in suppressing protrusion formation, suggests that the former mechanism of a cell-cell signal followed by paralysis of the migration apparatus is more likely.

Contact inhibition of locomotion can explain much of the behaviour observed in neural crest cells migrating *in vitro*. It can account for the gradual spreading of neural crest explants on fibronectin, as cells at the edge move consistently away from their neighbours to occupy the free space. Abercrombie stated that 'the outstanding effect that these collision phenomena have on a population of cells *in vitro*...is to produce the flow of cells from a high population density to a low one' (Abercrombie, 1980) and this is exactly what is observed in neural crest explants. Additionally, contact inhibition explains why neural crest cells eventually lose their persistence once migrating as individual cells. Control neural crest cells will migrate with high persistence as a sheet at the edge of the explant and will initially maintain this persistence as the individual cells break free from their neighbours. However individual cells left to migrate for many hours will eventually revert to random migration (Roberto Mayor, unpublished observation), probably due to a lack of contact-based directional cues from other cells.

Contact inhibition of locomotion can account for *in vitro* behaviour very well, but how far can it go towards explaining the migration of neural crest cells *in vivo*? I have shown that Dsh-mediated contact inhibition occurs for individual NC cells migrating *in vivo*, but it may also have a significant impact on the initial emigration of neural crest cells from the neural tube. After all, cells leaving the neural tube will be surrounded by other crest cells on all sides apart from in the direction in which they will migrate, and therefore the only direction in which they are not subject to contact inhibition. Recent data from Carlos Carmona-Fontaine in our laboratory supports this idea by demonstrating that contact inhibition only occurs between two neural crest cells (homotypic contact inhibition) and not with other cell types (heterotypic contact inhibition). Neural crest cells will aggressively invade pieces of

mesodermal tissue cultured next to a neural crest explant, but not another neural crest explant with the cells from both explants spreading to form a monolayer. Neural crest cells have been described to exhibit a contact inhibition-like reaction with somatic cells. Avian neural crest cells will depolarise and change direction upon contact with somatic cells in an *in vitro* confrontation assay (Gooday and Thorogood, 1985). So, neural crest cells exhibit contact inhibition with some cell types, although not with others. This kind of heterotypic contact inhibition may be involved in guidance of neural crest cells along their migration pathways. Notably, neural crest cells do not show contact inhibition with head mesoderm, which is a tissue normally used as a substrate for their migration, but do show contact inhibition with somite tissue, parts of which are not permissive to neural crest migration. In addition to guidance by heterotypic contact inhibition, homotypic contact inhibition between neural crest cells themselves is likely to play a significant role in migration away from other neural crest cells and hence the neural tube. In a computer model of neural crest migration, where a large number of particles starting at one end of a screen have to reach a target at the other end by random movement, particles with contact inhibition travel much more persistently and reach the target much sooner than those without (Carlos Carmona-Fontaine, unpublished data). This suggests that contact inhibition of locomotion could play a significant role in helping neural crest cells to reach their targets efficiently.

The discovery of PCP-mediated contact inhibition in the neural crest raises the possibility of a role for contact inhibition in other embryonic processes. Vertebrate gastrulation, in particular, is known to require non-canonical Wnt signalling (Wallingford et al., 2002). Similar behaviour to neural crest cells has been observed in the head mesoderm, which migrate as a coherent cell aggregate across the fibronectin-coated inner blastocoel roof during *Xenopus* gastrulation (Winklbauer and Selchow, 1992). Isolated head mesoderm cells have been shown to migrate randomly and are only able to travel persistently, following extracellular matrix guidance cues, when present in a group of cells (Winklbauer et al., 1992). A contact inhibition-like mechanism may be playing a role in this cell migration and potentially in many other embryonic processes. Another area open to investigation is the role of PCP signalling in the cellular processes already known to be mediated by contact inhibition. For example, the movement of epithelial sheets during wound healing is thought to be controlled by contact inhibition, which polarises the cells at the leading

edge of migration and also halts migration when the two sides of the wound meet (Abercrombie, 1967). While β-catenin-dependent Wnt signalling is known to be activated at the hair follicles of wound sites, non-canonical Wnt signalling has recently been shown to be up-regulated in the wound itself and the forced expression of Wnt5a promotes regeneration (Fathke et al., 2006). Therefore PCP signalling may be involved in the regulation of contact inhibition during wound healing.

Loss of contact inhibition may also be an important event during malignant invasion, as various malignant cell types behave differently to normal cells *in vitro* and are not so strictly controlled by contact inhibition (Abercrombie, 1979). Others such as Sarcoma cells exhibit homotypic contact inhibition of movement but lack heterotypic contact inhibition with other cell types such as fibroblasts (Abercrombie and Heaysman, 1976). Although it has become clear that the relationship between contact inhibition and cancer is not straightforward, as the degree of contact inhibition varies between malignant cell types (Heaysman, 1978), loss of contact inhibition of locomotion is likely to be one of many factors contributing to malignancy. Neural crest cells, like many cancers, display homotypic but not heterotypic contact inhibition and furthermore DshDEP+ neural crest cells lack even homotypic contact inhibition and are highly invasive. Several members of the non-canonical Wnt pathway are known to be tumour suppressor genes, whose inhibition is associated with malignancy. Wnt5a, a PCP ligand, is down regulated in a number of cancerous cell types including leukaemia, neuroblastomas and thyroid carcinomas (reviewed in (Pukrop and Binder, 2008). Loss of Wnt5a is also associated with a poor prognosis in patients with colon and breast cancer, suggesting a role in invasion and metastasis (Dejmek et al., 2005; Jonsson et al., 2002). Other downstream components of the PCP pathway including several Frizzleds, Dsh and members of the Rho GTPase family have also been implicated in a variety of human cancers (Katoh, 2005; Ridley, 2004). Further investigation may reveal that these roles in cancer cell invasion may be in part due to effects on PCP-mediated contact inhibition. Certainly the role for Dsh/PCP signalling in controlling contact inhibition of locomotion during neural crest migration is likely to be conserved in a variety of embryonic and adult processes.

# 8. General Discussion

## 8.1. A molecular model of neural crest migration

In the course of this thesis I have described essential roles for PCP signalling and Syndecan-4 in controlling neural crest migration in *Xenopus* and zebrafish embryos and have begun to uncover the mechanism by which they control cell migration *in vitro* and *in vivo*. The key findings can be summarised as follows: i) PCP signalling is required for neural crest migration and Dsh localises to the cell membrane in migrating neural crest cells, ii) Syndecan-4 is essential for neural crest migration, where it signals upstream of the PCP pathway and is required for Dsh recruitment to the cell membrane, iii) Both Dsh and Syn4 control persistence but not speed of migration of neural crest cells *in vitro* and *in vivo*, iv) Syn4 and Dsh control persistence by regulating the directional formation of cell protrusions, v) Syn4 and Dsh control the activity of Rho GTPases to modulate cell protrusions with Syn4 repressing Rac, while Dsh activates RhoA vi) PCP signalling also controls contact inhibition of locomotion in neural crest cells migrating *in vitro* and *in vivo*. Taken together, these conclusions allow a stepwise model to be proposed, which can explain how an individual neural crest cell is able to establish and maintain directional migration (illustrated in Figure 8.1). For the purposes of simplicity, here I shall be only considering the migration of a neural crest cell *in vitro*, but based on the data presented I propose that an equivalent mechanism is operating *in vivo*:

1) Plating on fibronectin results in the attachment and spreading of neural crest cells at the edge of the explant. Attachment to fibronectin is likely to involve engagement of Syndecan-4 and hence its activation and clustering. Activated Syn4 recruits Dishevelled to the entire cell membrane (Fig 8.1A).
2) Cell-cell interactions concentrate Dsh activity at the points of contact between cells. For cells at the edge of the explant, this will result in Dsh becoming localised at the 'back' of the cell, in the direction of the mass of cells in the explant (Fig 8.1B).
3) Dsh activity at the back of the cell will activate RhoA, which will act as a repressor of Rac. Additionally, continued Syn4 signalling contributes to the

repression of Rac. This leads to low levels of Rac in the cell body and polarises Rac activity at the leading edge (Fig 8.1B).

4) Polarised Rac activity leads to the production of protrusions at the leading edge and hence forward movement in that direction. Initially this is likely to be the only direction open to migration, as cell protrusion formation at the back of the cell will be inhibited by continued contact inhibition from other neural crest cells.
5) Eventually the cell may break away from its neighbours, but persistence can be maintained for some time by continued activation of RhoA by Dsh, and continued suppression of Rac by Syn4, probably in response to interactions with fibronectin in the extracellular matrix (Fig 8.1C). Additionally, contact inhibition of locomotion at collision events with other neural crest cells will contribute to persistent movement away from other cells.

This is the most coherent way to assemble the data presented here into a model, which is able to explain the intrinsic behaviour of neural crest cells cultured on a fibronectin substrate, in the absence of signalling from chemoattractants. Much of the data taken from *in vitro* experiments are also reproducible *in vivo*, and therefore it is likely that many aspects of this model also hold true in the embryo.

### *8.1.1. The interaction between Syn4 and PCP signalling*

In this model, I have placed Dsh and the PCP pathway downstream of Syndecan-4, but the evidence for this is mixed and the exact interaction of Syn4 with the PCP pathway remains unclear. Munoz and colleagues (2006) suggest that Dsh acts downstream of Syn4, as the effects of a *syn4* Mo on *Xenopus* gastrulation can be rescued by activation of Dsh/PCP using DshΔN. This is also the case for neural crest migration (Fig 4.6). Syn4 signalling to Dsh has been proposed to be the result of a direct interaction between Syn4, Fzd7 and Dsh, as they co-immunoprecipitate in an *in vitro* pull down assay (Munoz et al., 2006). A recent study has also shown that Fzd7 physically interacts with the PDZ protein, Syntenin, which is recruited to the membrane alongside Dsh upon activation of PCP signalling and which is required for convergent extension in *Xenopus* (Luyten et al., 2008).

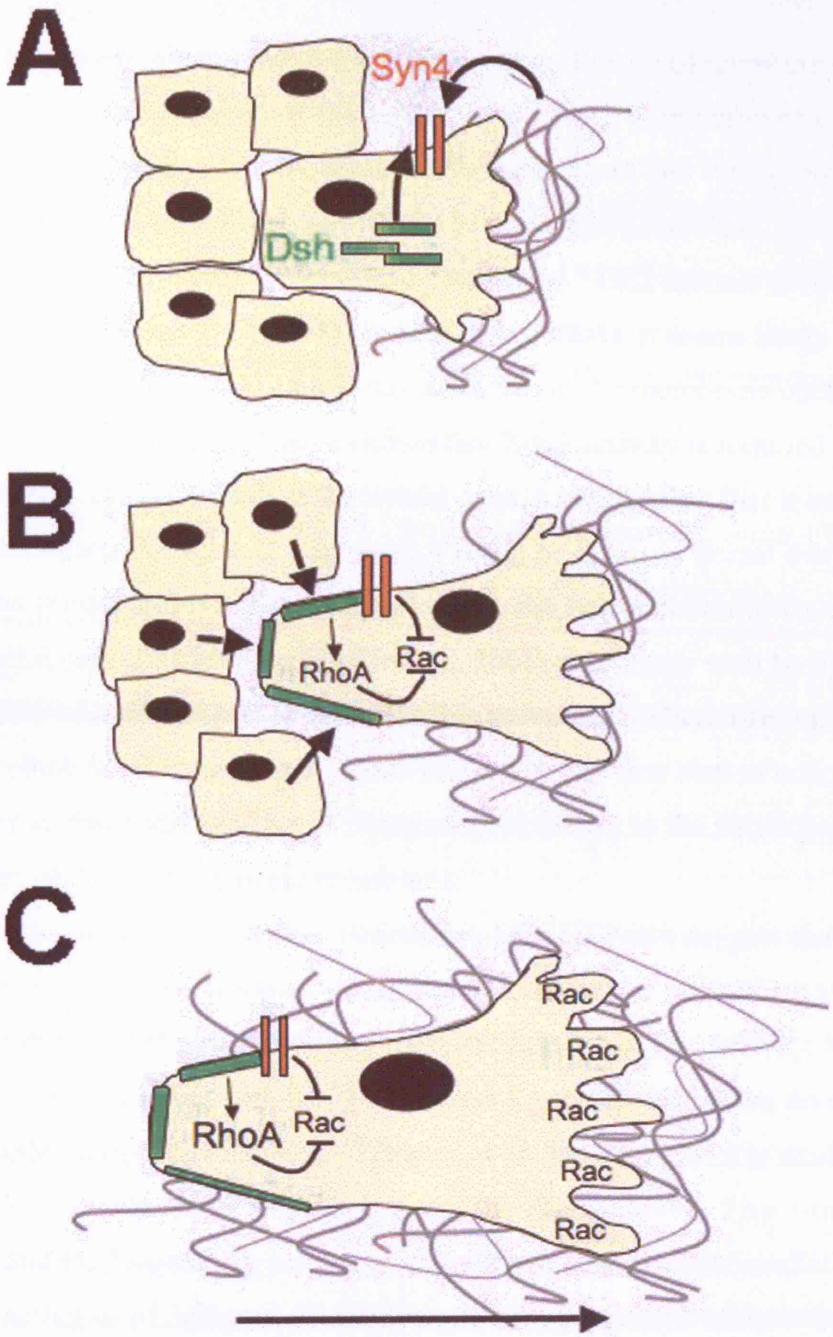


**Figure 8.1. Model of neural crest migration**

**(A)** A neural crest cell leaving a group of cells comes into contact with fibronectin in the extracellular matrix (grey lines) resulting in the activation of Syn4 (shown in red), which recruits Dsh (green) to the membrane. **(B)** Signalling from neighbouring cells concentrates Dsh at the cell contacts, where it activate RhoA. **(C)** Repression of Rac by Syn4 and activation of RhoA by Dsh at the back of the cell maintain polarised Rac activity and cell protrusion formation at the leading edge, resulting in persistent migration.

Syntenin is also known to bind to the PDZ-binding domain of members of the syndecan family including Syn4 (Grootjans et al., 1997; Zimmermann et al., 2001) and therefore may facilitate the interaction between Syn4 and PCP proteins. Luyten et al (2008) propose that it acts as a scaffold to link Syn4 and Fzd7, since its PDZ1 domain binds preferentially to Syndecans, while the PDZ2 domain favours binding to Frizzled7 (Grootjans et al., 2000; Luyten et al., 2008). It seems likely that a complex of many different proteins may assemble at the membrane upon activation of Syn4 and Fzd7. Crucially I have shown that Syn4 activity is required for the membrane localisation of Dsh in the neural crest, a localisation that is essential for PCP signalling and for contact inhibition. Plating of *Xenopus* dorsal marginal zone explants on fibronectin is sufficient to stimulate the translocation of Dsh to the plasma membrane (Marsden and DeSimone, 2001) and it may well be Syndecan-4 that interacts with fibronectin to facilitate this movement. Therefore, I present a model in which Syn4 is upstream of Dsh and where the first step of neural crest migration requires Syn4 binding to fibronectin, resulting in the subsequent recruitment of Dsh to the plasma membrane.

On the other hand, the data concerning Rho GTPases suggest that the interaction may be more complex than a linear Syndecan-4 to Fzd/Dsh signalling pathway. Inhibition of Syn4 leads to a massive increase in Rac activity, while PCP signalling levels correlate with the level of RhoA activity. However, no clear effect is discernable on the converse Rho GTPases, with RhoA apparently unaffected by Syn4 and Rac unresponsive to modulation of the PCP pathway. This would suggest that Syn4 and PCP signalling are acting though two separate but parallel pathways to affect the activities of different Rho GTPases. Ultimately both pathways have the same outcome, which is the repression of Rac activity, resulting in its limitation to the leading edge. One possibility is that Syn4 plays a dual role in the regulation of neural crest migration; firstly by facilitating activation of the PCP pathway by membrane recruitment of Dsh, and secondly by a separate, more direct, downstream pathway which results in the repression of Rac. Therefore Syn4 and PCP signalling are acting synergistically to co-ordinate neural crest migration, with PCP signalling primarily providing input from surrounding neural crest cells while Syn4 provides information from the extracellular matrix. Thus both signals are able to feed into the

same pathway to establish and maintain polarity in neural crest cells, through the regulation of Rho GTPases.

*8.1.2. Alternative intracellular signalling pathways*

I have principally addressed the role of Rho GTPases downstream of Syn4 and Dsh in controlling neural crest migration. However a myriad of intracellular signalling pathways have been implicated in the regulation of cell migration, and there is no doubt that a complex network of signalling is likely to be active in the migrating neural crest. One family of molecules that may well play a key role in neural crest migration are the various protein kinase C (PKC) isoforms, in particular PKCα. Activation of PKCα has been suggested to be one of the primary mechanisms by which Syn4 controls cell spreading and the recruitment of cytoskeletal proteins to focal adhesions. Syn4 and PKCα co-localise to focal adhesions, where Syn4 is able to directly activate PKCα (Lim et al., 2003; Oh et al., 1997b). Activation of PKCα by phorbol ester treatment can drive the recruitment of FA components such as talin and vinculin to nascent focal adhesions, while PKC inhibitors inhibit focal adhesion formation (Woods and Couchman, 1992). PKCα physically interacts with Syn4, binding to its cytoplasmic variable domain and forming a ternary complex with $PIP_2$ (Koo et al., 2006; Oh et al., 1998). Substitution of tyrosine and lysine residues in this variable region have been shown to abolish PKCα binding and interfere with Syn4 function (Bass et al., 2007; Horowitz et al., 1999; Lim et al., 2003). I show that this mutation also negates the ability of Syn4 to rescue neural crest migration in embryos where *syn4* has been inhibited by Mo injection (Fig 4.8). This implies that PKCα binding and activation downstream of Syn4 is essential for neural crest migration. Bass et al (2007) propose that PKCα mediates the interaction between Syn4 and Rac, as the Y188L mutant is unable to stimulate the wave of Rac activation observed with full length Syn4. However they also show that the Y188L mutant is able to rescue persistent migration in *syn4*-/-fibroblasts. The same mutant is unable to rescue migration of neural crest cells in *Xenopus*, hinting at a possible requirement *in vivo*, which is not observed *in vitro*. Interestingly, activation of PKCα by Syn4 has been shown to be dependent on Syn4 phosphorylation by another PKC isoform, PKCδ (Chaudhuri et al., 2005; Murakami et al., 2002). PKCδ is also required for convergent extension movements in *Xenopus* and furthermore, animal cap cells lacking PKCδ are unable to recruit Dsh to the plasma membrane following

stimulation by Fzd7 mRNA (Kinoshita et al., 2003). This is consistent with the role of Syn4 in recruiting Dsh to the plasma membrane.

In addition, PCP signalling also has the potential to activate various PKC isoforms downstream. Overexpression of Wnt5 or Wnt11 increase the frequency of the waves of $Ca^{2+}$ release in zebrafish embryos and results in the activation of calcium-sensitive PKC as well as calcium/calmodulin-dependent kinase II (Kuhl et al., 2000; Slusarski et al., 1997a; Slusarski et al., 1997b). This has been proposed to be a putative third branch of the Wnt-signalling pathway known as wnt/calcium signalling. However, DshDEP+ has been shown to be a strong activator of calcium flux in zebrafish embryos, stronger even than full length Dsh (Sheldahl et al., 2003), suggesting that this pathway is also a downstream response of the planar cell polarity pathway. In fact, it is becoming increasingly clear that non-canonical Wnts activate a whole network of signalling, rather than separate linear pathways (Kestler and Kuhl, 2008). Therefore PCP signalling in the neural crest is likely to have a variety of wide-ranging effects.

Several other molecules, apart from Rho GTPases, have been proposed to be downstream effectors of PCP signalling. Daam1, which facilitates the binding of RhoA to Dsh (Habas et al., 2001), also has independent effects on the actin cytoskeleton. A member of the formin family of proteins, Daam1 is able to bind to Profilin1, which is able to induce stress fibre formation without affecting RhoA activation status (Sato et al., 2006). Inhibition of Daam1 or Profilin also disrupts *Xenopus* gastrulation (Sato et al., 2006). Another potential mediator of non-canonical Wnt signalling is the Jun kinase (JNK) signalling cascade. Dsh induces JNK activity in *Drosophila* and mammalian cells, an activity which is dependent on the DEP domain of Dsh (Boutros et al., 1998; Li et al., 1999; Moriguchi et al., 1999). The JNK pathway results in activation of the transcription factor, AP-1, and has been implicated in a variety of cellular processes including proliferation, differentiation, apoptosis and the stress response (Weston and Davis, 2007), but its role in non-canonical Wnt signalling is unclear. Rac and Cdc42 have been shown to stimulate JNK activation (Coso et al., 1995; Hall, 2005) and it has been suggested that PCP signalling activates JNK via Rac, as a dominant negative form of Rac inhibits the Dsh-stimulated activation of JNK *in vitro* (Habas et al., 2003). However the picture is unclear as conflicting reports suggest that inhibiting Rac does not affect JNK activation by Dsh (Li et al., 1999). There are still many details of the PCP pathway

that remain to be resolved, but it seems likely that a whole intracellular signalling network is activated in the neural crest, stimulated by activation of Syn4 and Dsh and that many other molecules will work in conjunction with Rho GTPases to regulate neural crest cell migration.

### *8.1.3. The role of the extracellular matrix*

The interaction between Syn4 and fibronectin is central in controlling neural crest migration, but this interaction has not been greatly examined in this thesis. The extra-cellular matrix has long been implicated in neural crest migration, with fibronectin in particular thought to play a crucial role (Perris and Perissinotto, 2000). Not only is fibronectin ubiquitously expressed around the migrating neural crest (Newgreen and Thiery, 1980), but it is the only ECM component that is able to support *Xenopus* neural crest migration *in vitro* (Alfandari et al., 2003). *In vivo* also, treatment with antibody inhibitors of fibronectin or its integrin binding partners completely block cranial neural crest migration (Boucaut et al., 1984; Bronner-Fraser, 1986b). It has generally been assumed that the interaction between neural crest cells and fibronectin is primarily mediated by integrins. A function-blocking monoclonal antibody against α5β1-integrin prevents attachment of neural crest cells to fibronectin *in vitro* (Alfandari et al., 2003). More generalised integrin inhibition by $Mn^{2+}$ treatment also inhibits neural crest cell motility (Strachan and Condic, 2008). Recent reports suggest that these integrin-fibronectin interactions are essential not just for migration, but also for the survival of neural crest cells. Neural crest cells have an increased rate of apoptotic death in avian embryos treated with an inhibitory antibody against α4β1 integrins, and the α5β1-integrin mutant mouse also shows a decrease in neural crest cell numbers (Testaz and Duband, 2001; Yang et al., 1993). Furthermore, neural crest cells lacking α4 or α5-integrins are able to migrate in chick embryos but show defects in survival and proliferation (Haack and Hynes, 2001). In many other cell types, attachment to the extracellular matrix requires co-ordinated signalling through both integrins and syndecans (Morgan et al., 2007). In the neural crest, integrin binding to fibronectin is required for survival, but engagement of Syn4 is essential for proper migration to take place. Alfandari et al (2003) show that while neural crest cells are able to attach and migrate on the cell binding domain (CBD) of fibronectin, they will preferentially migrate onto a substrate also containing the Hep-II fragment, which mediates the interaction with

Syn4. I have shown here that Syn4 is essential for the directional migration of neural crest cells and for the formation of cell protrusions and focal contacts and it is likely that the binding of Syn4 to fibronectin stimulates these processes.

So, how does a fibronectin-Syn4 interaction control neural crest migration? I propose that this interaction is one of the earliest to occur when neural crest cells emigrate from the neural tube, preceded only by integrin-ECM binding. I would also suggest that it is this interaction that is responsible for recruitment of Dsh to the plasma membrane, which is an essential event in establishing cell polarity. Plating of animal caps on fibronectin is known to be sufficient to bring Dsh to the membrane (Marsden and DeSimone, 2001) and I have shown that this is also the case in neural crest cells (Fig 3.8). However, treatment with the *syn4* Mo inhibits this translocation (Fig 4.7). Membrane localisation of Dsh is essential for PCP signalling and it has been suggested that recruitment of Dsh to the membrane may facilitate a switch from β-catenin signalling to the non-canonical Wnt pathway (Wallingford and Habas, 2005). During neural crest development a switch from canonical to non-canonical Wnt signalling also coincides with the onset of migration. It may be that signalling from the extra-cellular matrix controls this switch. The access of NC cells to fibronectin after EMT could provide a Syn4-mediated signal, which activates PCP signalling and stimulates the start of migration. Interestingly, neural crest explants taken from very young embryos (such as stage 15), well before the onset of migration, will rapidly attach and start to migrate when plated on fibronectin, far earlier than any migration would have taken place *in vivo*. Experiments using axolotl embryos, where neural crest cells exit from the neural tube but remain stationary for some time before migrating, point to a role for the extracellular matrix in regulating the timing of migration. Transplant of micro-membranes coated with ECM taken from more mature embryos or with fibronectin alone into the neural crest of these embryos is sufficient to stimulate a premature migration (Olsson et al., 1996; Perris and Perissinotto, 2000). This indicates that, in the axolotl at least, neural crest cells are fully competent to migrate after EMT, but require the proper environmental signals from the ECM before they embark upon their migration. Signalling from the extracellular matrix may play a similar role in higher vertebrates and any such signal is likely to involve Syn4-mediated recruitment of Dsh.

Fibronectin is also likely to play a continued role after the emigration of neural crest cells from the neural tube. It is expressed along the entire migration

pathways of neural crest cells (Alfandari et al., 2003; Thiery et al., 1982), so any interaction between Syn4 and fibronectin will occur constantly throughout migration. Syn4-mediated repression of Rac allows neural crest cells to maintain a persistent migration, and constant signalling from the extracellular-matrix is also likely to contribute to this. Bass et al (2007) show that regulation of Rac activity by Syn4 is essential for cells to be able to respond to turns in the fibronectin matrix. They created artificial fibronectin paths on 50μm gold stripes with a series of junctions. While normal fibroblasts were able to navigate along these pathways, Syn4 null cells failed to move along the stripes due to extensive lamellipodial extensions in all directions. Furthermore, cells expressing Syn4 with an Y188L mutation in the PKCα binding sites were able to follow straight lines but did not turn upon reaching a fibronectin junction, unlike wildtype cells. They suggest a model whereby Syn4 is able to sense changes in the matrix environment resulting in a PKCα-dependent activation of Rac, which allows the cell to change direction. In addition, continued suppression of Rac by Syn4 also allows cells to follow a narrow fibronectin pathway. It is likely that similar mechanisms are operating in neural crest cells *in vivo*, as they follow their fibronectin pathways through the embryo.

### *8.1.4. The role of external signalling molecules*

Chemotaxis has been suggested as one of the mechanisms to explain directional migration of neural crest cells; however there is no sound evidence for this proposal. Moreover persistent directional migration occurs *in vitro* in the absence of chemoattractants. Instead, interactions between the extracellular matrix, integrins, and levels of Rac and Syn4 have been shown to control persistent migration *in vitro* (Bass et al., 2007; Choma et al., 2004; Pankov et al., 2005). Here I propose a model to explain the migration of neural crest cells *in vivo* without any need for extrinsic signals from chemoattractants. Cell-cell interactions polarise neural crest cells and direct them away from the neural tube. Persistent migration is then maintained by continuous interaction between Syn4 and fibronectin as well as cell-cell signalling mediated by Dsh, both of which result in the activation of RhoA and suppression of Rac at the back of the cell. Furthermore, tissues expressing negative signals such as Ephrins and Semaphorins surround the neural crest migration pathways (Kuriyama and Mayor, 2008), and will contribute to guiding crest cells along the correct routes. This leaves no requirement for the kind of long-range gradient-based

chemoattraction, which is well known in other cellular systems such as axon guidance. Nevertheless, several chemoattractants are known to be expressed around the neural crest later in development and have been shown to guide the movement of neural crest derivatives such as enteric crest cells and dorsal root ganglia (Belmadani et al., 2005; Natarajan et al., 2002; Young et al., 2001). Additionally, the chemokine SDF-1 is expressed during the early stages of migration in the *Xenopus* cranial neural crest (Braun et al., 2002), although it is not certain whether it is acting as a chemoattractant or as a chemokinetic, migration-stimulating agent. Therefore it is not possible to completely rule out a role for chemotaxis in neural crest migration.

One class of extracellular signalling molecule that are vital for neural crest migration are the non-canonical Wnt ligands. Injection of dnWnt11 blocks cranial neural crest migration in *Xenopus* (De Calisto et al., 2005), and I have shown here that the same is true when Wnt11r is inhibited using a morpholino (Fig 3.6). Signalling from Wnt11R expressed adjacent to the neural crest is essential for proper migration, as migration is inhibited in wildtype crests transplanted to Wnt11R -/- embryos (Fig 3.7). However, it is not entirely clear how extra-cellular Wnt signalling from Wnt11 or Wnt11r fits into the model described previously. Dsh-mediated contact inhibition is sufficient to polarise neural crest cells by cell-cell contact without necessarily requiring an extracellular Wnt ligand. Wnt11R is expressed in the neural tube adjacent to the neural crest; so one possibility is that it provides a negative signal, which prevents crest cells from moving towards the midline. However if this were the case, inhibition of Wnt11r would be expected to result in a 'backwards' migration towards the neural tube rather the general inhibition of migration that is observed in *wnt11r* Mo embryos. Perhaps instead, the non-canonical ligands Wnt11 and Wnt11R, which flank the neural crest prior to migration, act to give the tissue an overall polarity. PCP signalling is well known to establish global tissue polarity in other systems. In the *Drosophila* wing, cell-cell signalling sets up a distal-proximal polarity across the tissue resulting in uniform hair growth at the distal side of each cell (Mlodzik, 2002). During convergent extension also, PCP signalling sets up an overall polarity with cells aligned along the same axis of intercalation. PCP ligands are required for vertebrate PCP signalling, with inhibition of Wnt5a or Wnt11 causing convergent extension defects in *Xenopus* and zebrafish (Heisenberg et al., 2000; Moon et al., 1993; Rauch et al., 1997; Tada and

Smith, 2000). However, as in the neural crest, the exact role that Wnt ligands play in controlling this process remains a mystery.

Another possibility is that non-canonical ligands serve simply as activators of the PCP pathway without conveying any directional cue. It is not known how the timing of neural crest migration is regulated in frogs or fish and I have suggested that cues from the extra-cellular matrix could be involved. It is also possible, as discussed in chapter 3, that it is the appearance of non-canonical Wnt ligands expressed in the vicinity of the neural crest that stimulate the beginning of neural crest migration. Witzel et al (2007) show that the accumulation of Dsh and Fzd7 at the contacts between zebrafish animal pole cells depends on the presence of Wnt11 in the medium and that without Wnt11, Dsh is uniformly distributed in the membrane. Therefore, the presence of an extracellular soluble Wnt ligand may be required to allow neural crest cells to respond to a cell-cell contact inhibition signal. The requirement for Wnt ligands during contact inhibition could be tested in cells migrating in the presence or absence of soluble Wnt protein, or by examining contact inhibition in cells lacking the wnt receptor, Fzd7. Clearly, there is much work to be done in elucidating further the molecular mechanisms by which PCP ligands control neural crest migration.

### *8.1.5. Collective versus individual cell migration*

The model of neural crest migration that I have presented relies on initial cell-cell contacts to polarise neural crest cells, while directional migration is maintained by Syn4 suppression of Rac in individually migrating cells. However *in vivo*, individual neural crest cells are rare and most cells migrate surrounded entirely by other neural crest cells. During my experiments following the migration of fluorescently labelled cranial neural crest cells (using graft experiments in *Xenopus* and the *sox10:egfp* zebrafish line), I found that the majority of cells form a coherent mass, which migrate together in a group. *In vivo* imaging of chick embryos has shown that even the comparatively disparate chick neural crest cells maintain long filopodial connections between cells some distance apart (Teddy and Kulesa, 2004). The migration of individual cells such as leukocytes or fibroblasts are some of the best characterised examples of cell migration, however it is becoming increasingly clear that many types of migration exist in which cells travel collectively (Friedl et al., 2004). In some cases, migration occurs by the movement of epithelial sheets, for

example in wound healing or blastopore closure in *Xenopus*, but perhaps a better comparison with neural crest migration is the collective migration of groups of mesenchymal cells. Several examples of this kind of migration can be found during development including the movement of non-involuting endocytic marginal cells during zebrafish gastrulation, the neuromast cells of the fish lateral line and border cell migration in the *Drosophila* ovary (Cooper and D'Amico, 1996; Montell, 2003; Rorth, 2007). Additionally a number of tumour types including melanoma, basal cell, colon and mammary carcinomas have been shown to use a similar mechanism of collective migration for invasion (Friedl et al., 2004). In many of these examples, the collective migration of a group of mesenchymal cells relies on two different cellular populations; cells at the leading edge of migration that produce lamellipodia, and 'following cells' further back, which are tightly connected to their neighbours and contract to generate forward movement. During neural crest migration *in vitro*, cells can also be divided into two populations with polarised leading cells that form cell protrusions and migrate persistently, while trailing cells follow behind, subjected to constant contact inhibition from their neighbours (Fig 7.1). The difference between leading and trailing cells is not intrinsic, and any cell is able to behave as a leading cell, given sufficient free space at the edge of an explant. Given the close proximity of neural crest cells to their neighbours observed in the embryo, similar populations are likely to exist during embryonic migration.

Recent evidence suggests that the PCP pathway plays a role in coordinating cell movement in *Drosophila* border cell migration, one of the best characterised examples of collective cell migration *in vivo* (Montell, 2003). In the *Drosophila* ovary, a cluster of cells known as border cells delaminate from the anterior epithelium of the egg chamber and migrate posteriorly towards the oocyte, carrying with them several non-migratory polar follicle cells. Bastock and Strutt (2007) show that RNAi knockdown of *dsh*, *fzd* or *strabismus* either in the border cells themselves or in the polar follicle cells disrupts migration and promotes the formation of abnormal actin protrusions. Additionally, Fzd and Strabismus localise to the junctions between border and polar follicle cells and they suggest that they establish tissue polarity across the migrating cluster, in a similar way to the control of epithelial tissue polarity in the *Drosophila* wing (Bastock and Strutt, 2007). Similarly in the neural crest, cell-cell signalling via the PCP pathway establishes a polarity, which results in the formation of protrusions at the front of leading cells only. As in

the neural crest, Bastock and Strutt also found that RhoA acts downstream of the PCP pathway in border cells and inhibition of RhoA perturbed border cell migration as a coherent mass. The Rho GTPases are likely to be as central to the regulation of collective cell movements as for individual cell migration. Interestingly, a recent study has shown roles for different Rho GTPases in leading and following cells. During invasion of a squamous cell carcinoma into an artificial 3D-matrix, fibroblastic leading cells require RhoA for their migration, while the carcinoma cells, which trail behind, require Cdc42 (Gaggioli et al., 2007). This hints at different mechanisms regulating the migration of leading versus non-leading cells. It is possible that similar different mechanisms may also be present in non-leading neural crest cells, as most of the data presented here was gathered from observation of neural crest cells migrating individually or at the leading edge of migration.

Collective cell migration has only just begun to be studied in depth and it is likely that much of the work in this field will also be applicable to the neural crest. In fact, it may be more appropriate to consider the neural crest as a single migratory entity, rather than a group of individual migrating cells. In this context, most neural crest cells will be constantly communicating with their neighbours, including PCP-mediated contact inhibition signaling. In this way, cells at the leading edge of migration will be inhibited from producing backwards protrusions by contact inhibition from the mass of cells behind them. Combined with Syn4-mediated signaling from the extracellular matrix, this will result in the activation of RhoA and suppression of Rac at the back of the cell and allow cells to maintain persistent directional migration. Cells at the back of the field, meanwhile, will be surrounded by inhibitory signaling from other cells, and will have little choice but to move forwards when space is vacated by the cells in front. By considering the neural crest in this way, it is possible to extent the model for migration proposed *in vitro* into an *in vivo* environment.

### 8.2. The neural crest as an example of cell migration *in vivo*

One of the greatest challenges currently facing biologists studying cell migration is the observation of cell migration *in vivo*. The migration of individual cells on 2D substrates has allowed the elucidation of some of the finer molecular details of the migratory process, however it is not known how far these mechanisms are conserved in 3-dimensions. Recent attempts to address this issue have involved the construction

of artificial 3D matrices (Even-Ram and Yamada, 2005). These have highlighted some key differences in cell migration in two and three dimensions. For example, $\alpha_v\beta_3$ integrin is not detected in the 3-D-matrix adhesions of fibroblasts, although it is a central constituent of those formed on 2-D substrates (Cukierman et al., 2001). This may be a consequence of the decreased rigidity of a 3D matrix, as the distribution of integrins is known to respond to mechanical stress from the matrix (Katsumi et al., 2005). Additionally, Focal adhesion kinase (FAK) is found to be less phosphorylated at residue Y397, a well known marker of its activation, in fibroblasts on a 3D matrix than on a 2D substrate (Cukierman et al., 2001). These differences have lead to the suggestion that some of the fundamental mechanisms for cell migration may be altered in 3 dimensions compared to two.

However, even a 3-D matrix does not accurately reproduce the complexity and diversity of the *in vivo* environment and there is a need for the development of new systems that allow the analysis of cell migration *in vivo*. The early embryo provides an *in vivo* environment that is relatively straightforward to study compared with living mammalian tissue, and the neural crest is one of the most striking examples of cell migration during development. Here I present data obtained through the analysis of *Xenopus* and zebrafish neural crest migration, both *in vivo* and *in vitro*. For the most part, my findings *in vitro* have been consistently reproducible *in vivo*. Inhibition of Syn4 and Dsh both disrupt neural crest migration in the embryo (Figures 3.3, 4.3 & 5.4) and on a 2-D fibronectin substrate (Figures 5.1 & 5.3). Furthermore the molecular mechanisms by which they control neural crest migration are also conserved. Neural crest cells lacking Syn4 lose persistence *in vitro* (Fig 5.1) and *in vivo* (Fig 5.4). Fibroblasts have been shown to have an increased persistence in three dimensions, corresponding to slightly lower levels of Rac activation (Pankov et al., 2005). However neural crest cells migrate with a similar persistence *in vitro* (persistence is 0.65, Fig 5.2) and in zebrafish embryos (Fig 5.4, persistence=0.61). Perturbation of Syn4 or Dsh also has similar effects on the number of cell protrusions and focal contacts *in vitro* and *in vivo*. Additionally, FRET analysis of Rho GTPases activity, performed here *in vivo* for the first time, reveals identical effects of Rho GTPases, with Syn4 repressing Rac and Dsh activating RhoA in *Xenopus* cells in both 2- and 3-dimensions. Likewise, contact inhibition occurs *in vivo* and *in vitro* and in both cases is dependent on PCP signalling. In fact, the only notable difference between neural crest migration *in vitro* and *in vivo* is the role of focal adhesion

kinase, which has an extended function *in vivo* where it regulates early events essential for the onset of migration. These data suggest that the basic mechanisms that regulate neural crest migration are in fact very similar *in vitro* and in the more complex embryonic environment. Indeed, neural crest migration *in vitro* seems to mimic the *in vivo* situation far better than has been reported in previous 3D matrix studies (Even-Ram and Yamada, 2005).

One of the central differences between migration in 2-D and 3-D is the shape of the cells. Cells migrating on a horizontal surface naturally adopt a more flattened morphology to allow maximum attachment, whereas cells migrating *in vivo* form a variety of shapes. Consequently, cell protrusions and attachments to the substrate often appear different. Focal adhesion formation is particularly affected, as attachment to the substrate occurs not just at the base of the cell, but all around its surface. Some reports have indicated that focal adhesions appear very different in three dimensions. Cukierman et al (2001) studied focal adhesions in 3D matrices and *in vivo* in mouse mesenchymal cells and found paxillin and α5-integrin distributed in long, thin, fibriller structures, which co-localise with fibronectin in the extracellular matrix. They also showed a co-localisation of paxillin and α5-integrin, which is not normally observed *in vitro*, where paxillin is associated with focal adhesions and α5-integrin is a constituent of the more mature fibriller adhesions (Cukierman et al., 2001). This suggests that it may not be possible to distinguish between the different types of focal contact *in vivo*. Focal adhesions have been proposed to act as mechanosensors and therefore any role that they play in a rigid 2 matrix, might be different in a more flexible 3D matrix (Wozniak et al., 2004). Here, staining with a phospho-paxillin antibody in zebrafish and *Xenopus* embryos shows distinctive accumulations of paxillin in the migrating neural crest. In *Xenopus*, some of these accumulations are fibriller but the majority of accumulations in both *Xenopus* and zebrafish appeared as smaller puncta, which are similar to those observed *in vitro*. This suggests that focal adhesions in 3-D may be more similar to those *in vitro* than has previously been described (Cukierman et al., 2001). The neural crest provides a good model for the study of focal adhesions *in vivo* and could no doubt provide much more information, especially if live imaging was applied.

In this thesis, I have shown that *Xenopus* and zebrafish embryos can be used to analyse the physical aspects of cell migration *in vivo* including the actin cytoskeleton and focal adhesions, as well as for undertaking dissection of the molecular

mechanisms. Of course, there will always be a necessity for *in vitro* models of cell migration, and the depth of analysis during embryology does not yet rival its *in vitro* counterparts. Yet with constantly improving imaging techniques, the embryo provides an excellent opportunity for studying cell migration *in vivo*. In particular, neural crest migration in zebrafish and *Xenopus* embryos is an exciting new model, which has a great deal of potential for the *in vivo* analysis of cell migration.

# 9. REFERENCES


**Aaku-Saraste, E., Hellwig, A. and Huttner, W. B.** (1996). Loss of occludin and functional tight junctions, but not ZO-1, during neural tube closure--remodeling of the neuroepithelium prior to neurogenesis. *Dev Biol* **180**, 664-79.

**Abercrombie, M.** (1967). Contact inhibition: the phenomenon and its biological implications. *Natl Cancer Inst Monogr* **26**, 249-77.

**Abercrombie, M.** (1970). Contact inhibition in tissue culture. *In Vitro* **6**, 128-42.

**Abercrombie, M.** (1979). Contact inhibition and malignancy. *Nature* **281**, 259-62.

**Abercrombie, M.** (1980). The Croonian Lecture, 1978: The Crawling Movement of Metazoan Cells. In *Proc. Royal Soc. London B, Biol Sci*, vol. 207 (ed., pp. 129-47.

**Abercrombie, M. and Ambrose, E. J.** (1958). Interference microscope studies of cell contacts in tissue culture. *Exp Cell Res* **15**, 332-45.

**Abercrombie, M. and Heaysman, J. E.** (1953). Observations on the social behaviour of cells in tissue culture. I. Speed of movement of chick heart fibroblasts in relation to their mutual contacts. *Exp Cell Res* **5**, 111-31.

**Abercrombie, M. and Heaysman, J. E.** (1954a). Invasiveness of sarcoma cells. *Nature* **174**, 697-8.

**Abercrombie, M. and Heaysman, J. E.** (1954b). Observations on the social behaviour of cells in tissue culture. II. Monolayering of fibroblasts. *Exp Cell Res* **6**, 293-306.

**Abercrombie, M. and Heaysman, J. E.** (1976). Invasive behavior between sarcoma and fibroblast populations in cell culture. *J Natl Cancer Inst* **56**, 561-70.

**Abu-Elmagd, M., Garcia-Morales, C. and Wheeler, G. N.** (2006). Frizzled7 mediates canonical Wnt signaling in neural crest induction. *Dev Biol* **298**, 285-98.

**Adler, P. N.** (2002). Planar signaling and morphogenesis in Drosophila. *Dev Cell* **2**, 525-35.

**Alexander, C. M., Reichsman, F., Hinkes, M. T., Lincecum, J., Becker, K. A., Cumberledge, S. and Bernfield, M.** (2000). Syndecan-1 is required for Wnt-1-induced mammary tumorigenesis in mice. *Nat Genet* **25**, 329-32.

**Alfandari, D., Cousin, H., Gaultier, A., Hoffstrom, B. G. and DeSimone, D. W.** (2003). Integrin alpha5beta1 supports the migration of Xenopus cranial neural crest on fibronectin. *Dev Biol* **260**, 449-64.

**Alfandari, D., Cousin, H., Gaultier, A., Smith, K., White, J. M., Darribere, T. and DeSimone, D. W.** (2001). Xenopus ADAM 13 is a metalloprotease required for cranial neural crest-cell migration. *Curr Biol* **11**, 918-30.

**Amsterdam, A. and Hopkins, N.** (2006). Mutagenesis strategies in zebrafish for identifying genes involved in development and disease. *Trends Genet* **22**, 473-8.

**Anderson, K. I., Wang, Y. L. and Small, J. V.** (1996). Coordination of protrusion and translocation of the keratocyte involves rolling of the cell body. *J Cell Biol* **134**, 1209-18.

**Aoki, Y., Saint-Germain, N., Gyda, M., Magner-Fink, E., Lee, Y. H., Credidio, C. and Saint-Jeannet, J. P.** (2003). Sox10 regulates the development of neural crest-derived melanocytes in Xenopus. *Dev Biol* **259**, 19-33.

**Asundi, V. K. and Carey, D. J.** (1995). Self-association of N-syndecan (syndecan-3) core protein is mediated by a novel structural motif in the transmembrane domain and ectodomain flanking region. *J Biol Chem* **270**, 26404-10.

**Axelrod, J. D.** (2001). Unipolar membrane association of Dishevelled mediates Frizzled planar cell polarity signaling. *Genes Dev* **15**, 1182-7.

**Axelrod, J. D., Miller, J. R., Shulman, J. M., Moon, R. T. and Perrimon, N.** (1998). Differential recruitment of Dishevelled provides signaling specificity in the planar cell polarity and Wingless signaling pathways. *Genes Dev* **12**, 2610-22.

**Aybar, M. J. and Mayor, R.** (2002). Early induction of neural crest cells: lessons learned from frog, fish and chick. *Curr Opin Genet Dev* **12**, 452-8.

**Aybar, M. J., Nieto, M. A. and Mayor, R.** (2003). Snail precedes slug in the genetic cascade required for the specification and migration of the Xenopus neural crest. *Development* **130**, 483-94.

**Baciu, P. C., Saoncella, S., Lee, S. H., Denhez, F., Leuthardt, D. and Goetinck, P. F.** (2000). Syndesmos, a protein that interacts with the cytoplasmic domain of syndecan-4, mediates cell spreading and actin cytoskeletal organization. *J Cell Sci* **113**, 315-324.

**Baeg, G. H., Lin, X., Khare, N., Baumgartner, S. and Perrimon, N.** (2001). Heparan sulfate proteoglycans are critical for the organization of the extracellular distribution of Wingless. *Development* **128**, 87-94.

**Barrallo-Gimeno, A. and Nieto, M. A.** (2005). The Snail genes as inducers of cell movement and survival: implications in development and cancer. *Development* **132**, 3151-61.
**Bass, M. D. and Humphries, M. J.** (2002). Cytoplasmic interactions of syndecan-4 orchestrate adhesion receptor and growth factor receptor signalling. *Biochem J* **368**, 1-15.
**Bass, M. D., Roach, K. A., Morgan, M. R., Mostafavi-Pour, Z., Schoen, T., Muramatsu, T., Mayer, U., Ballestrem, C., Spatz, J. P. and Humphries, M. J.** (2007). Syndecan-4-dependent Rac1 regulation determines directional migration in response to the extracellular matrix. *J Cell Biol* **177**, 527-38.
**Bastock, R. and Strutt, D.** (2007). The planar polarity pathway promotes coordinated cell migration during Drosophila oogenesis. *Development* **134**, 3055-64.
**Bastock, R., Strutt, H. and Strutt, D.** (2003). Strabismus is asymmetrically localised and binds to Prickle and Dishevelled during Drosophila planar polarity patterning. *Development* **130**, 3007-14.
**Bear, J. E., Svitkina, T. M., Krause, M., Schafer, D. A., Loureiro, J. J., Strasser, G. A., Maly, I. V., Chaga, O. Y., Cooper, J. A., Borisy, G. G. et al.** (2002). Antagonism between Ena/VASP proteins and actin filament capping regulates fibroblast motility. *Cell* **109**, 509-21.
**Bellmeyer, A., Krase, J., Lindgren, J. and LaBonne, C.** (2003). The protooncogene c-myc is an essential regulator of neural crest formation in xenopus. *Dev Cell* **4**, 827-39.
**Belmadani, A., Tran, P. B., Ren, D., Assimacopoulos, S., Grove, E. A. and Miller, R. J.** (2005). The chemokine stromal cell-derived factor-1 regulates the migration of sensory neuron progenitors. *J Neurosci* **25**, 3995-4003.
**Beningo, K. A., Dembo, M., Kaverina, I., Small, J. V. and Wang, Y. L.** (2001). Nascent focal adhesions are responsible for the generation of strong propulsive forces in migrating fibroblasts. *J Cell Biol* **153**, 881-8.
**Bernards, A. and Settleman, J.** (2005). GAPs in growth factor signalling. *Growth Factors* **23**, 143-9.
**Bernfield, M., Gotte, M., Park, P. W., Reizes, O., Fitzgerald, M. L., Lincecum, J. and Zako, M.** (1999). Functions of cell surface heparan sulfate proteoglycans. *Annu Rev Biochem* **68**, 729-77.
**Bloom, L., Ingham, K. C. and Hynes, R. O.** (1999). Fibronectin regulates assembly of actin filaments and focal contacts in cultured cells via the heparin-binding site in repeat III13. *Mol Biol Cell* **10**, 1521-36.
**Bolos, V., Peinado, H., Perez-Moreno, M. A., Fraga, M. F., Esteller, M. and Cano, A.** (2003). The transcription factor Slug represses E-cadherin expression and induces epithelial to mesenchymal transitions: a comparison with Snail and E47 repressors. *J Cell Sci* **116**, 499-511.
**Borchers, A., David, R. and Wedlich, D.** (2001). Xenopus cadherin-11 restrains cranial neural crest migration and influences neural crest specification. *Development* **128**, 3049-60.
**Borchers, A., Epperlein, H. H. and Wedlich, D.** (2000). An assay system to study migratory behavior of cranial neural crest cells in Xenopus. *Dev Genes Evol* **210**, 217-22.
**Bos, J. L., Rehmann, H. and Wittinghofer, A.** (2007). GEFs and GAPs: critical elements in the control of small G proteins. *Cell* **129**, 865-77.
**Boucaut, J. C., Darribere, T., Poole, T. J., Aoyama, H., Yamada, K. M. and Thiery, J. P.** (1984). Biologically active synthetic peptides as probes of embryonic development: a competitive peptide inhibitor of fibronectin function inhibits gastrulation in amphibian embryos and neural crest cell migration in avian embryos. *J Cell Biol* **99**, 1822-30.
**Boutros, M., Paricio, N., Strutt, D. I. and Mlodzik, M.** (1998). Dishevelled activates JNK and discriminates between JNK pathways in planar polarity and wingless signaling. *Cell* **94**, 109-18.
**Braun, M., Wunderlin, M., Spieth, K., Knochel, W., Gierschik, P. and Moepps, B.** (2002). Xenopus laevis Stromal cell-derived factor 1: conservation of structure and function during vertebrate development. *J Immunol* **168**, 2340-7.
**Bronner-Fraser, M.** (1986a). Analysis of the early stages of trunk neural crest migration in avian embryos using monoclonal antibody HNK-1. *Dev Biol* **115**, 44-55.
**Bronner-Fraser, M.** (1986b). An antibody to a receptor for fibronectin and laminin perturbs cranial neural crest development in vivo. *Dev Biol* **117**, 528-36.
**Brown, R. M. and Middleton, C. A.** (1981). Contact-induced spreading in cultures of corneal epithelial cells. *J Cell Sci* **51**, 143-52.
**Burridge, K. and Wennerberg, K.** (2004). Rho and Rac take center stage. *Cell* **116**, 167-79.
**Burstyn-Cohen, T. and Kalcheim, C.** (2002). Association between the cell cycle and neural crest delamination through specific regulation of G1/S transition. *Dev Cell* **3**, 383-95.
**Burstyn-Cohen, T., Stanleigh, J., Sela-Donenfeld, D. and Kalcheim, C.** (2004). Canonical Wnt activity regulates trunk neural crest delamination linking BMP/noggin signaling with G1/S transition. *Development* **131**, 5327-39.

**Cano, A., Perez-Moreno, M. A., Rodrigo, I., Locascio, A., Blanco, M. J., del Barrio, M. G., Portillo, F. and Nieto, M. A.** (2000). The transcription factor snail controls epithelial-mesenchymal transitions by repressing E-cadherin expression. *Nat Cell Biol* **2**, 76-83.
**Capelluto, D. G., Kutateladze, T. G., Habas, R., Finkielstein, C. V., He, X. and Overduin, M.** (2002). The DIX domain targets dishevelled to actin stress fibres and vesicular membranes. *Nature* **419**, 726-9.
**Carmona-Fontaine, C., Acuna, G., Ellwanger, K., Niehrs, C. and Mayor, R.** (2007). Neural crests are actively precluded from the anterior neural fold by a novel inhibitory mechanism dependent on Dickkopf1 secreted by the prechordal mesoderm. *Dev Biol* **309**, 208-21.
**Carney, T. J., Dutton, K. A., Greenhill, E., Delfino-Machin, M., Dufourcq, P., Blader, P. and Kelsh, R. N.** (2006). A direct role for Sox10 in specification of neural crest-derived sensory neurons. *Development* **133**, 4619-30.
**Chaudhuri, P., Colles, S. M., Fox, P. L. and Graham, L. M.** (2005). Protein kinase Cdelta-dependent phosphorylation of syndecan-4 regulates cell migration. *Circ Res* **97**, 674-81.
**Chen, B. H., Tzen, J. T., Bresnick, A. R. and Chen, H. C.** (2002). Roles of Rho-associated kinase and myosin light chain kinase in morphological and migratory defects of focal adhesion kinase-null cells. *J Biol Chem* **277**, 33857-63.
**Choi, S. C. and Han, J. K.** (2002). Xenopus Cdc42 regulates convergent extension movements during gastrulation through Wnt/Ca2+ signaling pathway. *Dev Biol* **244**, 342-57.
**Choi, S. C. and Han, J. K.** (2005). Rap2 is required for Wnt/beta-catenin signaling pathway in Xenopus early development. *Embo J* **24**, 985-96.
**Choma, D. P., Pumiglia, K. and DiPersio, C. M.** (2004). Integrin alpha3beta1 directs the stabilization of a polarized lamellipodium in epithelial cells through activation of Rac1. *J Cell Sci* **117**, 3947-59.
**Christiansen, J. H., Dennis, C. L., Wicking, C. A., Monkley, S. J., Wilkinson, D. G. and Wainwright, B. J.** (1995). Murine Wnt-11 and Wnt-12 have temporally and spatially restricted expression patterns during embryonic development. *Mech Dev* **51**, 341-50.
**Chrzanowska-Wodnicka, M. and Burridge, K.** (1996). Rho-stimulated contractility drives the formation of stress fibers and focal adhesions. *J Cell Biol* **133**, 1403-15.
**Coles, E. G., Gammill, L. S., Miner, J. H. and Bronner-Fraser, M.** (2006). Abnormalities in neural crest cell migration in laminin alpha5 mutant mice. *Dev Biol* **289**, 218-28.
**Collazo, A., Bronner-Fraser, M. and Fraser, S. E.** (1993). Vital dye labelling of Xenopus laevis trunk neural crest reveals multipotency and novel pathways of migration. *Development* **118**, 363-76.
**Cooper, M. S. and D'Amico, L. A.** (1996). A cluster of noninvoluting endocytic cells at the margin of the zebrafish blastoderm marks the site of embryonic shield formation. *Dev Biol* **180**, 184-98.
**Coso, O. A., Chiariello, M., Yu, J. C., Teramoto, H., Crespo, P., Xu, N., Miki, T. and Gutkind, J. S.** (1995). The small GTP-binding proteins Rac1 and Cdc42 regulate the activity of the JNK/SAPK signaling pathway. *Cell* **81**, 1137-46.
**Crawford, B. D., Henry, C. A., Clason, T. A., Becker, A. L. and Hille, M. B.** (2003). Activity and distribution of paxillin, focal adhesion kinase, and cadherin indicate cooperative roles during zebrafish morphogenesis. *Mol Biol Cell* **14**, 3065-81.
**Cukierman, E., Pankov, R., Stevens, D. R. and Yamada, K. M.** (2001). Taking Cell-Matrix Adhesions to the Third Dimension. *Science* **294**, 1708-1712.
**Curtis, A. S.** (1964). The Mechanism Of Adhesion Of Cells To Glass. A Study By Interference Reflection Microscopy. *J Cell Biol* **20**, 199-215.
**Czuchra, A., Wu, X., Meyer, H., van Hengel, J., Schroeder, T., Geffers, R., Rottner, K. and Brakebusch, C.** (2005). Cdc42 is not essential for filopodium formation, directed migration, cell polarization, and mitosis in fibroblastoid cells. *Mol Biol Cell* **16**, 4473-84.
**Dale, L. and Slack, J. M.** (1987). Fate map for the 32-cell stage of Xenopus laevis. *Development* **99**, 527-51.
**David, N. B., Sapede, D., Saint-Etienne, L., Thisse, C., Thisse, B., Dambly-Chaudiere, C., Rosa, F. M. and Ghysen, A.** (2002). Molecular basis of cell migration in the fish lateral line: role of the chemokine receptor CXCR4 and of its ligand, SDF1. *Proc Natl Acad Sci U S A* **99**, 16297-302.
**De Calisto, J., Araya, C., Marchant, L., Riaz, C. F. and Mayor, R.** (2005). Essential role of non-canonical Wnt signalling in neural crest migration. *Development* **132**, 2587-97.
**Dejmek, J., Dejmek, A., Safholm, A., Sjolander, A. and Andersson, T.** (2005). Wnt-5a protein expression in primary dukes B colon cancers identifies a subgroup of patients with good prognosis. *Cancer Res* **65**, 9142-6.
**del Pozo, M. A., Alderson, N. B., Kiosses, W. B., Chiang, H. H., Anderson, R. G. and Schwartz, M. A.** (2004). Integrins regulate Rac targeting by internalization of membrane domains. *Science* **303**, 839-42.

**Delannet, M., Martin, F., Bossy, B., Cheresh, D. A., Reichardt, L. F. and Duband, J. L.** (1994). Specific roles of the alpha V beta 1, alpha V beta 3 and alpha V beta 5 integrins in avian neural crest cell adhesion and migration on vitronectin. *Development* **120**, 2687-702.
**Delfino-Machin, M., Chipperfield, T. R., Rodrigues, F. S. and Kelsh, R. N.** (2007). The proliferating field of neural crest stem cells. *Dev Dyn* **236**, 3242-54.
**Denhez, F., Wilcox-Adelman, S. A., Baciu, P. C., Saoncella, S., Lee, S., French, B., Neveu, W. and Goetinck, P. F.** (2002). Syndesmos, a syndecan-4 cytoplasmic domain interactor, binds to the focal adhesion adaptor proteins paxillin and Hic-5. *J Biol Chem* **277**, 12270-4.
**Djiane, A., Riou, J., Umbhauer, M., Boucaut, J. and Shi, D.** (2000). Role of frizzled 7 in the regulation of convergent extension movements during gastrulation in Xenopus laevis. *Development* **127**, 3091-100.
**Dovas, A., Yoneda, A. and Couchman, J. R.** (2006). PKCbeta-dependent activation of RhoA by syndecan-4 during focal adhesion formation. *J Cell Sci* **119**, 2837-46.
**Dutton, K. A., Pauliny, A., Lopes, S. S., Elworthy, S., Carney, T. J., Rauch, J., Geisler, R., Haffter, P. and Kelsh, R. N.** (2001). Zebrafish colourless encodes sox10 and specifies non-ectomesenchymal neural crest fates. *Development* **128**, 4113-25.
**Eaton, S., Wepf, R. and Simons, K.** (1996). Roles for Rac1 and Cdc42 in planar polarization and hair outgrowth in the wing of Drosophila. *J Cell Biol* **135**, 1277-89.
**Echtermeyer, F., Baciu, P. C., Saoncella, S., Ge, Y. and Goetinck, P. F.** (1999). Syndecan-4 core protein is sufficient for the assembly of focal adhesions and actin stress fibers. *J Cell Sci* **112 (Pt 20)**, 3433-41.
**Echtermeyer, F., Streit, M., Wilcox-Adelman, S., Saoncella, S., Denhez, F., Detmar, M. and Goetinck, P.** (2001). Delayed wound repair and impaired angiogenesis in mice lacking syndecan-4. *J Clin Invest* **107**, R9-R14.
**Eisen, J. S. and Weston, J. A.** (1993). Development of the neural crest in the zebrafish. *Dev Biol* **159**, 50-9.
**Etienne-Manneville, S. and Hall, A.** (2001). Integrin-mediated activation of Cdc42 controls cell polarity in migrating astrocytes through PKCzeta. *Cell* **106**, 489-98.
**Etienne-Manneville, S. and Hall, A.** (2002). Rho GTPases in cell biology. *Nature* **420**, 629-35.
**Etienne-Manneville, S. and Hall, A.** (2003). Cdc42 regulates GSK-3beta and adenomatous polyposis coli to control cell polarity. *Nature* **421**, 753-6.
**Even-Ram, S. and Yamada, K. M.** (2005). Cell migration in 3D matrix. *Curr Opin Cell Biol* **17**, 524-32.
**Fathke, C., Wilson, L., Shah, K., Kim, B., Hocking, A., Moon, R. and Isik, F.** (2006). Wnt signaling induces epithelial differentiation during cutaneous wound healing. *BMC Cell Biol* **7**, 4.
**Feiguin, F., Hannus, M., Mlodzik, M. and Eaton, S.** (2001). The ankyrin repeat protein Diego mediates Frizzled-dependent planar polarization. *Dev Cell* **1**, 93-101.
**Fitzgerald, M. L., Wang, Z., Park, P. W., Murphy, G. and Bernfield, M.** (2000). Shedding of syndecan-1 and -4 ectodomains is regulated by multiple signaling pathways and mediated by a TIMP-3-sensitive metalloproteinase. *J Cell Biol* **148**, 811-24.
**Friedl, P., Hegerfeldt, Y. and Tusch, M.** (2004). Collective cell migration in morphogenesis and cancer. *Int J Dev Biol* **48**, 441-9.
**Gaggioli, C., Hooper, S., Hidalgo-Carcedo, C., Grosse, R., Marshall, J. F., Harrington, K. and Sahai, E.** (2007). Fibroblast-led collective invasion of carcinoma cells with differing roles for RhoGTPases in leading and following cells. *Nat Cell Biol* **9**, 1392-400.
**Galbraith, C. G., Yamada, K. M. and Sheetz, M. P.** (2002). The relationship between force and focal complex development. *J Cell Biol* **159**, 695-705.
**Gammill, L. S., Gonzalez, C., Gu, C. and Bronner-Fraser, M.** (2006). Guidance of trunk neural crest migration requires neuropilin 2/semaphorin 3F signaling. *Development* **133**, 99-106.
**Gao, Y., Dickerson, J. B., Guo, F., Zheng, J. and Zheng, Y.** (2004). Rational design and characterization of a Rac GTPase-specific small molecule inhibitor. *Proc Natl Acad Sci U S A* **101**, 7618-23.
**Garcia-Castro, M. I., Marcelle, C. and Bronner-Fraser, M.** (2002). Ectodermal Wnt function as a neural crest inducer. *Science* **297**, 848-51.
**Garriock, R. J., D'Agostino, S. L., Pilcher, K. C. and Krieg, P. A.** (2005). Wnt11-R, a protein closely related to mammalian Wnt11, is required for heart morphogenesis in Xenopus. *Dev Biol* **279**, 179-92.
**Garriock, R. J. and Krieg, P. A.** (2007). Wnt11-R signaling regulates a calcium sensitive EMT event essential for dorsal fin development of Xenopus. *Dev Biol* **304**, 127-40.

**Garriock, R. J., Warkman, A. S., Meadows, S. M., D'Agostino, S. and Krieg, P. A.** (2007). Census of vertebrate Wnt genes: isolation and developmental expression of Xenopus Wnt2, Wnt3, Wnt9a, Wnt9b, Wnt10a, and Wnt16. *Dev Dyn* **236**, 1249-58.
**Goley, E. D. and Welch, M. D.** (2006). The ARP2/3 complex: an actin nucleator comes of age. *Nat Rev Mol Cell Biol* **7**, 713-26.
**Gooday, D. and Thorogood, P.** (1985). Contact behaviour exhibited by migrating neural crest cells in confrontation culture with somitic cells. *Cell Tissue Res* **241**, 165-9.
**Goto, T., Davidson, L., Asashima, M. and Keller, R.** (2005). Planar cell polarity genes regulate polarized extracellular matrix deposition during frog gastrulation. *Curr Biol* **15**, 787-93.
**Goto, T. and Keller, R.** (2002). The planar cell polarity gene strabismus regulates convergence and extension and neural fold closure in Xenopus. *Dev Biol* **247**, 165-81.
**Grootjans, J. J., Reekmans, G., Ceulemans, H. and David, G.** (2000). Syntenin-syndecan binding requires syndecan-synteny and the co-operation of both PDZ domains of syntenin. *J Biol Chem* **275**, 19933-41.
**Grootjans, J. J., Zimmermann, P., Reekmans, G., Smets, A., Degeest, G., Durr, J. and David, G.** (1997). Syntenin, a PDZ protein that binds syndecan cytoplasmic domains. *Proc Natl Acad Sci U S A* **94**, 13683-8.
**Gu, J., Tamura, M., Pankov, R., Danen, E. H., Takino, T., Matsumoto, K. and Yamada, K. M.** (1999). Shc and FAK differentially regulate cell motility and directionality modulated by PTEN. *J Cell Biol* **146**, 389-403.
**Gubb, D. and Garcia-Bellido, A.** (1982). A genetic analysis of the determination of cuticular polarity during development in Drosophila melanogaster. *J Embryol Exp Morphol* **68**, 37-57.
**Gubb, D., Green, C., Huen, D., Coulson, D., Johnson, G., Tree, D., Collier, S. and Roote, J.** (1999). The balance between isoforms of the prickle LIM domain protein is critical for planar polarity in Drosophila imaginal discs. *Genes Dev* **13**, 2315-27.
**Gurdon, J. B. and Hopwood, N.** (2000). The introduction of Xenopus laevis into developmental biology: of empire, pregnancy testing and ribosomal genes. *Int J Dev Biol* **44**, 43-50.
**Haack, H. and Hynes, R. O.** (2001). Integrin receptors are required for cell survival and proliferation during development of the peripheral glial lineage. *Dev Biol* **233**, 38-55.
**Habas, R., Dawid, I. B. and He, X.** (2003). Coactivation of Rac and Rho by Wnt/Frizzled signaling is required for vertebrate gastrulation. *Genes Dev* **17**, 295-309.
**Habas, R., Kato, Y. and He, X.** (2001). Wnt/Frizzled activation of Rho regulates vertebrate gastrulation and requires a novel Formin homology protein Daam1. *Cell* **107**, 843-54.
**Hakeda-Suzuki, S., Ng, J., Tzu, J., Dietzl, G., Sun, Y., Harms, M., Nardine, T., Luo, L. and Dickson, B. J.** (2002). Rac function and regulation during Drosophila development. *Nature* **416**, 438-42.
**Hall, A.** (2005). Rho GTPases and the control of cell behaviour. *Biochem Soc Trans* **33**, 891-5.
**Hammerschmidt, M., Pelegri, F., Mullins, M. C., Kane, D. A., Brand, M., van Eeden, F. J., Furutani-Seiki, M., Granato, M., Haffter, P., Heisenberg, C. P. et al.** (1996). Mutations affecting morphogenesis during gastrulation and tail formation in the zebrafish, Danio rerio. *Development* **123**, 143-51.
**Harland, R. M.** (1991). In situ hybridization: an improved whole-mount method for Xenopus embryos. *Methods Cell Biol* **36**, 685-95.
**Heaysman, J. E.** (1978). Contact inhibition of locomotion: a reappraisal. *Int Rev Cytol* **55**, 49-66.
**Heisenberg, C. P., Tada, M., Rauch, G. J., Saude, L., Concha, M. L., Geisler, R., Stemple, D. L., Smith, J. C. and Wilson, S. W.** (2000). Silberblick/Wnt11 mediates convergent extension movements during zebrafish gastrulation. *Nature* **405**, 76-81.
**Henry, C. A., Crawford, B. D., Yan, Y. L., Postlethwait, J., Cooper, M. S. and Hille, M. B.** (2001). Roles for zebrafish focal adhesion kinase in notochord and somite morphogenesis. *Dev Biol* **240**, 474-87.
**Hens, M. D. and DeSimone, D. W.** (1995). Molecular analysis and developmental expression of the focal adhesion kinase pp125FAK in Xenopus laevis. *Dev Biol* **170**, 274-88.
**Hong, C. S. and Saint-Jeannet, J. P.** (2005). Sox proteins and neural crest development. *Semin Cell Dev Biol* **16**, 694-703.
**Hopwood, N. D., Pluck, A. and Gurdon, J. B.** (1989). A Xenopus mRNA related to Drosophila twist is expressed in response to induction in the mesoderm and the neural crest. *Cell* **59**, 893-903.
**Horowitz, A., Murakami, M., Gao, Y. and Simons, M.** (1999). Phosphatidylinositol-4,5-bisphosphate mediates the interaction of syndecan-4 with protein kinase C. *Biochemistry* **38**, 15871-7.
**Hsia, D. A., Mitra, S. K., Hauck, C. R., Streblow, D. N., Nelson, J. A., Ilic, D., Huang, S., Li, E., Nemerow, G. R., Leng, J. et al.** (2003). Differential regulation of cell motility and invasion by FAK. *J Cell Biol* **160**, 753-67.

**Hu, B., Jarzynka, M. J., Guo, P., Imanishi, Y., Schlaepfer, D. D. and Cheng, S. Y.** (2006). Angiopoietin 2 induces glioma cell invasion by stimulating matrix metalloprotease 2 expression through the alphavbeta1 integrin and focal adhesion kinase signaling pathway. *Cancer Res* **66**, 775-83.
**Hyatt, S. L., Klauck, T. and Jaken, S.** (1990). Protein kinase C is localized in focal contacts of normal but not transformed fibroblasts. *Mol Carcinog* **3**, 45-53.
**Iioka, H., Iemura, S., Natsume, T. and Kinoshita, N.** (2007). Wnt signalling regulates paxillin ubiquitination essential for mesodermal cell motility. *Nat Cell Biol* **9**, 813-21.
**Ilic, D., Furuta, Y., Kanazawa, S., Takeda, N., Sobue, K., Nakatsuji, N., Nomura, S., Fujimoto, J., Okada, M. and Yamamoto, T.** (1995). Reduced cell motility and enhanced focal adhesion contact formation in cells from FAK-deficient mice. *Nature* **377**, 539-44.
**Ilic, D., Kovacic, B., Johkura, K., Schlaepfer, D. D., Tomasevic, N., Han, Q., Kim, J. B., Howerton, K., Baumbusch, C., Ogiwara, N. et al.** (2004). FAK promotes organization of fibronectin matrix and fibrillar adhesions. *J Cell Sci* **117**, 177-87.
**Ishiguro, K., Kadomatsu, K., Kojima, T., Muramatsu, H., Tsuzuki, S., Nakamura, E., Kusugami, K., Saito, H. and Muramatsu, T.** (2000). Syndecan-4 deficiency impairs focal adhesion formation only under restricted conditions. *J Biol Chem* **275**, 5249-52.
**Itoh, R. E., Kurokawa, K., Ohba, Y., Yoshizaki, H., Mochizuki, N. and Matsuda, M.** (2002). Activation of Rac and Cdc42 Video Imaged by Fluorescent Resonance Energy Transfer-Based Single-Molecule Probes in the Membrane of Living Cells. *Mol. Cell. Biol.* **22**, 6582-6591.
**Jaffe, A. B. and Hall, A.** (2005). Rho GTPases: biochemistry and biology. *Annu Rev Cell Dev Biol* **21**, 247-69.
**Jia, L., Cheng, L. and Raper, J.** (2005). Slit/Robo signaling is necessary to confine early neural crest cells to the ventral migratory pathway in the trunk. *Dev Biol* **282**, 411-21.
**Jiang, Y., Liu, M. T. and Gershon, M. D.** (2003). Netrins and DCC in the guidance of migrating neural crest-derived cells in the developing bowel and pancreas. *Dev Biol* **258**, 364-84.
**Jonsson, M., Dejmek, J., Bendahl, P. O. and Andersson, T.** (2002). Loss of Wnt-5a protein is associated with early relapse in invasive ductal breast carcinomas. *Cancer Res* **62**, 409-16.
**Julius, M. A., Schelbert, B., Hsu, W., Fitzpatrick, E., Jho, E., Fagotto, F., Costantini, F. and Kitajewski, J.** (2000). Domains of axin and disheveled required for interaction and function in wnt signaling. *Biochem Biophys Res Commun* **276**, 1162-9.
**Kaksonen, M., Pavlov, I., Voikar, V., Lauri, S. E., Hienola, A., Riekki, R., Lakso, M., Taira, T. and Rauvala, H.** (2002). Syndecan-3-deficient mice exhibit enhanced LTP and impaired hippocampus-dependent memory. *Mol Cell Neurosci* **21**, 158-72.
**Katoh, M.** (2005). WNT/PCP signaling pathway and human cancer (review). *Oncol Rep* **14**, 1583-8.
**Katsumi, A., Naoe, T., Matsushita, T., Kaibuchi, K. and Schwartz, M. A.** (2005). Integrin activation and matrix binding mediate cellular responses to mechanical stretch. *J Biol Chem* **280**, 16546-9.
**Keller, R.** (2005). Cell migration during gastrulation. *Curr Opin Cell Biol* **17**, 533-41.
**Kestler, H. A. and Kuhl, M.** (2008). From individual Wnt pathways towards a Wnt signalling network. *Philos Trans R Soc Lond B Biol Sci* **363**, 1333-47.
**Keum, E., Kim, Y., Kim, J., Kwon, S., Lim, Y., Han, I. and Oh, E. S.** (2004). Syndecan-4 regulates localization, activity and stability of protein kinase C-alpha. *Biochem J* **378**, 1007-14.
**Kikuchi, A., Yamamoto, H. and Kishida, S.** (2007). Multiplicity of the interactions of Wnt proteins and their receptors. *Cell Signal* **19**, 659-71.
**Kimmel, C. B., Ballard, W. W., Kimmel, S. R., Ullmann, B. and Schilling, T. F.** (1995). Stages of embryonic development of the zebrafish. *Dev Dyn* **203**, 253-310.
**Kinoshita, N., Iioka, H., Miyakoshi, A. and Ueno, N.** (2003). PKC delta is essential for Dishevelled function in a noncanonical Wnt pathway that regulates Xenopus convergent extension movements. *Genes Dev* **17**, 1663-76.
**Kiyokawa, E., Hara, S., Nakamura, T. and Matsuda, M.** (2006). Fluorescence (Forster) resonance energy transfer imaging of oncogene activity in living cells. *Cancer Sci* **97**, 8-15.
**Klein, R.** (2004). Eph/ephrin signaling in morphogenesis, neural development and plasticity. *Curr Opin Cell Biol* **16**, 580-9.
**Kolodkin, A. L.** (1998). Semaphorin-mediated neuronal growth cone guidance. *Prog Brain Res* **117**, 115-32.
**Kontges, G. and Lumsden, A.** (1996). Rhombencephalic neural crest segmentation is preserved throughout craniofacial ontogeny. *Development* **122**, 3229-42.
**Koo, B. K., Jung, Y. S., Shin, J., Han, I., Mortier, E., Zimmermann, P., Whiteford, J. R., Couchman, J. R., Oh, E. S. and Lee, W.** (2006). Structural basis of syndecan-4 phosphorylation as a molecular switch to regulate signaling. *J Mol Biol* **355**, 651-63.

**Kozma, R., Ahmed, S., Best, A. and Lim, L.** (1995). The Ras-related protein Cdc42Hs and bradykinin promote formation of peripheral actin microspikes and filopodia in Swiss 3T3 fibroblasts. *Mol Cell Biol* **15**, 1942-52.
**Kragtorp, K. A. and Miller, J. R.** (2006). Regulation of somitogenesis by Ena/VASP proteins and FAK during Xenopus development. *Development* **133**, 685-695.
**Kraynov, V. S., Chamberlain, C., Bokoch, G. M., Schwartz, M. A., Slabaugh, S. and Hahn, K. M.** (2000). Localized Rac activation dynamics visualized in living cells. *Science* **290**, 333-7.
**Krotoski, D. M., Fraser, S. E. and Bronner-Fraser, M.** (1988). Mapping of neural crest pathways in Xenopus laevis using inter- and intra-specific cell markers. *Dev Biol* **127**, 119-32.
**Krull, C. E., Lansford, R., Gale, N. W., Collazo, A., Marcelle, C., Yancopoulos, G. D., Fraser, S. E. and Bronner-Fraser, M.** (1997). Interactions of Eph-related receptors and ligands confer rostrocaudal pattern to trunk neural crest migration. *Current Biology* **7**, 571.
**Ku, M. and Melton, D. A.** (1993). Xwnt-11: a maternally expressed Xenopus wnt gene. *Development* **119**, 1161-73.
**Kuhl, M., Sheldahl, L. C., Malbon, C. C. and Moon, R. T.** (2000). Ca(2+)/calmodulin-dependent protein kinase II is stimulated by Wnt and Frizzled homologs and promotes ventral cell fates in Xenopus. *J Biol Chem* **275**, 12701-11.
**Kuriyama, S. and Mayor, R.** (2008). Molecular analysis of neural crest migration. *Philos Trans R Soc Lond B Biol Sci* **363**, 1349-62.
**Kurokawa, K., Nakamura, T., Aoki, K. and Matsuda, M.** (2005). Mechanism and role of localized activation of Rho-family GTPases in growth factor-stimulated fibroblasts and neuronal cells. *Biochem Soc Trans* **33**, 631-4.
**Kwong, L., Wozniak, M. A., Collins, A. S., Wilson, S. D. and Keely, P. J.** (2003). R-Ras promotes focal adhesion formation through focal adhesion kinase and p130(Cas) by a novel mechanism that differs from integrins. *Mol Cell Biol* **23**, 933-49.
**LaBonne, C. and Bronner-Fraser, M.** (1998). Neural crest induction in Xenopus: evidence for a two-signal model. *Development* **125**, 2403-14.
**Lauffenburger, D. A. and Horwitz, A. F.** (1996). Cell migration: a physically integrated molecular process. *Cell* **84**, 359-69.
**Laukaitis, C. M., Webb, D. J., Donais, K. and Horwitz, A. F.** (2001). Differential dynamics of alpha 5 integrin, paxillin, and alpha-actinin during formation and disassembly of adhesions in migrating cells. *J Cell Biol* **153**, 1427-40.
**Le Douarin, N. M. and Teillet, M. A.** (1974). Experimental analysis of the migration and differentiation of neuroblasts of the autonomic nervous system and of neurectodermal mesenchymal derivatives, using a biological cell marking technique. *Dev Biol* **41**, 162-84.
**LeDouarin, N. M. and Kalcheim, C.** (1999). The Neural Crest: Cambridge University Press.
**Li, L., Yuan, H., Xie, W., Mao, J., Caruso, A. M., McMahon, A., Sussman, D. J. and Wu, D.** (1999). Dishevelled proteins lead to two signaling pathways. Regulation of LEF-1 and c-Jun N-terminal kinase in mammalian cells. *J Biol Chem* **274**, 129-34.
**Lim, S. T., Longley, R. L., Couchman, J. R. and Woods, A.** (2003). Direct binding of syndecan-4 cytoplasmic domain to the catalytic domain of protein kinase C alpha (PKC alpha) increases focal adhesion localization of PKC alpha. *J Biol Chem* **278**, 13795-802.
**Lin, X. and Perrimon, N.** (1999). Dally cooperates with Drosophila Frizzled 2 to transduce Wingless signalling. *Nature* **400**, 281-4.
**Lin, X., Wei, G., Shi, Z., Dryer, L., Esko, J. D., Wells, D. E. and Matzuk, M. M.** (2000). Disruption of gastrulation and heparan sulfate biosynthesis in EXT1-deficient mice. *Dev Biol* **224**, 299-311.
**Liu, S., Liu, F., Schneider, A. E., St Amand, T., Epstein, J. A. and Gutstein, D. E.** (2006). Distinct cardiac malformations caused by absence of connexin 43 in the neural crest and in the non-crest neural tube. *Development* **133**, 2063-73.
**Lo, C. W., Cohen, M. F., Huang, G. Y., Lazatin, B. O., Patel, N., Sullivan, R., Pauken, C. and Park, S. M.** (1997). Cx43 gap junction gene expression and gap junctional communication in mouse neural crest cells. *Dev Genet* **20**, 119-32.
**Locascio, A. and Nieto, M. A.** (2001). Cell movements during vertebrate development: integrated tissue behaviour versus individual cell migration. *Curr Opin Genet Dev* **11**, 464-9.
**Longley, R. L., Woods, A., Fleetwood, A., Cowling, G. J., Gallagher, J. T. and Couchman, J. R.** (1999). Control of morphology, cytoskeleton and migration by syndecan-4. *J Cell Sci* **112 (Pt 20)**, 3421-31.
**Lucas, J. M., Nikolic, I. and Hens, M. D.** (2002). cDNA cloning, sequence comparison, and developmental expression of Xenopus rac1. *Mech Dev* **115**, 113-6.

**Luster, A. D., Alon, R. and von Andrian, U. H.** (2005). Immune cell migration in inflammation: present and future therapeutic targets. *Nat Immunol* **6**, 1182-90.
**Luyten, A., Mortier, E., Campenhout, C. V., Taelman, V., Degeest, G., Wuytens, G., Lambaerts, K., David, G., Bellefroid, E. J. and Zimmermann, P.** (2008). The PDZ Protein Syntenin Directly Interacts with Frizzled 7 and Supports Non-canonical Wnt Signaling. *Mol Biol Cell* **19**, 1594-604.
**Makita, R., Mizuno, T., Koshida, S., Kuroiwa, A. and Takeda, H.** (1998). Zebrafish wnt11: pattern and regulation of the expression by the yolk cell and No tail activity. *Mech Dev* **71**, 165-76.
**Marchant, L., Linker, C., Ruiz, P., Guerrero, N. and Mayor, R.** (1998). The inductive properties of mesoderm suggest that the neural crest cells are specified by a BMP gradient. *Dev Biol* **198**, 319-29.
**Marlow, F., Topczewski, J., Sepich, D. and Solnica-Krezel, L.** (2002). Zebrafish Rho kinase 2 acts downstream of Wnt11 to mediate cell polarity and effective convergence and extension movements. *Curr Biol* **12**, 876-84.
**Marsden, M. and DeSimone, D. W.** (2001). Regulation of cell polarity, radial intercalation and epiboly in Xenopus: novel roles for integrin and fibronectin. *Development* **128**, 3635-47.
**Marsden, M. and DeSimone, D. W.** (2003). Integrin-ECM interactions regulate cadherin-dependent cell adhesion and are required for convergent extension in Xenopus. *Curr Biol* **13**, 1182-91.
**Matthews, H. K., Marchant, L., Carmona-Fontaine, C., Kuriyama, S., Larrain, J., Holt, M. R., Parsons, M. and Mayor, R.** (2008). Directional migration of neural crest cells in vivo is regulated by Syndecan-4/Rac1 and non-canonical Wnt signaling/RhoA. *Development* **135**, 1771-80.
**Mayor, R., Morgan, R. and Sargent, M. G.** (1995). Induction of the prospective neural crest of Xenopus. *Development* **121**, 767-77.
**McLarren, K. W., Litsiou, A. and Streit, A.** (2003). DLX5 positions the neural crest and preplacode region at the border of the neural plate. *Dev Biol* **259**, 34-47.
**McLean, G. W., Carragher, N. O., Avizienyte, E., Evans, J., Brunton, V. G. and Frame, M. C.** (2005). The role of focal-adhesion kinase in cancer - a new therapeutic opportunity. *Nat Rev Cancer* **5**, 505-15.
**Medina, A., Reintsch, W. and Steinbeisser, H.** (2000). Xenopus frizzled 7 can act in canonical and non-canonical Wnt signaling pathways: implications on early patterning and morphogenesis. *Mech Dev* **92**, 227-37.
**Meyer, D., Stiegler, P., Hindelang, C., Mager, A. M. and Remy, P.** (1995). Whole-mount in situ hybridization reveals the expression of the Xl-Fli gene in several lineages of migrating cells in Xenopus embryos. *Int J Dev Biol* **39**, 909-19.
**Miller, J. R., Hocking, A. M., Brown, J. D. and Moon, R. T.** (1999). Mechanism and function of signal transduction by the Wnt/beta-catenin and Wnt/Ca2+ pathways. *Oncogene* **18**, 7860-72.
**Mlodzik, M.** (2002). Planar cell polarization: do the same mechanisms regulate Drosophila tissue polarity and vertebrate gastrulation? *Trends Genet* **18**, 564-71.
**Moissoglu, K. and Schwartz, M. A.** (2006). Integrin signalling in directed cell migration. *Biol Cell* **98**, 547-55.
**Monsoro-Burq, A. H., Wang, E. and Harland, R.** (2005). Msx1 and Pax3 cooperate to mediate FGF8 and WNT signals during Xenopus neural crest induction. *Dev Cell* **8**, 167-78.
**Montell, D. J.** (2003). Border-cell migration: the race is on. *Nat Rev Mol Cell Biol* **4**, 13-24.
**Moody, S. A.** (1987). Fates of the blastomeres of the 16-cell stage Xenopus embryo. *Dev Biol* **119**, 560-78.
**Moolenaar, W. H., van Meeteren, L. A. and Giepmans, B. N.** (2004). The ins and outs of lysophosphatidic acid signaling. *Bioessays* **26**, 870-81.
**Moon, R. T., Campbell, R. M., Christian, J. L., McGrew, L. L., Shih, J. and Fraser, S.** (1993). Xwnt-5A: a maternal Wnt that affects morphogenetic movements after overexpression in embryos of Xenopus laevis. *Development* **119**, 97-111.
**Morgan, M. R., Humphries, M. J. and Bass, M. D.** (2007). Synergistic control of cell adhesion by integrins and syndecans. *Nat Rev Mol Cell Biol* **8**, 957-69.
**Moriguchi, T., Kawachi, K., Kamakura, S., Masuyama, N., Yamanaka, H., Matsumoto, K., Kikuchi, A. and Nishida, E.** (1999). Distinct domains of mouse dishevelled are responsible for the c-Jun N-terminal kinase/stress-activated protein kinase activation and the axis formation in vertebrates. *J Biol Chem* **274**, 30957-62.
**Mostafavi-Pour, Z., Askari, J. A., Parkinson, S. J., Parker, P. J., Ng, T. T. and Humphries, M. J.** (2003). Integrin-specific signaling pathways controlling focal adhesion formation and cell migration. *J Cell Biol* **161**, 155-67.
**Munoz, R. and Larrain, J.** (2006). xSyndecan-4 regulates gastrulation and neural tube closure in Xenopus embryos. *ScientificWorldJournal* **6**, 1298-301.

**Munoz, R., Moreno, M., Oliva, C., Orbenes, C. and Larrain, J.** (2006). Syndecan-4 regulates non-canonical Wnt signalling and is essential for convergent and extension movements in Xenopus embryos. *Nat Cell Biol* **8**, 492-500.
**Murakami, M., Horowitz, A., Tang, S., Ware, J. A. and Simons, M.** (2002). Protein kinase C (PKC) delta regulates PKCalpha activity in a Syndecan-4-dependent manner. *J Biol Chem* **277**, 20367-71.
**Nakagawa, S. and Takeichi, M.** (1995). Neural crest cell-cell adhesion controlled by sequential and subpopulation-specific expression of novel cadherins. *Development* **121**, 1321-32.
**Nakagawa, S. and Takeichi, M.** (1998). Neural crest emigration from the neural tube depends on regulated cadherin expression. *Development* **125**, 2963-71.
**Nakaya, M. A., Habas, R., Biris, K., Dunty, W. C., Jr., Kato, Y., He, X. and Yamaguchi, T. P.** (2004). Identification and comparative expression analyses of Daam genes in mouse and Xenopus. *Gene Expr Patterns* **5**, 97-105.
**Natarajan, D., Marcos-Gutierrez, C., Pachnis, V. and de Graaff, E.** (2002). Requirement of signalling by receptor tyrosine kinase RET for the directed migration of enteric nervous system progenitor cells during mammalian embryogenesis. *Development* **129**, 5151-60.
**Newgreen, D. and Thiery, J. P.** (1980). Fibronectin in early avian embryos: synthesis and distribution along the migration pathways of neural crest cells. *Cell Tissue Res* **211**, 269-91.
**Newgreen, D. F.** (1989). Physical influences on neural crest cell migration in avian embryos: contact guidance and spatial restriction. *Dev Biol* **131**, 136-48.
**Nieuwkoop, P. D. and Faber, J.** (1967). Normal Table of *Xenopus laevis* (Doudin). Amsterdam: Elsevier-North Holland Publishing.
**Nimnual, A. S., Taylor, L. J. and Bar-Sagi, D.** (2003). Redox-dependent downregulation of Rho by Rac. *Nat Cell Biol* **5**, 236-41.
**Nobes, C. D. and Hall, A.** (1995a). Rho, rac and cdc42 GTPases: regulators of actin structures, cell adhesion and motility. *Biochem Soc Trans* **23**, 456-9.
**Nobes, C. D. and Hall, A.** (1995b). Rho, rac, and cdc42 GTPases regulate the assembly of multimolecular focal complexes associated with actin stress fibers, lamellipodia, and filopodia. *Cell* **81**, 53-62.
**Nobes, C. D. and Hall, A.** (1999). Rho GTPases control polarity, protrusion, and adhesion during cell movement. *J Cell Biol* **144**, 1235-44.
**Oakley, R. A., Lasky, C. J., Erickson, C. A. and Tosney, K. W.** (1994). Glycoconjugates mark a transient barrier to neural crest migration in the chicken embryo. *Development* **120**, 103-14.
**Oh, E. S., Woods, A. and Couchman, J. R.** (1997a). Multimerization of the cytoplasmic domain of syndecan-4 is required for its ability to activate protein kinase C. *J Biol Chem* **272**, 11805-11.
**Oh, E. S., Woods, A. and Couchman, J. R.** (1997b). Syndecan-4 proteoglycan regulates the distribution and activity of protein kinase C. *J Biol Chem* **272**, 8133-6.
**Oh, E. S., Woods, A., Lim, S. T., Theibert, A. W. and Couchman, J. R.** (1998). Syndecan-4 proteoglycan cytoplasmic domain and phosphatidylinositol 4,5-bisphosphate coordinately regulate protein kinase C activity. *J Biol Chem* **273**, 10624-9.
**Ohkawara, B., Yamamoto, T. S., Tada, M. and Ueno, N.** (2003). Role of glypican 4 in the regulation of convergent extension movements during gastrulation in Xenopus laevis. *Development* **130**, 2129-38.
**Ohta, Y., Hartwig, J. H. and Stossel, T. P.** (2006). FilGAP, a Rho- and ROCK-regulated GAP for Rac binds filamin A to control actin remodelling. *Nat Cell Biol* **8**, 803-14.
**Olsson, L., Svensson, K. and Perris, R.** (1996). Effects of extracellular matrix molecules on subepidermal neural crest cell migration in wild type and white mutant (dd) axolotl embryos. *Pigment Cell Res* **9**, 18-27.
**Paddock, S. W. and Dunn, G. A.** (1986). Analysing collisions between fibroblasts and fibrosarcoma cells: fibrosarcoma cells show an active invasionary response. *J Cell Sci* **81**, 163-87.
**Palazzo, A. F., Joseph, H. L., Chen, Y. J., Dujardin, D. L., Alberts, A. S., Pfister, K. K., Vallee, R. B. and Gundersen, G. G.** (2001). Cdc42, dynein, and dynactin regulate MTOC reorientation independent of Rho-regulated microtubule stabilization. *Curr Biol* **11**, 1536-41.
**Palecek, S. P., Loftus, J. C., Ginsberg, M. H., Lauffenburger, D. A. and Horwitz, A. F.** (1997). Integrin-ligand binding properties govern cell migration speed through cell-substratum adhesiveness. *Nature* **385**, 537-40.
**Pankov, R., Cukierman, E., Katz, B. Z., Matsumoto, K., Lin, D. C., Lin, S., Hahn, C. and Yamada, K. M.** (2000). Integrin dynamics and matrix assembly: tensin-dependent translocation of alpha(5)beta(1) integrins promotes early fibronectin fibrillogenesis. *J Cell Biol* **148**, 1075-90.

**Pankov, R., Endo, Y., Even-Ram, S., Araki, M., Clark, K., Cukierman, E., Matsumoto, K. and Yamada, K. M.** (2005). A Rac switch regulates random versus directionally persistent cell migration. *J Cell Biol* **170**, 793-802.
**Penzo-Mendez, A., Umbhauer, M., Djiane, A., Boucaut, J. C. and Riou, J. F.** (2003). Activation of Gbetagamma signaling downstream of Wnt-11/Xfz7 regulates Cdc42 activity during Xenopus gastrulation. *Dev Biol* **257**, 302-14.
**Perissinotto, D., Iacopetti, P., Bellina, I., Doliana, R., Colombatti, A., Pettway, Z., Bronner-Fraser, M., Shinomura, T., Kimata, K., Morgelin, M. et al.** (2000). Avian neural crest cell migration is diversely regulated by the two major hyaluronan-binding proteoglycans PG-M/versican and aggrecan. *Development* **127**, 2823-42.
**Perris, R. and Perissinotto, D.** (2000). Role of the extracellular matrix during neural crest cell migration. *Mech Dev* **95**, 3-21.
**Pertz, O. and Hahn, K. M.** (2004). Designing biosensors for Rho family proteins--deciphering the dynamics of Rho family GTPase activation in living cells. *J Cell Sci* **117**, 1313-8.
**Pertz, O., Hodgson, L., Klemke, R. L. and Hahn, K. M.** (2006). Spatiotemporal dynamics of RhoA activity in migrating cells. *Nature* **440**, 1069-72.
**Pollard, T. D. and Borisy, G. G.** (2003). Cellular motility driven by assembly and disassembly of actin filaments. *Cell* **112**, 453-65.
**Pukrop, T. and Binder, C.** (2008). The complex pathways of Wnt 5a in cancer progression. *J Mol Med* **86**, 259-66.
**Puschel, A. W.** (2007). GTPases in semaphorin signaling. *Adv Exp Med Biol* **600**, 12-23.
**Raible, D. W., Wood, A., Hodsdon, W., Henion, P. D., Weston, J. A. and Eisen, J. S.** (1992). Segregation and early dispersal of neural crest cells in the embryonic zebrafish. *Dev Dyn* **195**, 29-42.
**Rauch, G. J., Hammerschmidt, M., Blader, P., Schauerte, H. E., Strahle, U., Ingham, P. W., McMahon, A. P. and Haffter, P.** (1997). Wnt5 is required for tail formation in the zebrafish embryo. *Cold Spring Harb Symp Quant Biol* **62**, 227-34.
**Reizes, O., Lincecum, J., Wang, Z., Goldberger, O., Huang, L., Kaksonen, M., Ahima, R., Hinkes, M. T., Barsh, G. S., Rauvala, H. et al.** (2001). Transgenic expression of syndecan-1 uncovers a physiological control of feeding behavior by syndecan-3. *Cell* **106**, 105-16.
**Ren, X. D., Kiosses, W. B., Sieg, D. J., Otey, C. A., Schlaepfer, D. D. and Schwartz, M. A.** (2000). Focal adhesion kinase suppresses Rho activity to promote focal adhesion turnover. *J Cell Sci* **113 (Pt 20)**, 3673-8.
**Richardson, A. and Parsons, T.** (1996). A mechanism for regulation of the adhesion-associated proteintyrosine kinase pp125FAK. *Nature* **380**, 538-40.
**Rickmann, M., Fawcett, J. W. and Keynes, R. J.** (1985). The migration of neural crest cells and the growth of motor axons through the rostral half of the chick somite. *J Embryol Exp Morphol* **90**, 437-55.
**Ridley, A. J.** (2004). Rho proteins and cancer. *Breast Cancer Res Treat* **84**, 13-9.
**Ridley, A. J. and Hall, A.** (1992). The small GTP-binding protein rho regulates the assembly of focal adhesions and actin stress fibers in response to growth factors. *Cell* **70**, 389-99.
**Ridley, A. J., Paterson, H. F., Johnston, C. L., Diekmann, D. and Hall, A.** (1992). The small GTP-binding protein rac regulates growth factor-induced membrane ruffling. *Cell* **70**, 401-10.
**Ridley, A. J., Schwartz, M. A., Burridge, K., Firtel, R. A., Ginsberg, M. H., Borisy, G., Parsons, J. T. and Horwitz, A. R.** (2003). Cell migration: integrating signals from front to back. *Science* **302**, 1704-9.
**Riento, K. and Ridley, A. J.** (2003). Rocks: multifunctional kinases in cell behaviour. *Nat Rev Mol Cell Biol* **4**, 446-56.
**Rohatgi, R., Ho, H. Y. and Kirschner, M. W.** (2000). Mechanism of N-WASP activation by CDC42 and phosphatidylinositol 4, 5-bisphosphate. *J Cell Biol* **150**, 1299-310.
**Rohatgi, R., Ma, L., Miki, H., Lopez, M., Kirchhausen, T., Takenawa, T. and Kirschner, M. W.** (1999). The interaction between N-WASP and the Arp2/3 complex links Cdc42-dependent signals to actin assembly. *Cell* **97**, 221-31.
**Rorth, P.** (2007). Collective guidance of collective cell migration. *Trends Cell Biol* **17**, 575-9.
**Rothbacher, U., Laurent, M. N., Deardorff, M. A., Klein, P. S., Cho, K. W. and Fraser, S. E.** (2000). Dishevelled phosphorylation, subcellular localization and multimerization regulate its role in early embryogenesis. *Embo J* **19**, 1010-22.
**Rothhut, B., Ghoneim, C., Antonicelli, F. and Soula-Rothhut, M.** (2007). Epidermal growth factor stimulates matrix metalloproteinase-9 expression and invasion in human follicular thyroid carcinoma cells through Focal adhesion kinase. *Biochimie* **89**, 613-24.

**Sadaghiani, B. and Thiebaud, C. H.** (1987). Neural crest development in the Xenopus laevis embryo, studied by interspecific transplantation and scanning electron microscopy. *Dev Biol* **124**, 91-110.
**Sander, E. E., ten Klooster, J. P., van Delft, S., van der Kammen, R. A. and Collard, J. G.** (1999). Rac downregulates Rho activity: reciprocal balance between both GTPases determines cellular morphology and migratory behavior. *J Cell Biol* **147**, 1009-22.
**Saoncella, S., Calautti, E., Neveu, W. and Goetinck, P. F.** (2004). Syndecan-4 regulates ATF-2 transcriptional activity in a Rac1-dependent manner. *J Biol Chem* **279**, 47172-6.
**Saoncella, S., Echtermeyer, F., Denhez, F., Nowlen, J. K., Mosher, D. F., Robinson, S. D., Hynes, R. O. and Goetinck, P. F.** (1999). Syndecan-4 signals cooperatively with integrins in a Rho-dependent manner in the assembly of focal adhesions and actin stress fibers. *Proc Natl Acad Sci U S A* **96**, 2805-10.
**Sasai, N., Mizuseki, K. and Sasai, Y.** (2001). Requirement of FoxD3-class signaling for neural crest determination in Xenopus. *Development* **128**, 2525-36.
**Sastry, S. K. and Burridge, K.** (2000). Focal adhesions: a nexus for intracellular signaling and cytoskeletal dynamics. *Exp Cell Res* **261**, 25-36.
**Sato, A., Khadka, D. K., Liu, W., Bharti, R., Runnels, L. W., Dawid, I. B. and Habas, R.** (2006). Profilin is an effector for Daam1 in non-canonical Wnt signaling and is required for vertebrate gastrulation. *Development* **133**, 4219-31.
**Schaller, M. D., Borgman, C. A., Cobb, B. S., Vines, R. R., Reynolds, A. B. and Parsons, J. T.** (1992). pp125FAK a structurally distinctive protein-tyrosine kinase associated with focal adhesions. *Proc Natl Acad Sci U S A* **89**, 5192-6.
**Schaller, M. D., Borgman, C. A. and Parsons, J. T.** (1993). Autonomous expression of a noncatalytic domain of the focal adhesion-associated protein tyrosine kinase pp125FAK. *Mol Cell Biol* **13**, 785-91.
**Schaller, M. D., Hildebrand, J. D. and Parsons, J. T.** (1999). Complex formation with focal adhesion kinase: A mechanism to regulate activity and subcellular localization of Src kinases. *Mol Biol Cell* **10**, 3489-505.
**Schaller, M. D., Hildebrand, J. D., Shannon, J. D., Fox, J. W., Vines, R. R. and Parsons, J. T.** (1994). Autophosphorylation of the focal adhesion kinase, pp125FAK, directs SH2-dependent binding of pp60src. *Mol Cell Biol* **14**, 1680-8.
**Schlaepfer, D. D., Mitra, S. K. and Ilic, D.** (2004). Control of motile and invasive cell phenotypes by focal adhesion kinase. *Biochim Biophys Acta* **1692**, 77-102.
**Sheldahl, L. C., Slusarski, D. C., Pandur, P., Miller, J. R., Kuhl, M. and Moon, R. T.** (2003). Dishevelled activates Ca2+ flux, PKC, and CamKII in vertebrate embryos. *J Cell Biol* **161**, 769-77.
**Shibata, K., Kikkawa, F., Nawa, A., Thant, A. A., Naruse, K., Mizutani, S. and Hamaguchi, M.** (1998). Both focal adhesion kinase and c-Ras are required for the enhanced matrix metalloproteinase 9 secretion by fibronectin in ovarian cancer cells. *Cancer Res* **58**, 900-3.
**Shih, J. and Keller, R.** (1992). Cell motility driving mediolateral intercalation in explants of Xenopus laevis. *Development* **116**, 901-14.
**Sieg, D. J., Hauck, C. R. and Schlaepfer, D. D.** (1999). Required role of focal adhesion kinase (FAK) for integrin-stimulated cell migration. *J Cell Sci* **112 (Pt 16)**, 2677-91.
**Slusarski, D. C., Corces, V. G. and Moon, R. T.** (1997a). Interaction of Wnt and a Frizzled homologue triggers G-protein-linked phosphatidylinositol signalling. *Nature* **390**, 410-3.
**Slusarski, D. C., Yang-Snyder, J., Busa, W. B. and Moon, R. T.** (1997b). Modulation of embryonic intracellular Ca2+ signaling by Wnt-5A. *Dev Biol* **182**, 114-20.
**Smith, A., Robinson, V., Patel, K. and Wilkinson, D. G.** (1997). The EphA4 and EphB1 receptor tyrosine kinases and ephrin-B2 ligand regulate targeted migration of branchial neural crest cells. *Current Biology* **7**, 561.
**Soderling, S. H. and Scott, J. D.** (2006). WAVE signalling: from biochemistry to biology. *Biochem Soc Trans* **34**, 73-6.
**Sokol, S. Y., Klingensmith, J., Perrimon, N. and Itoh, K.** (1995). Dorsalizing and neuralizing properties of Xdsh, a maternally expressed Xenopus homolog of dishevelled. *Development* **121**, 3487.
**Solnica-Krezel, L., Stemple, D. L., Mountcastle-Shah, E., Rangini, Z., Neuhauss, S. C., Malicki, J., Schier, A. F., Stainier, D. Y., Zwartkruis, F., Abdelilah, S. et al.** (1996). Mutations affecting cell fates and cellular rearrangements during gastrulation in zebrafish. *Development* **123**, 67-80.
**Songyang, Z., Fanning, A. S., Fu, C., Xu, J., Marfatia, S. M., Chishti, A. H., Crompton, A., Chan, A. C., Anderson, J. M. and Cantley, L. C.** (1997). Recognition of unique carboxyl-terminal motifs by distinct PDZ domains. *Science* **275**, 73-7.
**Spring, J., Paine-Saunders, S. E., Hynes, R. O. and Bernfield, M.** (1994). Drosophila syndecan: conservation of a cell-surface heparan sulfate proteoglycan. *Proc Natl Acad Sci U S A* **91**, 3334-8.

**Steffen, A., Rottner, K., Ehinger, J., Innocenti, M., Scita, G., Wehland, J. and Stradal, T. E.** (2004). Sra-1 and Nap1 link Rac to actin assembly driving lamellipodia formation. *Embo J* **23**, 749-59.
**Steventon, B., Carmona-Fontaine, C. and Mayor, R.** (2005). Genetic network during neural crest induction: From cell specification to cell survival. *Semin Cell Dev Biol* **16**, 647-54.
**Strachan, L. R. and Condic, M. L.** (2008). Neural crest motility on fibronectin is regulated by integrin activation. *Exp Cell Res* **314**, 441-52.
**Strigini, M. and Cohen, S. M.** (2000). Wingless gradient formation in the Drosophila wing. *Curr Biol* **10**, 293-300.
**Strutt, D. I.** (2001). Asymmetric localization of frizzled and the establishment of cell polarity in the Drosophila wing. *Mol Cell* **7**, 367-75.
**Strutt, D. I., Weber, U. and Mlodzik, M.** (1997). The role of RhoA in tissue polarity and Frizzled signalling. *Nature* **387**, 292-5.
**Subramanian, S. V., Fitzgerald, M. L. and Bernfield, M.** (1997). Regulated shedding of syndecan-1 and -4 ectodomains by thrombin and growth factor receptor activation. *J Biol Chem* **272**, 14713-20.
**Sumanas, S., Strege, P., Heasman, J. and Ekker, S. C.** (2000). The putative wnt receptor Xenopus frizzled-7 functions upstream of beta-catenin in vertebrate dorsoventral mesoderm patterning. *Development* **127**, 1981-90.
**Tachibana, K., Urano, T., Fujita, H., Ohashi, Y., Kamiguchi, K., Iwata, S., Hirai, H. and Morimoto, C.** (1997). Tyrosine phosphorylation of Crk-associated substrates by focal adhesion kinase. A putative mechanism for the integrin-mediated tyrosine phosphorylation of Crk-associated substrates. *J Biol Chem* **272**, 29083-90.
**Tada, M. and Smith, J. C.** (2000). Xwnt11 is a target of Xenopus Brachyury: regulation of gastrulation movements via Dishevelled, but not through the canonical Wnt pathway. *Development* **127**, 2227-38.
**Tahinci, E. and Symes, K.** (2003). Distinct functions of Rho and Rac are required for convergent extension during Xenopus gastrulation. *Dev Biol* **259**, 318-35.
**Takenawa, T. and Suetsugu, S.** (2007). The WASP-WAVE protein network: connecting the membrane to the cytoskeleton. *Nat Rev Mol Cell Biol* **8**, 37-48.
**Tan, S. S., Crossin, K. L., Hoffman, S. and Edelman, G. M.** (1987). Asymmetric expression in somites of cytotactin and its proteoglycan ligand is correlated with neural crest cell distribution. *Proc Natl Acad Sci U S A* **84**, 7977-81.
**Taneyhill, L. A., Coles, E. G. and Bronner-Fraser, M.** (2007). Snail2 directly represses cadherin6B during epithelial-to-mesenchymal transitions of the neural crest. *Development* **134**, 1481-90.
**Teddy, J. M. and Kulesa, P. M.** (2004). In vivo evidence for short- and long-range cell communication in cranial neural crest cells. *Development* **131**, 6141-51.
**Teel, A. L. and Yost, H. J.** (1996). Embryonic expression patterns of Xenopus syndecans. *Mech Dev* **59**, 115-27.
**Teillet, M. A., Kalcheim, C. and Le Douarin, N. M.** (1987). Formation of the dorsal root ganglia in the avian embryo: segmental origin and migratory behavior of neural crest progenitor cells. *Dev Biol* **120**, 329-47.
**Testaz, S. and Duband, J. L.** (2001). Central role of the alpha4beta1 integrin in the coordination of avian truncal neural crest cell adhesion, migration, and survival. *Dev Dyn* **222**, 127-40.
**Theisen, H., Purcell, J., Bennett, M., Kansagara, D., Syed, A. and Marsh, J. L.** (1994). dishevelled is required during wingless signaling to establish both cell polarity and cell identity. *Development* **120**, 347-60.
**Thiery, J. P., Duband, J. L. and Delouvee, A.** (1982). Pathways and mechanisms of avian trunk neural crest cell migration and localization. *Dev Biol* **93**, 324-43.
**Tkachenko, E., Elfenbein, A., Tirziu, D. and Simons, M.** (2006). Syndecan-4 clustering induces cell migration in a PDZ-dependent manner. *Circ Res* **98**, 1398-404.
**Tkachenko, E., Lutgens, E., Stan, R. V. and Simons, M.** (2004). Fibroblast growth factor 2 endocytosis in endothelial cells proceed via syndecan-4-dependent activation of Rac1 and a Cdc42-dependent macropinocytic pathway. *J Cell Sci* **117**, 3189-99.
**Tkachenko, E. and Simons, M.** (2002). Clustering induces redistribution of syndecan-4 core protein into raft membrane domains. *J Biol Chem* **277**, 19946-51.
**Topczewski, J., Sepich, D. S., Myers, D. C., Walker, C., Amores, A., Lele, Z., Hammerschmidt, M., Postlethwait, J. and Solnica-Krezel, L.** (2001). The zebrafish glypican knypek controls cell polarity during gastrulation movements of convergent extension. *Dev Cell* **1**, 251-64.
**Tree, D. R., Shulman, J. M., Rousset, R., Scott, M. P., Gubb, D. and Axelrod, J. D.** (2002). Prickle mediates feedback amplification to generate asymmetric planar cell polarity signaling. *Cell* **109**, 371-81.

**Tsuji, T., Ishizaki, T., Okamoto, M., Higashida, C., Kimura, K., Furuyashiki, T., Arakawa, Y., Birge, R. B., Nakamoto, T., Hirai, H. et al.** (2002). ROCK and mDia1 antagonize in Rho-dependent Rac activation in Swiss 3T3 fibroblasts. *J Cell Biol* **157**, 819-30.
**Uehata, M., Ishizaki, T., Satoh, H., Ono, T., Kawahara, T., Morishita, T., Tamakawa, H., Yamagami, K., Inui, J., Maekawa, M. et al.** (1997). Calcium sensitization of smooth muscle mediated by a Rho-associated protein kinase in hypertension. *Nature* **389**, 990-4.
**Ulrich, F., Krieg, M., Schotz, E. M., Link, V., Castanon, I., Schnabel, V., Taubenberger, A., Mueller, D., Puech, P. H. and Heisenberg, C. P.** (2005). Wnt11 functions in gastrulation by controlling cell cohesion through Rab5c and E-cadherin. *Dev Cell* **9**, 555-64.
**Usui, T., Shima, Y., Shimada, Y., Hirano, S., Burgess, R. W., Schwarz, T. L., Takeichi, M. and Uemura, T.** (1999). Flamingo, a seven-pass transmembrane cadherin, regulates planar cell polarity under the control of Frizzled. *Cell* **98**, 585-95.
**Valentin, G., Haas, P. and Gilmour, D.** (2007). The chemokine SDF1a coordinates tissue migration through the spatially restricted activation of Cxcr7 and Cxcr4b. *Curr Biol* **17**, 1026-31.
**Vallin, J., Girault, J. M., Thiery, J. P. and Broders, F.** (1998). Xenopus cadherin-11 is expressed in different populations of migrating neural crest cells. *Mech Dev* **75**, 171-4.
**Van Haastert, P. J. and Devreotes, P. N.** (2004). Chemotaxis: signalling the way forward. *Nat Rev Mol Cell Biol* **5**, 626-34.
**Veeman, M. T., Axelrod, J. D. and Moon, R. T.** (2003). A second canon. Functions and mechanisms of beta-catenin-independent Wnt signaling. *Dev Cell* **5**, 367-77.
**Vega, S., Morales, A. V., Ocana, O. H., Valdes, F., Fabregat, I. and Nieto, M. A.** (2004). Snail blocks the cell cycle and confers resistance to cell death. *Genes Dev* **18**, 1131-43.
**Vicente-Manzanares, M., Webb, D. J. and Horwitz, A. R.** (2005). Cell migration at a glance. *J Cell Sci* **118**, 4917-9.
**Villanueva, S., Glavic, A., Ruiz, P. and Mayor, R.** (2002). Posteriorization by FGF, Wnt, and retinoic acid is required for neural crest induction. *Dev Biol* **241**, 289-301.
**Vinson, C. R. and Adler, P. N.** (1987). Directional non-cell autonomy and the transmission of polarity information by the frizzled gene of Drosophila. *Nature* **329**, 549-51.
**Wallingford, J. B., Fraser, S. E. and Harland, R. M.** (2002). Convergent extension: the molecular control of polarized cell movement during embryonic development. *Dev Cell* **2**, 695-706.
**Wallingford, J. B. and Habas, R.** (2005). The developmental biology of Dishevelled: an enigmatic protein governing cell fate and cell polarity. *Development* **132**, 4421-36.
**Wallingford, J. B., Rowning, B. A., Vogeli, K. M., Rothbacher, U., Fraser, S. E. and Harland, R. M.** (2000). Dishevelled controls cell polarity during Xenopus gastrulation. *Nature* **405**, 81-5.
**Wallingford, J. B., Vogeli, K. M. and Harland, R. M.** (2001). Regulation of convergent extension in Xenopus by Wnt5a and Frizzled-8 is independent of the canonical Wnt pathway. *Int J Dev Biol* **45**, 225-7.
**Wang, Y., Macke, J. P., Abella, B. S., Andreasson, K., Worley, P., Gilbert, D. J., Copeland, N. G., Jenkins, N. A. and Nathans, J.** (1996). A large family of putative transmembrane receptors homologous to the product of the Drosophila tissue polarity gene frizzled. *J Biol Chem* **271**, 4468-76.
**Wang, Y. and Nathans, J.** (2007). Tissue/planar cell polarity in vertebrates: new insights and new questions. *Development* **134**, 647-58.
**Watanabe, N., Kato, T., Fujita, A., Ishizaki, T. and Narumiya, S.** (1999). Cooperation between mDia1 and ROCK in Rho-induced actin reorganization. *Nat Cell Biol* **1**, 136-43.
**Webb, D. J., Donais, K., Whitmore, L. A., Thomas, S. M., Turner, C. E., Parsons, J. T. and Horwitz, A. F.** (2004). FAK-Src signalling through paxillin, ERK and MLCK regulates adhesion disassembly. *Nat Cell Biol* **6**, 154-61.
**Webb, D. J., Parsons, J. T. and Horwitz, A. F.** (2002). Adhesion assembly, disassembly and turnover in migrating cells -- over and over and over again. *Nat Cell Biol* **4**, E97-100.
**Welch, H. C., Coadwell, W. J., Stephens, L. R. and Hawkins, P. T.** (2003). Phosphoinositide 3-kinase-dependent activation of Rac. *FEBS Lett* **546**, 93-7.
**Welch, M. D. and Mullins, R. D.** (2002). Cellular control of actin nucleation. *Annu Rev Cell Dev Biol* **18**, 247-88.
**Wells, C. M. and Ridley, A. J.** (2005). Analysis of cell migration using the Dunn chemotaxis chamber and time-lapse microscopy. *Methods Mol Biol* **294**, 31-41.
**Westerfield, M.** (2000). The zebrafish book. A guide for the laboratory use of zebrafish (Danio rerio). Univ. of Oregon Press, Eugene.
**Weston, C. R. and Davis, R. J.** (2007). The JNK signal transduction pathway. *Curr Opin Cell Biol* **19**, 142-9.
**Wheeler, G. N. and Hoppler, S.** (1999). Two novel Xenopus frizzled genes expressed in developing heart and brain. *Mech Dev* **86**, 203-7.

**Whiteford, J. R. and Couchman, J. R.** (2006). A conserved NXIP motif is required for cell adhesion properties of the syndecan-4 ectodomain. *J Biol Chem* **281**, 32156-63.
**Wilcox-Adelman, S. A., Denhez, F. and Goetinck, P. F.** (2002a). Syndecan-4 modulates focal adhesion kinase phosphorylation. *J Biol Chem* **277**, 32970-7.
**Wilcox-Adelman, S. A., Denhez, F., Iwabuchi, T., Saoncella, S., Calautti, E. and Goetinck, P. F.** (2002b). Syndecan-4: dispensable or indispensable? *Glycoconj J* **19**, 305-13.
**Winklbauer, R., Medina, A., Swain, R. K. and Steinbeisser, H.** (2001). Frizzled-7 signalling controls tissue separation during Xenopus gastrulation. *Nature* **413**, 856-60.
**Winklbauer, R. and Selchow, A.** (1992). Motile behavior and protrusive activity of migratory mesoderm cells from the Xenopus gastrula. *Dev Biol* **150**, 335-51.
**Winklbauer, R., Selchow, A., Nagel, M. and Angres, B.** (1992). Cell interaction and its role in mesoderm cell migration during Xenopus gastrulation. *Dev Dyn* **195**, 290-302.
**Winter, C. G., Wang, B., Ballew, A., Royou, A., Karess, R., Axelrod, J. D. and Luo, L.** (2001). Drosophila Rho-associated kinase (Drok) links Frizzled-mediated planar cell polarity signaling to the actin cytoskeleton. *Cell* **105**, 81-91.
**Witzel, S., Zimyanin, V., Carreira-Barbosa, F., Tada, M. and Heisenberg, C. P.** (2006). Wnt11 controls cell contact persistence by local accumulation of Frizzled 7 at the plasma membrane. *J Cell Biol* **175**, 791-802.
**Wolff, T. and Rubin, G. M.** (1998). Strabismus, a novel gene that regulates tissue polarity and cell fate decisions in Drosophila. *Development* **125**, 1149-59.
**Wong, H. C., Bourdelas, A., Krauss, A., Lee, H. J., Shao, Y., Wu, D., Mlodzik, M., Shi, D. L. and Zheng, J.** (2003). Direct binding of the PDZ domain of Dishevelled to a conserved internal sequence in the C-terminal region of Frizzled. *Mol Cell* **12**, 1251-60.
**Wong, H. C., Mao, J., Nguyen, J. T., Srinivas, S., Zhang, W., Liu, B., Li, L., Wu, D. and Zheng, J.** (2000). Structural basis of the recognition of the dishevelled DEP domain in the Wnt signaling pathway. *Nat Struct Biol* **7**, 1178-84.
**Woods, A. and Couchman, J. R.** (1992). Protein kinase C involvement in focal adhesion formation. *J Cell Sci* **101 (Pt 2)**, 277-90.
**Woods, A. and Couchman, J. R.** (1994). Syndecan 4 heparan sulfate proteoglycan is a selectively enriched and widespread focal adhesion component. *Mol Biol Cell* **5**, 183-92.
**Woods, A., Couchman, J. R., Johansson, S. and Hook, M.** (1986). Adhesion and cytoskeletal organisation of fibroblasts in response to fibronectin fragments. *Embo J* **5**, 665-70.
**Woods, A., Longley, R. L., Tumova, S. and Couchman, J. R.** (2000). Syndecan-4 binding to the high affinity heparin-binding domain of fibronectin drives focal adhesion formation in fibroblasts. *Arch Biochem Biophys* **374**, 66-72.
**Worthylake, R. A. and Burridge, K.** (2003). RhoA and ROCK promote migration by limiting membrane protrusions. *J Biol Chem* **278**, 13578-84.
**Wozniak, M. A., Modzelewska, K., Kwong, L. and Keely, P. J.** (2004). Focal adhesion regulation of cell behavior. *Biochim Biophys Acta* **1692**, 103-19.
**Wu, J., Saint-Jeannet, J. P. and Klein, P. S.** (2003). Wnt-frizzled signaling in neural crest formation. *Trends Neurosci* **26**, 40-5.
**Wunnenberg-Stapleton, K., Blitz, I. L., Hashimoto, C. and Cho, K. W.** (1999). Involvement of the small GTPases XRhoA and XRnd1 in cell adhesion and head formation in early Xenopus development. *Development* **126**, 5339-51.
**Yamaguchi, H., Wyckoff, J. and Condeelis, J.** (2005). Cell migration in tumors. *Curr Opin Cell Biol* **17**, 559-64.
**Yamaguchi, Y., Katoh, H., Yasui, H., Mori, K. and Negishi, M.** (2001). RhoA inhibits the nerve growth factor-induced Rac1 activation through Rho-associated kinase-dependent pathway. *J Biol Chem* **276**, 18977-83.
**Yang, J. T., Rayburn, H. and Hynes, R. O.** (1993). Embryonic mesodermal defects in alpha 5 integrin-deficient mice. *Development* **119**, 1093-105.
**Young, H. M., Hearn, C. J., Farlie, P. G., Canty, A. J., Thomas, P. Q. and Newgreen, D. F.** (2001). GDNF is a chemoattractant for enteric neural cells. *Dev Biol* **229**, 503-16.
**Yu, H. H. and Moens, C. B.** (2005). Semaphorin signaling guides cranial neural crest cell migration in zebrafish. *Dev Biol* **280**, 373-85.
**Zamir, E. and Geiger, B.** (2001). Components of cell-matrix adhesions. *J Cell Sci* **114**, 3577-9.
**Zhai, J., Lin, H., Nie, Z., Wu, J., Canete-Soler, R., Schlaepfer, W. W. and Schlaepfer, D. D.** (2003). Direct interaction of focal adhesion kinase with p190RhoGEF. *J Biol Chem* **278**, 24865-73.
**Zhang, Y., Thant, A. A., Hiraiwa, Y., Naito, Y., Sein, T. T., Sohara, Y., Matsuda, S. and Hamaguchi, M.** (2002). A role for focal adhesion kinase in hyluronan-dependent MMP-2 secretion in a human small-cell lung carcinoma cell line, QG90. *Biochem Biophys Res Commun* **290**, 1123-7.

**Zhu, S., Liu, L., Korzh, V., Gong, Z. and Low, B. C.** (2005). RhoA acts downstream of Wnt5 and Wnt11 to regulate convergence and extension movements by involving effectors Rho Kinase and Diaphanous: Use of zebrafish as an in vivo model for GTPase signaling. *Cell Signal* **18**, 359-72.
**Zigmond, S. H.** (2004). Formin-induced nucleation of actin filaments. *Curr Opin Cell Biol* **16**, 99-105.
**Zimmermann, P., Tomatis, D., Rosas, M., Grootjans, J., Leenaerts, I., Degeest, G., Reekmans, G., Coomans, C. and David, G.** (2001). Characterization of syntenin, a syndecan-binding PDZ protein, as a component of cell adhesion sites and microfilaments. *Mol Biol Cell* **12**, 339-50.